Processes of Vitrification in Scottish Iron Age Hillforts

Amanda-Jane Dolan

BSc (Hons), MLitt

January 2020

Thesis submitted for the degree of Doctor of Philosophy

Biological and Environmental Science

School of Natural Sciences

University of Stirling

Scotland

Quotation

“Understanding is a three-edged sword: your side, their side, and the truth.”

J. Michael Straczynski, Babylon 5, season 4, episode 6

Abstract

Iron Age Vitrified hillforts are a relatively common feature in the Scottish landscape. There are at least sixty confirmed examples spread across Scotland. How and why these hillforts were vitrified are unanswered questions to modern archaeologists. There has long been debate as to whether this vitrification was an act of construction or destruction and if vitrification was a destructive process, was this vitrification event intentional or accidental. This research sets out to firstly determine the provenance and variability of the building lithology and secondly, to understand the conditions of vitrification in Scottish Iron Age hillforts. Research was conducted on nine hillforts across Scotland taking in a variety of local geologies, but work focussed on Dun Deardail in Glen Nevis.

Dun Deardail was excavated for three seasons between 2015 and 2017. These three seasons of excavation produced samples of vitrified, burnt and unburnt rock, soil and charcoal. The provenance of the building materials at all of the hillforts included in this research has been found to have been local, with the building materials found to be mainly found from within one kilometre of the hillfort site. Variability across each hillfort was shown to be low, with each of the hillforts being constructed using only a few lithologies. Conditions of vitrification were determined using a variety of geochemical and petrological techniques. Experimental melts were carried out to study the effect of vitrification conditions on the melting process and vitrified material and compared to the evidence seen at the hillforts themselves. These melts allowed an exploration of the processes of the vitrification under controlled conditions, allowing the different variables and theories to be examined.

The minimum melting temperature of the rubble core at Dun Deardail was found to be approximately 1140˚C, and this result was mirrored at Craig Phadrig, The Torr and Knockfarrel, where similar temperatures were also calculated. This suggests that only partial melting took place, with this temperature being in between the solidus and liquidus temperatures of pelitic material.

Each of the hillforts researched was timberlaced in construction. This timberlacing allowed the transportation of the heat from the outside of the hillfort into the rubble

core. This allowed the core to remain at a temperature high enough to allow mineral melting, even when the outer face of the walls had cooled to below the solidus temperature.

Excavation of Dun Deardail identified very few items, and this suggests that the hillfort was cleared of goods before the fire. This may suggest that the fire was a deliberate act at the end of the hillfort's life. Perhaps a sort of ritual closure.

Compared with modern glass, the glasses formed during vitrification have shown a much lower degree of erosion over time due to an enrichment of calcium in the glass. This retardation of typical erosional properties of the vitrified material gives strength to the vitrified walls and prevents erosion, preserving these vitrified hillforts for future generations. Further study into this erosion should be undertaken to further understand the conservation of these, and similar, monuments.

Table of Contents

List of figures

List of tables

Temperature equations used throughout the thesis

Equation 1: Leeman and Scheidegger calculation (Leeman and Scheidegger, 1977)

$$T(Mg, ℃) = \left(\frac{8916}{\left(\ln\left(\frac{Mg(ol)}{Mg(gl)}\right)\right) + 4.29}\right) - 273 \quad \text{a)}$$

$$T(Fe, ℃) = \left(\frac{9016}{\left(\ln\left(\frac{Fe(ol)}{Fe(gl)}\right)\right) + 5.46}\right) - 273 \quad \text{b)}$$

Where Mg(ol) is the magnesium content of the olivine, Mg(gl) is the magnesium content of the glass, Fe(ol) is the iron content of the olivine and Fe(gl) is the iron content of the glass.

Equation 2: Jung and Pfander (Jung and Pfänder, 2007)

$$T(℃) = \frac{((\ln 93183) - \ln\left(\frac{Al}{Ti}\right)}{0.00813}$$

The Jung and Pfänder (2007) method is commonly used in metamorphic geology for determining the temperature in pelitic melts. This method uses the ratio of commonly occurring elements, aluminium and titanium, in pelitic rocks to give a temperature that the pelitic rock melted.

Equation 3: Wan et al (Wan et al, 2008)

$$T(℃) = \left(\frac{10000}{0.512 + 0.873Y_{Cr} - 0.91\ln(K_D)}\right) - 273$$

Where $Y_{Cr} = Cr/(\frac{Cr}{Al})$ and $K_D = \frac{Al_2O_3\ (ol)}{Al_2O_3\ (sp)}$

Equation 4: De Hogg et al (De Hogg et al, 2010)

$$T_{Al(ol)}(℃) = \left(\frac{9423 + 51.4p + 1860_{Cr\#}{}^{ol}}{(13.409 - \ln([Al]^{ol})}\right) - 273$$

Where $Cr_{\#}{}^{ol} = Cr/(Cr + Al)$ in olivine

Equation 5: Coogan et al (Coogan et al., 2014)

$$T(^{\circ}\mathrm{C}) = \left(\frac{10000}{0.575(0.162) + 0.884(0.043)Cr^{\#} - 0.897(0.025)\ln(Kd)}\right) - 273$$

Where $Cr^{\#} = Cr/(Cr + Al)$ in spinel and $Kd = \frac{Al_2O_3{}^{olivine}}{Al_2O_3{}^{spinel}}$

Acronyms commonly used

AOC	AOC Archaeology Group
BGS	British Geological Society
FCS	Forestry Commission Scotland
HES	Historic Environment Scotland
Highland HER	Highland Historic Environment Record
ICP	Inductively Coupled Plasma Mass Spectrometry
NERC	Natural Environment Research Council
OS	Ordinance Survey of the UK
PPL	Plane polarised light
p-XRF	Portable X-ray fluorescence
RCAHMS	the Royal Commission on the Ancient and Historical Monuments of Scotland
SEM-EDX	Scanning Electron Microscopy Dispersive X-Ray Analyzer
UoS	University of Stirling
XPL	Crossed polarised light
XRF	X-ray fluorescence

Acknowledgements

Dolly Parton sang “Workin’ 9 to 5, what a way to make a livin’. Barely getting’ by. It’s all takin’ and no givin’.” Listening to the lyrics of that song eleven years ago made me realise I wanted more from my career and to do so, I needed to get myself a degree. From this spark, I embarked on a university education from an undergraduate degree, followed by a masters and cumulating in this PhD. And this all started when Dr Iain Allison allowed me to start my BSc Earth Science, really quite by accident.

Just like Dolly Parton, I have always had strong female role models throughout my academic career. Dr Jaime Toney took a chance on me and gave me a summer prize internship in the BECS laboratory, and from then on, I was privileged to do my honour’s project and a further research project in Jaime’s BECS laboratory. From then on, I knew I wanted to do research. Dr Cristina Persano gave me my love of isotopes and was always there whenever I needed a shot of “pull yourself together”. And now my primary supervisor, Dr Clare Wilson, has been my guide throughout this PhD. Whenever my thoughts would drift onto some crazy idea or other, Clare would reign me back in again. Clare would keep me focused and guide me through to completion and kept me full of coffee at the McBob. Great thanks go out to each one of them. I would not be here without you.

I have been really fortunate with the support and differences between all of my supervisors. Dr Christian Schröder has always been there with Mössbauer chat, space stuff, along with a healthy dose of Star Wars. Christian also made me feel included and took me in under the wing of his research team. Matt Ritchie has the super enthusiasm of all things Dun Deardail. Probably all things to do with vitrified hillforts. And last, but by no means least, Dr Carol Lang, very much my geoarchaeological supervisor. All of my supervisors merged together to give me an excellent, very well sounded support system. It has been very much appreciated.

Thanks also go out to everyone in my lovely office but most importantly to Debs. You have been my rock throughout this whole thing. The person whom I could moan about everything and anything to and sound advice was always given without judgement. Your help has been very much appreciated.

My love of sci-fi has been the element that has been my escape and my grounding mechanism. Days spent watching Stargate, whether it be SG1 or Atlantis, while down

in the dungeon doing hundreds of p-XRF analyses, were numerous. Star Trek, of all types, and Babylon 5 have also very much played their parts. Spotify has kept me going with every musical genre that my head has wanted during my writing up period.

This PhD was share funded between Forestry and Land Scotland and the University of Stirling and this funding has been greatly appreciated.

Everyone at AOC has been a great help and allowed me to tag along during their excavations, teaching me excavation skills along the way. Special thanks go to Andy Heald and Martin Cook for everything.

George MacLeod has made some beautiful slides and was eternally patient with all of my SEM-EDS woes. Scott Jackson sorted all of my computer issues, as well as helping me to pick a new laptop that did everything that I needed it to do and came with the extras that I really turned out to need. Ronald Balfour sorted everything I needed to order for my research. From a furnace to melt rock to the crucibles to melt the rock in and helping me sort out my car hire for the fieldwork carried out. It was really helpful to be able to pick up my hire cars locally from the fantastic team at Arnold Clark in Hamilton Road. Lynn sorted all my cashflow and helped me spend my budget to the best of our ability. Charlie was always a highlight of the day when he was in the department, especially when he came to investigate what I was eating for lunch when sitting out by the loch.

Academic Twitter has been a wonderful source for networking and getting advice on various things to do with my research, career and PhD life in general.

My daughter Lily has joined me on my academic journey from when she was a tiny tot. She's put up with my studying and fieldtrips from a young age without complaint. I hope I have given her a love of science, the chance to question everything and a love of the outdoors.

And in my thanks, I have left the best until last. My parents, Wilma and John, have been there for me in every way through this entire adventure. As a single parent, I could not have done it without them, especially all the fieldwork and the school runs, and for this, I will be eternally grateful.

1 Introduction

Vitrified hillforts are a characteristic feature of the Scottish Iron Age and Early Historic Period (Ralston, 2004). The Iron Age was a time of change, and a further move towards farming and domestication and more permanent domestic structures were constructed from the Late Bronze Age onwards (Armit and Ralston, 1997). For the purposes of this, the definition of the Iron Age will be taken as from around 8th century BC until AD43. There have been frustratingly few excavations carried out on Scottish Iron Age vitrified hillforts, and this has created a situation where the chronological framework of these sites is rather vague. The excavation techniques of the early nineteenth century would leave modern-day archaeologists flabbergasted. Also, many of the earlier sites have not been carbon dated and the datable samples handled in ways which allow not modern-day dating to take place (Hunter and Carruthers, 2012).

1.1 Iron age hillforts

There is no absolute distinction between forts and enclosed settlement. The range is a continuum from tiny enclosed promontories through to large enclosed hillforts (Ralston, 2004) In this thesis, hillforts will be classified using the Atlas of Hillforts Lock, G. & Ralston (2017) criteria:

1. topographic position - sites which occupy a prominent/focal spot in the landscape;

2. the scale of enclosing works - sites with enclosing works which are designed to impress;

3. size of the enclosed area - sites with enclosing works that enclose an area >0.2 hectares.

The use of the term hillfort implies that these structures were used as military fortifications built to be used for defence and battle (Armit, 2005). There may have been a need for highly defensible positions at this time. Irish writings talk of the destruction of strongholds by fire (Hamilton, 1966). The term “hillfort” was first used in the early days of hillfort studies when the “on-trend” focus of enclosures was defence, fortitude and warring communities. Modern thinking sees these structures as more of a social space, perhaps with hierarchical connotations (Hunter and Carruthers, 2012). However, the term “hillforts” is still the commonly used term and will continue to be used to describe these structures.

Hodder (2011) believes in a “human-thing entanglement” and that this transfers over to structures and their uses. Each is dependent on each other and influence the purposes and emotion related to each of them. Through this approach, we can envisage that hillforts would have had an active role in allowing Iron Age people to make their mark on their world and experience their existence and significance in their environment. Hillforts may have had agency or even personhood in the eyes of the community and held a cosmological importance. This may be why so much energy went into the construction and maintenance of the hillfort. Therefore, the positioning of the hillforts may have been important to the community and may have provided protection to its users. There may have been some significant ritual use, and the landscape where the hillforts were built may have had a spiritual meaning for the builders (Dobres and Robb, 2000).

Geophysical analysis has shown that there are often wooden structures found within the hillfort ramparts. These may have been used for animal husbandry, storage, human living areas or social areas. Ingold (2011) reminds us that communities create networks with the landscape and with other communities. As these societies did not live in isolation, these hillforts may have been meeting places, especially as are they are often found at the junctions of several routes. Dun Deardail, for example, is found at the juncture between three valleys, and these valleys would have been the easiest ways of getting around or transporting goods and animals to market areas. Travelling people need areas for themselves and their animals to rest and refresh and to trade and make social bonds. In more modern times drovers’ tracks are still visible where people moved their animals from place to place, either for fresh grazing or to sell them at a market. It has often been the case in more modern societies where different groups will meet in areas for social gatherings, such as arranging marriages and treaties between different groups and so this may have been one of the hillforts uses (Hodder, 2011).

It has been suggested that these may have been communal dwelling areas and may have been more of a show of political power rather than just a display of physical strength (Feacham, 1966). These may have been seasonal in use in Scotland due to the harsh winter weather creating a lack of fresh water.

Using its simplest definition, enclosures are any structure separating one area from another (Thomas, 1997). Hillforts were defined previously as areas of enclosed space, and so, in the simplest of terms, hillforts can simply be considered as enclosures.

Figure 1 illustrates how it is believed that a Scottish Iron Age hillfort was constructed. Strong twin drystone walls would have been built directly on the bedrock, and these walls would have been filled with rubble and midden material to produce a rubble core. Hillforts, such as Craig Phadrig in Inverness, have been observed to have been built with differing numbers of ramparts and walls. These may have been either from the original construction or may have been added on later by subsequent settlement users (Ralston, 2006). Univallate hillforts have a single circuit of ramparts, bivallate a double circuit and multivallate have more than one layer. These outer works might not be complete circuits, and so will be notated as partial, and they may just defend the weakest approaches to the hillfort (Harding, 2012).

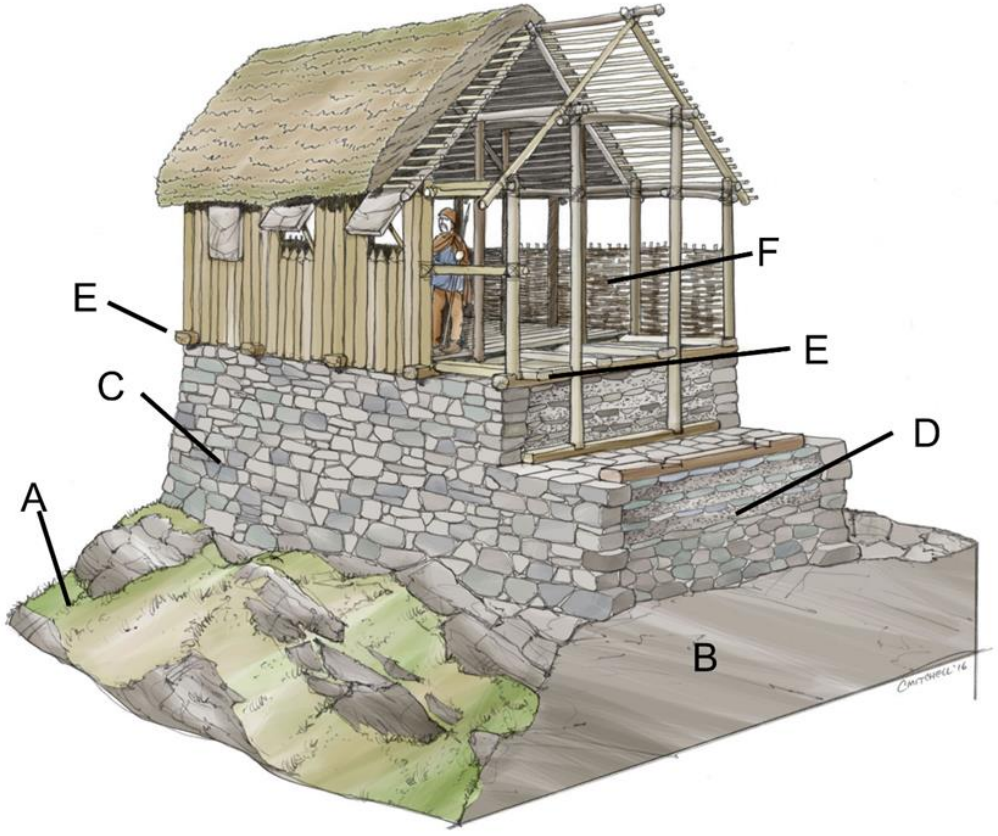

Figure 1:Hillfort construction from FLS.

Area A the natural grass slope, however, this may have been supplemented by dumping extra soil and rubble here to increase the incline. Area B is the natural rock that the hillfort is directly constructed on. Area C are the rampart walls. Area D is the rubble core between the walls. Areas E are highlighting the timberlacing in the structure. Area F illustrates the type of structure that may have been built on top of the hillfort.

Avery (1993) Distinguished between timberframed and timberfaced hillforts. Timberframed hillforts have widely spaced timbers supporting the front and rear walls of the rampart. This timberlacing provides a rigid framework to the structure, allowing wall faces to be built up at the outside and inside wall faces of the rampart. The fabric is further stabilised by filling the structure with a rubble core. Timberfaced ramparts, however, have been constructed with more substantial uprights, set closer together. These substantial upright timbers formed the main retaining wall.

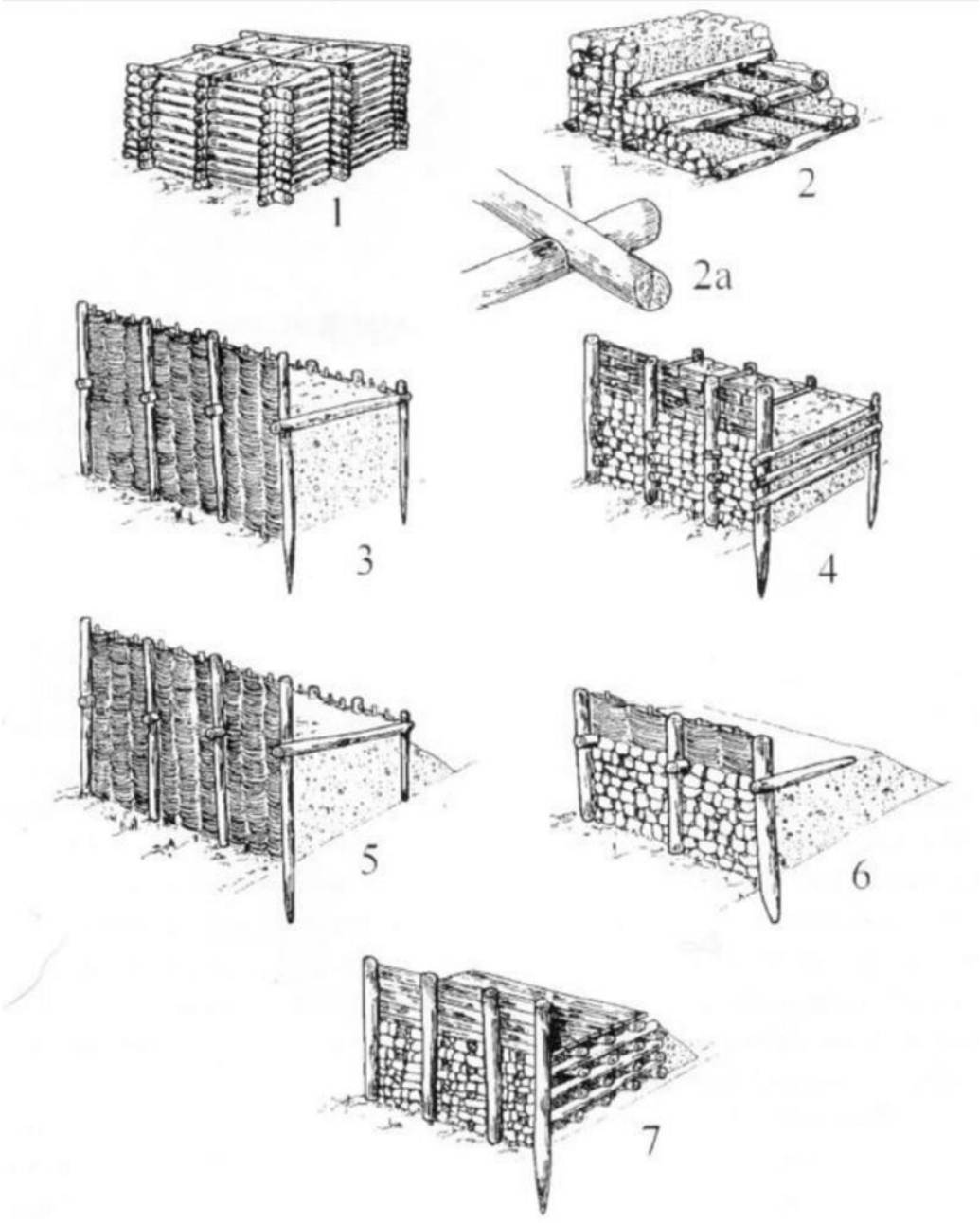

Figure 2: Evolution of timberfaced and timberlaced hillfort types (Driver, 2016).

Figure 2 illustrates some of these variations in timberframes and timberlacing construction techniques. This illustrates the various permutations found in hillfort structure. Image one illustrates a timberframed structure with a rubble core and no outer facing. Illustrations two, four and six are stonefaced timberframed dump rampart varieties, where the timberlacing has been filled with rubble and the walls created from stone. Images three and five are timberfronted dump ramparts, where they have no stone walls, but wood is used instead. Image seven represents timberlaced stonefaced hillfort with wooden superstructure on top (Driver, 2016).

Driver, (2016) calculated that the construction of Danebury hillfort would have taken 1700 five metre lengths of wood for the upright posts and around the same in horizontal timbers. This suggests that timberlacing is a resource-rich building practice. However, this timberlacing increases the strength of the structure so much that it made the use of resources worthwhile. In some hillforts, excavations have shown only horizontal beam holes with no sign of vertical timbers. Structures exhibiting this feature can be observed as a series of square holes in the wall facing in the period 2 rampart at Crinkley Hill, where unbonded, transverse timbers have been built through the stonework (Dixon, 1976). It was noted that there were two parallel rows of posts, sited 2.5 metres apart. These were set into the bedrock for stability. Several of these types of hillforts have been noted to have a stepping structure on the outside of the walls. Rainsborough Camp, Northamptonshire was also noted to have a stepping structure as did several structures in the Aran Islands and South West Ireland (Avery et al., 1967).

In some hillforts, excavations have shown only horizontal beam holes with no sign of vertical timbers. Structures exhibiting this feature can be observed as a series of square holes in the wall facing in the period 2 rampart at Crinkley Hill, where unbonded, transverse timbers have been built through the stonework (Dixon, 1976). It was noted that there were two parallel rows of posts, sited 2.5 metres apart. These were set into the bedrock for stability. Several of these types of hillforts have been noted to have a stepping structure on the outside of the walls. Rainsborough Camp, Northamptonshire was also noted to have a stepping structure as did several structures in the Aran Islands and South West Ireland (Avery et al., 1967) There are many examples of stone-faced, timberlaced ramparts in Britain. These ramparts contain a crisscross timber framework within the rampart core. In England, examples of these timberlaced hillforts can be seen

in Hollingburu, Sussex (Curwen, 1932) and Uffington (Miles et al., 2003). In Scotland, this hillfort type is quite prolific and have been studied since the late 19th century through excavations on Castlelaw, Abernethy (Christison, 1898, 1899). Stone-faced hillforts without any sign of timber supports have been observed. The period 2 rampart at site A at Stanwick is an excellent example of this architecture (Wheeler, 1954)

Many of the settlements with earthen banks have also been shown to have had ditches surrounding the structure and material from these ditches would have been used to create the earthen bank hillfort. The product of these ditches was often used in the building of dump ramparts (Harding, 2012). However, at Uffington, the material from the ditches was stockpiled and selectively used in building the dump rampart (Miles et al. 2003). At Stanwick, East Yorkshire, the ditch appears to have been constructed so to collect water, perhaps as a moat feature to impede access to the rampart (Wheeler, 1954).

Various types of entrances have been discovered in hillfort ramparts (Harding, 2012). Many hillforts have extra defensive features near the entrance, such as a thickening of the walls or a passage where those who wish to enter must pass through. Two commonly encountered entrances are simple openings and raised entrances.

Simple openings, which might be just a break in the wall, or a timber gate may have been constructed might the main ramparts may turn inward or outward and be widened and heightened to control the entrance. Many hillforts have extra defensive areas near the entrance, such as a thickening of the walls or a passage and so, if used for defence, a simple entrance might not be all that would be required. In some hillforts, a basic narrowing of the entrance was all that was needed (Alexander, 2002). Linear holloway entrances are straight parallel pairs of ramparts dominating the entrance, projecting either inward, outward, or occasionally overlapped along the main rampart. Complex, multiple overlapping outer works are often featured on later hillforts. These may consist of staggered or interleaved multivallate ramparts, zig-zag entrance ways, sling platforms and well-planned lines of fire (Harding, 2012).

Elevated entrances are ones which were off the ground and probably accessed using a ladder or steps formation. These were used in some hillforts that had previously been thought not to have any entrance in evidence. Dunnideer, Strathdon is one such hillfort

(Cook, 2010) as was Finavon (Alexander, 2002). The entrance from the hillfort at Forandenny was built higher than the surviving wall and showed no evidence of its existence anymore (Bell, 1893).

1.2 Geographical extent

According to Lock and Ralston, (2017), there are 4147 hillforts in the United Kingdom and Ireland that fit these criteria. This breaks down as follows (in population order):

- Scotland: 1695
- England: 1225
- Wales: 690
- Ireland: 475
- Northern Ireland: 30
- Isle of Man: 30

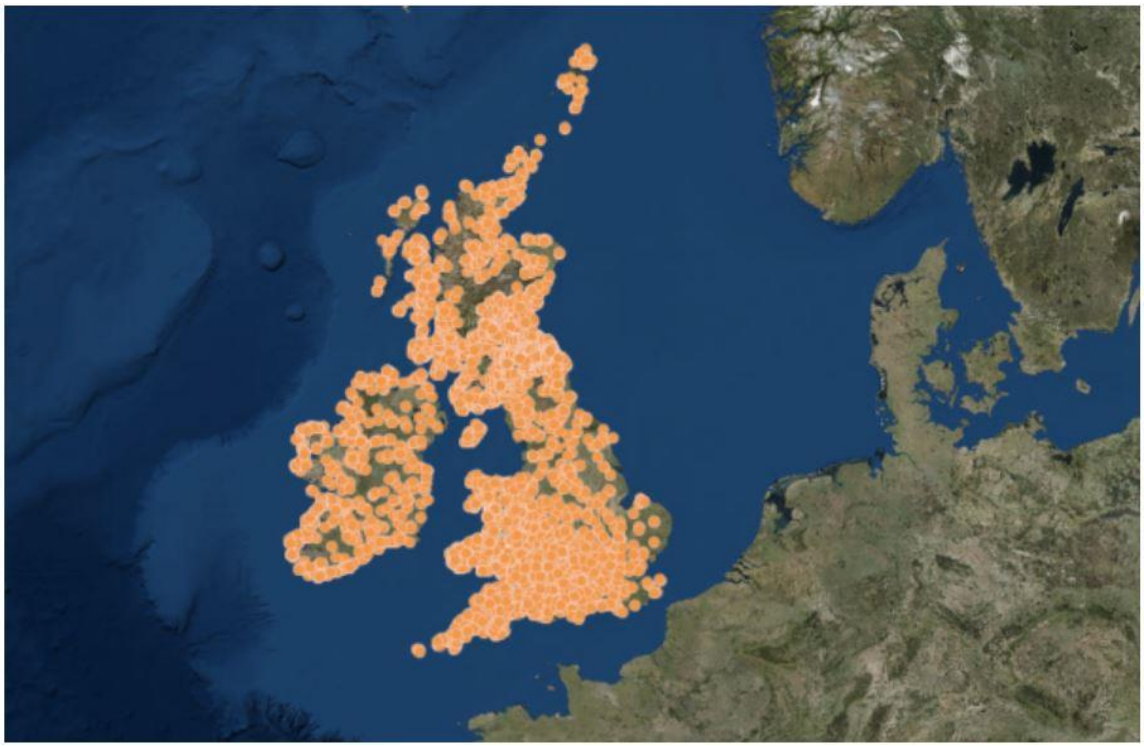

Figure 3: UK and Ireland hillfort locations, taken from the online hillfort atlas (Lock & Ralston, 2017) .

As shown in Figure 3, there is a broad spread of hillforts in The United Kingdom and Ireland, and they are not restricted to a small area of the country. They are spread over various geologies and elevations and not restricted to one area or land type (Lock, G. & Ralston, 2017).

1.3 Vitrified hillforts

Vitrified hillforts are hillforts that have been burned so such an extent that the walls and/or rubble core melts and fuses the lithology (Mackie, 1967). The rocks constructing the hillfort are heated to such a high temperature in a fire that they become melted and often glassy. The material is a vesicular, vuggy, frothy mixture of material, and may surround and fuse less altered pieces of rock (Youngblood et al., 1978). John Honeyman in 1868 first recognised that hillforts were constructed from loose materials that had become bound together into a solid mass by the thermal melting of easily fused materials. Honeyman thought that there was abundant evidence that the cementing material had run down among loose stone in melt drops and small streams, and these remained as they cooled. Scottish Iron Age hillforts are particularly associated with vitrification. The actual temperature reached during this vitrification has been a disputed area since Williams (1777) brought these structures to light.

Figure 4 shows an example of an excavated vitrified clast from Dun Deardail, Fort William. Melted rock material has glued together the other lithologies that have been heated but not melted, and vesicles are evident within the melt where the rock has boiled and lost its molecular water (A). Some of the lithologies have been dehydrated and are friable (B), and layered ones have had their layers disrupted, depending on their mineralogy (C).

There are approximately 80 known vitrified hillforts in Scotland (Lock & Ralston, 2017), and their spread is shown in Figure 5.

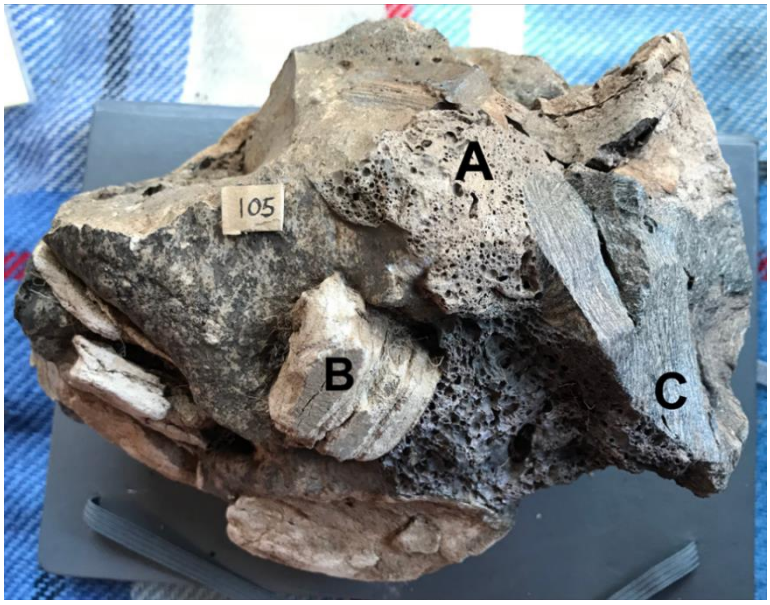

Figure 4:Vitrified rock clast from Dun Deardail, Glen Nevis, Fort William.

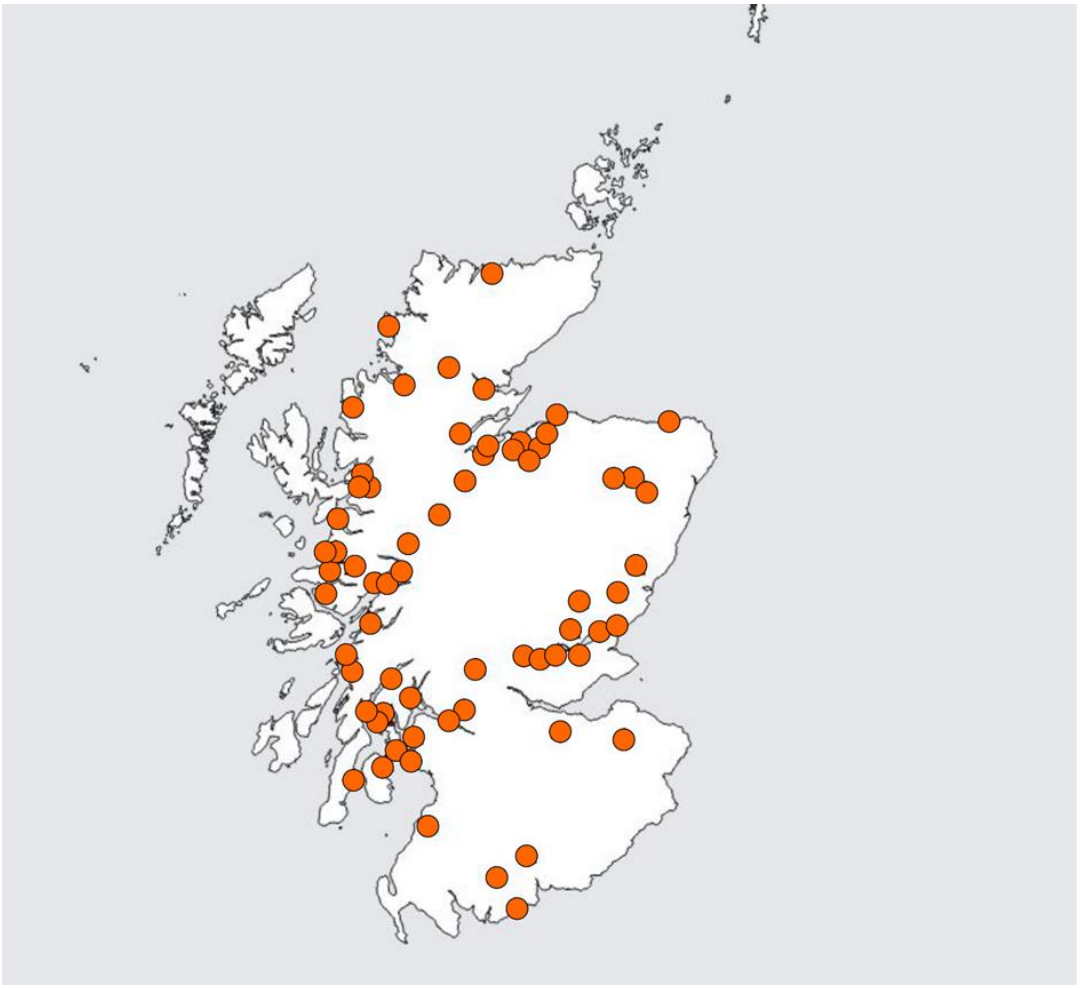

Figure 5:Vitrified hillfort locations in Scotland constructed from data from Canmore.

The main themes of Nisbet's studies (1974, 1975) have been firstly to discover whether geology influences where the hillforts were built. Nisbet speculated that they had been constructed on or with one specific type of rock that is good for melting and fusing other rocks? And also, whether the local rock was always used in the construction of the ramparts or if the rock was imported from outside the site area. Nisbet found that the hillfort locations were chosen more for their situation rather than a common geological feature. Construction materials also turned out to be mainly sourced from the local areas. Kresten (1993) explored the geologies of vitrified hillforts in Sweden. Here the building materials were predominantly gneissic granite and amphibolite.

1.3.1 Vitrification of hillforts

The degree of vitrification that has been noted varies from site to site. Some vitrification appears crumbly, some are well welded, and some have lots of dripping and textures. The colour of the vitrification is typically representative of the local unvitrified country-rock. Melting of biotite and other mafic minerals creates darker glasses, whereas melting of feldspars produces the lightest. These correspond to the partitioning of mafic (for example FeO, MgO and CaO) and silicic (for example SiO_2, Al_2O_3 and K_2O) materials (Youngblood et al., 1978).

Youngblood et al. (1978) further categorised the melting forms in vitrified rock samples into three groups depending on melt qualities and chemical analysis (Table 1).

The first group, typified in Scotland by Tap O'Noth, are granitic type melts. These are typified by rocks high in silicon, aluminium, sodium and potassium, and, depleted in silicon and sodium. The melt glasses are enriched in aluminium, calcium, potassium, iron, magnesium and titanium. The colour of these glasses is also determined by the chemical composition, with the darker glasses containing higher concentrations of iron, titanium, calcium and magnesium, compared to the lighter glasses. The first group of melt type shows a trend in glass away from the composition of the country-rock. The bulk chemistry shows a decrease in quartz and an increase if the sum of feldspars, albite, anorthite and orthoclase. This produces an overprinting variation in the glass, which is reflected in higher diopside, olivine and hypersthene values for darker glasses.

Group two melts, typified in Scotland by Finavon and Abbey Craig, consist of amphibolites and so contain less silica and more iron, magnesium and calcium

compared to group one felsic melts. In the glasses, the magnesium, iron and calcium are depleted whereas the silicon, aluminium, potassium and sodium are increased. This is reflected in an increase in normative quartz, albite and orthoclase and a decrease in anorthite and hypersthene.

Group three melts, typified in Scotland by Dunnideer, are ones that are defined in having more than two rock types used in building the walls. The glasses have a whole range of compositions, and it is typical for the less abundant elements to be enriched in the glass. At Mote of Mark, south-west Scotland, is composed of greywacke and granitic glasses, enriched in aluminium and calcium and is depleted in potassium. This is reflected by an increase in normative anorthite and a decrease in orthoclase.

Table 1: Hillfort groupings as per Youngblood et al., (1978).

	Hillfort melt groups		
	Group 1	Group 2	Group 3
Hillfort	Puy de Gaudy	Finavon	Braes
	Donnersberg	Abbey Craig	Mote of Mark
	Chateauvieux		Dunnideer
	La Courbe		
	Tap O'Noth		

Although there have been relatively few geochemical studies of vitrified hillforts, the results of these have been able to reveal something about the process of vitrification.

The distribution of phosphorus indicates local melting. The phosphate content in vitrified samples from Dunnideer shows that the phosphate content is highly variable, with variability between 3 and trace detected in thin section. This is due to the preferential melting of apatite in the diorite, and this implies a lack of convective mixing during melting. This indicates that the rocks were only just melted and so were still in a viscous state (Youngblood et al., 1978).

When the residual materials were analysed, they contained quartz, feldspar and smaller quantities of biotite and pyroxene. The quartz grains are highly fractured, and this implies the temperature reached over 1000°C (Leger et al., 1962). Feldspar grains are observed to have partially reabsorbed boundaries or reaction rims and have the optical properties of glass but the composition of feldspar. Materials often observed crystallising out are often magnetite and titanomagnetite and also, less frequently,

spinel. Some glasses were found to be lower in silicon, and higher in aluminium, iron and magnesium and these glasses tended to devitrify forming fibrous pyroxene (Leger et al., 1962; Youngblood et al., 1978).

Daubrée, (1881a & 1881b) observed feldspar, pyroxene and, in smaller quantities, spinel and humboldtine in vitrified samples from several vitrified hillforts. These formed the melt and were observed in highest abundance clustered around the wood casts. 99% of iron and the trace quantities nickel and manganese were found in the reduced state, indicating strong reducing conditions.

It has been suggested that trends be explained by partial melting. At constant pressure, the chemical composition of the phases present is a function of the temperature, so the first liquid formed is the predicted composition. In a granitic system, feldspars, biotite and accessory minerals contribute iron, magnesium, alkalis and aluminium to the melt. In mafic systems, plagioclase, feldspar, quartz, if present, and potassium melt first then contribute silicon, aluminium and potassium. The composition of the glasses follows this predicted behaviour; thus, there are no anomalous enrichments (Helz, 1976).

Overprinting in melts show three different effects. Firstly, in-situ melting of minerals creates chemical variations in the glass. Secondly, the distribution of calcium, sodium, potassium and aluminium, in the glass is determined by the feldspar composition of the source rock. Feldspar varies in each system, and thus the elements are enriched in varying amount (Winkler, 1967). The third effect is that the degree of fusion varies for each hillfort (Helz, 1976).

The chemical behaviour of the melt can be explained by partial melting. Youngblood et al., (1978) hypothesised that vitrification had occurred in-situ and that there was no evidence of selected fusibility of rock types to increase the chance of vitrification. Also, except for the increase in phosphorus amounts, there is no evidence of fluxes. Trace element analysis for zinc, copper, vanadium and phosphorous may indicate enrichment of organic content in the core, but this may just be the result of the core being used to dispose of midden materials, such as bone and shell, when the walls were being built. This chemical analysis agrees with the findings of Daubrée, (1881a); Daubrée, (1882); Christison et al., (1905) & Brothwell et al., (1974), however the glass results from partial melting does not answer the debate on whether vitrification was a constructive or

destructive process. Youngblood et al. (1978) believed that It might take a large scale burning to answer this question.

Phosphorus quantities are anomalous in many vitrified hillforts. The phosphorus in Braes, Chateauvieux and Finavon shows a small enrichment whereas there is a large increase at Dunnideer, Donnersburg and Puy de Gaudy. The greatest increase in phosphorus is in dark glasses, which highly fluoresce under an electron beam. At Dunnideer the phosphorus was be derived from the apatite melting. However, at Donnergberg and Puy de Gaudy, the phosphorus is particularly high, and it has suggested that this may be caused by midden bones dumped in the rubble core during construction. As well as evidence from excavations, the chemical analysis shows calcium levels are also high. In all cases, chemical analysis has also shown that the FeO: Fe_2O_3 ratio is higher in the glasses than the country-rock. This indicates that the melting environment was highly reducing and produced a loss of water. This suggests that the fire was contained with a lack of oxygen, like a kiln or a wood gas generator. This would produce gas that would make the structure burn at a higher temperature as per the formula:

$$\mathbf{H_2O + C \rightarrow CO + 2H}$$

and this may have helped the burning reach the temperature for partial melting (Youngblood et al., 1978).

The reaction

$$\mathbf{Albite + Orthoclase + quartz + H_2O}$$

defines the solidus temperature to be approximately 925°C, at atmospheric pressure and the liquidus over 1000°C (Huang & Wyllie, 1975). In a basaltic system, the solidus will be higher than 1000°C and the liquidus around 1300°C (Voldan, 1962). Yoder and Tilley (1962) confirmed this by geological investigations in natural basaltic systems. Melting relations demonstrated that vitrified hillforts fall in the range that Voldan, (1962) suggested. A more precise definition of vitrification temperature would require the consideration of other parameters. Diffusion of heat would be a slow process, and this would be because of the dense wall and is backed up by the reducing conditions. Minor chemical constituents, including water, changes the characteristics of the system and tends to depress the solidus temperature.

A detailed study could yield individual temperature data for each hillfort. Youngblood et al. (1978) believed that all the data generated for every hillfort would fall into the range stated above. In lesser vitrified hillforts the temperature would most probably be lower than one with vast quantities of vitrification. Future research could also include a geochemical study of the elemental distribution pattern in surface vs interstitial glasses in source rocks compared to timbers, brushwood, peat and other combustible material. Zinc, copper, vanadium and phosphorus may be useful indicators in flow and surface areas, and this could be compared to internal partial melting and may show flux use or additional combustible material. This could involve experimental melts and glasses at known temperatures.

1.3.2 Fuel sources

Scotland in the Iron Age was already experiencing a period of deforestation as land use was changing due to increases in farming practices. However, there would still have been a substantial covering of woodland in the areas where hillforts are found (Armit, I. & Ralston, 1997). The amount of timber needed to vitrify a hillfort would have been immense, and Brothwell et al. (1974) suggested that one hillfort may have needed sixty-five tons of wood. It has been suggested that the internal timber-lacing may have helped the fire spread through the stone structure, thus spreading the heat and facilitating melting of the stone. Timber-framing and timber-facings could also provide a source of fuel. In many cultures, it is common to burn animal dung. Throughout Scottish history, people have burned peat. Peat has been found, unconsumed, in vitrified remains from Dun Deardail, Fort William. This suggests use in the rubble core or wall (Duff, 1961). It may have been a filler for spaces in the wall structure or an intentional addition to assisting in the burning process. Further archaeobotanical and geoarchaeological research needs to be done to investigate what other fuel sources may have been used in these fires, and so other sources of fuel must be taken into consideration.

1.3.3 Fluxes

Fluxes are materials that have been added, other than stone, to lower the temperature of the melting temperature of the rock (Nisbet, 1974). At their simplest fluxes can include water, charcoal and potash. Wood or peat fuels and the ash from their burning would

have produced potash (K_2O) and should be traceable in chemical analysis studies of the rock and surrounding burnt soil.

Miller, (1858) penned a story they had heard about the finding of seaweed in an unnamed hillfort. The vitrification showed distinct impressions of a kelp weed and so suggested that this was added to the core. Enriched soda (Na_2O) in the soil or rock may point to this sort of addition. However, soda can also be formed from other common sources.

Shell casts were found by Christison et al. (1905) in vitrified material from Duntroon forts. Shells produce lime (CaO) when burnt, and lime helps to increase the temperature of the burn. This may show that the shells were added intentionally to raise the temperature and increase the chances of vitrification taking place. However, the occurrence of shells might just be a sign that the builders of the hillfort used the rubble core as a place to dump their midden waste.

At many excavations, burnt bone has been unearthed. Childe and Thorneycroft, (1937b) found bone in the vitrified material of Rahoy. It has also been suggested that some of the casts attributed to wood may be burnt bone casts (Childe and Thorneycroft, 1937a; Hanle, 1960). This additional material is not a flux for partial melting within blocks of breccia (Daubrée, 1881b) and the existence of this material does not imply constructive intent but may suggest it. These bones may have just been used to fill spaces in the wall or core, as they may have used anything available such as peat, brush or mud. Or may only have been midden deposits in the core.

1.4 Theories of vitrification and previous replica studies

How vitrification of hillforts occurred is still being debated and is important as it informs the many competing theories that exist around the timing, function and purpose of vitrification.

Christison, (1898) pointed out that there was a great variety of vitrified forts in terms of hillfort shape and size. However, vitrification appears to have started from the top and only reaches the bottom accidentally. Furthermore, Christison felt that vitrification was too regular, thorough and continuous to be formed by accidental or incidental means. In some cases, Christison determined that the rocks had been brought some distance as if the builders could tell between fusible and less fusible rocks and this made a difference

to their selection. Christison's observations have led some researchers to suggest that vitrification may have been a process to give stability and strength to the walls.

It is presumed that builders wanted rampart walls to withstand attack and early walls with just vertical facing and timbers would have been easier to destroy. Caesar noted that it was difficult to set fire to the hillforts. Thus Nisbet (1974) suggested that vitrification may have been part of a new constructional technique designed to strengthen the ramparts. Other researchers have concurred, for example, Brothwell et al. (1974) noted the high temperatures required for vitrification and the geographical distribution of sites imply careful planning and construction. They and others think that vitrification was an intentional process to strengthen walls. However, Christison (1898) disagreed with the construction hypothesis and had difficulty explaining it all.

From cremations of bodies to ritualistic destruction of buildings, fire has been used ritualistically for millennia. Many early Scottish cultures burned structures to the ground when at the end of the structures use. It has been suggested that these structures were burned down as part of a societal event. A closure of that part of the life of the social group and this would have been a huge, probably emotional, event (Noble and Brophy, 2011). This sort of event would have taken months of planning, weeks of preparation and would have been talked about and stories told about for years afterwards. Being able to burn your own hillfort to the ground would also have been a great show of power. You had the control over those who would do the work to prepare for the burning event, such as gather the combustible material for stacking outside to carrying out the inferno that the hillfort destruction would have been. It would have been particularly humiliating to be forced to burn down your own hillfort by an opposing army. Everyone from miles around would have seen the burning event, and so news of the defeat would be spread further.

Not many finds have been excavated from any hillfort and so if it were to be either a surprise attack from an opposing army or a humiliating forcing of a group to burn their own hillfort down then you would expect there to have been more finds left behind. However, these sites have been reused over history, and so perhaps that is also a reason why there are so few personal finds at any excavated hillfort so far.

Tytler (1790) demonstrated that Craig Phadrig was not a volcanic phenomenon but was caused by the burning of the timbers and stone making up the walls. Tyler suggested an accidental burning happening when a fire, such as from a bloomery, a beacon fire or a hearth, went out of control and started a fire in the wood in the walls. This could be especially probable given the siting of these hillforts as they would be quite exposed to the wind, helping spread the fire from the original source. Tytler also thought that it would be unlikely for an opposing force to be able to stand close enough to the hillfort to be able to establish a fire of the intensity needed to burn the timbers and vitrify the walls. MacCulloch (1814) disagreed with this idea of vitrification being accidental and believed that an accidental fire would not have created such extreme vitrification.

Paton (1928) suggested that a beacon site or bloomery, close to the wall, may have been the cause of the vitrification. However, microscopic study does not show the bloomery material that would have been expected on either of these sites, such as metal depleted slag deposits (Brothwell et al., 1974). This theory has largely been dismissed due to the depth and intensity of vitrification on some sites (Cotton, 1954; Nisbet, 1974)

The scale of vitrified hillforts implies a large-scale technological commitment. It is unknown if each fort was a single planned project or if they were all linked as some sort of large-scale project? The quantity of fuel needed would have been huge, dry and not rotten to provide good combustion. Childe and Thorneycroft, (1937a) calculated that it would have required thirty-five tons of timber to vitrify Rahoy fort.

Nisbet (1974 and 1975) wondered if the structure and methods of construction of the hillfort could be determined using geological methods and if this construction was in any way significant to the way the hillfort burned. Nisbet wanted to investigate in detail how the vitrification happened by examining the physical, chemical and mineralogical changes that had taken place, if the rates of heating and cooling could be determined and if any fluxes were used.

Many large-scale vitrifications have been attempted but none of these have been particularly successful and only produced limited vitrification. There have also been some experimental beacon burnings to ascertain if the hypothesis that an accidental out of control beacon fire may have set alight to the hillfort and therefore produce the observed vitrification.

The first documented vitrification account was carried out in 1782, using 40,000 bricks to attempt to produce a stronger battery platform than was already in use. This attempt produced virtually no vitrification, and so was not repeated (Cotton, 1954). In 1906 McHardy (1906) tested the beacon fire hypothesis and after three failed attempts decided that a beacon fire would not vitrify a layer of rock. Additions of hay, moss and damp brushwood managed to achieve a glaze on the rocks. McHardy had more success using slow-burning techniques, over an eighteen-hour period, using damp materials. This method produced a reducing, low oxygen environment, and it appears that they achieved a temperature of between 1000 and 1200°C. 1937: Childe & Thorneycroft (1937) performed two large-scale experiments to determine if they could burn and vitrify rocks at temperatures between 800 and 1100°C. They discovered that the burn reached the maximum temperature after around five hours. When the experiment was repeated again, the maximum temperature was achieved at five hours, and carbon monoxide flames were evident in the burn for at least seven hours longer. The wood in the fire was converted into charcoal by distillation, an endothermic reaction. This suggested an environment with reduced oxygen content and that low oxygen content combined with the resulting charcoal in contact with the rocks produce a higher temperature than what could be achieved by burning wood alone. This led Childe and Thorneycroft to assume that burning could produce a high enough temperature to produce vitrification and that this fire could be kindled externally or internally by combustible items against the rampart walls. They also concluded that the rocks that melted would have had to have contained a suitable mixture of minerals along with silica. Duff (1961) maintained that vitrification was used as a strengthening process during the build of the hillfort and that the process could be replicated using peat in the burn. They suggested that this lowered the temperature required for surface vitrification to occur.

Ralston (1986) conducted an experimental firing of the pine-laced rampart at Plean Colliery, Aberdeenshire, in conjunction with the television programme Arthur C Clarke's Mysterious World, made by Yorkshire Television. The rampart burned for 28 hours, and the fire was kept burning by multiple additions of wood and refuse, including items such as mattresses, donated from Aberdeen City Council. They did not achieve extensive vitrification on any part of the rampart. However, small fist-sized pockets of vitrification were found. Ralston concluded that it would have taken a lot of

resources to produce the levels of vitrification seen in vitrified hillforts. Ralston also concluded that the walls did not seem strengthened by the vitrification and that vitrification was most probably a deliberate act of destruction.

In 2001, Mainland executed a community vitrification attempt at the Lower Falls, Glen Nevis in 2001. The burn used ten tonnes of Sitka spruce, donated by the Forestry Commission Scotland (FCS). FCS also donated the infill material for between the main rampart walls and the composition of this was the rock that was local to the area. Other materials used in building and covering the rampart were sand, soil and peat, in varying concentrations over the wall so that the effect of their presence could be analysed. Part of the main timber frame was constructed using seasoned oak to discover the differences that types of wood would have on the burn temperature. They experimented with various building methods across the rampart, using different interlacing designs. Once the fort was built, it was left for four weeks to dry. Thermocouples were built into the rampart in several locations to allow the measurement of heat over the rampart throughout the burn. On burning the temperature initially dropped in the core; however, the outside edge of the rampart reached 1700°C. The fire burned for twenty hours however rain put the flames out after this time, but the core remained hot. Six days later, a trench was dug through the core, and it was discovered that the core was still warm. However, very little vitrified material was found.

There have also been many furnace-based vitrification experiments. In 1814 MacCulloch carried out experimental furnace experiments, utilising samples of amygdaloids in a conglomerate matrix. From these experiments, MacCulloch found that the amygdaloids fused to glass at around 1390°C; however, the conglomerate parts did not start to melt until about 1670°C. A pumice-like material was produced by Miller in 1840 while burning rock samples (Nisbet, 1974). Forbes experimented with melting mica-schist in 1868, melting the material in moderate heat and slight pressure to produce a blended rock, similar to that found in vitrified hillforts (Haswell, 1869).

Cadell explored high temperature melting when various rocks and a piece of cast iron was heated in a glost kiln for up to thirteen hours with the temperature gradually ramped up to 1650°C and the temperature held for twenty-two hours. The door was then opened to allow rapid chilling of the rocks (Nisbet, 1974).

Thorneycroft experimented with rock in a furnace, taking the temperature up to between 1100 and 1150°C. These rocks were petrologically examined, and these rocks appeared to be similar to the vitrified hillfort samples that Childe and Thorneycroft had observed in the field. Thorneycroft decided that an adequate draft was essential to the vitrification process and that this could be achieved by placing stacks of wood over the top of the structure to make it like a blast furnace with air rapidly passing through the space (Childe, 1935).

Wadsworth melted sandstone to determine the theoretical melting temperatures that hillforts may have been exposed to and analysed the resulting melt by x-ray diffraction and thermoanalysis (Wadsworth et al., 2015).

The effects of an open charcoal furnace were explored by Kresten. Small-scale experiments using gneissic granite and amphibolite were heated in an open charcoal furnace. However, the vitrified material was not produced, even when a forced draft was applied for several hours. Kresten concluded that as water plays such a critical part in vitrification and in the open-hearth system, water can easily escape melting does not occur. However, in a sealed system, water can become a supercritical fluid allowing vitrification to occur at lower temperatures than speculated (Kresten et al., 1993).

1.5 Aims and objectives of this research

This study aims to investigate the processes and products of vitrification of Iron Age Scottish hillforts through the detailed study of Dun Deardail vitrified hillfort and the targeted study of vitrified hillforts from across Scotland. The objectives of this study are as follows:

1) To establish the provenance and variation of the building materials used in the hillfort ramparts. It has also been suggested that the building materials used in the construction of Dun Deardail were chosen to enhance the vitrification process. This leads to the following research questions:

> 1a) Have local rocks been used in the construction of Dun Deardail or have other materials been brought in from elsewhere?
>
> 1b) Have the rocks for the construction of Dun Deardail been selected for their melting properties?

These questions will be answered in Chapter 5 Results – archaeological materials and discussed in Chapter 6, section 6.2: Dun Deardail provenance and material proportions. The provenance was examined using visual analysis, geochemical analysis and petrology of samples recovered during three seasons of excavation of Dun Deardail Iron Age vitrified hillfort and comparing the results with the local rock found within a short distance of the hillfort.

2) The temperature and conditions of the rock during the vitrification process were explored in order to understand how the hillfort was vitrified. This leads to the questions:

> 2a) What temperatures were needed to facilitate the vitrification of Dun Deardail?
>
> 2b) Were fluxes intentionally used at Dun Deardail to help the burning process and allow the rocks to melt at lower temperatures than without?
>
> 2c) What was the oxidation state of the melt inside the vitrifying structure?
>
> 2d) Has the vitrification event been a fast or slow burn?
>
> 2e) Are these temperatures and conditions uniform around the hillfort?
>
> 2f) Was the build of Dun Deardail such that it facilitated easier vitrification of the hillfort?

These questions will be answered in Chapter 5: Results, in which we can answer the questions raised involving the conditions of vitrification of Dun Deardail. Conditions were determined using geochemical analysis and petrological study, with the results corroborated by recreating the vitrification using in controlled laboratory conditions using furnace melting of local rock. The methodology for techniques used in Chapter 5 was tested using the experimental melts results contained in Chapter 4, and this will also allow exploration of the theories of how vitrification occurred.

3) To understand Dun Deardail, its conditions of vitrification must be understood in a broader Scottish context. This leads to the questions:

> 3a) Was Dun Deardail unique in its provenance of building materials or are other Scottish vitrified hillforts similar?

3b) Have the same temperatures been required for vitrification of Dun Deardail compared with other vitrified hillforts in Scotland?

3c) Were fluxes found in Dun Deardail also found in other Scottish vitrified hillforts?

3d) Were the oxidation states of the melt inside the vitrifying structures alike?

3e) Was the build type found at Dun Deardail mirrored in the build of other Scottish vitrified hillforts?

These will be answered in Chapter 5, section 5.2: Secondary case study sites . Consistency of hillfort construction and vitrification were determined by hillfort site visits, visual analysis and geochemical analysis of in-situ material. Samples from two vitrified excavated hillforts were also examined as well as one unvitrified excavated hillfort.

Chapter 6 will be a discussion chapter bringing the research questions together and discussing and comparing results that have been determined in previous chapters with current theories of vitrification in Scottish Iron Age hillforts.

And finally, Chapter 7 brings all of the results and discussion together as a final thesis conclusion.

2 Research design – study areas

Nine Iron Age vitrified hillforts sites were chosen to cover varying geology and locations across Scotland.

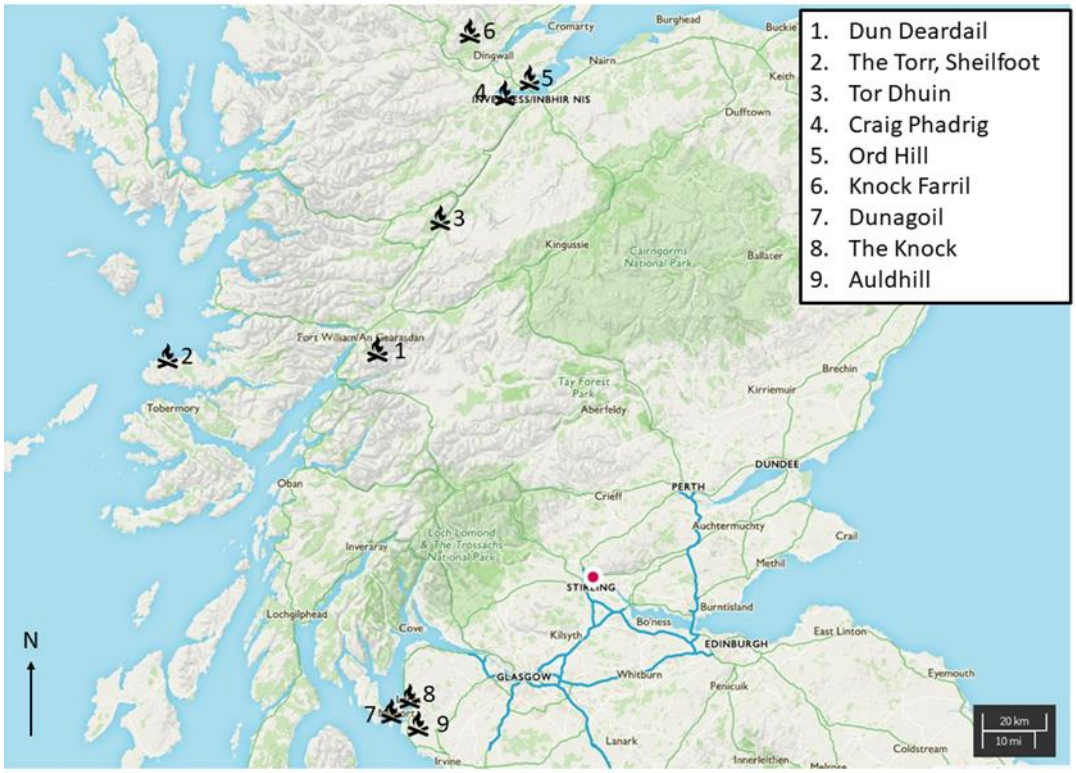

Figure 6: Map of study sites. Adapted from OS online mapping.

2.1 Dun Deardail

The primary study site, Dun Deardail (NN12707012), is situated on the west coast of Scotland in Glen Nevis (Figure 6). Dun Deardail was chosen as the primary study site due to its being excavated at the start of the PhD project, and this allowed reasonable access to the excavation and good excavation records. The ability to tailor the project around the three-year excavation of a site allowed specific research questions to be asked. Dun Deardail remained unexcavated until the AOC excavations of 2015-2017, each of fourteen-day duration. Dun Deardail is a univallate, timberlaced, vitrified contour hillfort located in Glen Nevis, facing Ben Nevis, 300 metres above sea level, on the north-facing spur of Sgurr Challum (Figure 7). The hillfort has a total enclosed area of 1.7ha. (Lock & Ralston, 2017)

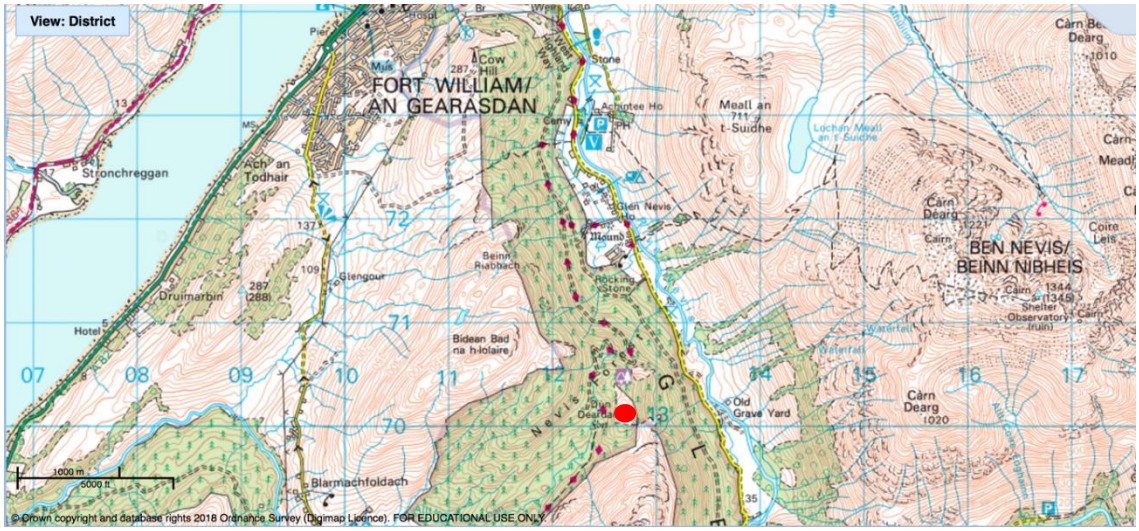

Figure 7:Location of Dun Deardail in relation to Fort William and Ben Nevis (OS mapping downloaded from Edina Digimap).

Dun Deardail is misshapen oval shape (Figure 8), in that the hillfort has a bulge to the south with rough dimensions of 46m x 28m. The inner area shows two distinct regions, delineated by a break in slope. The lower, south-west, area is 30x28m, whereas the higher citadel area measures 20x15m.

The rampart walls were likely to have been around 5m wide and around the same in height.

Figure 8:Dun Deardail from above (Dun Deardail excavation project design, Ellis et al., 2015)

Dun Deardail is sited in an area which contains several types of geology of mainly metamorphic and igneous rocks (Figure 9). The hillfort is situated on the Ballachulish Limestone Formation consisting of calcareous pelite. Sgurr Chalum, the mountain that Dun Deardail sits on the shoulder of is composed of the Leven Schist Formation, a metamorphic bedrock comprising Pelite and Calcsilicate. Ben Nevis sits to the North West of the site and is composed of granites and hornblende andesite lava. One km from the site is The Fort William Formation composed of psammite and semipelite. There are also bands of quartz diorite and pelite with a 2km radius (BGS NERC, 2018).

The local area is covered with superficial glacial deposits of sand, gravel and smaller stones, up to cobble-sized (Wentworth, 1922; BGS NERC, 2018). In addition to this, the landscape is littered with dropstones (BGS NERC, 2018).

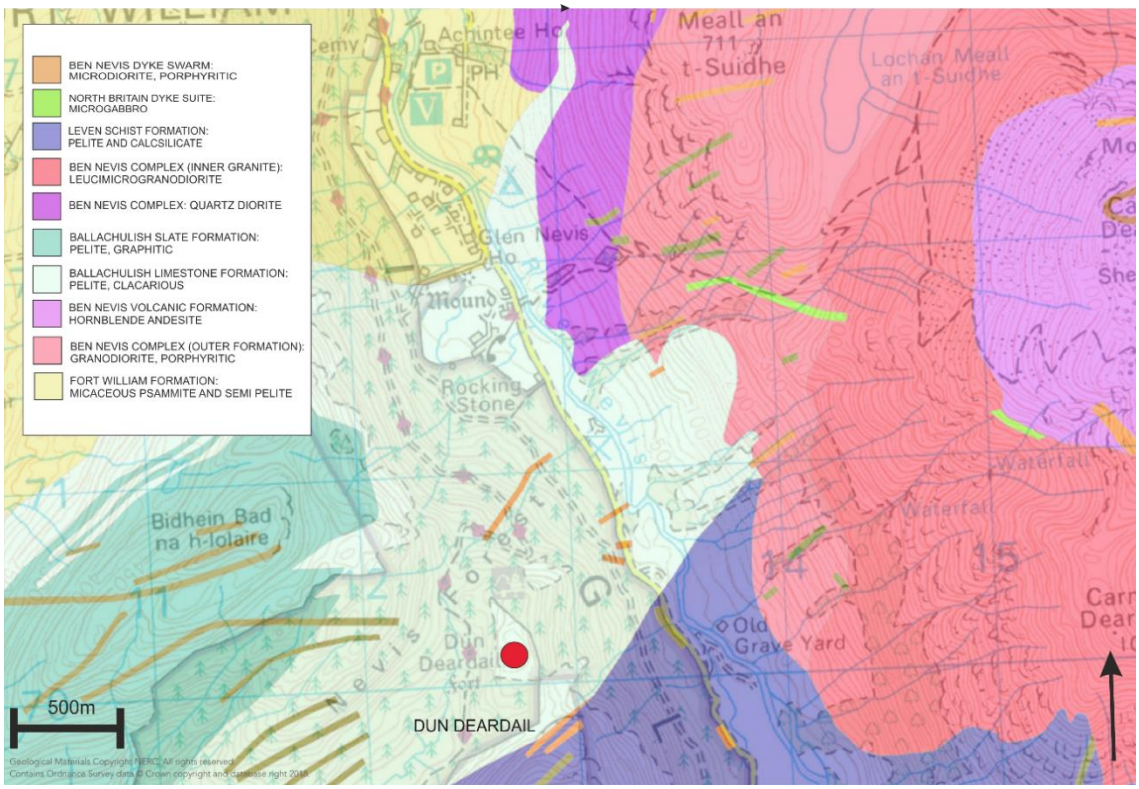

Figure 9: Geology of Dun Deardail and the surrounding area (BGS NERC, 2018).

Williams, (1777) first identified the hillfort followed by the first depiction in an OS map in 1870. An earthworks survey, producing a sketch plan and description was carried in 1888 (Christison, 1889). The hillfort was noted by Angus Graham and Gordon Childe in 1943, followed by a report by RCAHMS in 1956 as part of the Survey of Marginal Landscapes. Helen Nisbet visited Dun Deardail and studied the

hillfort and recorded much of the rampart using photography (Nisbet, 1974, 1975). The structure was scheduled in 1995 following a visit by Highland Council in 1994. Matt Ritchie visited and described the site in 2009 as part of the Forestry Commission for Scotland's conservation management project (Ritchie, 2009). As a prequel to the AOC excavations between 2015 and 2017, in 2010, Headland Archaeology was commissioned to carry out an earthwork survey consisting of a plan and survey (Headland Archaeology, 2011a). During the AOC 2015-2017 excavation (Figure 10), trenches two and four of the first season of excavation (2015) involved going over the walls of the enclosure. Trench three went up to the inner edge of the vitrification. In the second season of excavation (2016) trench six was opened to go over the enclosure wall where the entrance to the hillfort was suggested to be found and was the only trench to investigate the walls.

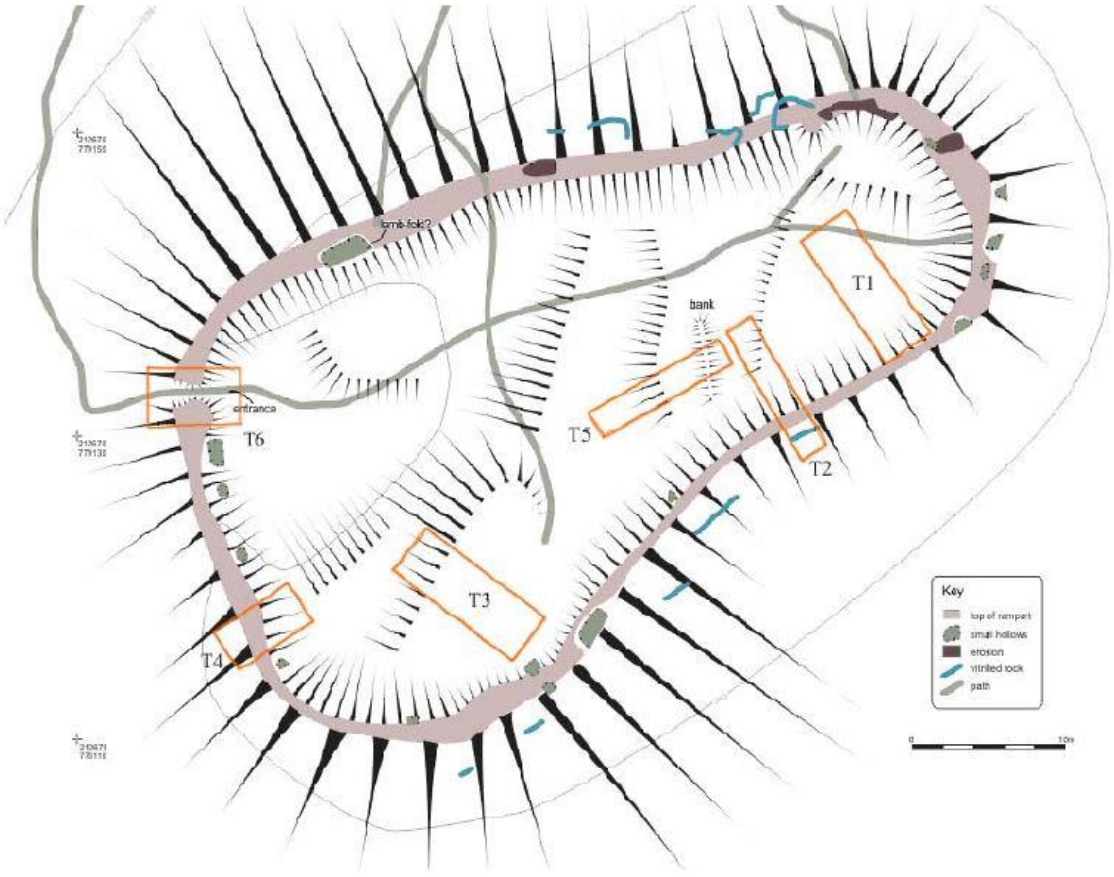

Figure 10: Trench locations for Dun Deardail excavations 2015-2017. (AOC Archaeology Group, 2015).

2.2 Other sites

Eight other hillforts (Figure 6, page 23 and Figure 11) were chosen to allow information to be gained from contrasting sites with differences in geology and location and allowing for a broader spread to cover north to south and east to west. Seven of these sites were not excavated during the research. The Knock was excavated during the research period, and Craig Phadrig was excavated in 2015 by AOC.

Figure 11:Sites and information regarding their vitrification status and whether excavated or not

Craig Phadrig (Figure 6, page 23, site 4) has been included as a secondary excavated site. There is a considerable contrast in excavation history between Dun Deardail and Craig Phadrig. Craig Phadrig has had several, well-documented excavations and surveys since its discovery.

A secondary burnt but not vitrified site, The Knock in Largs, Ayrshire, (Figure 6, page 23, site 8) has also been included here to determine the difference that geology makes on the process of vitrification.

As shown in Figure 6, page 23 and Figure 11, six further secondary vitrified sites will also be compared with the excavated sites above: Knockfarrel, Ord Hill, Tor Dhuin, The Torr Sheilfoot, Dunagoil and Auldhill Portencross. Each of these sites was not excavated as part of this project. However, these sites were visited and analysed in-situ using visual and portable XRF analysis

As well as comparing the hillforts included as a group, the hillforts will be compared in smaller geographical groups broken down to Ayrshire (The Knock, Dunagoil and Auldhill Portencross), Inverness shire (Knockfarrel, Craig Phadrig and Ord Hill) and Fort William and Ardnamurchan peninsula (Dun Deardail, Tor Dhuin and The Torr Shielfoot).

2.2.1 Craig Phadrig

Figure 12: Oblique aerial view of Craig Phadrig (Canmore).

Craig Phadrig, Figure 12 (NH64004527) is a partial bivallate, partial multivallate, timberlaced, vitrified, subrectangular contour hillfort just outside Inverness (Figure 13). The site consists of an oval-shaped fort, angled north-west to south-east (Figure 14). The inner rampart consists of a massive vitrified structure. An outer rampart surrounds this inner rampart structure, and this is terraced down onto the slopes below. The total enclosed area is 0.6ha with internal dimensions of 72m northeast to southwest by 22m

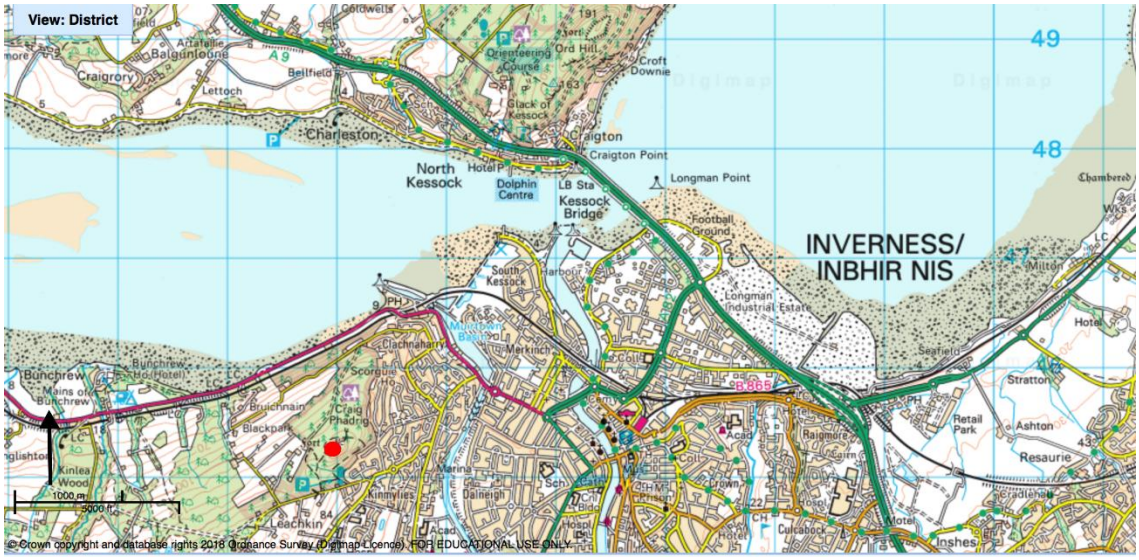

Figure 13:Location of Craig Phadrig in relation to Inverness (OS mapping downloaded from Edina Digimap).

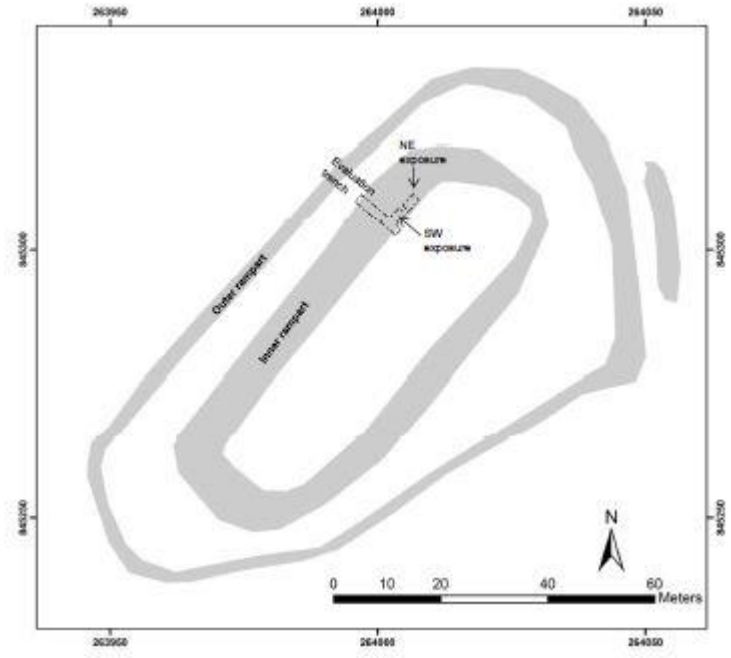

Figure 14: Craig Phadrig trench locations (Peteranna and Birch, 2015).

Craig Phadrig is sited in an area dominated by sedimentary rocks (Figure 15). It is sited on the Kilmuir conglomerate Formation, formed between 383 and 393 million years ago (BGS NERC, 2018), and is found within a repeating sequence of sandstone and conglomerate. Pelite deposits exist around 4km to the west of the site.

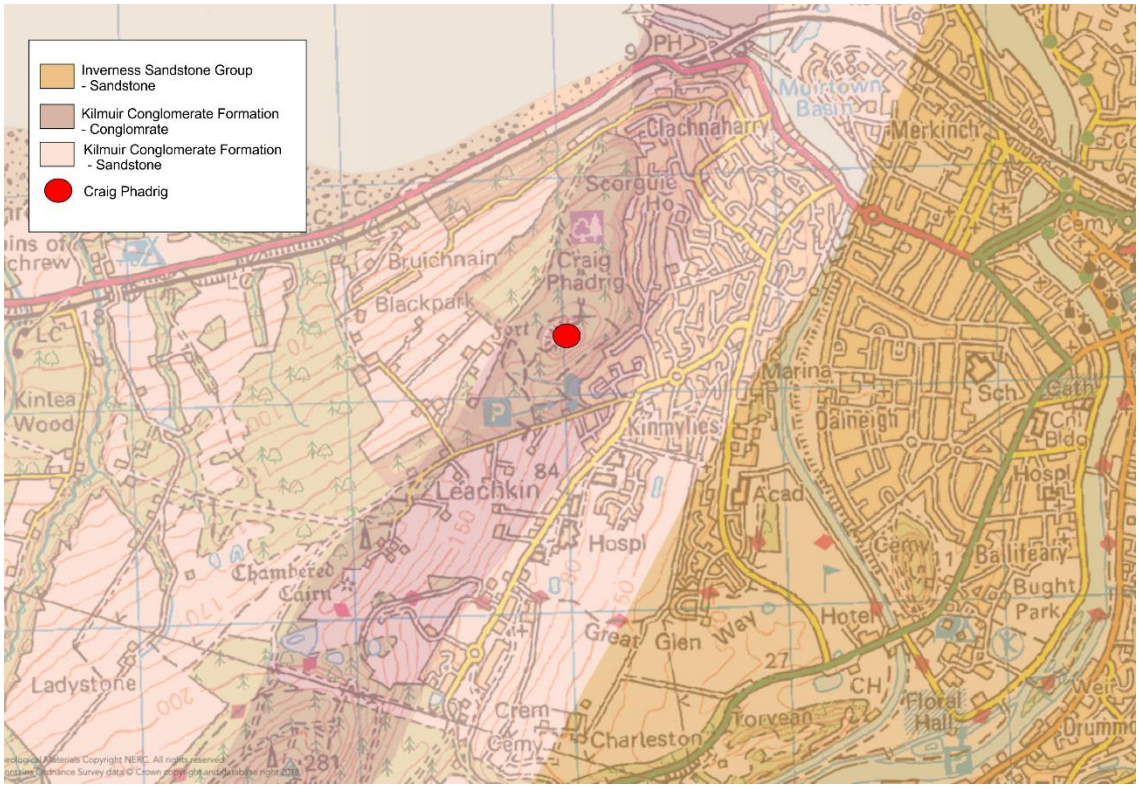

Figure 15:Geology of Craig Phadrig and surrounding area (BGS NERC, 2018)

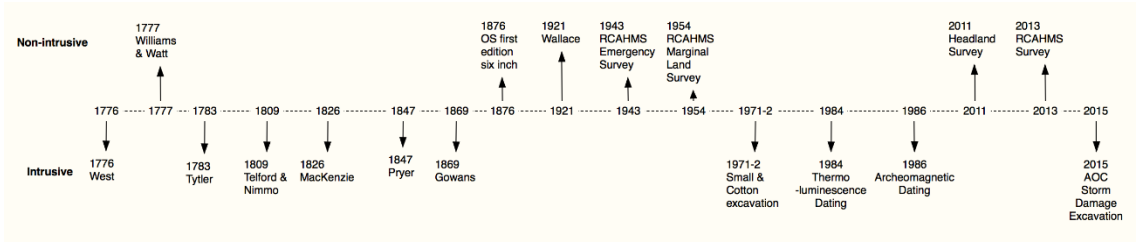

Figure 16:Previous excavations and examinations of Craig Phadrig.

The first excavation was carried out in 1776 and, as shown in Figure 16, several other excavations were carried out over time until the 2015 emergency excavation carried out by AOC in 2015. In addition, a number of other non-intrusive surveys were carried out, with the majority of these being carried out Ordinance Survey map surveys.

2.2.2 Knockfarrel

Several spellings are used throughout the literature for Knockfarrel, and so it has been decided to follow the OS mapping version for clarity. Knockfarrel (NH50485852), between Dingwall and Strathpeffer (Figure 17) is a lozenge-shaped, stone walled, contour vitrified hillfort.

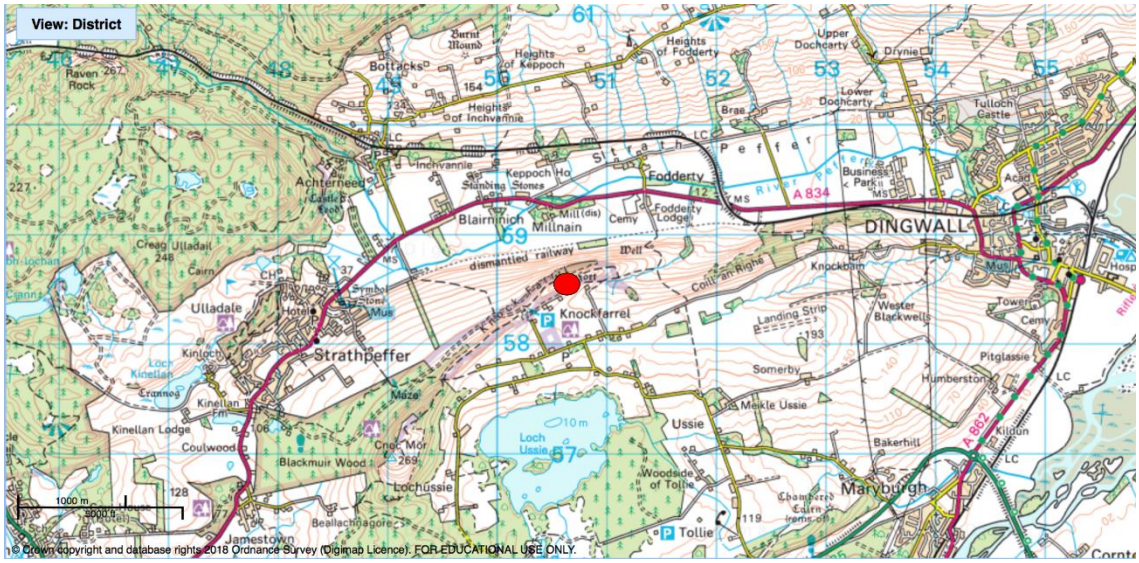

Figure 17:OS map of Knockfarrel location (OS mapping downloaded from Edina Digimap).

Knockfarrel stands on the Cnoc Fyrish Conglomerate Formation, formed approximately 389 to 393 million years ago. The hillfort is adjacent to the Braemore Mudstone Formation, formed approximately 393 to 408 million years ago (BGS NERC, 2018) ().

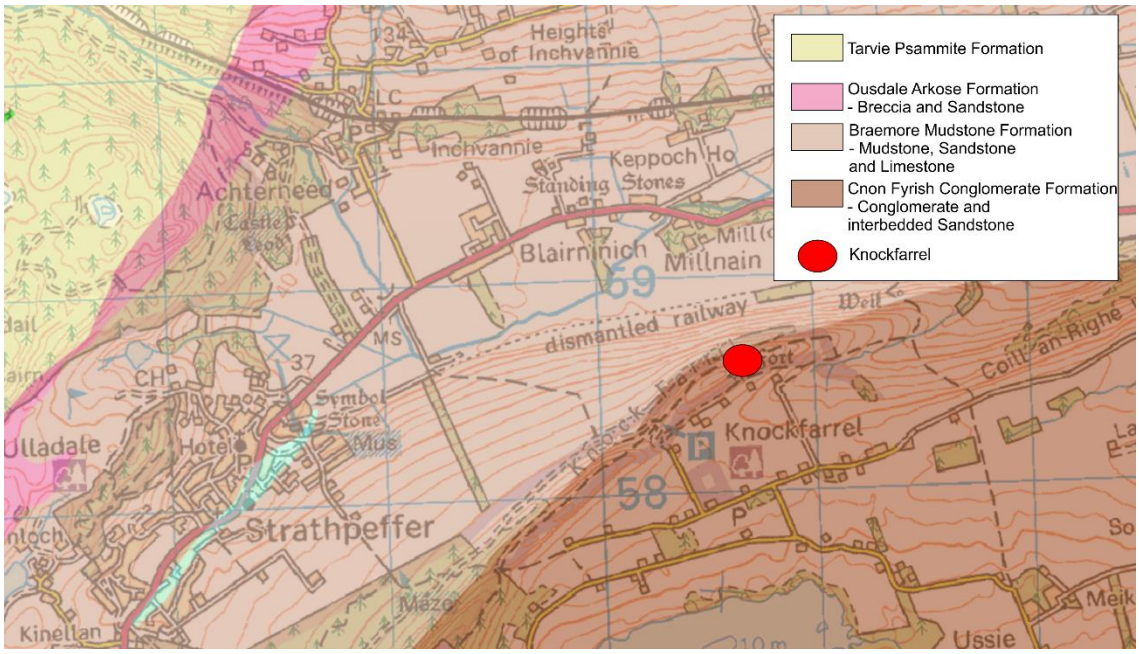

Figure 18:Geology of Knockfarrel and surrounding area (BGS NERC, 2018)

The first mention of Knockfarrel was a description of the hillfort by John Williams in 1777 (Williams, 1777). A depiction on the 1st edition OS map of the area followed in 1873. Following on from these early notes of the hillfort's existence, two earthworks surveys were carried out. The first survey was carried out by Fraser in 1905 and the

second by Wallace in 1819 (Fraser, 1906; Wallace, 1918). In 1965, and also in 1970, the OS resurveyed the area for the 1:2500 map and, following on from the 1965 survey; the hillfort was scheduled in 1969. The rampart was cored for thermoluminescence dating (TL dating) in 1985 by David Sanderson (Sanderson and Placido, 1985). This led to TL dates being published, however, as of yet, there has been no carbon dating performed on the hillfort. An earthworks survey, including a plan and a description, was completed by Headland Archaeology in 2011 on behalf of the Forestry Commission for Scotland (Headland Archaeology, 2011b). One of the things that makes this hillfort stand out is that it has wingwalls running at either end of the hillfort for 50m. This would have made the fort look bigger than it really was for those passing by. The total enclosed area of the hillfort is 0.3ha with the interior being 118m from northeast to southwest by 30m transversely. Walls on the rampart were 3m whereas the height of the wingwalls was measured at 7m on the southwest. An earlier wall was identified on the east flank of the fort, however no sign on vitrification on this earlier wall (Lock, G. & Ralston, 2017).

2.2.3 Ord Hill

Ord Hill (NH66404910) is an irregularly shaped, partial univallate, partial bivallate contour hillfort, with a stone wall construction with unconfirmed reports of vitrification, in a hilltop location overlooking Inverness (Figure 19).

Figure 19: Location of Ord Hill, 1 and Craig Phadrig, 2, for comparison (OS mapping downloaded from Edina Digimap).

As with Craig Phadrig, Ord Hill has been built on the Kilmuir Conglomerate Formation (Figure 20) and so, as vitrification was not observed during a recent site visit, this makes it an excellent comparison site for Craig Phadrig.

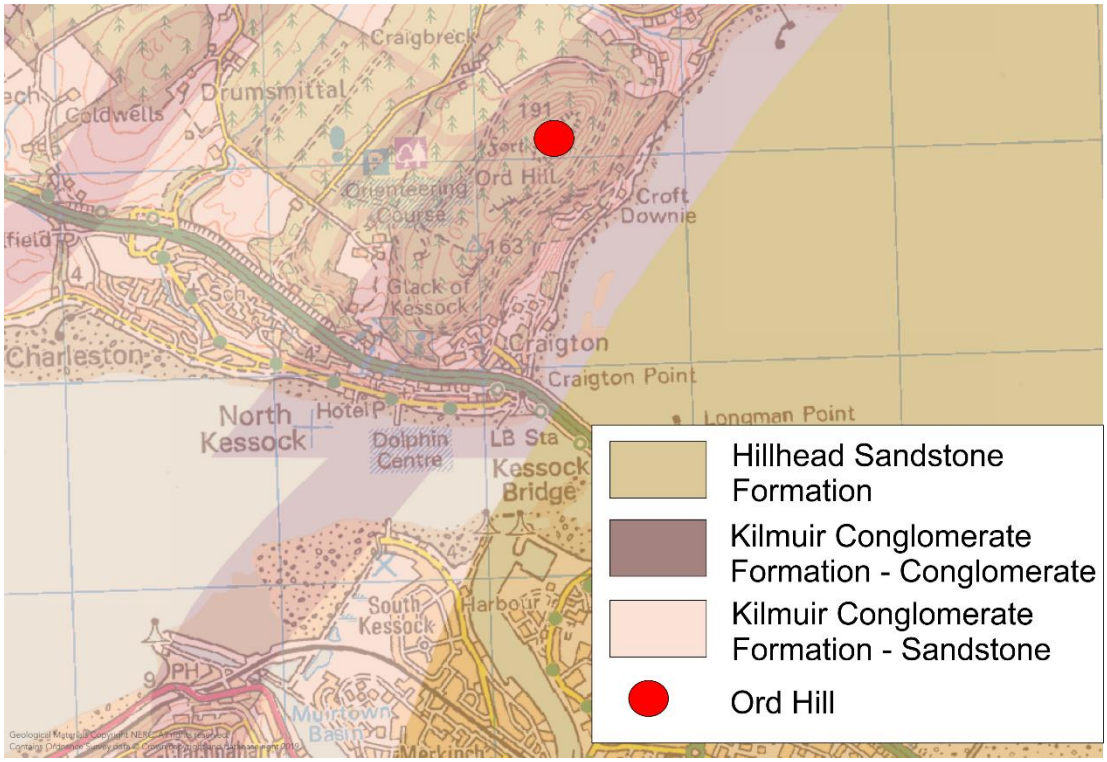

Figure 20:Geology of Ord Hill and the surrounding area (BGS NERC, 2018)

The hillfort was first identified, and noted, in 1824 (MacKenzie, 1857). The first map depiction by the OS followed in 1872. An earthwork survey was carried out as part of area surveys in 1819 (Wallace, 1918). The hillfort was described in 1955 during a survey of prehistoric monuments of the Black Isle, Inverness-shire (Woodham, 1955). An earthworks survey, including a sketch plan, was carried out by RCAHMS in 1957. The hillfort was scheduled in 1965. An earthworks survey, at 1;2500, was carried out by the OS in 1970. In 1974 the site was visited by the OS and then visited by RCAHMS in 1978. The hillfort was rescheduled in 1993. Highland HER visited and photographed the site in 2002. A plan, description and earthwork survey of the site was carried out by Headland Archaeology in 2011. A visit by myself and Strat Halliday in 2015 revealed no sign of vitrification on the site (Lock, G. & Ralston, 2017). The hillfort has an enclosed area of 1.6ha with dimensions of 265m from northeast to south-west by a maximum of 110m transversely. The walls of the rubble core reach a maximum thickness of 6m.

2.2.4 The Torr

The Torr, Shielfoot (NM66227018) is a partial univallate, partial bivallate, stone walled, heavily vitrified contour hillfort situated on a hilltop, ridge position, located on the Ardnamurchan peninsula (Figure 21).

Figure 21:Location of The Torr, Sheilfoot. (OS mapping downloaded from Edina Digimap).

The Torr was built on the Morar Schists formation, consisting of semipelite and psammite, formed approximately 541 to 1000 million years ago. The plane to the west of the hillfort is formed from the Lower Morar Psammite Formation, formed 541 to 1000 million years ago (Figure 22, BGS NERC, 2018).

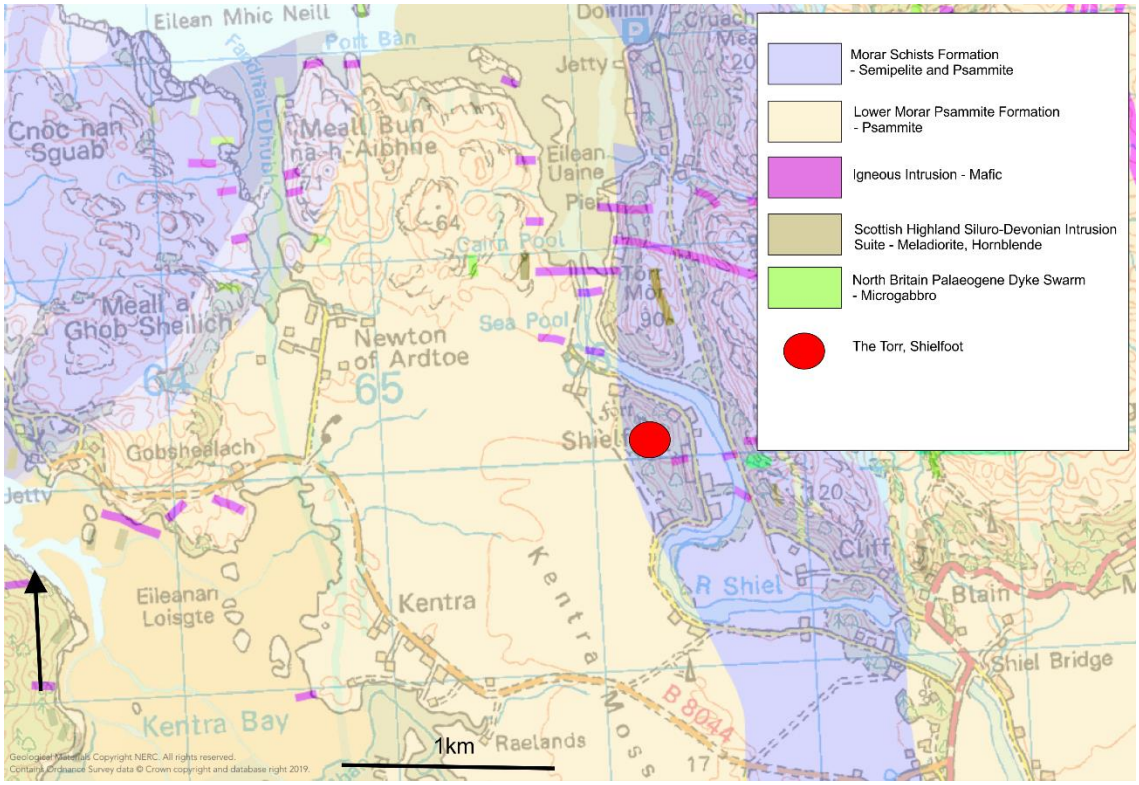

Figure 22:Geology of The Torr and the surrounding area (BGS NERC, 2018)

The hillfort has an enclosed area of 0.12ha with the main enclosure being 90m north-west to south-east by 17m wide at the south-east end, tapering to 4m at the north-west end. The inner vitrified core stands at 2.7m high, whereas the outside core shows no sign of vitrification. A small dun, around 7.5m in diameter, is located at the northeast end of the hillfort. There is also a small outer annexe to the south-east end of the hillfort. A possible entrance opened onto a sloping terrace with probable access being up to the south-west flank of the ridge. The heavily forested site has been photographed from the air, by RCAHMS Aerial Survey in 1978, 2009 and 2011(Lock, G. & Ralston, 2017).

2.2.5 Torr Dhuin

Torr Dhuin (NH348069) is a partial bivallate, partial multivallate, vitrified contour situated on a knoll 3.5km south-west of Fort Augustus, Figure 23.

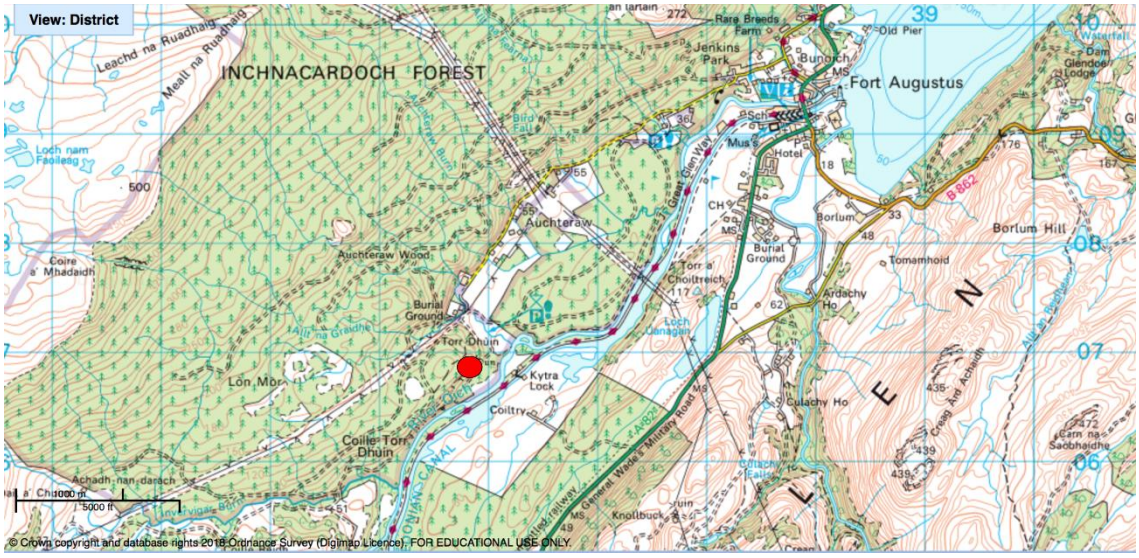

Figure 23:Location of Tor Dhuin. (OS mapping downloaded from Edina Digimap).

Torr Dhuin sits on a metamorphised igneous intrusion consisting of amphibolite and quartz-xenolithic, formed approximately 419 to 4000 million years ago. This intrusion is surrounded by the West Highland Gneiss Intrusion, consisting of granite and gneissose, formed 541 to 1000 million years ago (Figure 24, (BGS NERC, 2018).

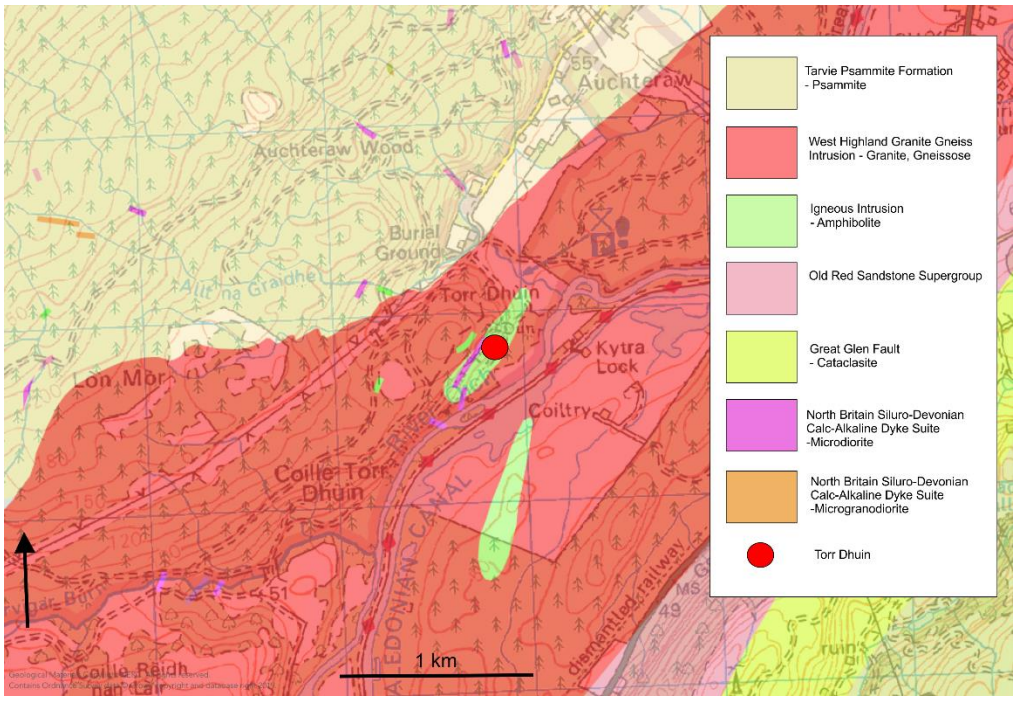

Figure 24:Geology of Torr Dhuin and the surrounding area (BGS NERC, 2018).

Torr Dhuin was first identified as a hillfort by Thomas Pennant in 1772 (Pennant, 1772) and mapped by the OS in 1871. Ross described it in 1915 (Ross, 1915). An earthwork survey and recording was carried out by Wallace in 1921 (Wallace, 1921). RCAHMS

described the site in 1957 which led to its scheduling in 1969. The OS undertook several surveys in 1970, 1974 and 1979 leading to the revised listing on the OS map (Lock & Ralston, 2017). The fort was subject to an archaeological survey in 2010 by Headland Archaeology (Headland Archaeology, 2011a). The site consists of three roughly concentric lines of defence, where the inner encloses the knoll summit. The inner wall, which may be the youngest of the three structures, consists of a heavily vitrified wall, best preserved in the north and west flanks, which has been reduced to rubble and is more than 3.5m in thickness. The middle rampart extends around the shoulder of the summit area. The site has a total enclosed area of 0.1ha consisting of 10m north-north-east by south-south-west by 10m transversely for the inner structure to 38m by 18m for the outer rampart wall, which extends around the foot of the knoll on the north-west and south. Walls vary in thickness from 1.7m up to 3.0m in the south (Lock & Ralston, 2017).

2.2.6 Dunagoil

Dunagoil, Figure 25, (NS08475312) is a partial univallate, stonewalled vitrified hillfort which uses a cliff edge as one of its defensive sides. The hillfort has a total enclosed area of 0.2ha, with interior measurements o 85m east-southeast to west-southwest by up to 20m transversely, with a wall thickness of up to 3.6m and massive vitrification of its core on the south-southwest side (Lock & Ralston, 2017).

The site sits on the Clyde Plateau Volcanic Formation, 331 to 347 million years old, and the Kinnesswood Formation 347 to 383 million years old (Figure 25).

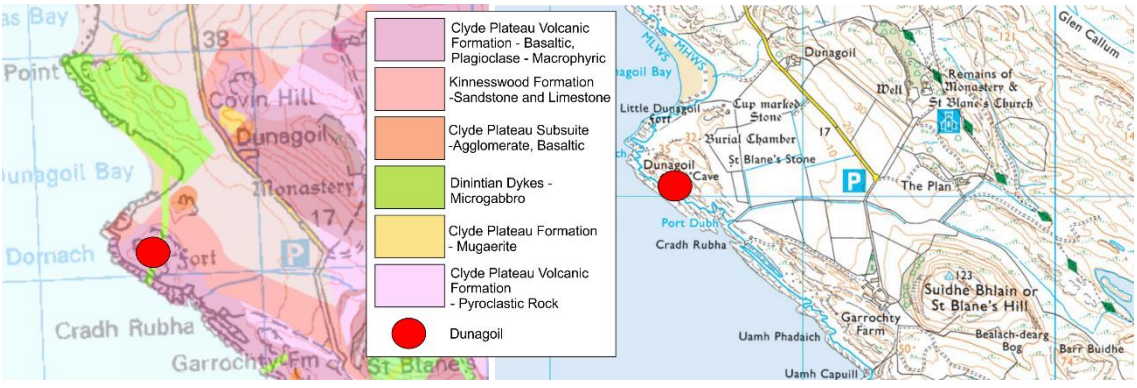

Figure 25:Geological and OS maps of Dunigoil and surrounding area.

Dunagoil and its neighbour Little Dunagoil were first surveyed on an estate map of 1780, and the forts were depicted in 1863 on the first edition OS 25-inch map, Argyle

and Bute 1869, sheet 227 and noted by Ross in 1880 (Ross, 1880). The hillforts were then described, in detail, by the Reverent JK Hewison (Hewison, 1893). Marshall and Mann carried out the first excavations in 1914, 1915 and 1919 (Mann, 1915, 1925; Marshall, 1915). An emergency survey and description was carried out by RCAHMS in 1943, followed by photographic evidence taken by Nisbet in 1958 (Nisbet, 1975). Following this, the site was first scheduled in 1953. Kenneth Steer visited the site in 1975 and 1976 as part of the updating of the OS survey map. Two seasons of excavations were carried out in the site area by Harding, Ralston and Burgress and this led to the belief that the site was more extensive than first believed (Harding et al.,1995; Harding, 1997).An RCAHMS survey of 2009-2010 suggested that this larger site was from later agricultural landscape usage and not from the time that Dunagoil was first occupied (Geddes and Hale, 2010). The hillfort was then rescheduled in 1993 (Lock and Ralston, 2017).

2.2.7 Auldhill – Portencross

Auldhill hillfort, Figure 26, (NS17834910), is a univallate contour vitrified hillfort in a hilltop location. The hillfort has an internal area of 0.3ha and has internal dimensions of 110m from northwest to southeast by up to 28m transversely. The core consists of both vitrified and burnt stone material, and this core appears to be around 3m in thickness in both areas (Lock and Ralston, 2017).

The hillfort sits on the Portencross Sandstone Formation, 393 to 419 million years old, and is cut by the Central Scotland Late Carboniferous Tholeiitic Dyke Swarm, 299 to 331 million years old (Figure 26).

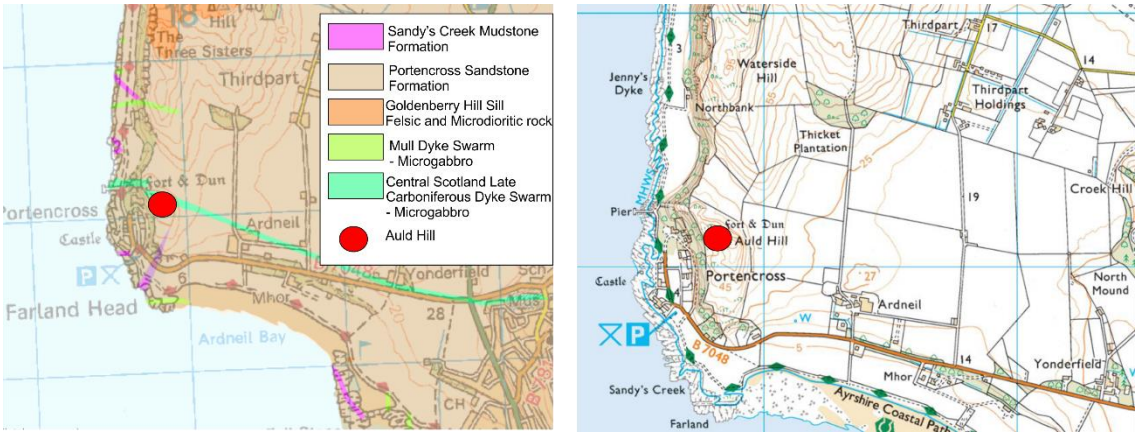

Figure 26:Geological and OS maps for Auld Hill.

Auldhill is a multigenerational site excavated by Caldwell et al., (1998) over ten weeks between 1987 and 1989. Excavation has shown that this vitrified hillfort was timberlaced in construction, and thermoluminescent dating has given an age of 3.3ka ±10% (Strickertsson et al., 1988). However, it is likely that the actual date of vitrification is later than this and probably Early Iron Age. The Auldhill site was first surveyed in 1855, but the hillfort was missed entirely, and only the later Motte and Bailey and stone castles were noted. The hillfort was first noted in 1862 by William Keddie where Keddie noted the remaining vitrification (Keddie, 1868). In 1943 Childe and Graham surveyed the site as part of the wartime emergency survey programme (Childe and Graham, 1943) which was followed by a visit from RCAHAMS in 1952 and a resurvey visit by the OS to revise the 1:2500 map in 1968 and 1972.

2.2.8 The Knock

Figure 27: Oblique aerial view of The Knock ramparts facing south east (https://canmore.org.uk/collection/1015448)

The Knock (NS20286286), Figure 27 and Figure 28, is a partial univallate hilltop contour hillfort with 2 ditches present, situated 3km north of Largs in North Ayrshire. The hillfort is oval in plan with an enclosed area of 0.9ha, with the internal space being 50m from north to south, 29m transversely with heights ranging from 0.9m high internally to 1.8-2.4m externally.

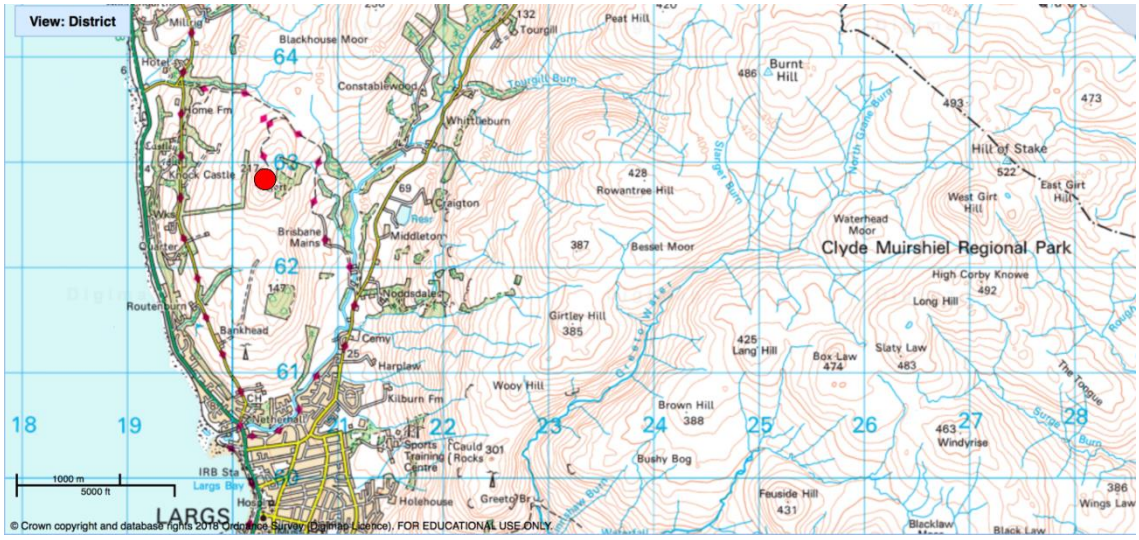

Figure 28:Location of the Knock, 2km north of Largs. OS map extracted from Digimap).

The knock sits directly on the Clyde Plateau Substrate consisting of Basalt, Plagioclase-Olivine-Clinopyroxene-Macrophytic. This is surrounded by basaltic pyroclastic rock. Surrounding this is The Kelly Burn Sandstone Formation. Several dykes cut through the area, consisting of felsite, basalt and microgabbro and olivine-basalt. Within 2km, there is also olivine-macrophyric basalt, tuff and agglomerate and microporphyritic basalt (Figure 29, BGS NERC, 2018).

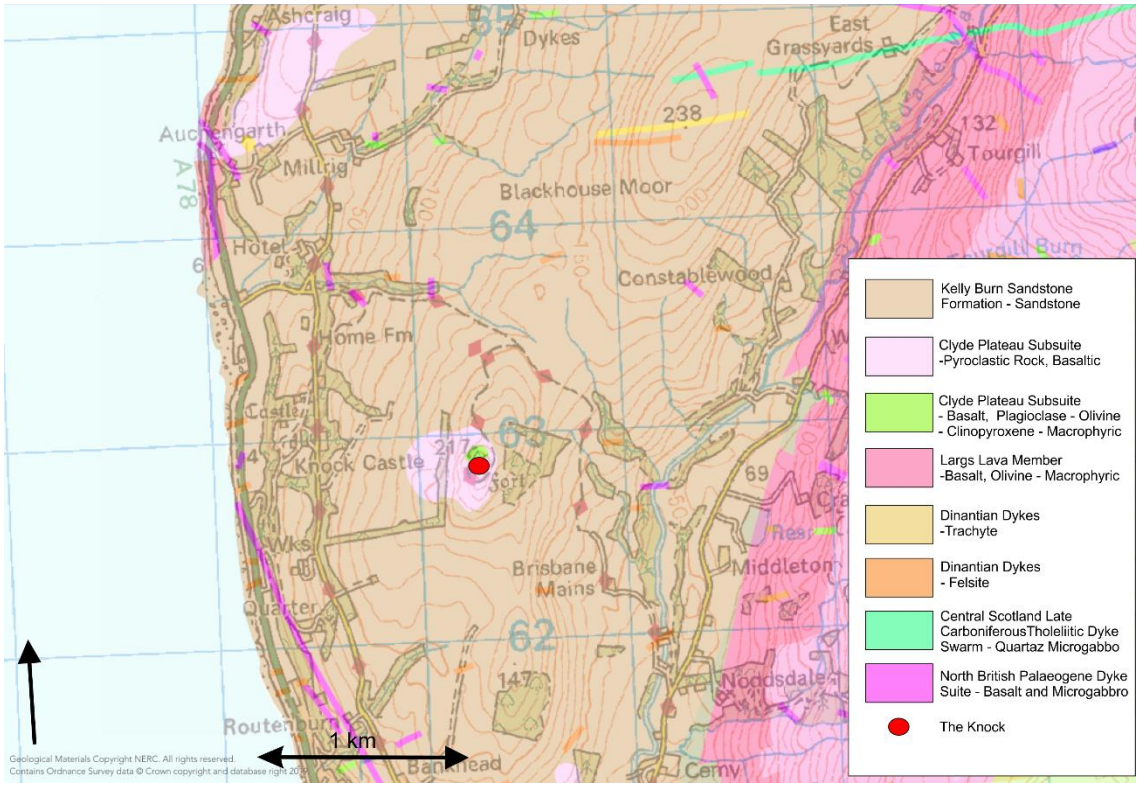

Figure 29:Geology of The Knock and surrounding area (BGS NERC, 2018).

As documented in, The Knock was first depicted in 1855 in the first edition of the 25-inch OS map, Ayrshire, 1857, sheet 3.4. David Christion noted the hillfort in 1893 and a little later by John Smith (Christison, 1893; Smith, 1895). In 1942 Childe and Graham carried out an emergency survey for RCAHMS (Childe and Graham, 1943) followed by another in 1952. In 1956 the OS published a revised plan at 1:2500 and then revisited in 1983. This led to The Knock being scheduled in 1961. RCAHMS undertook detailed aerial photographs in both 1983 and 2005 (Lock and Ralston, 2017). As part of this research, the hillfort was first excavated in 2016 by Lang from the University of York, where one trench was excavated over the period of one week (Lang, 2016).

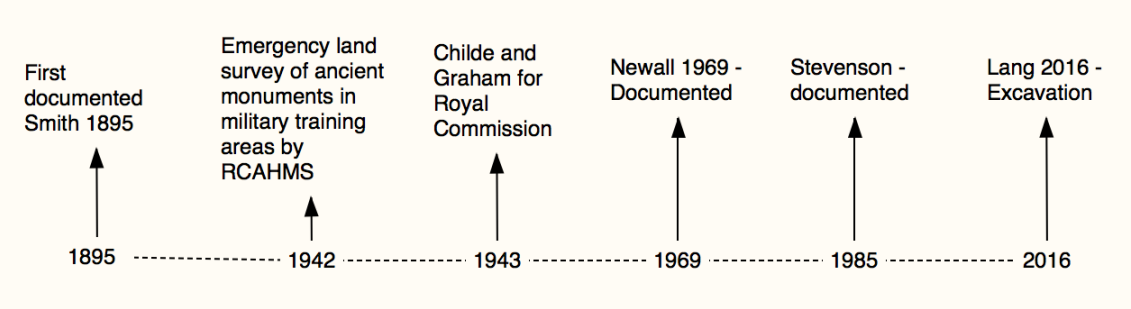

Figure 30:Excavation history of The Knock, Ayrshire.

2.3 Sampling strategy and rationale

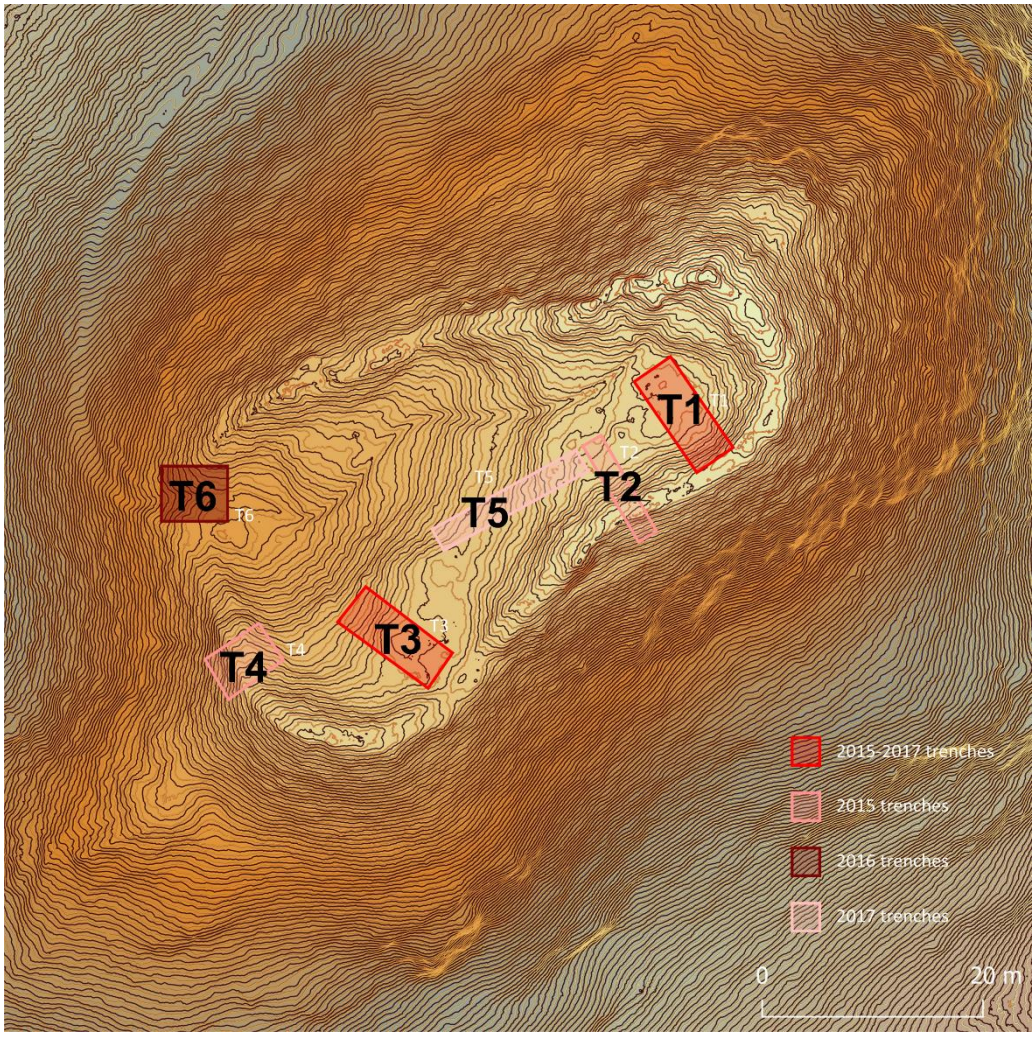

Figure 31: Excavated trenches at Dun Deardail, where samples were collected over three seasons (copyright FCS by Skyscape survey)

Three seasons of fieldwork at Dun Deardail, running from 2015 until 2017, were carried out by AOC Archaeology Group (AOC). Samples of the rubble core and soil were collected from the open trenches (Figure 31), with each sample being given a project number, context number, find number and material code. Rock samples collected included burnt rock, vitrified rock clusters and unvitrified rock. Soils represented areas that were burned and unburned, and each was sampled from a secure context. Samples were removed from the hillside each night and, at the end of the excavation period, moved to the AOC office in Loanhead, Edinburgh. Once at the University of Stirling, the vitrified and burnt rock samples were given a unique rock reference, as detailed in Table 2 and Table 3.

Table 2:Vitrified samples excavated over all trenches over seasons one and two

Trench 1

Sample number	AOC number	context number
DDV1	1021	1009
DDV2	1022	1005
DDV3	1022	1005
DDV4	1022	1005
DDV5	1022	1005
DDV6	1011	1009
DDV7	1009	1012
DDV8	110	101
DDV9	111	100
DDV10	112	100
DDV11	113	100
DDV12	114	100
DDV13	115	100
DDV14	116	100
DDV15	117	100
DDV16	118	100
DDV17	119	100
DDV18	120	100

Trench 2

Sample number	AOC number	context number
DDV19	SF217	205
DDV20	SF218	205
DDV21	SF219	205
DDV22	SF220	205
DDV23	SF221	205
DDV24	SF222	205
DDV25	SF223	205
DDV26	SF224	205
DDV27	SF225	205
DDV28	SF226	205
DDV29	SF227	205
DDV30	SF228	205
DDV31	SF229	205
DDV32	204	201
DDV33	205	201
DDV34	206	201
DDV35	207	201
DDV36	208	201
DDV37	209	201
DDV38	210	201
DDV39	211	201
DDV40	212	201
DDV41	213	201
DDV42	214	201
DDV43	215	201
DDV44	216	201
DDV45	230	205
DDV46	231	205

Trench 3

Sample number	AOC number	context number
DDV47	3011	3008
DDV48	3020	3016
DDV49	317	300

Trench 4

Sample number	AOC number	context number
DDV50	SF410A	401
DDV51	SF410B	401
DDV52	SF410C	401
DDV53	SF410D	401
DDV54	SF410E	401
DDV55	SF410F	401
DDV56	SF410G	401
DDV57	SF410H	401
DDV58	SF410I	401
DDV59	SF410J	401
DDV60	SF410K	401
DDV61	SF410L	401
DDV62	400	400
DDV63	404	401
DDV64	405	401
DDV65	406	401
DDV66	407	401
DDV67	408	401
DDV68	409	401
DDV69	411	401
DDV70	412	401
DDV71	413	401
DDV72	414	401
DDV73	415	401
DDV74	416	401
DDV75	417	401
DDV76	418	401
DDV77	419	401
DDV78	420	401
DDV79	421	401
DDV80	422	401
DDV81	423	401
DDV82	424	401

Trench 6

Sample number	AOC number	context number
DDV83	601	601
DDV84	602	601
DDV85	603	601
DDV86	604	601
DDV87	605	601
DDV88	606	601
DDV89	607	601
DDV90	608	601
DDV91	609	601
DDV92	610	601
DDV93	611	601
DDV94	612	601
DDV95	613	601
DDV96	614	601
DDV97	615	601
DDV98	616	601
DDV99	617	601
DDV100	618	601
DDV101	619	601
DDV102	620	601
DDV103	621	601
DDV104	622	601
DDV105	623	601
DDV106	624	601
DDV107	625	601
DDV108	626	601
DDV109	627	601
DDV110	629	601
DDV111	630	601
DDV112	631	602
DDV113	632	602
DDV114	633	602
DDV115	634	602
DDV116	635	602
DDV117	636	602
DDV118	637	602
DDV119	638	602
DDV120	639	602
DDV121	640	602
DDV122	641	602
DDV123	642	602
DDV124	643	602
DDV125	645	602
DDV126	647	602
DDV127	648	602
DDV128	649	602
DDV129	651	604
DDV130	652	604
DDV131	653	602
DDV132	654	601
DDV133	655	601
DDV134	667	602

Table 3:Burnt samples analysed from Dun Deardail year two excavation

Sample number	Trench number	AOC number	Context number
B1	1	1008	1009
B2	1	1005	1020
B3	1	1004	1009
B4	1	1019	1009
B5	1	1009	1009
B6	1	1018	1010
B7	1	1017	1010
B8	3	3019	3016

Sample number	Trench number	AOC number	Context number
B9	6	668	604
B10	6	661	601
B11	6	625	601
B12	6	646	604
B13	6	657	604
B14	6	658	601
B15	6	662	601
B16	6	663	601
B17	6	664	601
B18	6	665	601
B19	6	666	601
B20	6	670	604
B21	6	671	601

Forty local rock samples of each of the different rock types were sampled from outside of the scheduled area during seasons two and three. These rocks types were sampled from a radius of 3km from the site. These samples were recorded and given unique sample numbers and the 8 figure Ordinance Survey (OS) grid reference taken for the location of the sampling recorded (Figure 32). These samples were taken back to the University of Stirling (UoS) for storage.

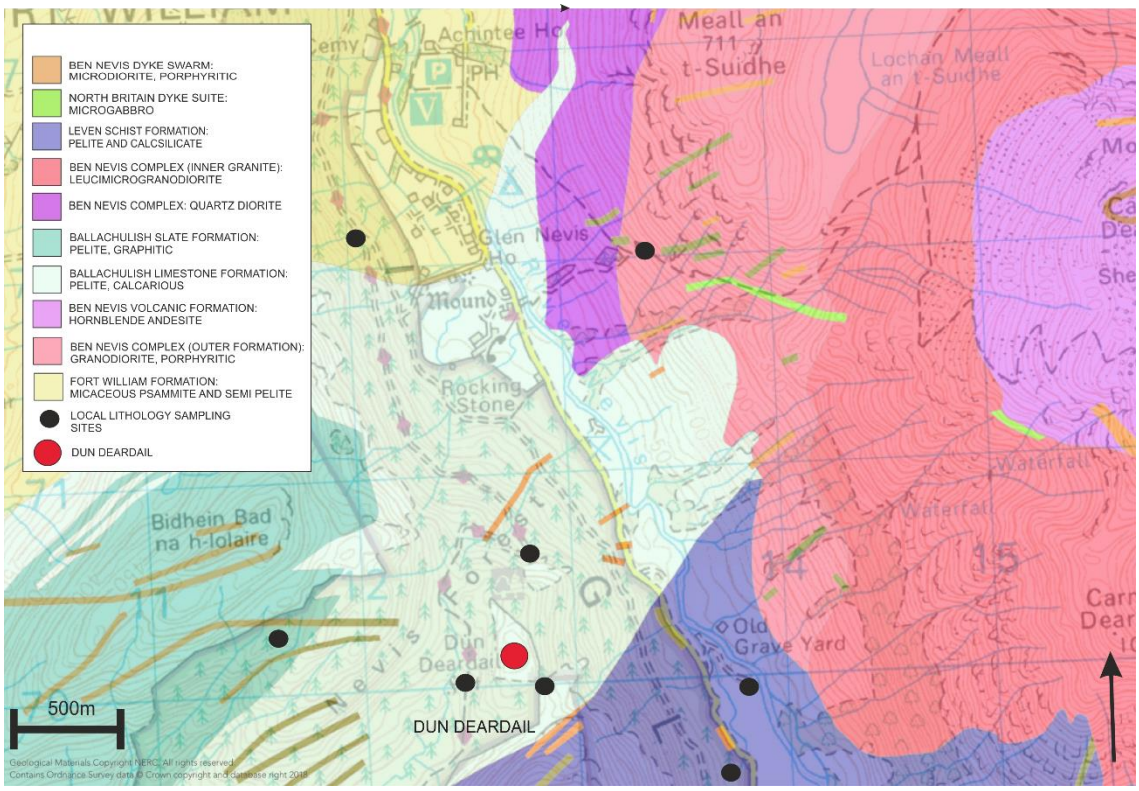

Figure 32: Dun Deardail local rock sampling locations (BGS NERC, 2018).

Table 4:Dun Deardail lithology and quantity of local rock sampled

Lithology (as shown in geological map)	Quantity
Pelite, calcitic	40
Pelite, graphitic	40
Pelite and psammite, micaeous	40
Calcsilicate	40
Granite	40

An emergency excavation of Craig Phadrig was carried out in early 2014 by AOC Archaeology Group (AOC). Samples of the rubble core were collected from the open trench (Figure 33), with each sample being given a project number, context number, find number and material code. Rock samples collected included burnt rock and vitrified rock clusters and untouched rock (Table 5). Samples were removed from the hillside each night and, at the end of the excavation period, moved to the AOC office in Loanhead, Edinburgh.

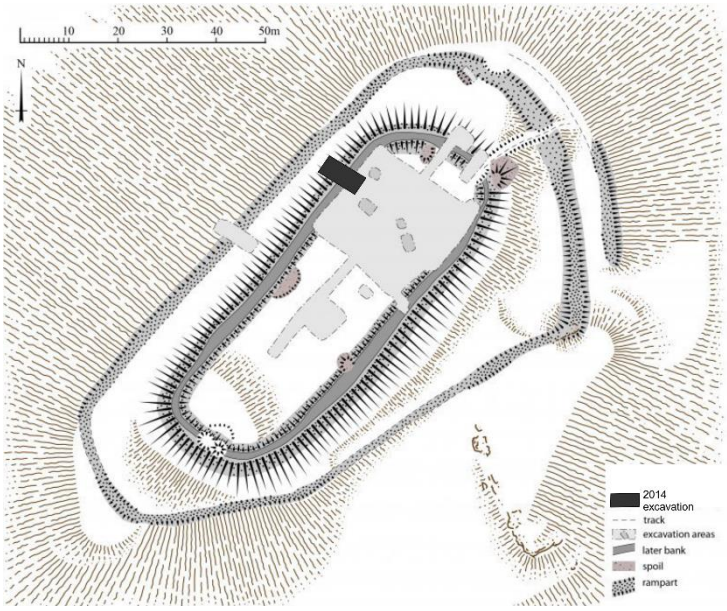

Figure 33:Plan of Craig Phadrig and location of the 2015 rescue excavation by AOC (Canmore)

Table 5: Excavated and local Craig Phadrig rock samples.

a) Craig Phadrig excavated samples

sample ref	Grid ref or AOC number	sample ref	Grid ref or AOC number	sample ref	Grid ref or AOC number	sample ref	Grid ref or AOC number
CP1	NH64054528	CP7	NH64054528	CP13	70011-6	CP19	70011-12
CP2	NH64054528	CP8	70011-1	CP14	70011-7	CP20	70011-13
CP3	NH64054528	CP9	70011-2	CP15	70011-8	CP21	70011-14
CP4	NH64054528	CP10	70011-3	CP16	70011-9	CP22	70011-15
CP5	NH64054528	CP11	70011-4	CP17	70011-10	CP23	70011-16
CP6	NH64054528	CP12	70011-5	CP18	70011-11	CP24	70011-17

b) Craig Phadrig local samples

Sample	Lithology	number
Kilmuir Conglomerate formation	Conglomerate	15
	Sandstone	15

Local rock was sampled from exposures outside of the scheduled area (Table 5). These rocks were chosen to represent the rock types found in the hillfort structure and excavated clasts. These samples were given unique sample numbers and stored in the University of Stirling.

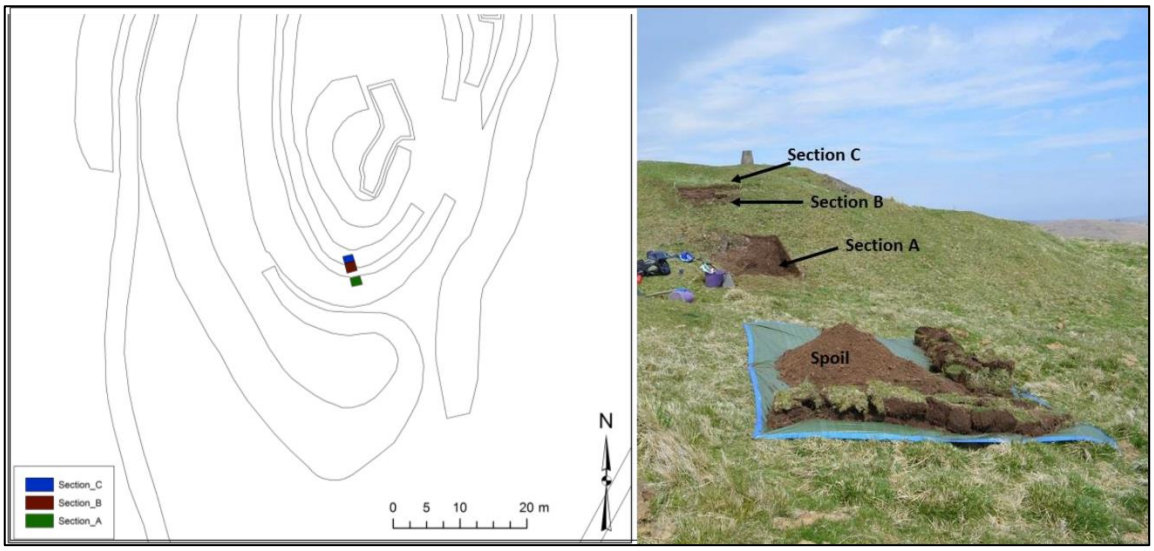

Figure 34: Location of excavation areas of The Knock (adapted from Lang, 2016).

The Knock was excavated by Lang, (2016) in May 2016. One week of excavation was carried out and three sections of the southern rampart were investigated (Figure 34). Burnt sandstone rocks and local rock from outside of the scheduled area were collected for laboratory analysis (Table 6). These samples were given original sample names and stored at the University of Stirling.

Table 6: Excavated and local samples for The Knock.

Excavated samples					
Sample number	Section number	Sample number	Section number	Sample number	Section number
KH01	1	KH11	2	KH21	3
KH02	1	KH12	2	KH22	3
KH03	1	KH13	2	KH23	3
KH04	1	KH14	2	KH24	3
KH05	1	KH15	2	KH25	3
KH06	1	KH16	2	KH26	3
KH07	1	KH17	2	KH27	3
KH08	1	KH18	2	KH28	3
KH09	1	KH19	2	KH29	3
KH10	1	KH20	2	KH30	3

Local rock samples							
Sample number	Grid ref	Sample number	Grid ref	Sample number	Grid ref	Sample number	Grid ref
KHSS1	NS20516269	KHSS11	NS20516269	KHSS21	NS20296275	KHSS31	NS20296275
KHSS2	NS20516269	KHSS12	NS20516269	KHSS22	NS20296275	KHSS32	NS20296275
KHSS3	NS20516269	KHSS13	NS20516269	KHSS23	NS20296275	KHSS33	NS20296275
KHSS4	NS20516269	KHSS14	NS20516269	KHSS24	NS20296275	KHSS34	NS20296275
KHSS5	NS20516269	KHSS15	NS20516269	KHSS25	NS20296275	KHSS35	NS20296275
KHSS6	NS20516269	KHSS16	NS20516269	KHSS26	NS20296275	KHSS36	NS20296275
KHSS7	NS20516269	KHSS17	NS20516269	KHSS27	NS20296275	KHSS37	NS20296275
KHSS8	NS20516269	KHSS18	NS20516269	KHSS28	NS20296275	KHSS38	NS20296275
KHSS9	NS20516269	KHSS19	NS20516269	KHSS29	NS20296275	KHSS39	NS20296275
KHSS10	NS20516269	KHSS20	NS20516269	KHSS30	NS20296275	KHSS40	NS20296275

Samples from Knockfarrel and The Torr were kindly donated for sampling and are shown below in Table 7.

Table 7: Vitrified rock samples from a) Knockfarrel and b) The Torr.

a) Knockfarrel samples	
Sample ref	**Grid ref**
KF1	NH5050658 521
KF2	NH5050658 521

b) The Torr samples				
Sample ref	**Grid ref**		**Sample ref**	**Grid ref**
T1	NM662187 0178		T4	NM663567 0180
T2	NM662187 0178		T5	NM662187 0178
T3	NM662187 0178		T6	NM662187 0178
T4	NM663567 0180		T7	NM662497 0166

3 Analytical methods

The analytical methods described here are the protocols developed to carry out the experimental melts and the analytical techniques used to obtain the analytical data.

3.1 Experimental melts

Youngblood et al., (1978) suggested that further experimental trace element geochemical work should be carried out on surface glass compared to interstitial melts. They supposed that experimental determination of melt temperature of representative glasses and study of partial melting of source rocks at different temperatures would be beneficial for the study of the melting processes in vitrified hillfort studies. And so, following on from that this chapter will conduct laboratory furnace experimental melting on rocks local to Dun Deardail to determine if processes of vitrification can be recreated in laboratory settings. Experimental furnace melts have been used to recreate some of the vitrification processes in a controlled environment allowing validation of the methods used and informing the conclusions reached. Melting was carried out in alumina crucibles due to the heat resistance and stability of the mineral. Three different crucible sizes and shapes were used (Figure 35). This allowed flexibility in experimental design.

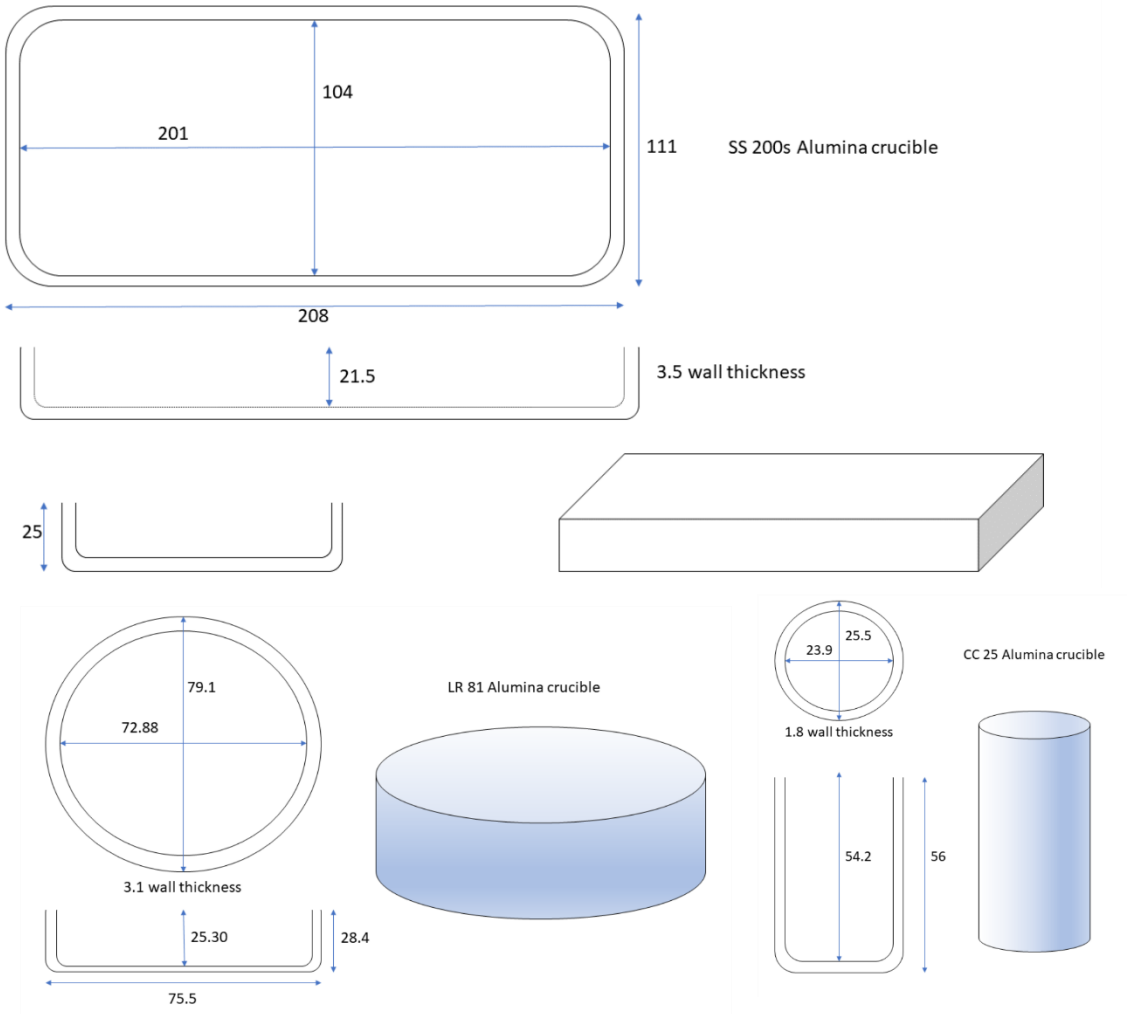

Figure 35:Alumina crucible dimensions. All measurements are in mm.

Table 8, Table 9 and Table 10 show the experimental melts carried out and the conditions that they were run under.

Firstly, it was necessary to determine the melting temperatures of the most common rock types found during the 2015 excavation. The temperatures were chosen to cover the Hornblende-Hornfels, Pyroxene-Hornfels and Sanidine facies, which should cover the lithology found in the surrounding areas of each of the research hillforts. This allowed melting temperatures of the different lithologies to be determined. The effect that the heating and cooling rates had on the melt also needed to be investigated. This was used to determine the conditions used in the subsequent experiments. The melts were carried out using pelite as per Table 8. Observations during season one excavation of Dun Deardail suggest that a mixture of clast sizes were used in the building of the walls and rubble core of the hillfort. This experiment investigated how differences in

these sizes affects the melting properties of the rocks involved. Once these three properties were known for the common lithologies found at Dun Deardail they could be used to determine further melting experiments to further knowledge about the vitrification processes in vitrified hillforts.

Table 8: Table of melts carried out for single lithology melts and ramp changes for pelite and calcite.

Methodology for each melt follows. Pebble sized rocks were used and placed in an 80mm diameter crucible with a ramp of 5 ℃ per minute, unless specified. These were cooled slowly to prevent damage to the heating coils of the furnace. Each temperature was run with 6 replicate samples to allow for error.

Melt completed		650˚C	750˚C	850˚C	950˚C	1050˚C	1150˚C	1250˚C	1350˚C	1400˚C
Single lithologies:	Pelite	✓	✓	✓	✓	✓	✓	✓	✓	✓
	Calcsilicate	✓	✓	✓	✓	✓	✓	✓	✓	✓
	Granite	✓	✓	✓	✓	✓	✓	✓	✓	✓
	Calcite	✓	✓	✓	✓	✓	✓	✓	✓	✓
	Sandstone	✓	✓	✓	✓	✓	✓	✓	✓	✓
Ramp change, pelite	Fast up				✓	✓	✓	✓	✓	
	Fast down				✓	✓	✓	✓	✓	
	Slow up				✓	✓	✓	✓	✓	
	Slow down				✓	✓	✓	✓	✓	
Ramp change, calcite	Fast up				✓	✓	✓	✓	✓	
	Fast down				✓	✓	✓	✓	✓	
	Slow up				✓	✓	✓	✓	✓	
	Slow down				✓	✓	✓	✓	✓	
Mixed lithology:	Pelite and calcsilicate				✓	✓	✓	✓	✓	
	Pelite and granite				✓	✓	✓	✓	✓	
	Pelite and quartz				✓	✓	✓	✓	✓	
	Pelite, Calcsilicate and granite				✓	✓	✓	✓	✓	
	Pelite, Calcsilicate, quartz and granite				✓	✓	✓	✓	✓	

Table 9:Table of melts carried out for Single melt

(for narrowing down the melting temperature of single lithologies), remelting the melts, flux use, covered rocks, anoxic melts and differences between charcoal and wood additions. Methodology for each melt follows. Pebble sized rocks were used and placed in an 80mm diameter crucible with a ramp of 5 ℃ per minute, unless specified. These were cooled slowly to prevent damage to the heating coils of the furnace. Each temperature was run with 6 replicate samples to allow for error.

Melt completed	Lithology	Temperature range experiment carried out at										
		1060˚C	1080˚C	1100˚C	1120˚C	1140˚C	1160˚C	1180˚C	1200˚C	1220˚C	1240˚C	1260˚C
Single lithologies: Melt temperature	Pelite	x	x	✓	✓	✓	✓	✓	✓	✓	✓	✓
	Calcsilicate	x	x	✓	✓	✓	✓	✓	✓	✓	✓	✓
	Calcsilicate - layered	x	x	✓	✓	✓	✓	✓	✓	✓	✓	✓
Single lithologies: Melt remelt	Pelite	x	x	✓	✓	✓	✓	✓	✓	✓	✓	✓
	Calcsilicate	x	x	✓	✓	✓	✓	✓	✓	✓	✓	✓
	Calcsilicate - layered	x	x	✓	✓	✓	✓	✓	✓	✓	✓	✓
Fluxes:	Wood	✓	✓	✓	✓	✓	✓	✓	x	x	x	x
	Charcoal	✓	✓	✓	✓	✓	✓	✓	x	x	x	x
	Bone	✓	✓	✓	✓	✓	✓	✓	x	x	x	x
	Shells	✓	✓	✓	✓	✓	✓	✓	x	x	x	x
	Seaweed	✓	✓	✓	✓	✓	✓	✓	x	x	x	x
Covered	Mud	✓	✓	✓	✓	✓	✓	✓	x	x	x	x
	Pelite	✓	✓	✓	✓	✓	✓	✓	x	x	x	x
Anoxic/reducing pelite used for melt	charcoal -small	✓	✓	✓	✓	✓	✓	✓	x	x	x	x
	Charcoal - large	✓	✓	✓	✓	✓	✓	✓	x	x	x	x
	Seal - small	✓	✓	✓	✓	✓	✓	✓	x	x	x	x
	Seal - large	✓	✓	✓	✓	✓	✓	✓	x	x	x	x
Differences that charcoal or wood make	Charcoal	✓	✓	✓	✓	✓	✓	✓	x	x	x	x
	Wood	✓	✓	✓	✓	✓	✓	✓	x	x	x	x

Table 10:Table exploring the change in melt time for different grain sizes as per, Wentworth, (1922).

Samples placed in an 80mm diameter crucible with a ramp of 5 ℃ per minute. These were cooled slowly to prevent damage to the heating coils of the furnace. Each temperature was run with 6 replicate samples to allow for error.

		Time for melting at 1150˚C (minutes)				
Melt completed		240	360	480	600	720
Grain Size:	Granule	✓	✓	✓	✓	✓
	Pebble	✓	✓	✓	✓	✓
	Cobble	✓	✓	✓	✓	✓

Excavated clasts from Dun Deardail show a mixture of different rock types in the vitrified clasts. This experiment investigated the effects, if any, that a mixed lithology has on the melt.

Crystal size on exterior surfaces of vitrified rock clasts are small, suggesting a fast cooling time. However, crystal size in the interior of vitrified rock clasts is larger suggesting a slower cooling rate inside the clast. This suggests that the outside has solidified quickly keeping the heat in, like a tea cosy would to a teapot, keeping the inside warmer allowing the crystals time to form well-shaped crystal structures. A “tea cosy” effect may also have allowed less fuel to be used during the vitrification burn. The hypothesis originates from cooking methods used in primitive, rural communities, where food and charcoal and buried in earth and straw to allow cooking to continue with minimal resources. This negates the need for the vast quantities of fuel that have previously been suggested. This melt experiment was used to test the theory that clasts wrapped in hot melted rock stay hot and are well insulated, allowing melting to continue past the point of the fire.

In the large, rectangular crucible, pebble-sized fragments of pelite, quartz and calcsilicate rocks were placed on a crucible and covered in pelite. The ratio of the base rocks was: 40% pelite, 30% calcsilicate, 20% granite and 10% quartz. Another equal quantity of pelite was placed around the rocks.

The addition of fluxes lowers the temperature that the rocks melt and help to create a melting pathway for the resulting reactions to take place (Nisbet, 1974). Several items that could have been used as fluxes have been discovered in excavated vitrified hillforts: Seaweed (Miller, 1858), shells (Christison et al., 1905) and bones (Childe and Thorneycroft, 1937b).

From this, seaweed, shells and bones were placed under pelite samples and melted at as per Table 9 for 8 hours. The results from these melts were compared with samples that were melted in melt 1.

Three methods of producing a reducing environment have been used in this study:

1. Using charcoal to remove the excess oxygen from the furnace chamber as the rocks melt and solidify,
2. Allowing the pelite on the outside of the rock clasts to melt and seal in the inner core of rocks, therefore preventing oxygen from entering the inner core,
3. Encasing the rocks using a mud coating.

1. Charcoal: charcoal was placed throughout pebble-sized fragments of pelite, quartz and calcsilicates to replicate the melting of the ramparts and rubble core around the timber lacing at Dun Deardail. This was heated as per Table 9 for 24 hours and allowed to cool. These were run in six replicates

2. Pebble-sized fragments of pelite, quartz and calcsilicate rocks were placed on a crucible and covered in pelite grains. This was heated as per Table 9 for 24 hours and allowed to cool. These were run in six replicates.

3. Pebble-sized fragments of pelite, quartz and calcsilicate rocks were placed on a crucible and covered in micaceous mud. This was heated as per Table 9 for 24 hours and allowed to cool. These were run in six replicates.

Each of the methods (1-3) above were also repeated with the samples being placed inside alumina tubes (Table 9) with the above conditions. This should amplify the anoxic conditions by containing the sample from the outside oxygen-containing atmosphere. This replicates the conditions that may have been formed during vitrification.

3.1.1 Can the temperature of vitrification be determined by geochemical methods?

There have been several documented methods using elemental ratios to calculate maximum melt temperatures. Five of these have been explored to determine if any of these can give an approximate maximum temperature that the vitrification occurred at. These five methods were chosen as they best represented the rock types that often occur at vitrified hillforts and also were based on standard atmospheric pressure or the

pressure was part of the calculation and so could be compensated for and are commonly used in metamorphic geology. Each of these method uses the different ratios of elements between the melted area of the clast and the original. The equations can be found in page xvii where their uses within metamorphic geology are discussed in greater detail.

This experiment also demonstrated that the original temperature of formation of the pelite does not interfere with the reset melting temperature from the vitrification event and that a relict temperature was not what was being calculated. Samples produced in the first pelite series of melts were used to determine if this method of temperature determination is suitable for pelitic melts in vitrified hillforts.

3.2 Archaeological Methodological Techniques

Geochemical data was collected for this thesis using portable X-Ray Fluorescence (p-XRF), scanning electron microscopy (SEM-EDS), petrology and Mössbauer spectroscopy. p-XRF, SEM-EDS, petrology, Mössbauer and visual analyses were conducted at the University of Stirling. Visual and p-XRF analyses were also carried out in-situ on site. Figure 36 reiterates the research questions, and this section illustrates how these questions will be answered.

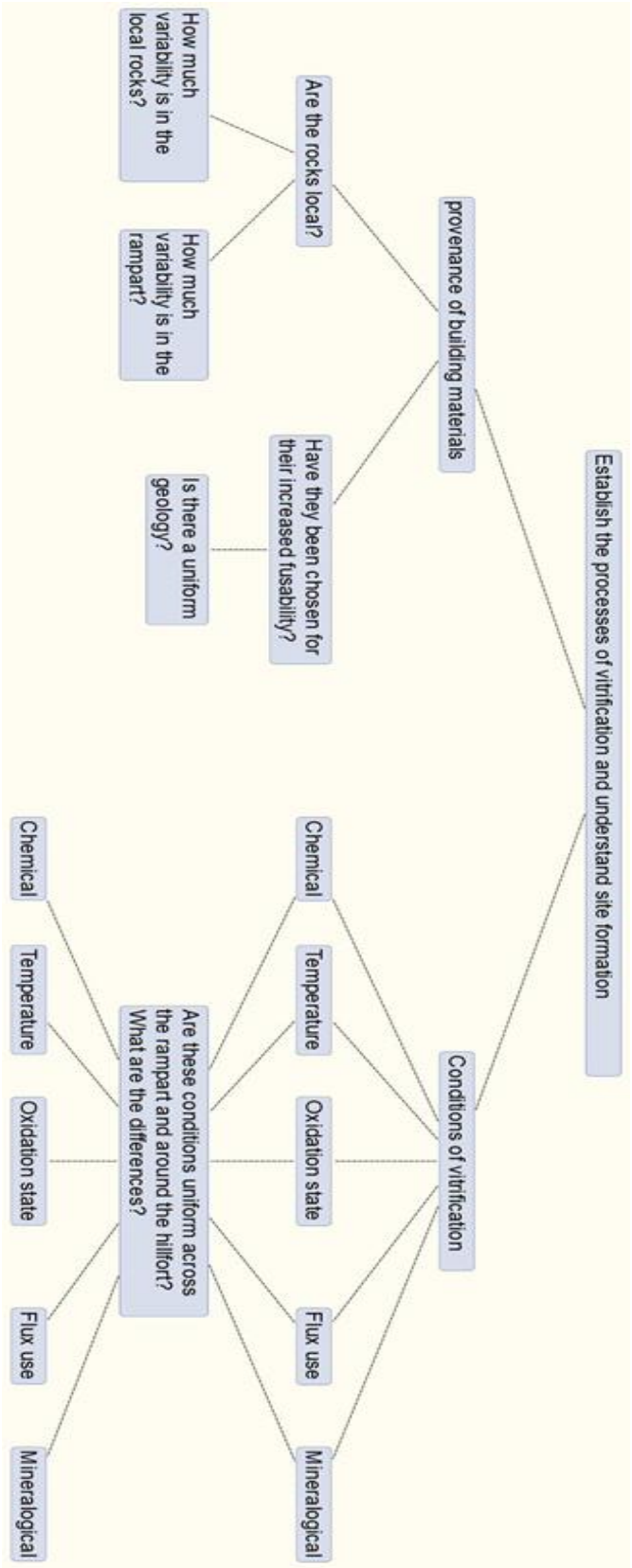

Figure 36:Research questions for this PhD.

Samples of vitrified, burnt and local material were collected, along with soil samples from trench 6 at Dun Deardail. Table 11 shows the analysis carried out on different presentations of these samples. Soils were also analysed by p-XRF.

Table 11:Analysis carried out on each type of sample.

	Visual	p-XRF	SEM-EDS	Petrology
In-Situ	✓	✓		
Excavated	✓	✓		
Cut	✓	✓	✓	
Slides	✓		✓	✓

3.2.1 Visual clast identification

Visual examination is a basic but vital first step in the analysis of any rock type. This allows larger-scale observations to be undertaken, and this allows recognition of patterns and changes that might not be observed in smaller scales.

Laboratory samples fell into four forms: Vitrified rock extracted from the site during the two years of excavation, burnt excavated rock, unvitrified unburnt excavated rock and collected local lithologies from outside the excavation area, both returned to the University of Stirling. In-situ samples were identified and analysed in the field and not returned to the University of Stirling.

Laboratory samples were rinsed with water to remove mud. Once the outer clast observation had been made, the samples were then cut using a Petrocut mounted saw. For in-situ samples, the rocks were observed as they were found on-site to prevent damage to the scheduled archaeological site.

Visual identification of the rock types in the samples was carried out using a hand lens, with a magnification of ten times. Physically observing the vitrified clasts also allowed for recognition and recording of deformations, presence of vesicles and presence of casts. This also allowed casts to be identified as this may suggest fluxes were intentionally used to improve the heating capability of the fire. Cast prints in the vitrified clasts allowed observations to be made to the presence of shells, seaweed and other potential flux materials. The laboratory samples were then cut open, and the freshly cut face was observed using a hand lens.

This allowed lithological identification of the rocks that make up the clasts and samples. Melt patterns and suture lines could also be observed at this stage. Each sample was

also photographed to allow a record to be kept of samples that have had destructive testing performed on them after the visual analysis was complete

To determine the rock name the BGS metamorphic identification flow chart, Figure 37, can be followed. From this, comparisons can be made between rocks used to build the walls and rubble core and also compare these to the native surrounding rock. This allows the determination of the provenance of the building materials.

From observations under the petrological microscope, the quantities of quartz, feldspar and mica can be plotted as a ternary diagram to allow direct comparison between rocks (Figure 38). For carbonate classed rocks, two different ternary diagrams are used. The first one is used for rock where there is less than 50% carbonate or calcsilicate-rock and at least 50% quartz ± feldspar ± mica. The second carbonate ternary is for the subdivision of rocks containing more than 50% carbonate and calcsilicate minerals. These ternaries are standard BGS diagrams for assigning metamorphic rock names (Robertson, 1999).

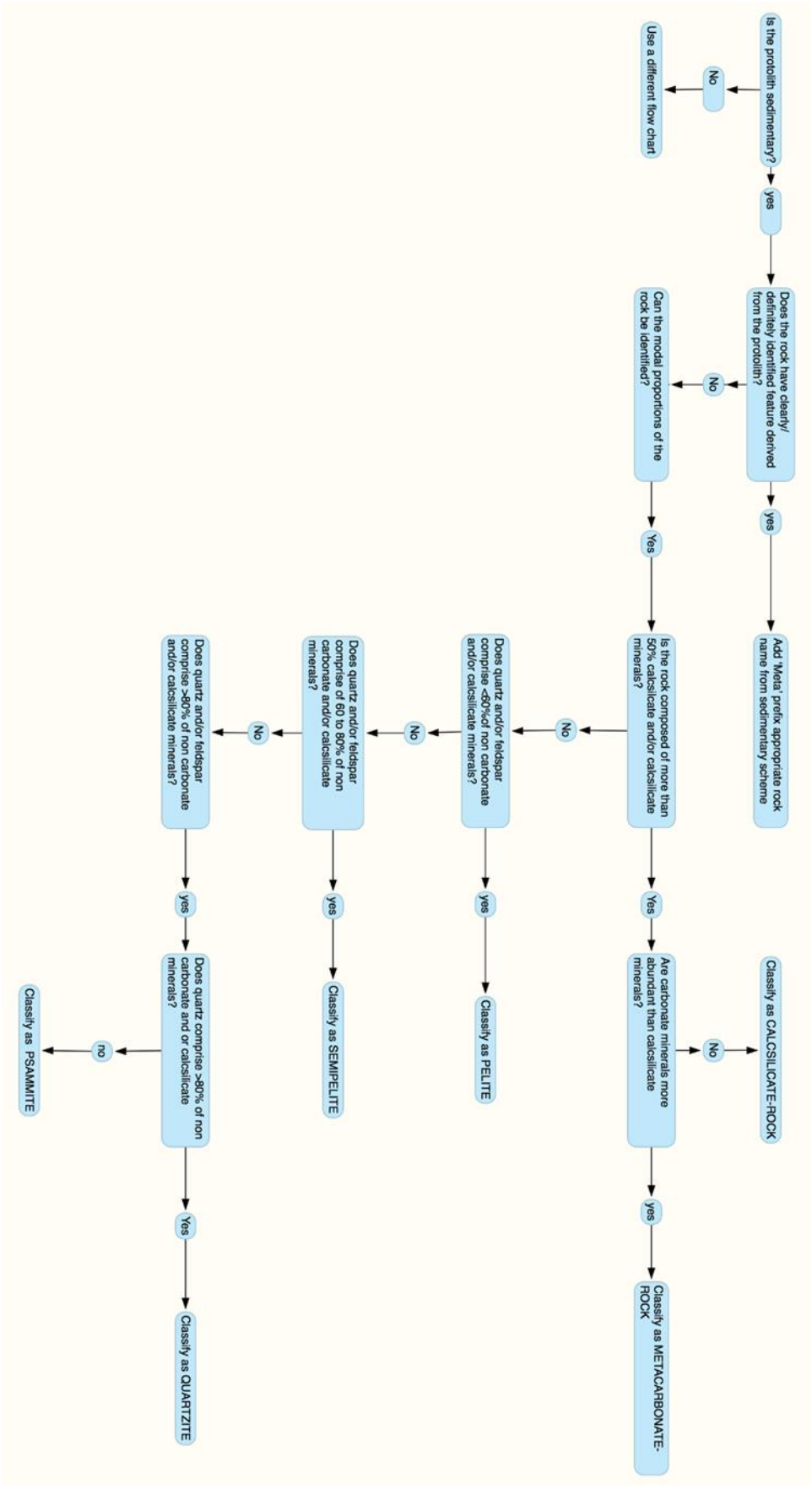

Figure 37: Flow chart for determination of sedimentary protolith metamorphic rock. Adapted from Robertson, 1999.

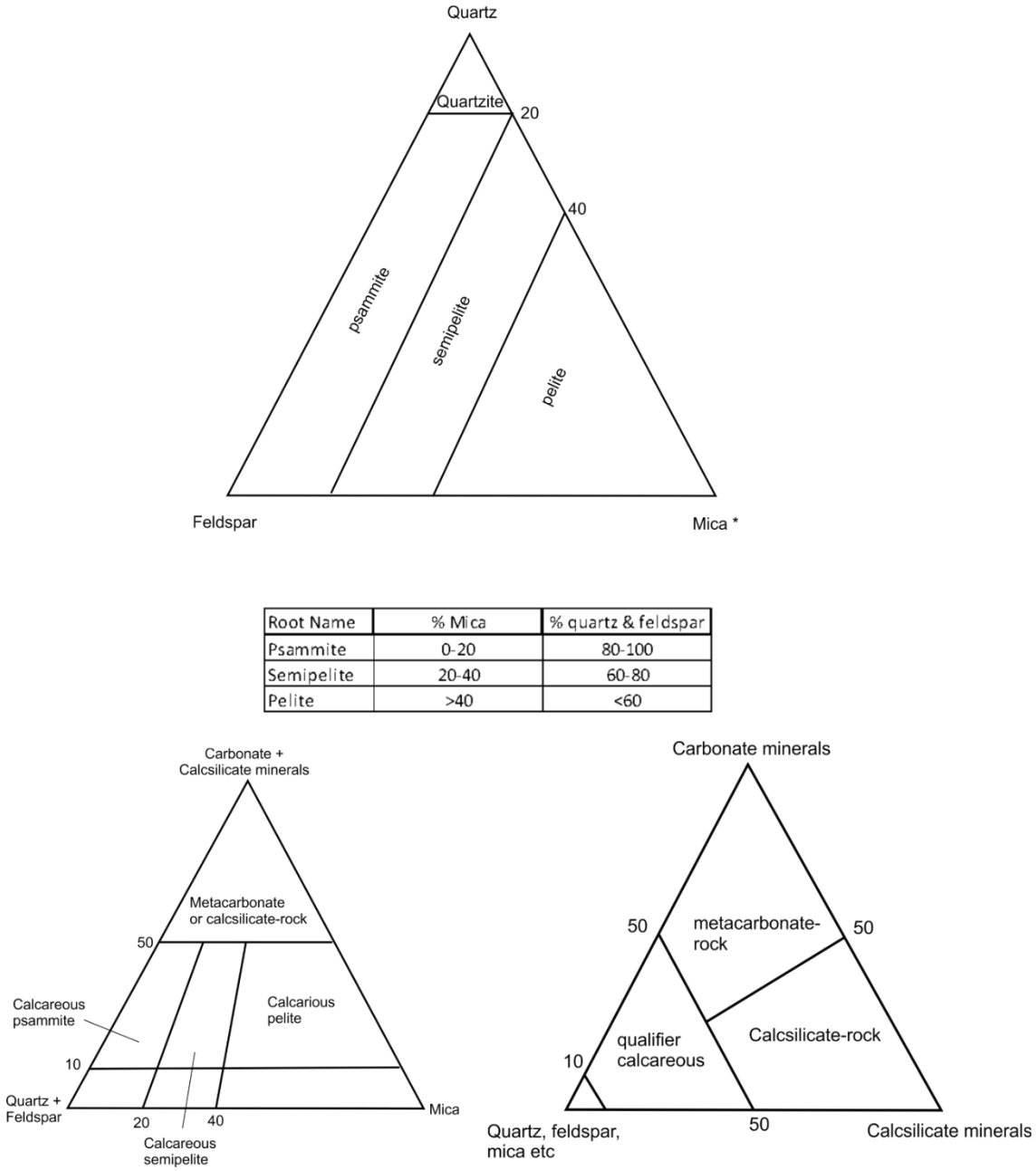

Root Name	% Mica	% quartz & feldspar
Psammite	0-20	80-100
Semipelite	20-40	60-80
Pelite	>40	<60

*Figure 38:Subdivision of rocks composed largely of quartz ± feldspar ± mica. Adapted from Robertson, 1999. * Mica includes all components other than quartz and feldspar.*

3.2.2 Portable X-ray Fluorescence (p-XRF)

The p-XRF analytical method was used to investigate the bulk geochemistry of geological samples. ICP-OES may also have been used to give the same results as p-XRF. However, the hydrofluoric acid digestion step makes the analysis time consuming, and the advantage of slightly better detection levels of the ICP-OES is cancelled out by the ease of use and portability of the p-XRF (Ramsey et al., 1995). This allowed the use of the instrument in the field and results that were comparable

with those obtained in the laboratory. As p-XRF is a fast technique, at around one minute per reading, this allowed many more samples to be analysed in comparison with SEM or petrology, giving better statistical power (Lemière, 2018). p-XRF is a non-destructive technique that can be used in the laboratory or the field with comparable results. The technique was originally used as a mining tool, and so detection limits for the method are appropriate to those needed for the elements analysed (Arne et al.,, 2014). This technique is also used for non-destructive provenance determination of lithic artefacts in archaeology and geoarchaeology (Jones et al., 1997; Shackley, 2011).

Samples for p-XRF were analysed both in-situ and ex-situ in the laboratory. In-situ analysis of the hillfort ramparts was undertaken as the restrictions of a scheduled monument prevented the taking of samples outside the excavated trenches and would have damaged the archaeological site. Excavated samples were water rinsed and cut open to reveal the inner rocks then allowed to air dry to prevent scattering of the X-rays, oven-drying has been shown to be unnecessary (Ge et al., 2005).

Excavated samples were placed on the lead sample holder and run on the mining programme of the p-XRF with a sixty-second analysis time per reading. Samples were run using the Mining Cu/Zn setting with filter timings of Main 15s, Low 10s, High 10s and Light 25s. Spot size of 8mm was used. No helium was used for sample analysis so that the samples analysed in-situ would be comparable. In-situ samples were analysed by removing moss from the outside of the vitrified clast. The rock was allowed to dry slightly to reduce the scattering of X-rays that damp rock would produce. Slight dampness of the rock should only very slightly increase the scattering of X-rays, and this results in a negligible loss of returning x-rays (Ge et al., 2005). In-situ samples were analysed using the same programme and analytical conditions as in the laboratory. However, the p-XRF was used handheld and the results downloaded to Excel once back in the laboratory.

Each reading was repeated five times, and multiple areas of each sample were measured to account for any anomalies in the sample. A minimum of three areas on smaller samples and five areas on larger samples were sampled. These figures were limited by rock sample size compared with p-XRF spot size used (8mm). The p-XRF sample size was determined from pre-existing research and preliminary testing of standard samples

(Hall et al., 2012). Areas targeted for analysis were the areas of melt, areas of heat damage, dehydrated rock and areas where there was no visible alteration of the rock.

The Thermo Fisher Scientific Nitron XL3 analyzer p-XRF is served and calibrated annually by ThermoScientific. An internal instrument check is carried out with each use along with a SiO2 check, which used a quartz rock, to ensure daily results are comparable with those from previous days. There are also quarterly checks carried out using certified check standards: CCRMP – Till4, NIST 2780, NIST 2709a, RCRA and SiO2. The data showing the analytical capabilities of the instrument are shown in Appendix. This data was used to ascertain the provenance of the samples using standard geological classification diagrams, discussed in the results chapter, to determine provenance and melt changes across the samples.

The elements analysed were: silicon (Si), iron (Fe), manganese (Mn), chromium (Cr), vanadium (V), titanium (Ti), calcium (Ca), potassium (K), aluminium (Al), barium (Ba), niobium (Nb), zirconium (Zr), strontium (Sr), rubidium (Rb), sulphur (S), magnesium (Mg), zinc (Zn), bismuth (Bi), arsenic (As), selenium (Se), gold (Au), lead (Pb), tungsten (W), copper (Cu), nickle (Ni), cobalt (Co), phosphorus (P), chlorine (Cl), antimony (Sb), tin (Sn), cadmium (Cd), palladium (Pd), silver (Ag) & molybdenum (Mo).

3.2.3 Petrology

Petrology is the examination of a thin section rock sample slide using a petrological microscope. These slides contain thin sections of rock around 30μm thick, allowing light to pass through it. This allows the user to identify minerals and textures of the rock using plane polarised light (PPL) and crossed polarised light (XPL), hence allowing a full rock identification and a rock formation history (MacKenzie and Guilford, 1980). This analysis was conducted on the *ex-situ* vitrified and unvitrified hillfort samples and from the local country-rock.

Two different microscope models were used for petrology: Olympus BX41 and Olympus BX51 with an attached camera and visual output facilities.

Minerals making up a rock can be identified using petrology. This allows rock identification and observations about how the rock may have changed since formation can be observed. Many minerals have set temperatures that they are formed and are

destroyed at. These minerals are called Index Minerals. These minerals can be used to determine the temperature that a rock solidified at. This can be used to determine the maximum temperature that the rocks in a vitrified hillfort melted at (Eskola, 1920). Therefore, petrology should be able to help determine the temperature of the melt of the hillfort and the provenance of the material used to build the hillfort.

Petrological thin-section slides were produced from samples of vitrified rock clasts, and country-rock, using University of Stirling petrological slide production method adapted to suit vitrified clasts, adapted from MacLeod, (2018). Rock sections were cut using a Buehler Petrocut, with a diamond-tipped blade, to 10mm thick. These slices were dried then impregnated with resin to hold any friable pieces of rock together. The resin was set overnight, then ground on a lapping plate, Logitech LP50, using 15μm calcinated aluminium oxide in water. This ensured a flat uniform surface. The sample slice was bonded to a 75x110mm glass slide using 301 epoxy resin and clamped overnight in spring-mounted jigs. The majority of the excess rock was removed using the Petrocut saw and the slide ground on the LP40/50 to 30-40μm thickness. The slide was then polished on a Logitech CL40 polishing machine using 3μm diamond in an oil suspension. The residual oil was then removed using solvent. As the samples were to be analysed using SEM, as well as by petrological microscope, no coverslip was attached to the top of the slide.

These slides were observed using a petrological microscope using plane polarised light (PPL) and cross polarised light (XPL). Magnifications of 10x and 20x were used, and entire slides were observed. Mineral formations and structures were noted, and images of areas that contained index minerals or minerals undergoing change were recorded using the image capture camera attached to the microscope. Index minerals observed (Table 12) will give a temperature range that the minerals formed under, at ground pressure (Eskola, 1920).

Table 12:Index mineral formation, at specific temperatures, in pelitic rocks, (Eskola, 1920)

Facies	Albite-Epidote-hornfels	Hornblende-hornfels	Pyroxene-hornfels	Sanidinite facies
Temperature range	**250-450℃**	**450-650℃**	**650-800℃**	**800℃+**
minerals extinct	Zeolites	Epidote, Chlorite, Actinolite	Muscovite, Hornblende, Microcline	Quartz, Orthoclase
minerals appear	Albite, Actinolite, Muscovite, Biotite, Microcline, Laumonite	Hornblende, Corderite	Orthopyroxene, Garnet, Orthoclase	Sanidine
pelite, psammite	Andelusite, Chlorite, Biotite, Quartz, Albite, Epdote	Muscovite, Andalusite, Biotite, Corderite, Quartz, Plagioclase	Corderite, Quartz, Silliminite, Andalusite, Orthoclase, Biotite, Garnite	Corderite, Mullite,Sanidine, Tridymite, Enstatite, Hypersthene, Silliminite, Corumdum
Carbonate rocks, Calc-silicates	Calcite, Dolomite, Epidote, Tremolite, Actinolite	Calcite, Dolomite, Tramolite, Quartz, Grossular, Plagioclase, Diopside, Talc	Diopside, Grossular, Wollastonite, Fosterite, Spinel, Biotite	Wollastonite, Anothite, Diopside

Areas of interest were also photographed using Image software for offline analysis. As the rocks types in the samples excavated and used to produce petrological slides are mainly of metamorphized mudstone (pelite and psammite), the minerals in these categories were sought for temperature range determination.

3.2.4 SEM-EDS

SEM-EDS was carried out using self-supporting cut rock slices 10mm thick and petrology slides.

A Zeiss Evo MA15 with InCA X Max 50mm^2 SEM-EDS was used for the analysis. The analysis conditions were: Accelerating Voltage – 20kV, Filament energy – 2.569A, Beam Current - 100µA, Working distance – 9mm, Count time – 60 seconds. The average spot size used was 550 and was chosen to maintain a count rate between 5 – 10 kcps with a dead time <45%. Analyses were run under partial pressure (60 Pa) to prevent surface charging without requiring sample coating.

The Zeiss EVO MA15 SEM-EDS undergoes an annual service by Zeiss and carries out its own internal checks on startup. Biotite and Muscovite certified reference standards (registered standard number 11409), provided by Micro-Analysis Consultants Ltd, were used to ensure that the instrument was returning sensible and comparable results. Aztec data collection software was used to interpret and visualise the data produced.

Figure 39 illustrates the typical areas of measurement when using the SEM. **A – D** illustrates measuring across a crystal to determine if there are differences across the crystal from edge to centre. **E – H** illustrates measurements following the edge of a crystal to determine differences in the edge structure of the crystal. **I – K** illustrates the measuring of the melt that has cemented the crystals together to determine if the melt is homogenous or has differing components in it. Spot **I** also allowed the analysis of the coating surrounding the vesicles.

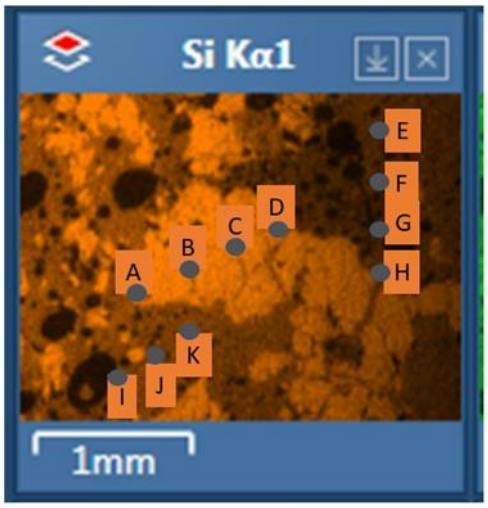

Figure 39:Areas of SEM measurement, as detailed above.

Analyses, using spot measurements, line measurements and scans, were focused on areas of pelite, quartz and calcite, as this is where the changes caused by vitrification occurred, areas of change and areas where no burning or melting occurred. In each area, ten readings were taken for reproducibility. In some areas, that were of limited size, such as around some of the vesicles, fewer readings were able to be taken. Results were used to compare the elemental composition of the vitrified samples to the burnt and natural rocks.

3.2.5 Mössbauer spectroscopy

Mössbauer spectroscopy works using recoilless emission and absorption of gamma rays by specific nuclei in a solid. This nuclear resonance has extremely high energy resolution. Information from these hyperfine interactions is provided by the hyperfine parameters, which can be determined by experimentation determining the line positions in a Mössbauer spectrum. The isomer shift represents the energy difference between the source and absorber nuclei (Gütlich et al., 2011).

Using data generated from analysing vitrified, burnt and unburnt rocks, it was hoped the burn temperature difference across the rock could be analysed. This technique has previously been used in pottery, slag and rampart temperature analysis (Gebhard et al., 2004a, 2004b). This analysis was used to provide independent confirmation of the vitrification temperatures derived using petrological and geochemical methods. In addition to temperature analysis, Mössbauer allows us to tell whether the vitrification occurred in an oxidising or reducing environment. Using Mössbauer the oxidation state of the iron can be determined, and from this, we can deduce whether the rock formed in an oxygen-rich or poor environment (Gebhard et al., 2004b).

Samples analysed by Mössbauer were previously cut for other techniques. The samples analysed were chosen as they exhibited varying degrees of vitrification across them and, after p-XRF analysis, contained sufficient iron to produce readings. These vitrified samples were compared to unburnt and unvitrified samples. Mössbauer analysis was carried out across the differing degrees of vitrification to allow changes to be detected.

The field methods, sample preparation and analytical techniques used in this research project have been described in this chapter. The application of these methods and techniques has resulted in high-quality data which will be presented in the following chapters:

Chapter 4 – Results – Experimental melts results, where these methods were used in the investigation of the melt of the local lithology, with different conditions and compositions. This chapter also looked at the proposed methods that would be used in sample analysis and determined if they were fit for purpose or not.

Chapter 5 – Results – Archaeological Materials, where the methods were used to demonstrate the provenance and variability of the building rocks making up Dun Deardail and also the conditions of vitrification will also be discussed here. Whether Dun Deardail is unique in its construction, provenance and conditions will be explored and the analytical methods used in this determination.

4 Results – experimental melts

This chapter disseminates the results for the experimental laboratory melts, described in Analytical methods: Experimental melts, page 48, so to approximately replicate what is happening in the field and to determine that the methods used to answer the research questions are appropriate for this study.

The experimental melts will determine the melting temperatures and conditions of the lithologies used at Dun Deardail, as determined during the Dun Deardail excavation seasons. From this, the changes in the conditions, such as grain size differences, oxidation state and fluxes, during vitrification was explored. Several methods of minimum melt temperature determination using results from the geochemical analysis have also evaluated.

4.1 Melting temperatures of common rock types

4.1.1 Visual

Visual assessment was carried out on all melts and documented in Table 13. This looked at the temperature that a rock melted at and also the reactions that occurred to that rock.

As shown in Table 13, pelite rocks showed no change between 650˚C and 750˚C and then began to show signs of oxidation and colour change on the outer surfaces by 850˚C. By 1150˚C the rock had melted and become fluid, and vesicles began to form by 1250˚C. By 1400˚C, large vesicles have formed in the melt where water has been boiled off from the inter-rock minerals (Figure 40).

Table 13:Visual analysis of single lithological melts.

x- visually unaltered, o- signs of outer oxidation, m- melt evident, ml-melted layers, d-dehydrated, f-friable

Melt completed	Conditions	Lithology	Temperature range experiment carried out at								
			650˚C	750˚C	850˚C	950˚C	1050˚C	1150˚C	1250˚C	1350˚C	1400˚C
Single lithologies:	Pebble size	Pelite	x	x	o	o	o	m	m	m	m
		Calcsilicate	x	x	o	o	o	o	ml	ml	ml
		Granite	x	x	x	x	f	f	f	f	f
		Calcite	x	x	x	d+f	d+f	d+f	d+f	d+f	d+f
		Sandstone	x	x	x	x	x	x	x	x	x

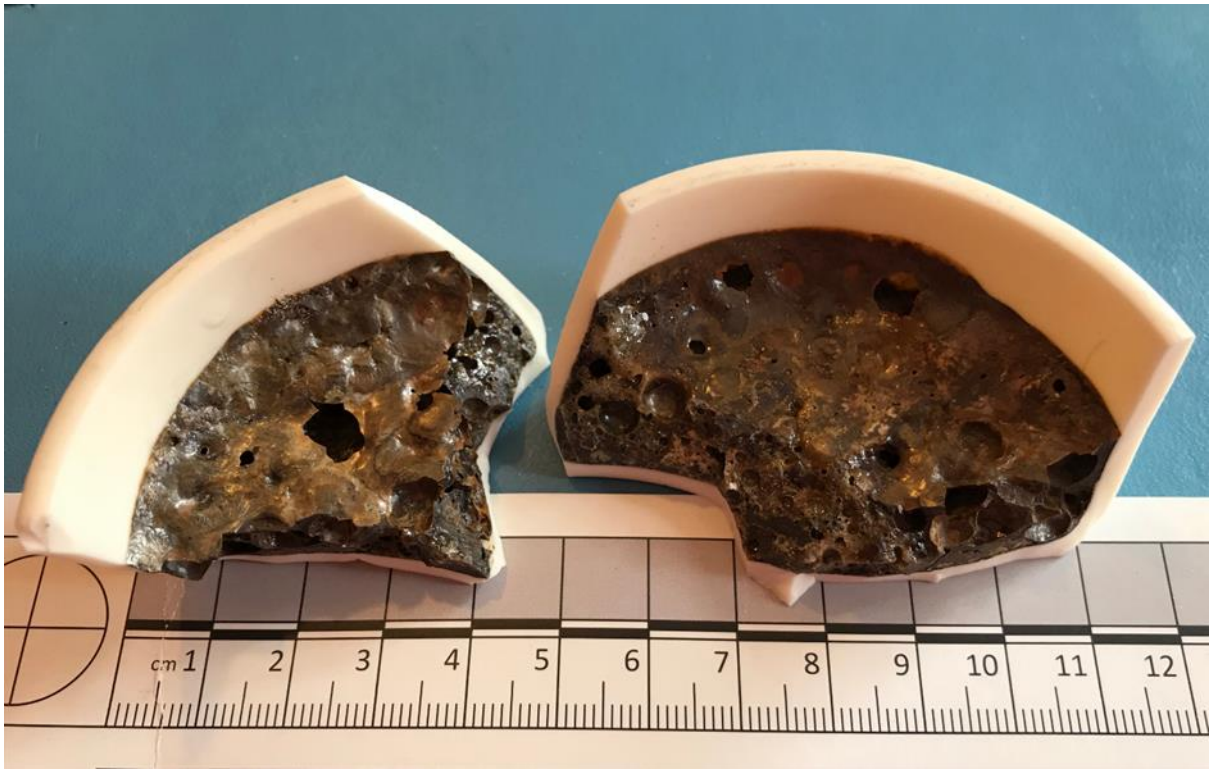

Figure 40:Pelitic melt at 1400˚C.

The calcite was shown to become progressively friable in the temperature range (Table 13), and by 1400˚C, the surface had become powdery. Granite also increased its friability as heating increased with colouring, also reducing as the heat increased (Figure 41).

Figure 41:Progression of the dehydration and friability of granite as temperature increases between 750 and 1250˚C.

The melting temperature of the lithologies that were found to melt (pelite and calcsilicate) was determined using smaller increments in temperature increase until melting was observed, by appearing glassy on the outside of the material (Table 14).

Figure 42 illustrates the situation when a layered pelitic, quartz and calcite was melted. This is a common rock, found on the hillside surrounding Dun Deardail. The different rock types stayed together when heated, with the pelitic rock producing a glaze over the other rocks. The pelitic rock showed signs of melting and formed vesicles. In contrast, the quartz has partially melted at the edges, and the calcitic layers have dehydrated.

Table 14:Melting temperatures of various lithologies during controlled temperature melting.

o - signs of outer oxidation but no melt occurred, m- melt evident, ml-melted layers

Melt completed	Conditions	Lithology	Temperature range experiment carried out at								
			1100˚C	1120˚C	1140˚C	1160˚C	1180˚C	1200˚C	1220˚C	1240˚C	1260˚C
Single lithologies: Melt temperature	Pebble size	Pelite	o	m	m	m	m	m	m	m	m
		Calcsilicate	o	o	o	o	o	m	m	m	m
		Calcsilicate - layered	o	ml	ml	ml	ml	ml	ml	ml	ml

Figure 42:Pelite, calcite and quartz layers after and before melting at 1160˚C.

Kresten et al., (1993) suggested that vitrification may have been undertaken in sections, leading to some areas being re-melted at the joins to each section of vitrification. To determine if re-melting a rock made any difference to the temperature of the melt, the following rocks were melted twice. Firstly, the rock was taken to the temperature that melting was evident and then allowed to cool to room temperature. The rock was then reheated to the original melting temperature, and this was then increased in 20˚C

increments until the rock melted. As shown in Table 15, the temperature of melting on reheating was forty degrees higher than the original melting temperature.

Table 15:Remelting temperature of previously melted rock.

o- signs of outer oxidation, m- melt evident, ml-melted layers

Melt completed	Conditions	Lithology	Temperature range experiment carried out at								
			1100˚C	1120˚C	1140˚C	1160˚C	1180˚C	1200˚C	1220˚C	1240˚C	1260˚C
Single lithologies: Melt remelt	Pebble size	Pelite	o	o	o	m	m	m	m	m	m
		Calcsilicate	o	o	o	o	o	o	o	m	m
		Calcsilicate - layered	o	o	o	ml	ml	ml	ml	ml	ml

4.1.2 Effect of grain size

The grain size was investigated to determine if a smaller grain size, based on the Wentworth Scale (Wentworth, 1922) facilitated faster melting. As shown in Table 16, pelite granules melted when subjected to 1150˚C for 240 minutes, whereas for pelite cobbles 600 minutes at 1150˚C were needed.

Table 16:Table exploring the change in melt time for different grain sizes as per, Wentworth, (1922).

X- no visual sign of melt, m-melted after the specified time.

		Time for melting at 1150˚C (minutes)				
Melt completed		240	360	480	600	720
Grain Size:	Granule (2-4mm)	m	m	m	m	m
	Pebble (4-64mm)	x	x	m	m	m
	Cobble (64-256mm)	x	x	x	m	m

4.2 Mixed lithologies

Although it is known that when rocks touch, they can lower the melting point of each other, the effect of this on melt temperature has not been investigated for vitrified hillforts. A melt mix was created that resembles the mixture of lithologies observed in the field during excavation.

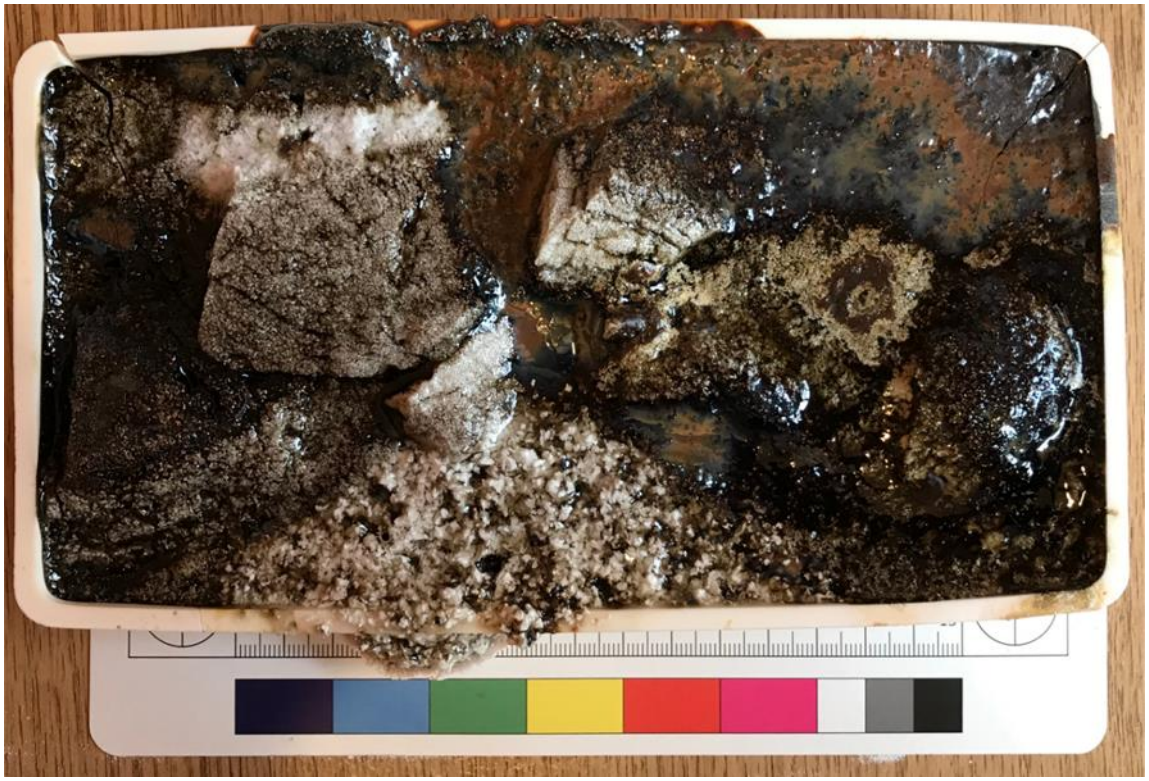

Figure 43:Pelite, calcsilicate, quartz and granite mixed melt at 1250˚C.

Visual assessments of the mixed lithology melts are shown in Table 17 and illustrated in Figure 43 and Figure 44. The mixed lithologies heated to below 1150˚C showed evidence of only oxidation. Above 1150˚C, the pelite melted, granite became friable and lost colour and the calcsilicate fractured. The quartz started partial melting at the edge of the rock at 1250˚C and melting continued at 1350˚C. This indicates that the temperatures of rock melt have been lowered, quite substantially in the case of quartz, as would be expected when combined with a melting material, such biotite from the pelite (Kresten et al., 1993).

Table 17:Temperature-controlled mixed lithology melts.

o- signs of outer oxidation, m- melt evident, ml-melted layers, d-dehydrated, f-friable

		Temperature range experiment carried out at				
Melt completed		950˚C	1050˚C	1150˚C	1250˚C	1350˚C
Mixed lithology:	Pelite and calcsilicate	o	o	m+d	m+d+f	m+d+f
	Pelite and granite	o	o	m+f	m+f	m+f
	Pelite and quartz	o	o	m+x	m+pm	m+m
	Pelite, Calcsilicate and granite	o	o	m+d+x	m+d+x	m+d+x
	Pelite, Calcsilicate, quartz and granite	o	o	m+d+x+f	m+d+m+f	m+d+m+f

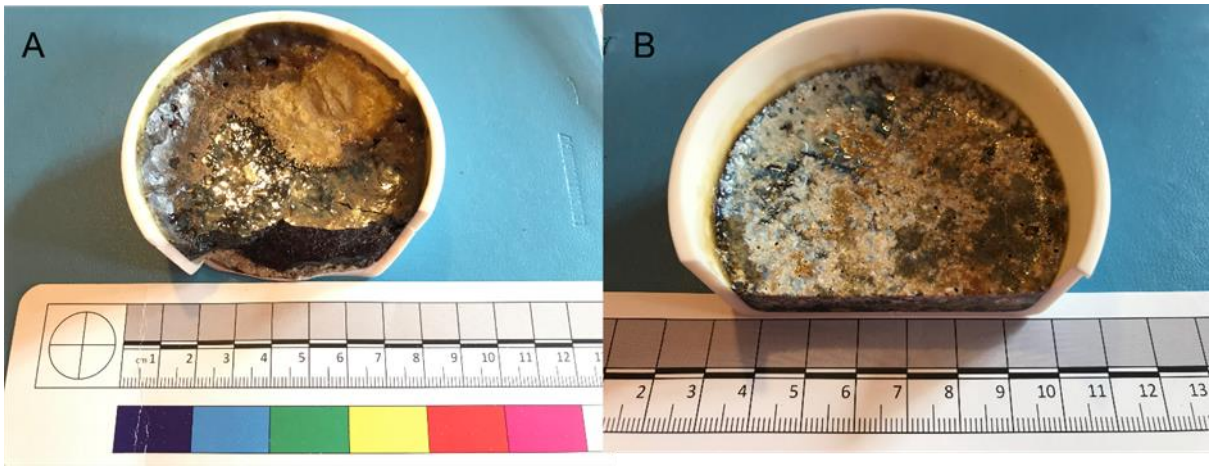

Figure 44:Mixed lithology melt mix at 1300˚C.

The resulting melt was analysed using p-XRF to determine if the elemental composition of the mixed melt was the same as the original sample, and so this could be used to confirm provenance from excavated samples, or if other elements entered the mix from the other lithologies in the mix, meaning that p-XRF of the melt mix could not be used to determine provenance as the melt would be different to the original source.

p-XRF data shows an increase in silicon in the melt mix in comparison with the rock before melting (Table 18). Most of the other elemental data remain as a similar composition. However, magnesium has dropped in the 1350˚C melt mix. This shows that for provenance analysis, the unmelted areas in a clast or rock must be the area that is analysed for an accurate fingerprint to be obtained.

Table 18: p-XRF data of the melted mix melts

Sample		Zn	Fe	Ti	Ca	K	Al	P	Si	Mg
original	Average	62	34073	4685	1480	39051	94410	1058	272251	7838
1150 mix melt	Average	67	33963	4685	1493	39687	94288	1060	269916	7664
1250 mix melt	Average	63	33991	4685	1515	40067	92483	1005	293913	6964
1350 mix melt	Average	64	32283	4685	1518	39840	90079	985	333517	5910

As shown in Figure 45, the edges of the quartz crystals are beginning to degrade and dissolve into the melt as it comes into contact with biotite crystals, which have lowered the melting temperature of the quartz. The crystals are also showing signs of distress with different extinction angles showing over single crystals.

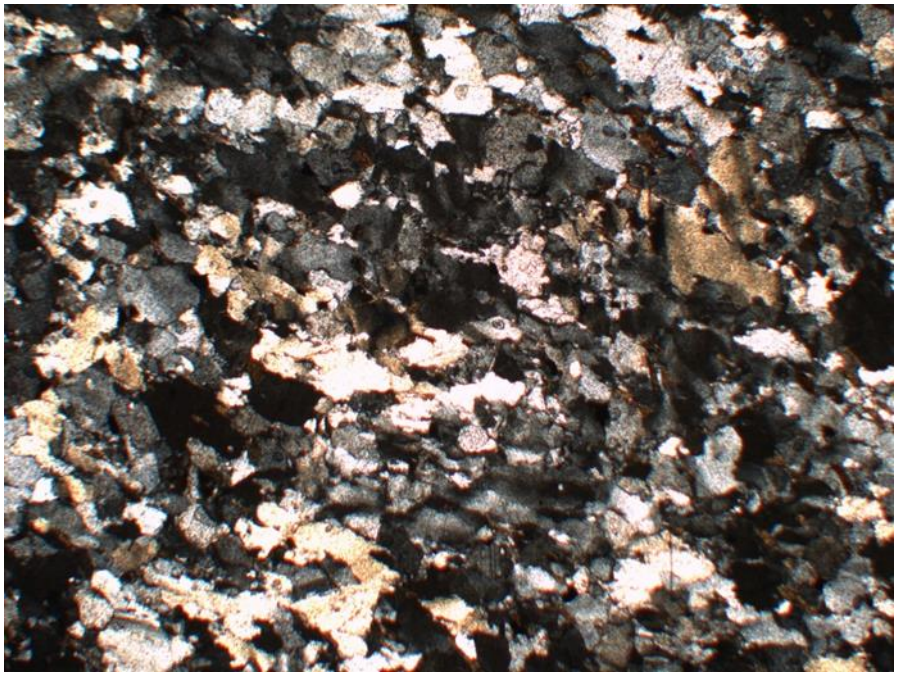

Figure 45:XPL of mixed lithology (quartz and biotite visible here) illustrating the damage to the edges of the quartz as it melts into the melt mix due to the biotite lowering of the quartz melting temperature .

4.3 Varying experimental conditions

As illustrated in Table 19, bones, illustrated in Figure 46, allow the rocks to melt at a lower temperature and create an increased phosphate value. Shell reduced to powder, and visual examination showed some of the powder was incorporated into the melt. This, however, did not appear to affect the melt temperature. Wood and charcoal have the most significant effect in lowering the melt temperature.

Figure 46: Burnt bones used as a flux in melting experiment.

Table 19:Changes fluxes make to a pelite melt under temperature-controlled conditions.

o- signs of outer oxidation but no melting visible, m- melt evident, pm – partial melting evident.

		Temperature range experiment carried out at						
Melt completed		1060˚C	1080˚C	1100˚C	1120˚C	1140˚C	1160˚C	1180˚C
Fluxes:	Pelite	o	o	o	m	m	m	m
	Wood	o	o	m	m	m	m	m
	Charcoal	o	o	m	m	m	m	m
	Bone	o	o	pm	m	m	m	m
	Shells	o	o	o	m	m	m	m
	Seaweed	o	o	pm	m	m	m	m

Table 20 show the elemental differences caused by the addition of different fluxes into the melt. Figure 47 shows this information in a spider diagram, with the diagram compared to the original pelitic sample. This allows us to see the changes compared to the results that the original sample gave. This works well in cases like this where the range in concentrations between the elements are quite extensive (zinc results are all in double figures whereas silicon results are in six figures).

Zinc shows a small change between fluxes, with the most substantial change in the seaweed samples. Iron, Titanium and aluminium show virtually no change in any of the

samples. There were small changes in the calcium and potassium in all of the samples with charcoal and wood, showing the most significant change. All samples had raised levels of magnesium, with no sample showing a more considerable increase than any of the others. The most significant change out of all the elements, in the majority of samples, was phosphorous.

Table 20: Average p-XRF results for flux incorporating melts.

SAMPLE		Zn	Fe	Ti	Ca	K	Al	P	Si	Mg
Original	Average	62	34073	4685	1480	39051	94410	1058	272251	7838
Charcoal	Average	57	33108	4714	1732	48183	91747	1520	267370	8729
Wood	Average	58	32820	4429	1685	44868	92174	1476	251442	8661
Bones	Average	72	35265	4661	1642	42208	96249	1649	253145	8780
Shell	Average	62	34941	4609	1584	40509	92912	1204	274321	8507
Seaweed	Average	79	35463	4455	1628	41092	94873	1371	279476	8664

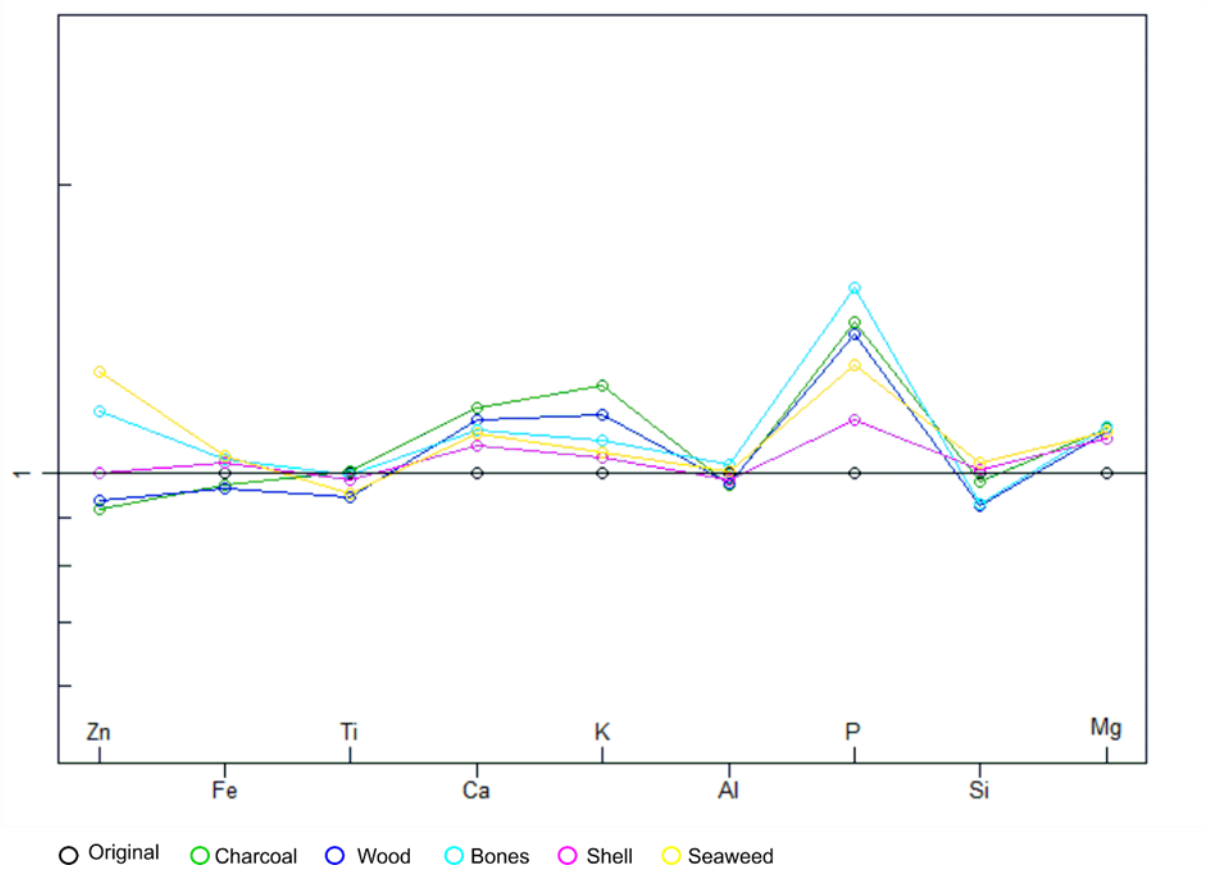

Figure 47:Spider diagram illustrating the differences in elemental composition in the flux inclusion melt compared to the original rock

The petrology did not show much effect from adding flux to the melt, apart from the wood and charcoal melts, where charcoal is visible in the melt

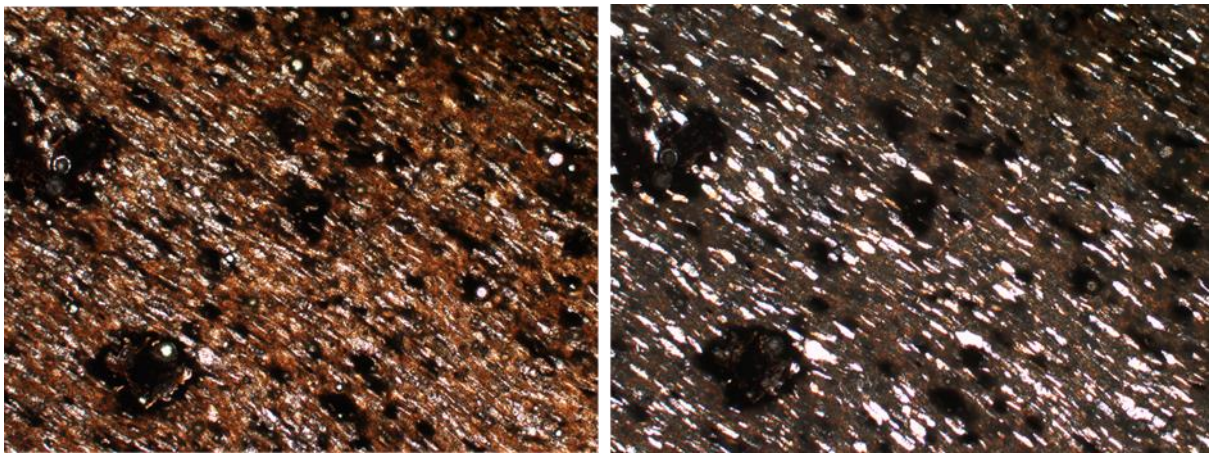

Figure 48:Charcoal pieces (dark areas) visible in the melt. 1160˚C charcoal melt in XPL and PPL.

Preliminary Mössbauer analysis suggests that the final solidified melt in vitrified hillforts were formed in an anoxic environment. This was also suggested in work by (Gebhard et al., 2004b). This may have occurred when all the oxygen was used up in the fire in a sealed environment. To see if the anoxic environment had much influence in the way the rocks melted anoxic furnace melting experiments were set up as per Table 21. However, the samples analysed by Mössbauer Spectroscopy contained too low an iron concentration for reasonable Mössbauer Spectroscopy results to be obtained. It would have been good to have samples that contained more iron to test this theory further; however, the samples used from the representative areas did not contain a high enough level and so no further Mössbauer Spectroscopy carried out on samples has been included in this thesis.

In investigating the effects of producing a reducing environment, Table 21, it was noted that that charcoal containing tube melted at a slightly lower temperature than without its presence. Trying to create a seal in the furnace was not particularly effective, and the melt temperature did not change.

Table 21: Visual analysis of an anoxic environment during the melt.

x- did not melt, pm – partial melt, m- melt evident.

		Temperature range experiment carried out at						
Melt completed		1060˚C	1080˚C	1100˚C	1120˚C	1140˚C	1160˚C	1180˚C
Anoxic/reducing pelite used for melt	charcoal -small	x	x	m	m	m	m	m
	Charcoal - large	x	x	m	m	m	m	m
	Seal - small	x	x	x	m	m	m	m
	Seal - large	x	x	x	m	m	m	m

During SEM-EDS analysis, it was observed that the iron surrounding the vesicles was pure iron rather than iron oxide. This lack of iron oxide suggests that the environment when the vesicles were forming was anoxic.

Understanding more about the speed at which the rocks were heated and cooled may provide clues to how the hillforts were heated to produce vitrification. Excavation has confirmed wide scale burning through the presence of ash and charcoal from wooden beams. Whether this has been a fast fire or a fire that has remained hot for several days has been unknown. However, it has been previously suggested that the vitrification processes in hillforts have not been a quick process (Youngblood et al., 1978).

The temperature ramp speed did not make a marked difference in what melted (Table 22); however, a difference in the heated rock was observed in the calcite experiment (Table 23). Those that were heated quickly showed signs of cracking and sometimes exploding before the melt temperature occurred. Those that had a slower temperature ramp were more likely to dehydrate.

Table 22:Visual analysis of the effects of heating and cooling speed on the alteration of a pelitic pebble.

o- signs of outer oxidation but no melting, m- melt evident

Melt completed	Conditions	ramp speed	Temperature range experiment carried out at				
			950˚C	1050˚C	1150˚C	1250˚C	1350˚C
Ramp change	Pelite, pebble size	Fast up	o	o	m	m	m
		Fast down	o	o	m	m	m
		Slow up	o	o	m	m	m
		Slow down	o	o	m	m	m

Table 23:Visual analysis of the effects of heating and cooling speed on the alteration of a calcite pebble.

f- friable, c- cracked, d-dehydrated, e-exploded

Melt completed	Conditions	ramp speed	Temperature range experiment carried out at				
			950˚C	1050˚C	1150˚C	1250˚C	1350˚C
Ramp change	calite, pebble size	Fast up	f	e	e	e	e
		Fast down	f	c	c	c	c
		Slow up	f	d	d	d	d
		Slow down	f	d	d	d	d

One way to reduce the vast amount of wood needed may have been for the melt to have created its own insulation. Two theories around insulation are that the mud was packed into the walls and when heated this solidified and helped contain the heat. The other idea is that the surface rock melt covered the inner melted rocks and kept in the heat.

Both effects are like a tea cosy keeping a teapot warm and would mean that more vitrification could be done with fewer resources.

Table 24 shows that the insulation did not make much difference to the melting temperature of the pelite. However, on further inspection, the insulated samples took several hours longer to cool than uninsulated pelite samples run at the same time suggesting that an insulating effect did occur in the experiment and this could have held in heat during a scaled-up burning and vitrification event.

Table 24:The alteration of pelitic rock insulated using either mud or layers of melted pelite.

x- did not melt, pm-partial melt, m- melt evident.

		Temperature range experiment carried out at						
Melt completed		1060˚C	1080˚C	1100˚C	1120˚C	1140˚C	1160˚C	1180˚C
Covered	Mud	o	o	pm	m	m	m	m
	Pelite	o	o	pm	m	m	m	m

4.4 Assessing different geochemical methods to determine melt temperature

Several geochemical calculations have previously been used in geology for determination of melt temperature using element ratio analysis. The ones chosen for use in this research have been listed at the start of this thesis, on page xvii. Five geochemical methods were chosen in this study for their suitability to vitrified hillfort studies. Part of these compatibility issues was finding calculations that were either for standard atmospheric pressure or this being able to be considered during the calculation. The samples also had to be able to be analysed and treated in a way that was compatible with the laboratory facilities. The final suitability of these calculations was determined using samples of pelite melted at known temperatures and the final melts being analysed using SEM-EDS.

The Leeman and Scheidegger (1977) equations, Equation 1: Leeman and Scheidegger calculation (Leeman and Scheidegger, 1977), use the ratio between either the magnesium content or the iron content in the olivine and glass melt on the vitrified clasts to give a maximum temperature of the melt in ˚C. Friend et al., (2016) analysed some vitrified samples from three Scottish Iron Age vitrified hillforts, and this analysis returned credible results. However, the method was not tested on laboratory-produced known temperature samples and so has been included in the experimental melts section.

Table 25 shows the calculated melt temperatures obtained using both of the Leeman and Scheidegger calculations (Equation 1: Leeman and Scheidegger calculation (Leeman and Scheidegger, 1977)) for the furnace melted samples. Figure 49 illustrates the range of temperatures calculated for each equation compared with the actual furnace temperature.

Table 25: Calculated T(°C) for the coexisting olive and glass

Melt number	Sample	Mg(ol)	Mg(gl)	Fe(ol)	Fe(gl)	T, Mg(˚C)	T, Fe(˚C)
1	1150	1.82	0.26	2.13	0.75	1157	1113
2	1150	1.13	0.16	2.35	0.85	1155	1119
3	1150	1.30	0.21	2.45	0.98	1186	1141
4	1150	1.25	0.18	2.78	1.03	1159	1124
5	1150	1.37	0.21	3.33	1.19	1173	1116
6	1150	1.35	0.22	2.87	1.12	1188	1136
1	1250	1.53	0.36	2.43	1.40	1281	1227
2	1250	1.68	0.37	2.57	1.51	1263	1232
3	1250	2.00	0.41	2.79	1.67	1245	1236
4	1250	2.56	0.32	2.9	1.86	1127	1254
5	1250	2.16	0.33	2.36	1.45	1172	1243
6	1250	1.55	0.35	2.65	1.59	1270	1237
1	1350	1.45	0.41	2.51	1.98	1333	1310
2	1350	1.53	0.49	2.57	2.05	1369	1313
3	1350	1.43	0.44	2.58	2.19	1357	1330
4	1350	1.38	0.47	2.67	2.46	1388	1354
5	1350	1.49	0.48	2.37	2.12	1371	1345
6	1350	1.39	0.41	2.99	2.45	1345	1320
1	1400	1.37	0.46	2.48	2.50	1384	1381
2	1400	1.42	0.50	2.69	2.65	1399	1374
3	1400	1.58	0.57	2.80	2.87	1406	1386
4	1400	1.44	0.54	2.69	2.74	1419	1384
5	1400	1.39	0.46	2.46	2.67	1379	1403
6	1400	1.38	0.54	2.67	2.75	1432	1387

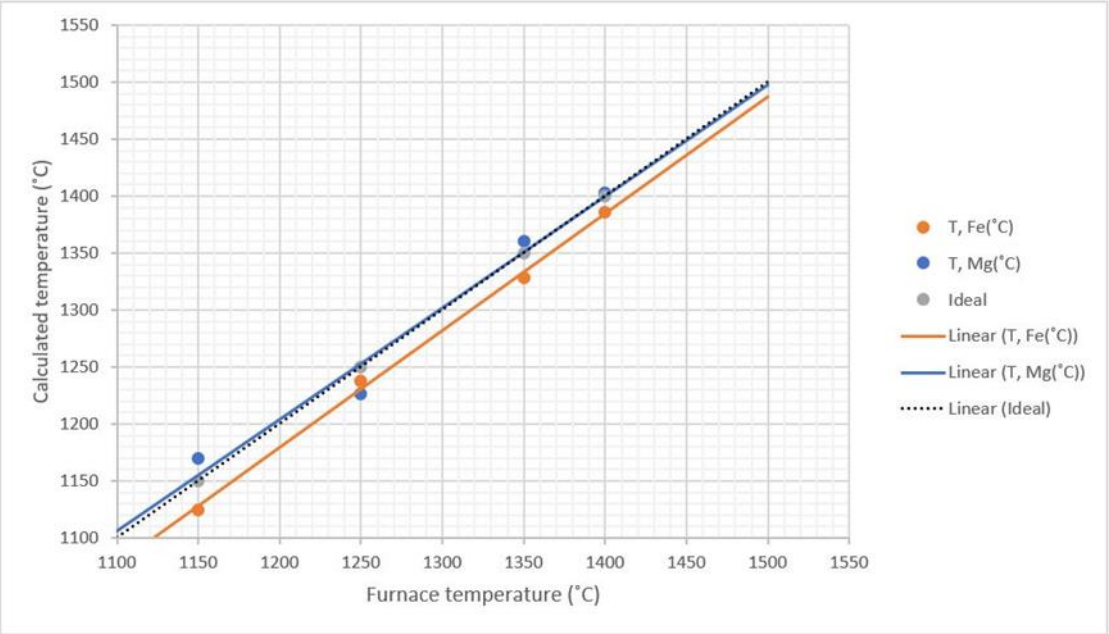

Figure 49:Calculated temperature range for pelitic rocks, melted at known temperatures, compared to furnace temperature.

The Jung and Pfänder, (2007) equation, Equation 2: Jung and Pfander (Jung and Pfänder, 2007), uses the ratio between titanium and aluminium in the melt to determine maximum melt temperature in ˚C.

The results from Jüng and Pfander (2007) calculation, using ratios of titanium and aluminium, are shown in Table 26. These temperatures do not correlate well to the actual temperature of melting.

Table 26:Temperature (°C) calculated using Titanium and aluminium ratios as per Jüng and Pfander (2007)

SAMPLE	Ti	Al	ratio	T(˚C)
Unmelted	4069	87201	21.43	1030
1050	3905	81918	20.98	1033
1150	3902	55302	14.17	1081
1250	3384	57584	17.02	1059
1350	2764	79575	28.79	994
1400	12057	45522	3.78	1244

For the Wan et al. (2008) (Equation 3: Wan et al (Wan et al, 2008)), De Hogg et al. (2010)(Equation 4: De Hogg et al (De Hogg et al, 2010)) and Coogan et al. (2014)(Equation 5: Coogan et al (Coogan et al., 2014)) equations, Due to lack of chromium detected in any of the samples, most likely because the chromium concentrations were below instrumental detection limits of SEM-EDS, the Wan et al (2008), De Hoog et al., (2010)

and (Coogan et al., 2014) calculations could not be assessed for these samples and so could not be used in this study.

5 Results – archaeological materials

This chapter will determine the results from the analysis of the building materials used in the construction of the study vitrified hillforts. Visual and geochemical work, as detailed in section 3.2 Analytical Methodological Techniques. The results from Dun Deardail will first be discussed followed by the results from the comparison hillforts and the research questions have been answered by following the flow diagram shown in Figure 50.

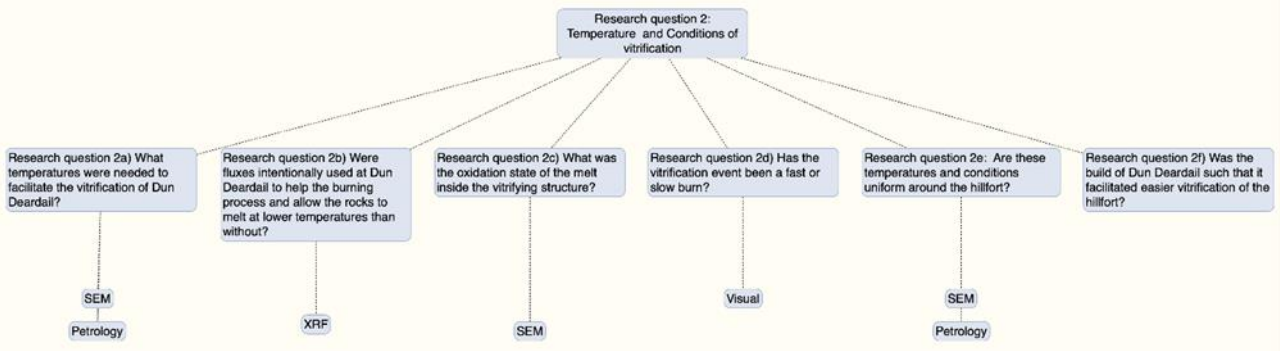

Figure 50:Research design questions and methods for answering them.

5.1 Dun Deardail materials

Figure 51 illustrates the excavated trenches used in these analyses and also the areas that were used for visual and p-XRF analysis. This was used to ensure as full a coverage of the rampart as would be allowed under the terms of the scheduled monument consent.

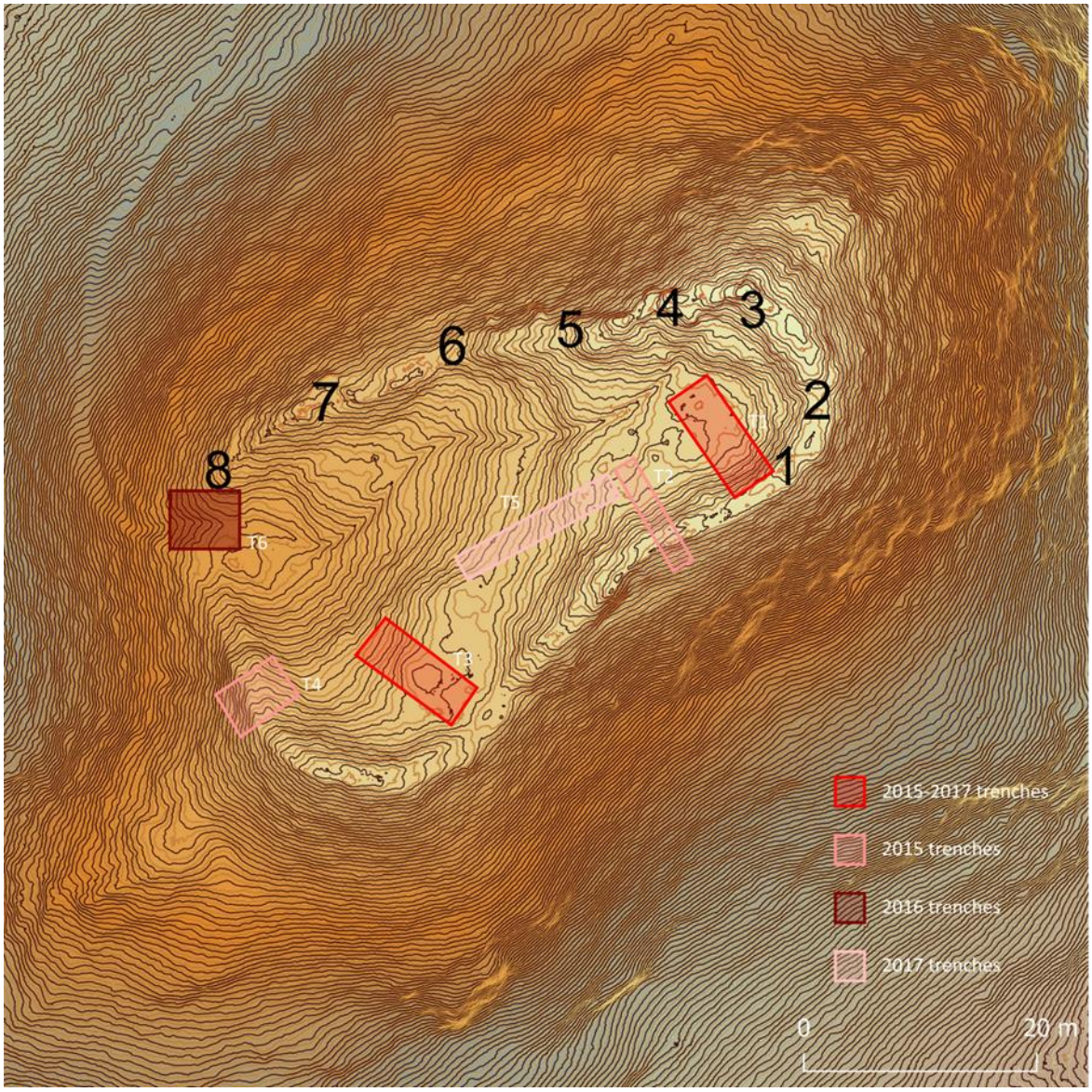

Figure 51: p-XRF measurement sites and excavated trench locations

(base map copyright FCS by Skyscape Survey)

5.1.1 Visual

Three hundred and thirty excavated clasts, vitrified, burnt and unburnt unvitrified samples, from five of the excavated trenches, were visually evaluated, and the mixture of lithologies for each clast recorded (Table 27). As shown in Chapter 4, Experimental melts results, it was observed that it is mainly the pelitic rocks that melt during vitrification and so to do a count just on numbers of types of lithology available would be meaningless as the pelitic rocks would have melted into one or two areas. To account for this, the lithology was analysed on area percent of each of the lithologies. Eight areas on the vitrified remains were also visually appraised in-situ. The lithology content

was compared to the geology of the surrounding landscape within a two-kilometre radius of the site.

Table 27:Comparison between local lithology and building materials in the hillfort

Lithology	Local geology	Trench 1	Trench 2	Trench 3	Trench 4	Trench 6
Calcaroius pelite	✓	✓	✓	✓	✓	✓
Graphitic pelite	✓	✓	✓	✓	✓	✓
Calcsilicate	✓	✓	✓	✓	✓	✓
Granite	✓	✓	✓	✓	✓	✓
Pelite	✓	✓	✓	✓	✓	✓
Quartz	✓	✓	✓	✓	✓	✓
Leucomicrograndiorite	✓					
Hornblende andesite	✓					
Granodiorite	✓					

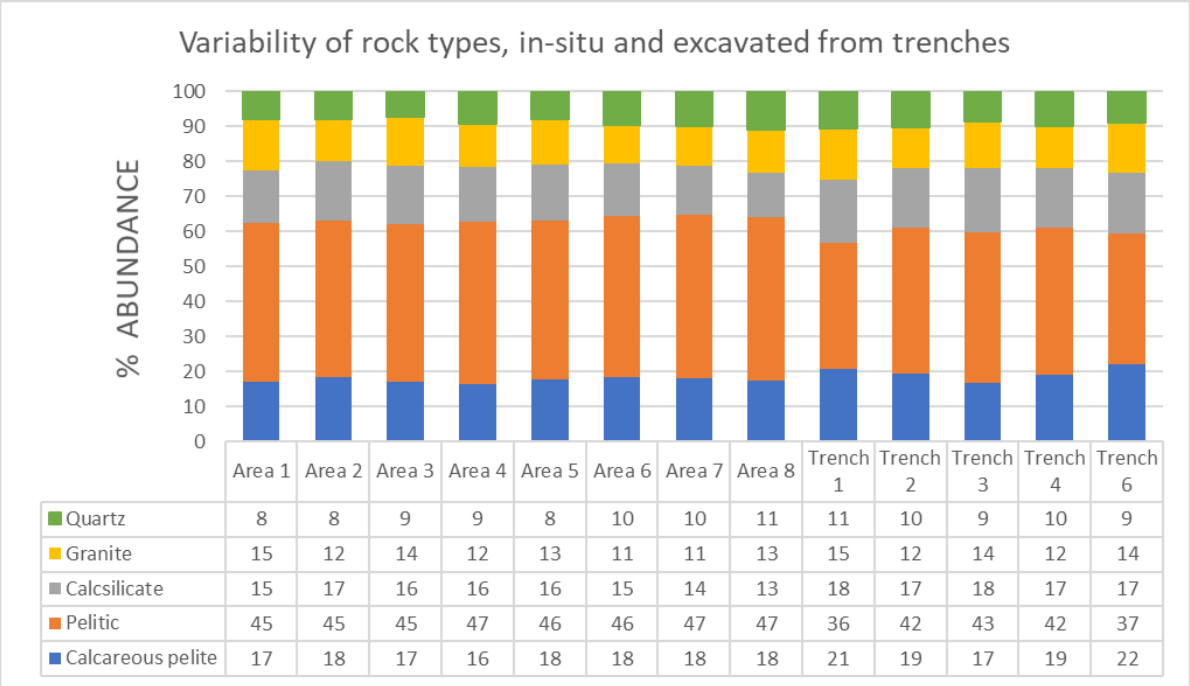

	Area 1	Area 2	Area 3	Area 4	Area 5	Area 6	Area 7	Area 8	Trench 1	Trench 2	Trench 3	Trench 4	Trench 6
Quartz	8	8	9	9	8	10	10	11	11	10	9	10	9
Granite	15	12	14	12	13	11	11	13	15	12	14	12	14
Calcsilicate	15	17	16	16	16	15	14	13	18	17	18	17	17
Pelitic	45	45	45	47	46	46	47	47	36	42	43	42	37
Calcareous pelite	17	18	17	16	18	18	18	18	21	19	17	19	22

Figure 52: Variability of rock types, in-situ and excavated from trenches in % abundance.

Figure 52 shows that almost half of the area percent for the clasts are pelitic. This pelitic element was found to be glassy on the outside and often full of vesicles on the inside. Almost twenty percent of the lithology was each of layered calcareous pelite and calcsilicate. The calcite component of this rock type was dehydrated in the burnt and the vitrified samples, and this was evident in the layers of the layered calcareous pelite. This shows that the composition across all excavated trenches are similar, and there is not one that has been supplemented with any other lithological types, other than what has been found in all other trenches, with pelitic rocks being the majority area percent

rock type in all of the trenches, followed almost equally by layer calcareous pelite and calcsilicate. The full breakdown for these areas can be viewed in Appendix C – Supplementary graphs and tables, including statistics

As with the visual analysis on the excavated clasts, the lithological determination of the in-situ vitrified areas was done on an area percent model due to the problem that the pelitic rocks had been incorporated into the vitrified melt areas and so this caused a problem if the analysis was just done on a simple numerical clast count. Figure 52 illustrates the lithological make-up of the in-situ areas of the vitrified remains. This shows that the greatest area of the vitrified remains is associated with pelitic material. With calcareous pelite, layered calcsilicate, granite and quartz also heavily featured in the vitrified material. Therefore, it can be seen that pelitic rocks have made up the majority of the lithologies that make up the rubble core of Dun Deardail. This pattern is consistent around the remains of the hillfort and there is a lack of variability in the build of the hillfort.

Cut excavated samples, uncut excavated sample and in-situ samples on the rampart remains were observed for minerals visible, evidence of melting and dehydration and deformation. Figure 53 gives an example of a cut vitrified clast excavated from Dun Deardail. Several other example photographs have been included throughout this thesis and have also been uploaded to the link provided in the appendix. From results from the experimental melts results in chapter 4, the melting temperatures and rock characteristics have been identified these can be classes are known elements and allow visual comparison with what has been observed on Dun Deardail. In the experimental melts, the pelitic material had become fluid and boiled by 1140˚C, leaving vesicles, like those seen in Figure 53. Area A shows the pelitic mix melt, containing vesicles. Area B is dehydrated calcitic layers. Area C is the vesicled calcsilicate. These are all consistent with the experimental melt results from around 1140˚C. This suggests that the melt reached at least this temperature.

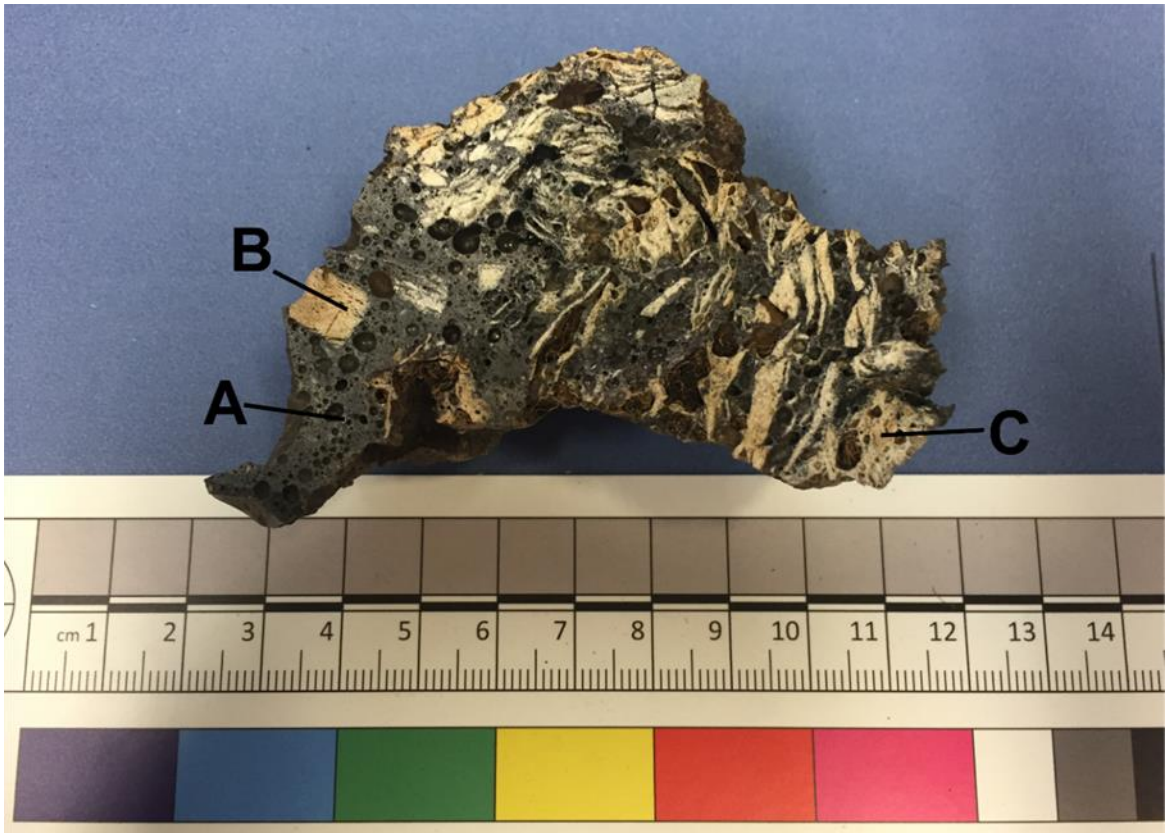

Figure 53:Slice of a vitrified clast from Dun Deardail.

Figure 54: Left, mixed lithologies melted in the furnace at 1150˚C. Right, excavated sample from Dun Deardail, trench 6.

Figure 54 illustrates the similarities between the furnace melted rock and the excavated samples found at Dun Deardail. The vitrified clasts are generally solid and visually show little sign of weathering or degradation. They can be dropped onto a solid surface from a height of one and a half metres and no damage occurs. The calcitic areas are

slightly friable on some clasts, and the areas that are granite are a little more friable, and some will crumble to the touch.

During the 2015-2017 excavation seasons of Dun Deardail, many pieces of burnt bone were found in the rubble in all the trenches (Cook, 2015; Cook and Heald, 2016; Cook et al., 2017). Figure 55 displays the cast marks that are observed on most of the clasts. The prints appear to be from where the melted rock has set onto charred timbers. As these prints go through the rubble core, this informs that the Dun Deardail was timberlaced. Large charcoal beams were also uncovered running through the rubble core, during excavation. Some of these beams had disintegrated into their constituent ashes, as was observed during excavation. Melted rock pipes are also visible on many of the clasts (Figure 55 right). These would have been formed as the melted rock would still have been very viscous, like when you squash a partially melted marshmallow between two chocolate digestives. The melted rock is too viscous to run out so is squashed with the weight of the remaining structure above.

Figure 55:DD29 showing cast marks and pipes

5.1.2 p-XRF

The p-XRF analysis was carried out on the excavated clasts from the excavations carried out in 2015 and 2016. Samples from five trenches were examined. Thirteen samples from trench one, thirteen samples from trench two, three samples from trench three, fifteen samples from trench four and thirteen samples from trench six. These numbers were constrained by samples that were of the correct size to cut on the

Petrosaw and sample availability in each trench. No samples were collected from trench five as it does not come in contact with the wall. GCD Toolkit for R was used to produce the data plots (Janoušek et al., 2006).

Table 28 shows the average p-XRF results of cut excavated clasts from each of the trenches. The data was used to construct a ternary diagram, using aluminium, silicon and iron as its ends, as these are common rock-forming elements found in pelitic rocks. A spider graph has also been created to illustrate the differences in elements detected in excavated clasts compared with the elements found in local pelitic rock and also with rock from Craig Phadrig, The Torr and Knockfarrel. This diagram has been normalised to the local rock to allow this comparison. The data has also been used to create two plates of bivariate plots to allow visual representation of different elements compared mainly to silicon and three against iron. Again, with these plots, the main elements found in rock building minerals were used for comparison, as the differences between these can show a fingerprint for local rock used. If the compositions are similar, then it is likely that the rocks are from the same source. These diagrams have been used for all of the p-XRF geochemical work.

Table 28: XRF elemental data on average pelitic rock measured from each trench

sample	Si	Fe	Mn	Cr	Ti	Ca	K	Al	Ba	Nb	Zr	Sr	Rb	Mg	Zn	P
Units	%	%	ppm	ppm	%	%	%	%	ppm	ppm	ppm	ppm	ppm	%	ppm	%
Local	278892	52101	622	181	4828	31355	28681	76100	827	14	259	142	133	39082	162	1468
Trench 1	305360	58016	627	186	4300	32180	29750	86710	815	15	249	148	144	36538	154	1505
Trench 2	318164	50413	649	180	4087	30115	30191	80499	861	14	282	152	132	38290	157	1527
Trench 3	274545	50862	614	182	3980	26842	26557	88696	953	19	284	157	121	42209	153	1360
Trench 4	309548	52845	623	180	4327	32156	32310	85230	867	15	237	154	127	35954	144	1468
Trench 6	301639	54284	647	180	4222	31056	27769	85801	807	13	251	158	131	37247	159	1416

The ternary diagram in Figure 56 illustrates that the composition of aluminium, silicon and iron are very similar between the trenches and also compared to the local rock and illustrates the differences with rock from Craig Phadrig, The Torr and Knockfarrel. This is further evidenced in the spider plot of Figure 57. also suggest that the pelite is local, with most readings falling in the same areas as each other.

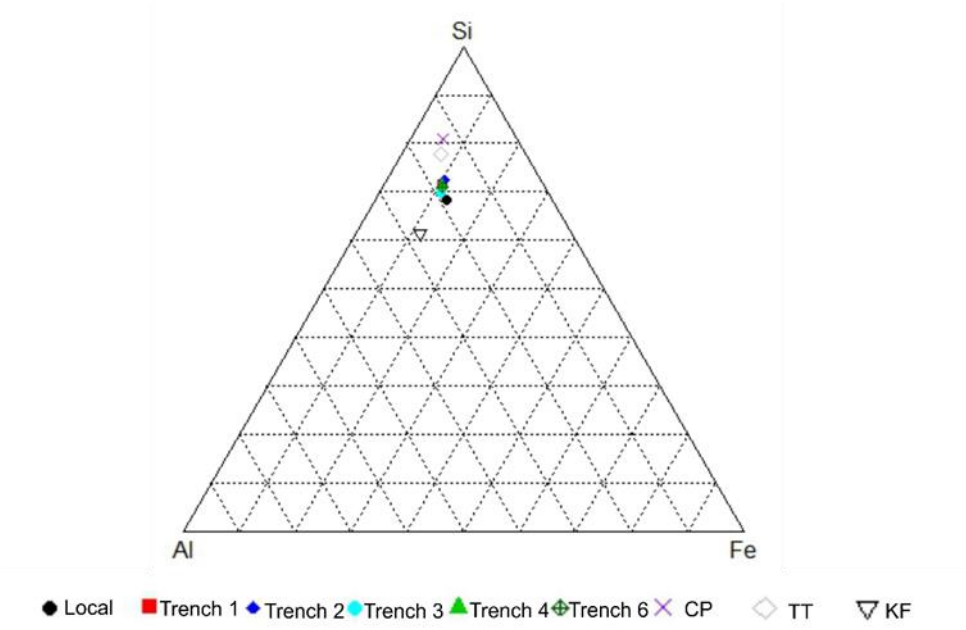

Figure 56: Aluminium - Silicon - Iron ternary diagram of p-XRF data for pelitic clasts excavated from trenches compared with local pelitic rock and samples from Craig Phadrig (CP), The Torr (TT) and Knockfarrel (KF)

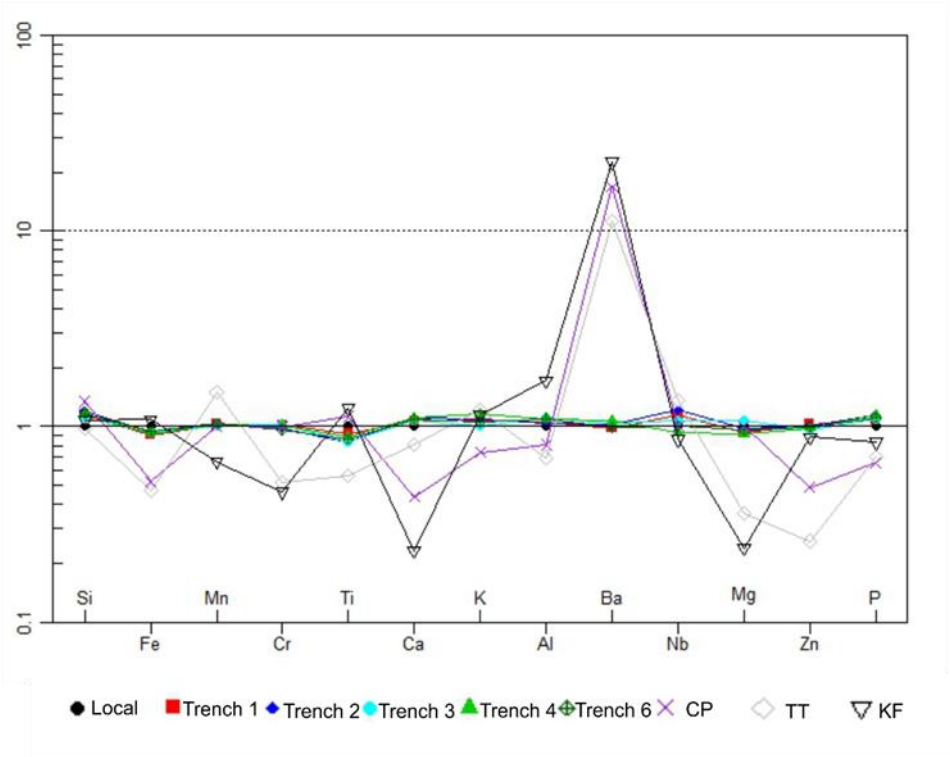

Figure 57: Elemental spider plot for average p-XRF results from pelitic samples excavated from all trenches and with samples from the local geology, compared to local rock and samples from Craig Phadrig (CP), The Torr (TT) and Knockfarrel (KF).

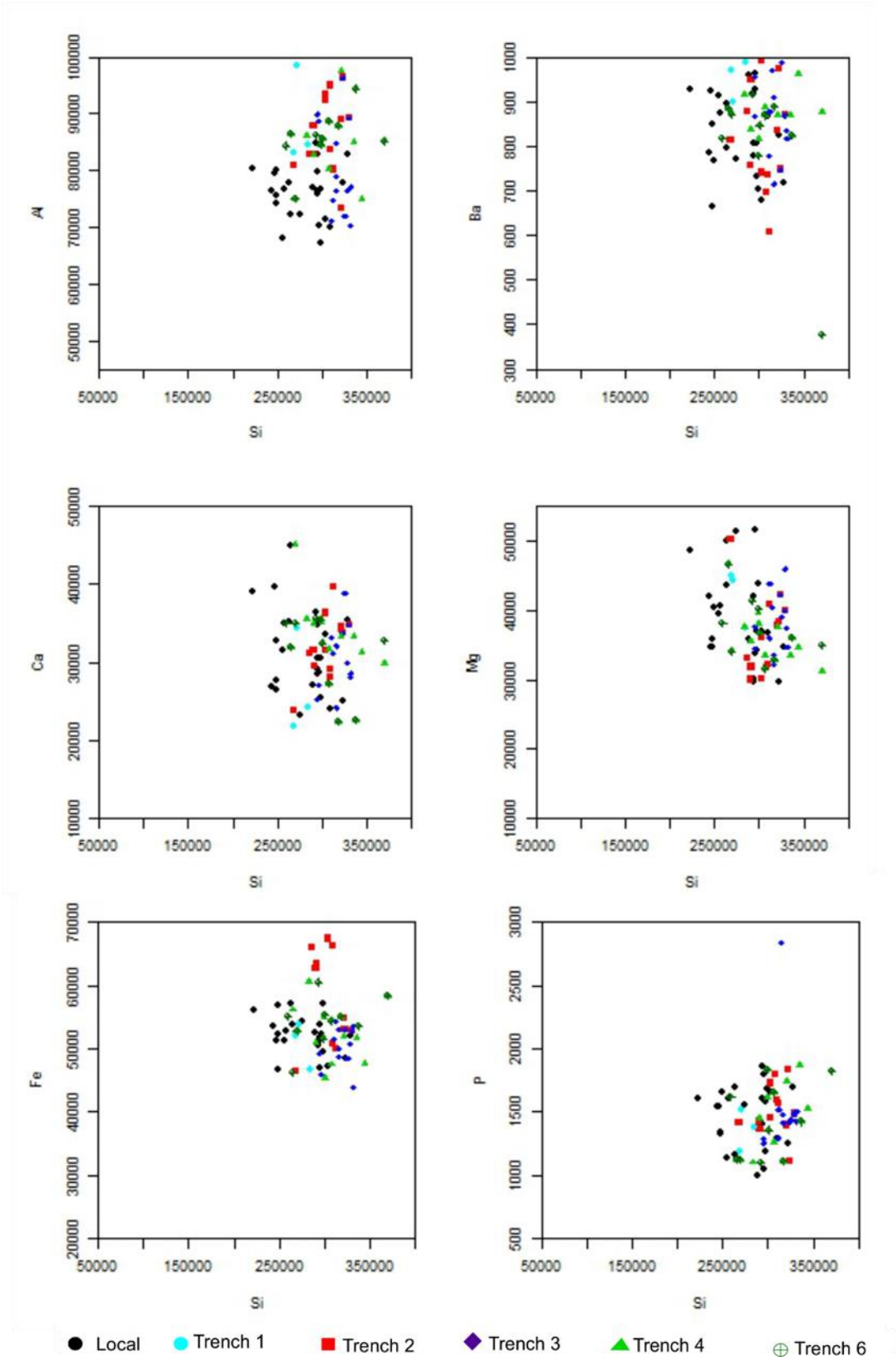

Figure 58: Bivariate box plots of p-XRF data for the pelitic portions of the clasts from all trenches compared with each other and to the local pelitic rock.

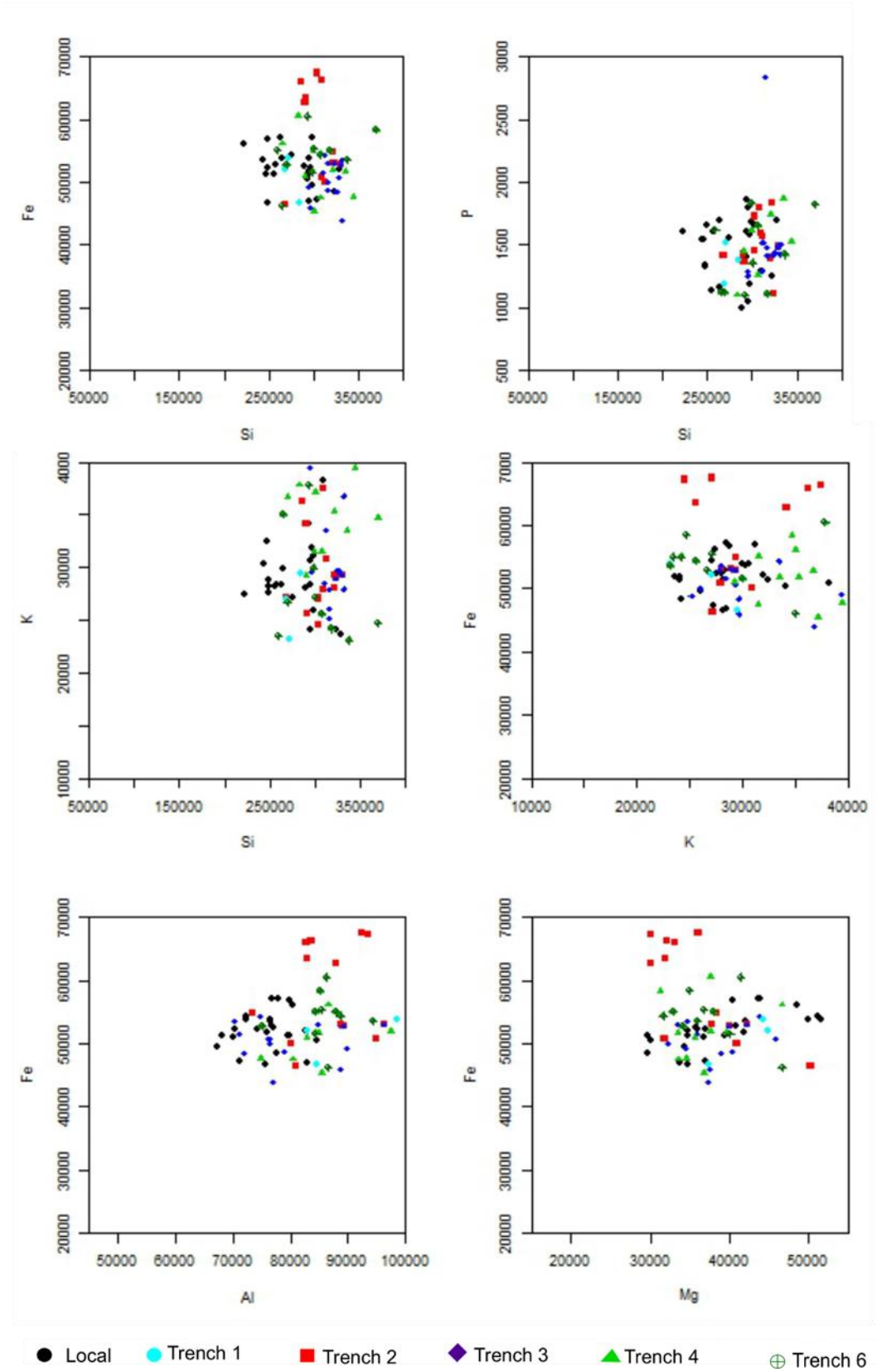

Figure 59: Bivariate box plots of p-XRF data for the pelitic portions of the clasts from all trenches compared with each other and to the local pelitic rock.

the p-XRF data, displayed in Table 29, for the quartz rocks were displayed as ternary, spider and bivariate plots. In the ternary diagram, Figure 60, the silicon is displayed as divided by one hundred and the iron is multiplied by ten, due to quartz having such high silicon and low iron quantity. This allows the data ternary diagram to be visible, rather than being clumped at the silicon end.

Table 29: p-XRF elemental data on average quartz rock measured from each trench.

sample	Si	Fe	Ti	Ca	K	Al	Ba	S	P
Units	%	%	%	%	%	%	ppm	%	%
Local	459970	362	46	200	2516	8350	200	520	868
Trench 1	463494	326	44	194	2661	8806	183	536	864
Trench 2	462100	346	41	178	2771	8884	198	528	852
Trench 3	470778	379	38	204	2888	8911	180	489	847
Trench 4	448477	349	47	190	2472	9046	167	543	885
Trench 6	449522	376	44	203	2550	8483	189	553	914

Figure 60 and Figure 61 illustrate the similarities between the elements between the trenches and also with the local rock and illustrates the differences with rock from Craig Phadrig, The Torr and Knockfarrel. This is further backed up by the results from the bivariate plots Figure 62 and Figure 63. The results suggest that the quartz used in the construction is local.

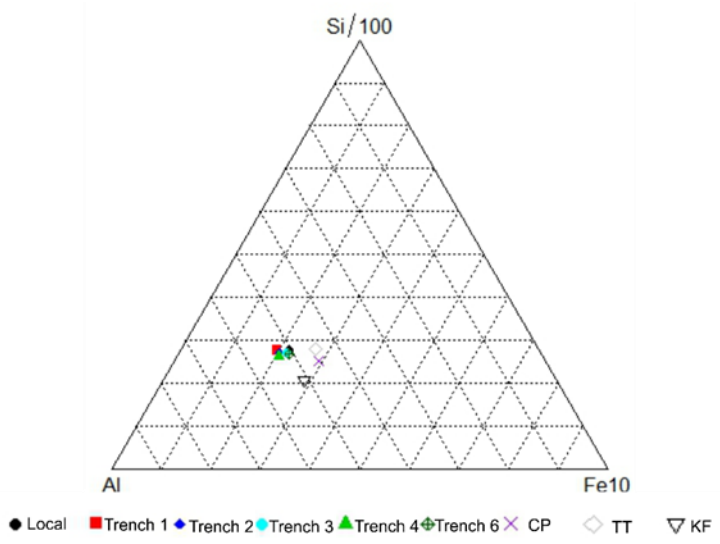

Figure 60: Aluminium - Silicon - Iron ternary diagram of p-XRF data for quartz clasts excavated from trenches compared with local quartz rock and samples from Craig Phadrig (CP), The Torr (TT) and Knockfarrel (KF)

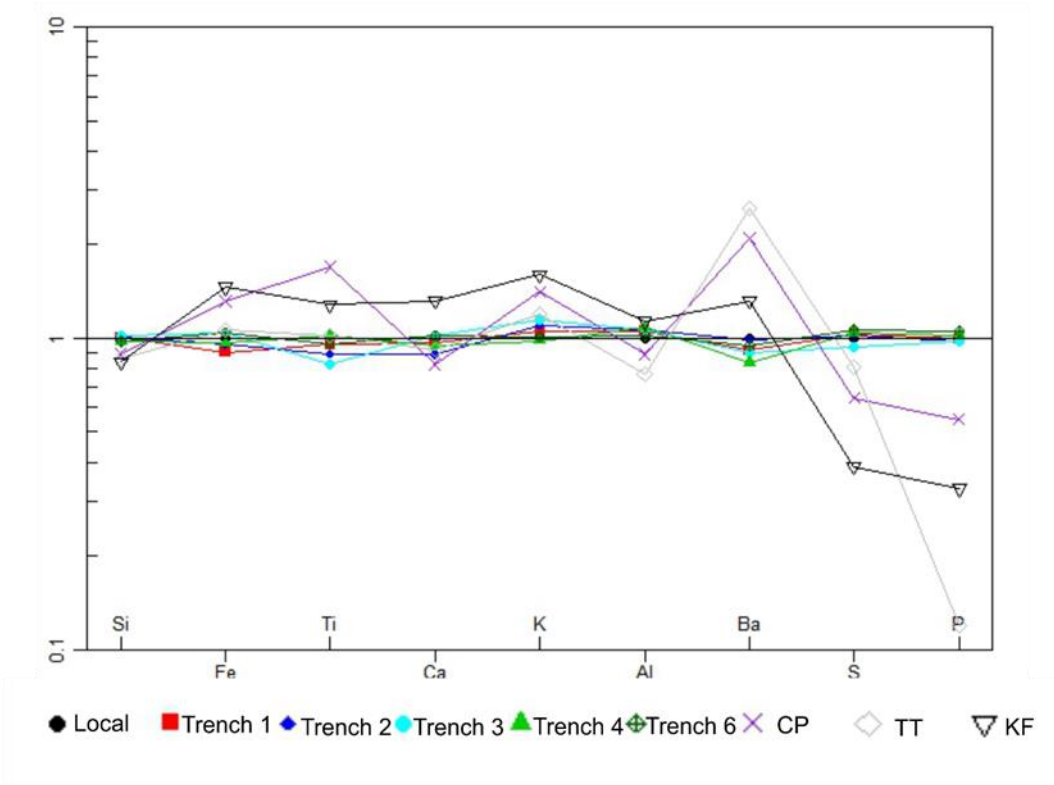

Figure 61: Spider plot of average p-XRF data of quartz rocks from excavated trenches compared with local quartz rock, compared to local rock and samples from Craig Phadrig (CP), The Torr (TT) and Knockfarrel (KF).

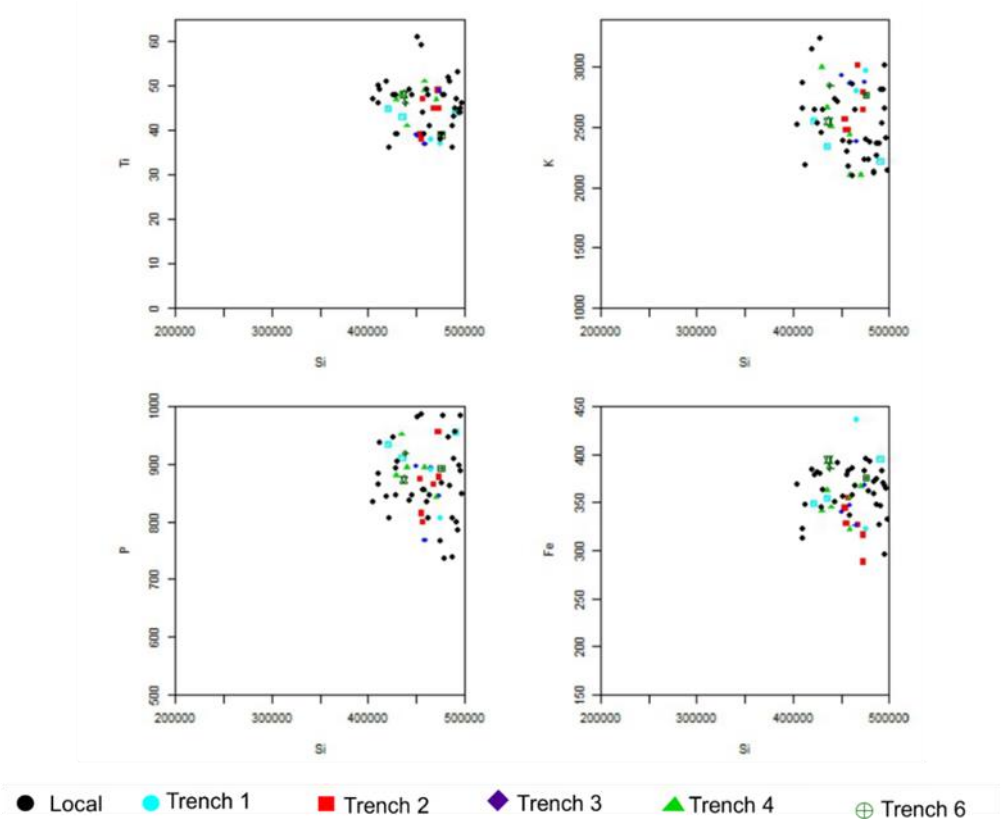

Figure 62: Bivariate plots of p-XRF data of quartz rocks from excavated trenches compared with local quartz rock.

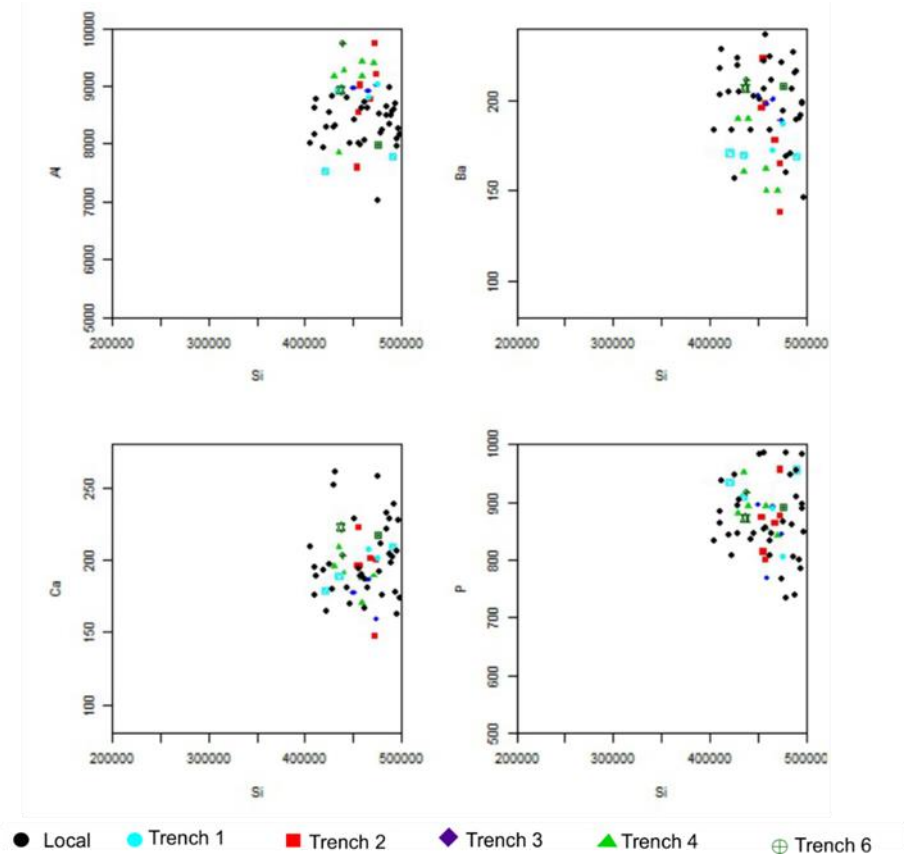

Figure 63: Bivariate plots of p-XRF data of quartz rocks from excavated trenches compared with local quartz rock.

the p-XRF data, displayed in Table 30, for the calcsilicate rocks was displayed as ternary, spider and bivariate plots.

Table 30: p-XRF elemental data on average calcsilicate rock measured from each trench.

SAMPLE	Si	Fe	Mn	Cr	V	Ti	Ca	K	Al	Ba	Nb	Zr	Sr	Rb	S	Mg	Zn	P	Cl
Units	%	%	ppm	ppm	ppm	%	%	%	%	ppm	ppm	ppm	ppm	ppm	%	%	ppm	%	ppm
Local	210399	39143	449	157	155	4981	75950	43773	66122	764	14	205	60	129	269	54212	201	1532	91
Trench 1	227819	36356	429	153	157	4839	76546	48588	64386	828	15	197	54	131	299	44520	169	1702	99
Trench 2	203159	37913	440	157	180	4936	78424	43817	61497	796	16	223	44	144	299	45337	198	1646	96
Trench 3	206626	32813	456	198	182	6051	78087	45352	67859	851	19	269	51	129	405	54635	210	1559	101
Trench 4	203645	39705	465	178	196	5791	79816	51724	64920	886	19	256	56	173	428	53127	213	1606	96
Trench 6	185953	44659	425	203	193	5114	80799	42192	63820	794	18	220	55	151	384	50462	201	1780	93

Figure 52, Figure 53 and Figure 53 illustrate the similarities between the elements between the trenches and also with the local rock and illustrates the differences with rock from Craig Phadrig, The Torr and Knockfarrel. This is further backed up by the results from the bivariate plots Figure 54 and Figure 55. The results suggest that the calcsilicate rock used in the construction is local.

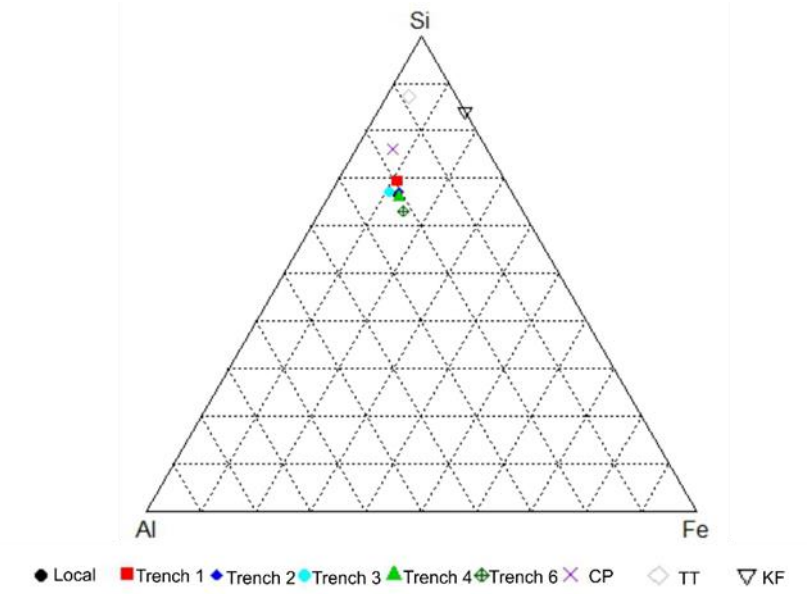

Figure 64: Aluminium - Silicon - Iron ternary diagram of p-XRF data for calcsilicate clasts excavated from trenches compared with local calcsilicate rock and samples from Craig Phadrig (CP), The Torr (TT) and Knockfarrel (KF).

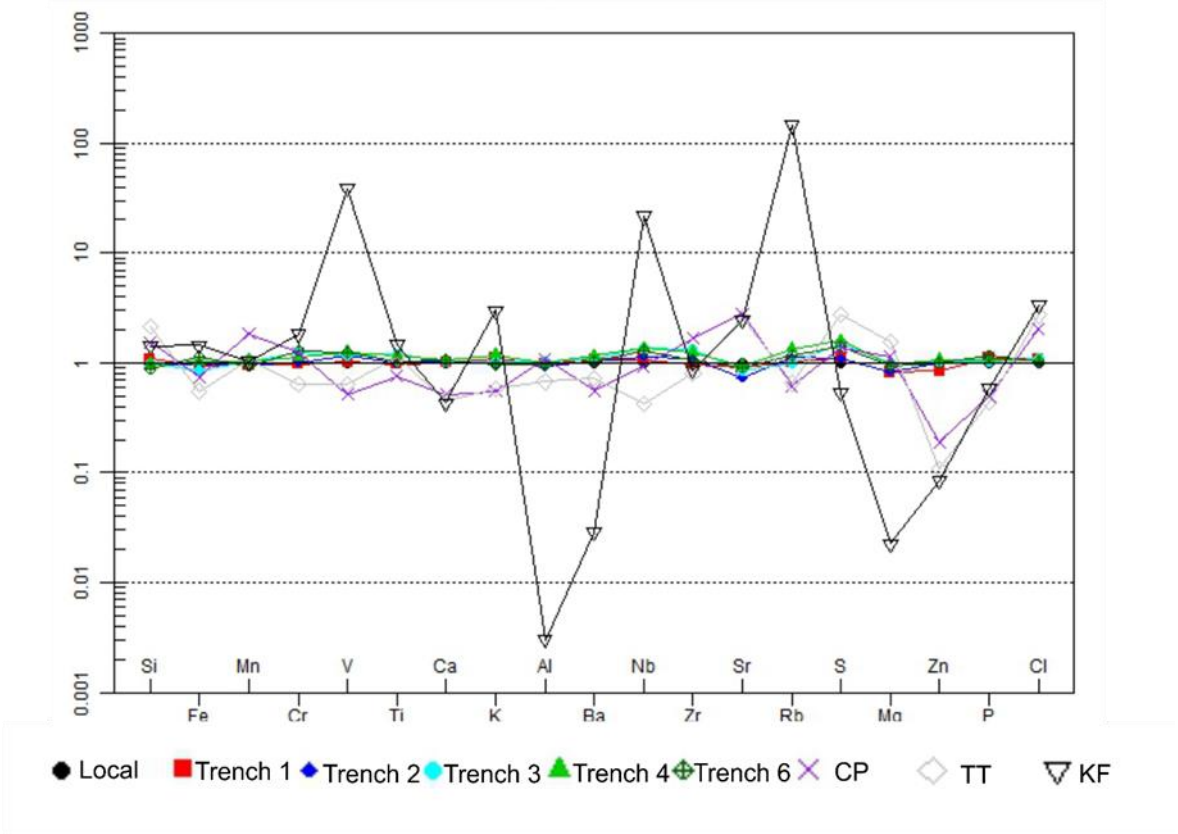

Figure 65: Spider plot of average p-XRF data of calcsilicate rocks from excavated trenches compared with local calcsilicate rock, compared to local rock and samples from Craig Phadrig (CP), The Torr (TT) and Knockfarrel (KF).

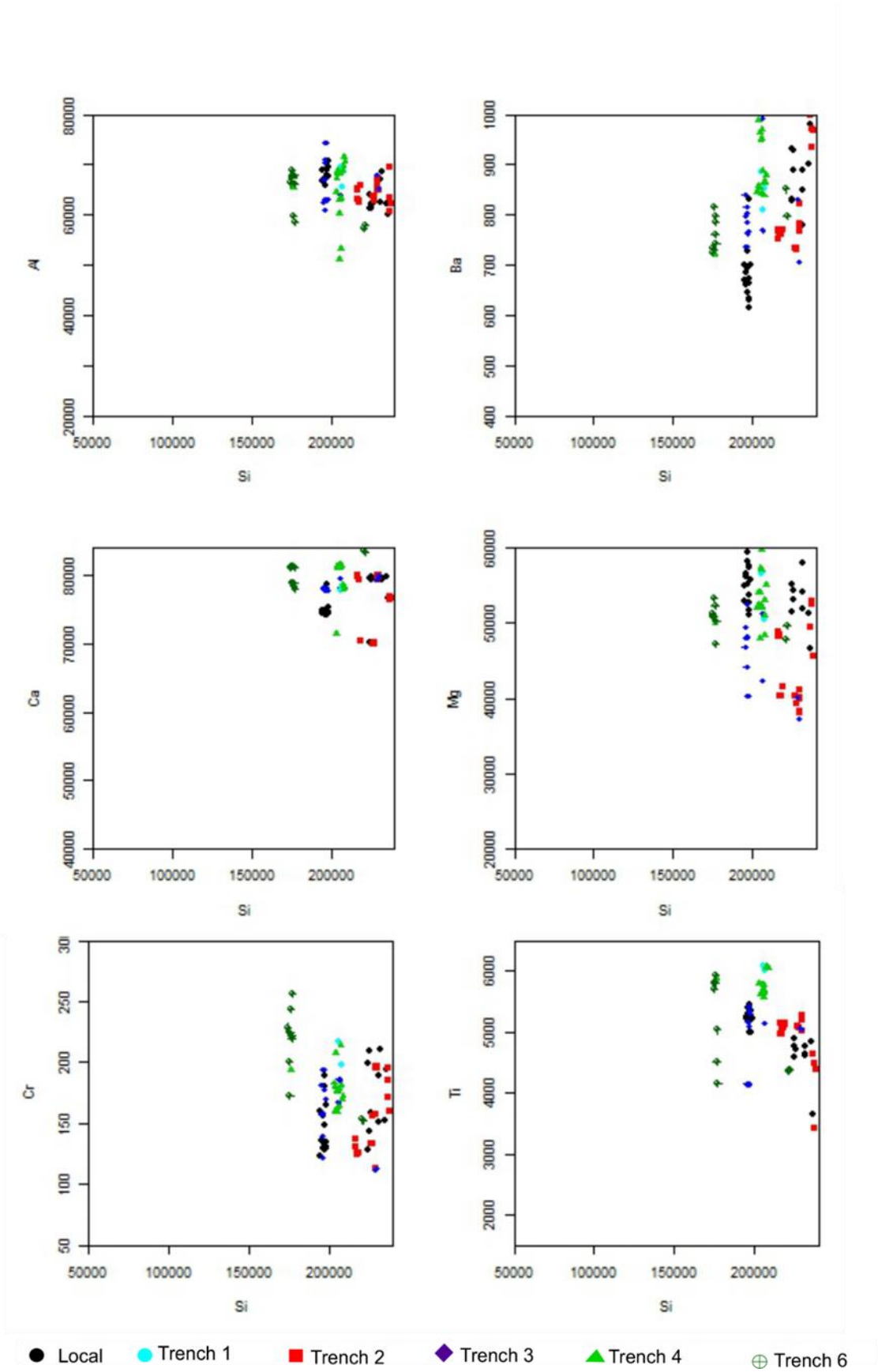

Figure 66: Bivariate plots of p-XRF data of calcsilicate rocks from excavated trenches compared with the local calcsilicate rock.

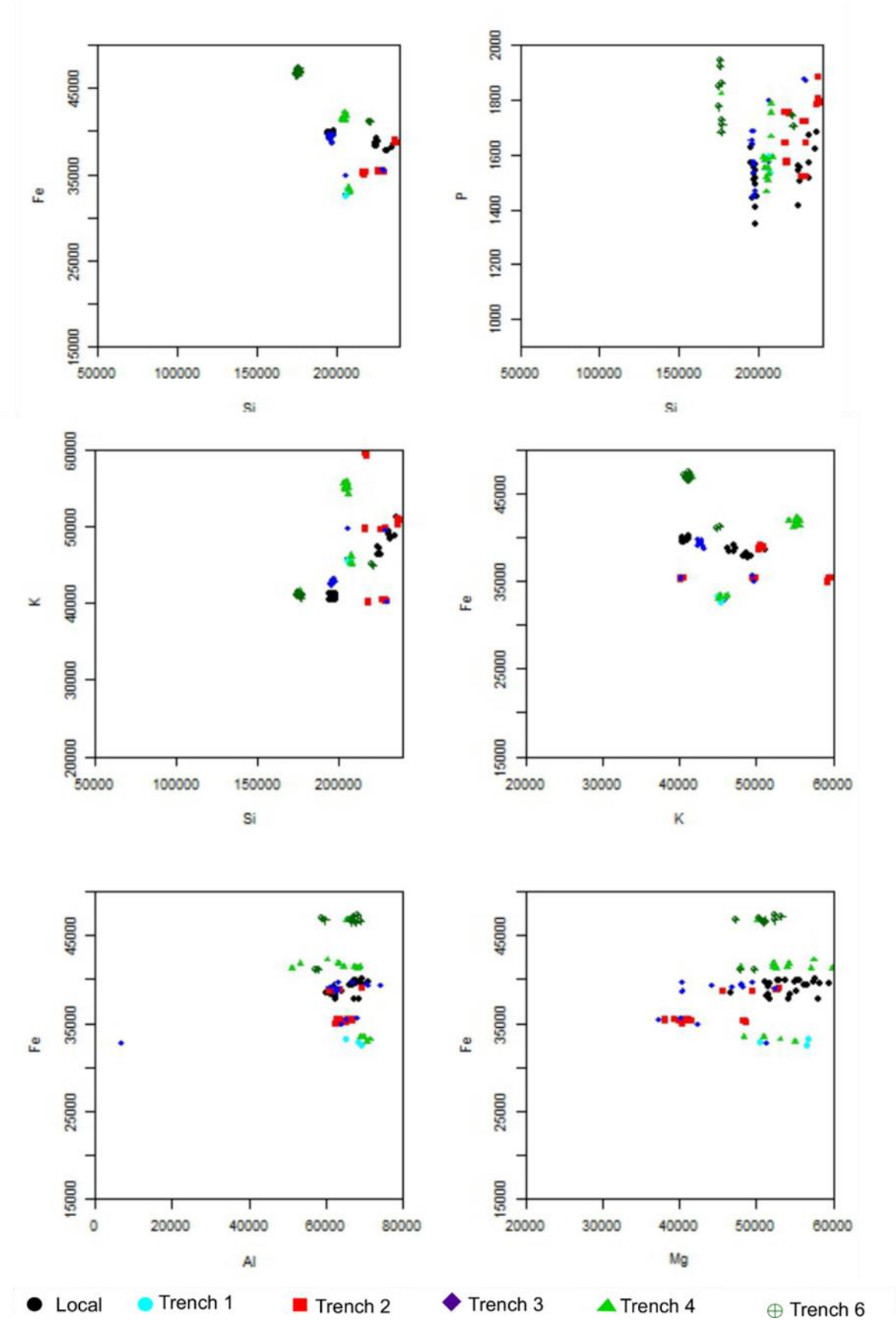

Figure 67: Bivariate plots of p-XRF data of calcsilicate rocks from excavated trenches compared with the local calcsilicate rock.

Eight areas in the vitrified remains were assessed visually and analysed using p-XRF (Figure 56). These areas, combined with the excavated trenches, also shown in Figure 56, give provenance results for around the entire hillfort.

The p-XRF analysis was carried out at the points shown in Figure 56 during the second excavation season in 2016, using the Thermo Fisher Scientific Nitron XL3 analyzer p-XRF in handheld mode.

The p-XRF results for the pelitic portions of the vitrified material in the areas shown in Figure 56. The data from the in-situ analysis was combined with the data from the p-XRF analysis on the pelitic portions of the excavated material to produce p-XRF data for all around the vitrified remains, shown in Table 31. This data was used to produce a spider plot, normalised to local pelitic rock, Figure 68, and two plates of bivariate plots, Figure 69 and Figure 70.

Table 31: p-XRF results for all pelitic samples, in-situ and excavated.

sample	Si	Fe	Mn	Cr	Ti	Ca	K	Al	Ba	Nb	Zr	Sr	Rb	Mg	Zn	P
Units	%	%	ppm	ppm	%	%	%	%	ppm	ppm	ppm	ppm	ppm	%	ppm	%
Local	278892	52101	622	181	4828	31355	28681	76100	827	14	259	142	128	39082	162	1468
Area 1	244811	50035	554	175	4404	29598	27866	77524	800	16	268	140	96	42488	144	1640
Area 2	272155	48003	640	172	5213	35405	23808	73437	763	15	235	128	103	48549	158	1386
Area 3	249895	47916	602	179	4779	37286	24912	69650	788	15	232	155	123	47049	136	1650
Area 4	250278	50723	566	175	4573	37720	26855	73720	888	17	229	135	122	39882	152	1577
Area 5	285111	45201	552	182	4342	34066	27044	72596	775	17	252	169	132	43719	165	1612
Area 6	225808	48327	595	189	4660	34854	26223	76328	844	16	256	139	141	46461	137	1512
Area 7	259220	50342	603	184	4696	33551	26628	78080	897	17	277	126	125	48855	152	1670
Area 8	267238	48222	573	179	4515	33390	22997	73520	779	18	267	122	122	49241	155	1650
Trench 1	305360	58016	627	186	4300	32180	29750	86710	815	15	249	148	144	36538	154	1505
Trench 2	318164	50413	649	180	4087	30115	30191	80499	861	14	282	152	132	38290	157	1527
Trench 3	274545	50862	614	182	3980	26842	26557	88696	953	19	284	157	121	42209	153	1360
Trench 4	309548	52845	623	180	4327	32156	32310	85230	867	15	237	154	127	35954	144	1468
Trench 6	301639	54284	647	180	4222	31056	27769	85801	807	13	251	158	131	37247	159	1416

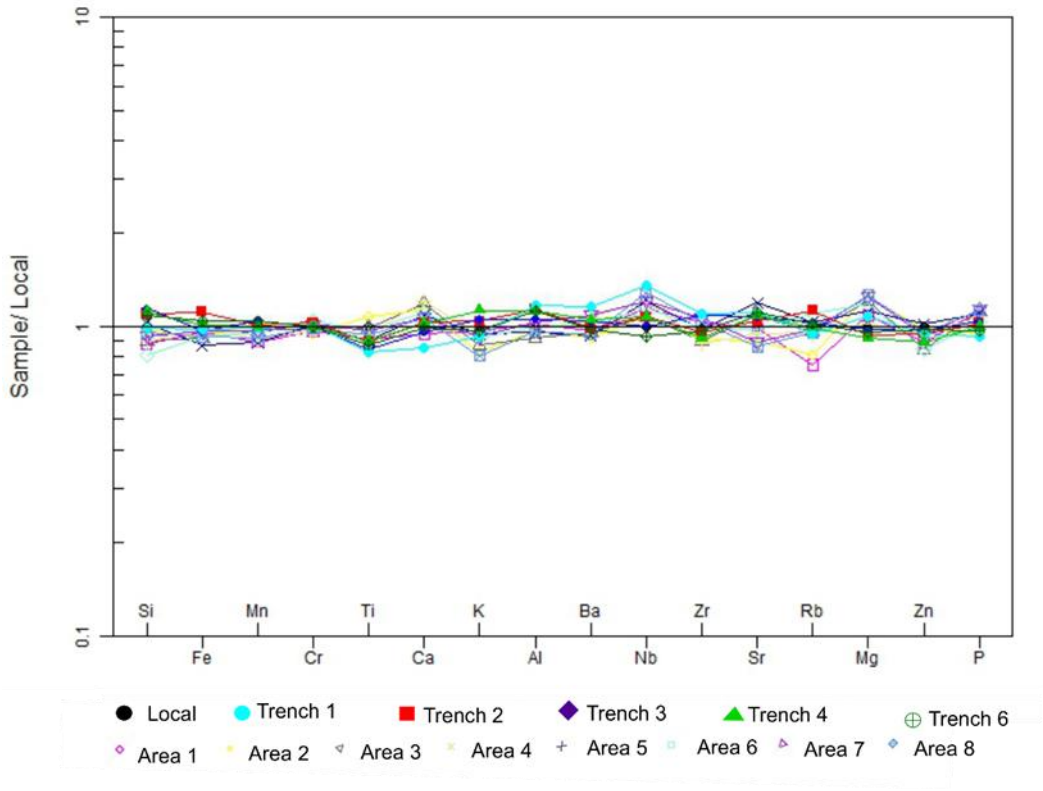

Figure 68: Spider plot of pelitic rocks from in-situ p-XRF analysis from areas shown in Figure 56 compared with local pelitic rock, normalised to local rock, using data from Table 26. As it was shown earlier in the chapter that each hillfort has a distinct fingerprint, other hillforts have been omitted from this chart.

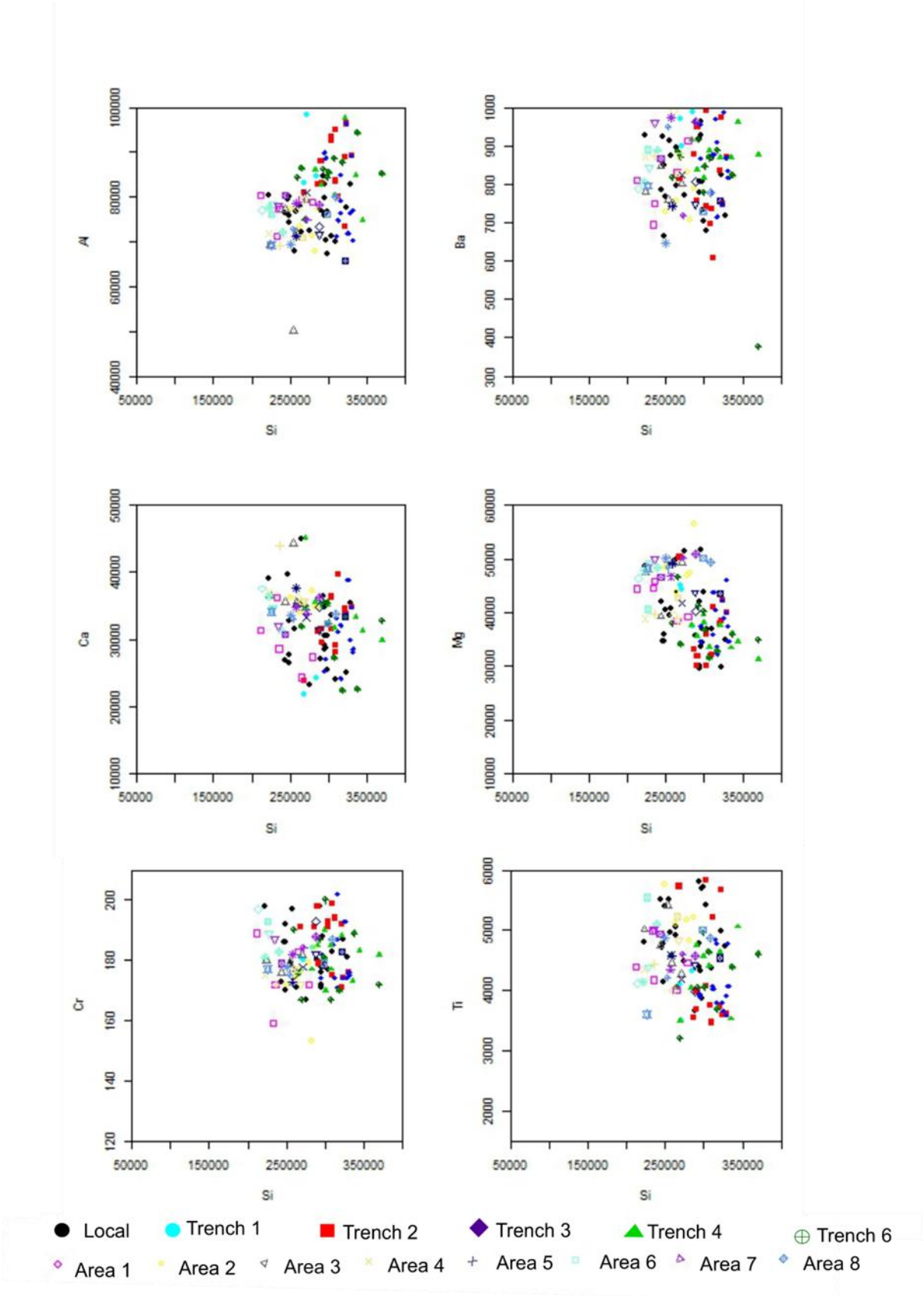

Figure 69: Bivariate plots of pelitic rocks from in-situ p-XRF analysis from areas shown in Figure 56 compared with the local pelitic rock.

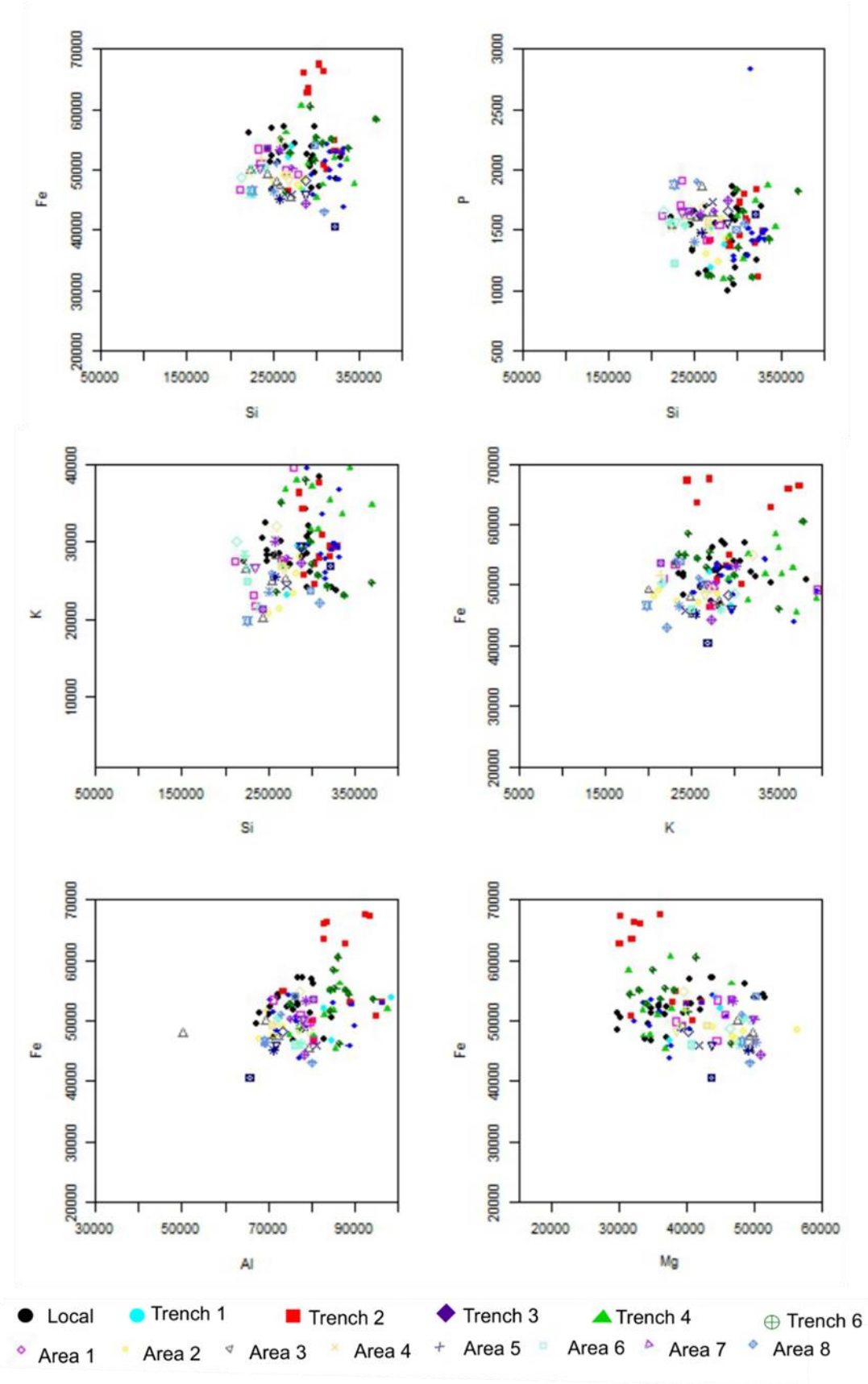

Figure 70: Bivariate plots of pelitic rocks from in-situ p-XRF analysed from areas shown in Figure 56 compared with the local pelitic rock.

The p-XRF results for the quartz portions of the vitrified material in the areas shown in Figure 51 was combined with the data from the laboratory p-XRF analysis on the quartz portions of the excavated material to produce p-XRF data for quartz material all around the vitrified remains, shown in Table 32. This data was used to produce a spider plot, normalised to local pelitic rock, Figure 71, and two plates of bivariate plots, Figure 72 and Figure 73.

Table 32: p-XRF results for all quartz samples, in-situ and excavated.

sample	Si	Fe	Ti	Ca	K	Al	Ba	S	P
Units	%	%	%	%	%	%	ppm	%	%
Local	459970	362	46	200	2516	8350	200	520	868
Area 1	459028	353	66	176	2709	8593	163	523	837
Area 2	461593	330	47	185	2599	8127	173	550	841
Area 3	444066	401	42	161	2644	8079	186	507	919
Area 4	477028	354	47	168	2594	8218	182	468	859
Area 5	477436	375	44	167	2753	8015	198	545	762
Area 6	452961	388	51	174	2549	8612	217	513	838
Area 7	422529	360	47	184	2667	7968	190	510	852
Area 8	405428	381	46	210	2682	8148	188	523	879
Trench 1	463494	326	44	194	2661	8806	183	536	864
Trench 2	462100	346	41	178	2771	8884	198	528	852
Trench 3	470778	379	38	204	2888	8911	180	489	847
Trench 4	448477	349	47	190	2472	9046	167	543	885
Trench 6	449522	376	44	203	2550	8483	189	553	914

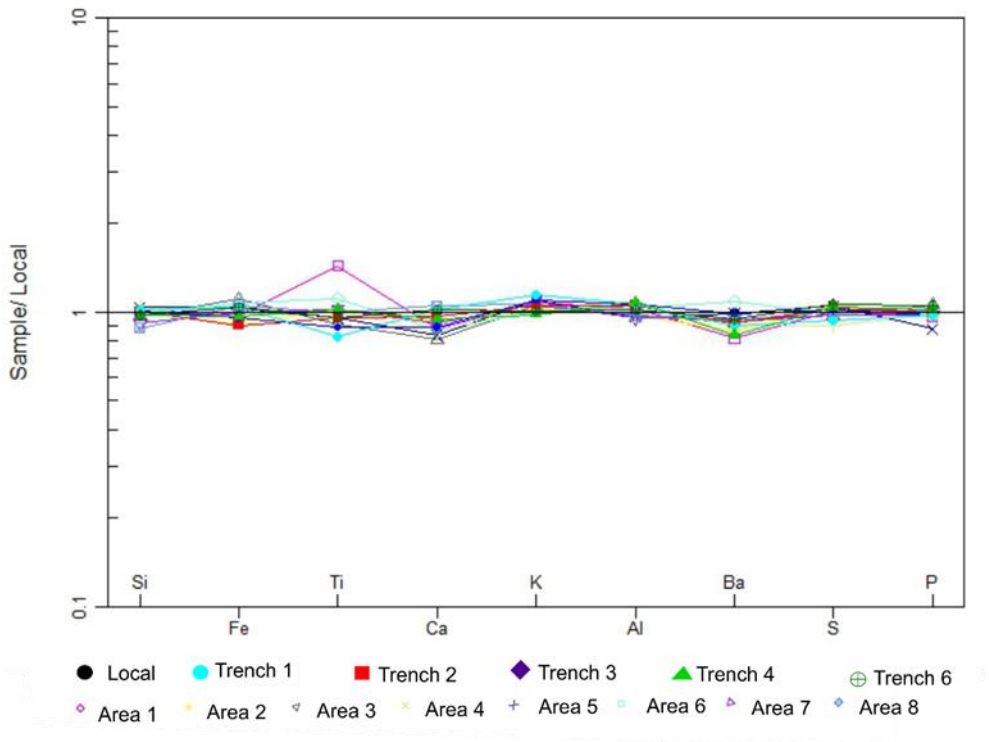

Figure 71: Spider plot of quartz rocks from in-situ p-XRF analysis from areas shown in Figure 56 compared with local quartz rock, normalised to local rock, using data from Table 29. As it was shown earlier in the chapter that each hillfort has a distinct fingerprint, other hillforts have been omitted from this chart.

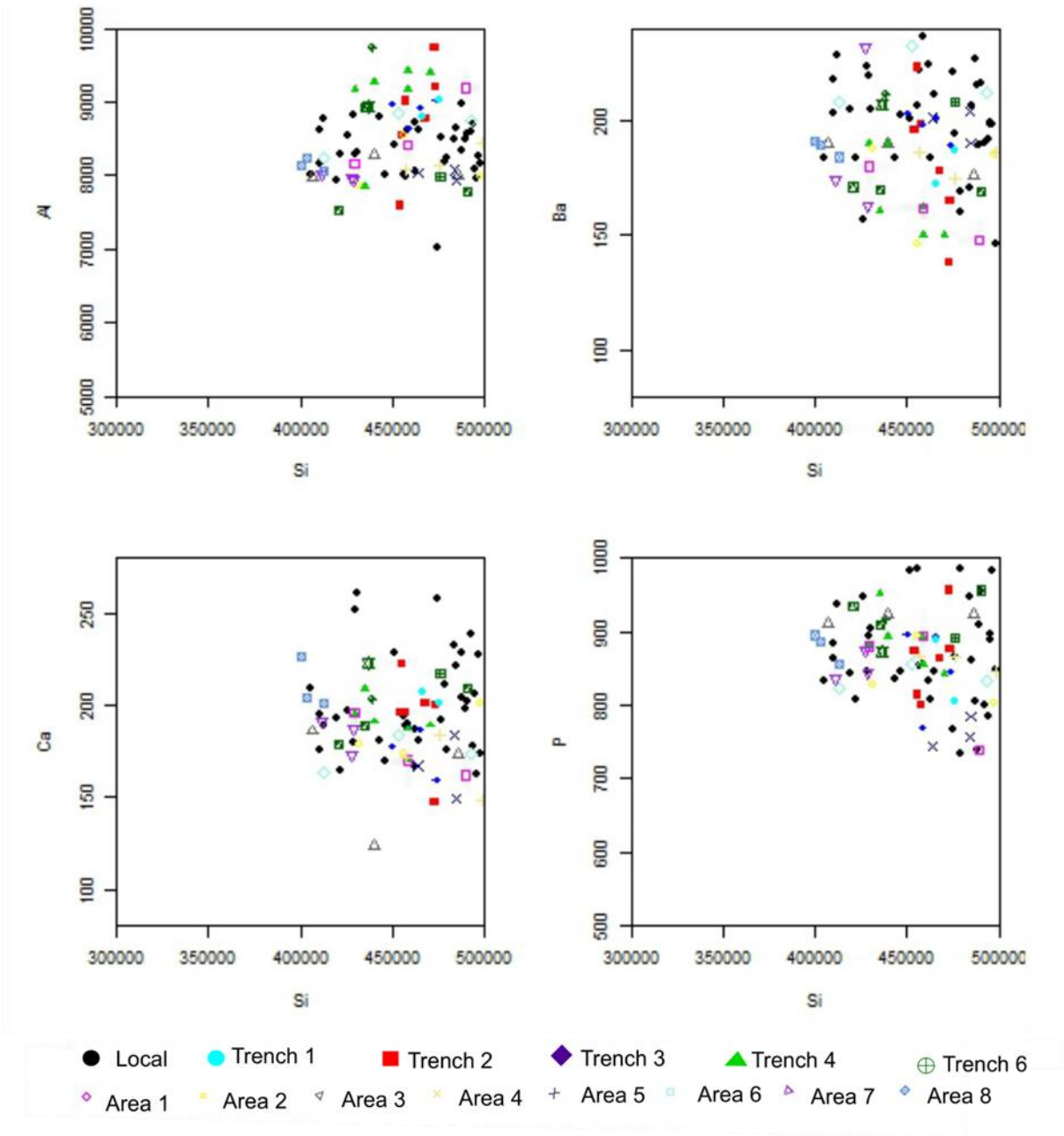

Figure 72: Bivariate plots of quartz rocks from in-situ p-XRF analysed from areas shown in Figure 56 compared with local quartz rock.

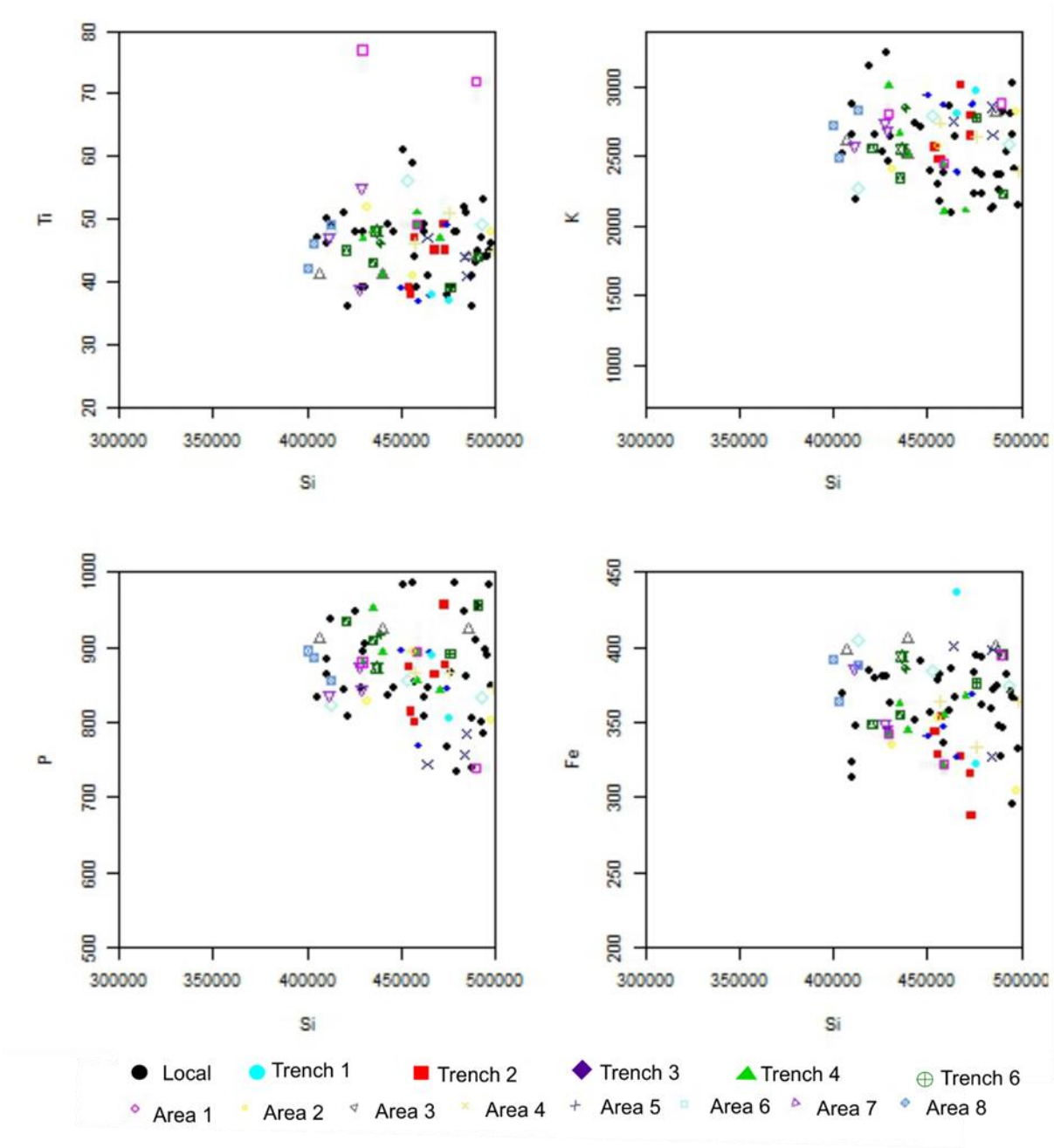

Figure 73: Bivariate plots of quartz rocks from in-situ p-XRF analysed from areas shown in Figure 56 compared with local quartz rock.

The p-XRF results for the calcsilicate portions of the vitrified material in the areas shown in Figure 51 was combined with the data from the p-XRF analysis on the calcsilicate portions of the excavated material to produce p-XRF data for calcsilicate material all around the vitrified remains, shown in Table 33. This data was used to produce a spider plot, normalised to local pelitic rock, Figure 74, and two plates of bivariate plots, Figure 75 and Figure 76.

Table 33: p-XRF results for all calcsilicate samples, in-situ and excavated.

SAMPLE	Si	Fe	Mn	Cr	V	Ti	Ca	K	Al	Ba	Nb	Zr	Sr	Rb	S	Mg	Zn	P	Cl
Units	%	%	ppm	ppm	ppm	%	%	%	%	ppm	ppm	ppm	ppm	ppm	%	%	ppm	%	ppm
Local	210399	39143	449	157	155	5022	75950	43773	66122	751	14	205	60	129	269	54212	201	1532	91
Area 1	199509	39911	407	161	164	4921	70213	48063	65517	687	14	158	57	138	258	54763	177	1480	96
Area 2	204425	38886	435	144	157	4935	74181	46408	65275	741	17	159	59	130	268	49136	186	1583	93
Area 3	192978	38630	469	164	180	5119	63417	49579	65406	715	18	187	51	127	303	45396	184	1519	93
Area 4	194517	41555	498	196	166	5039	65434	52589	63600	732	16	186	58	136	285	48212	184	1522	89
Area 5	199326	42161	516	177	169	4988	60332	54925	63370	738	16	185	61	126	310	54428	180	1494	84
Area 6	215295	40118	455	180	175	5139	63233	57053	67010	722	17	179	63	146	307	49304	189	1501	90
Area 7	238066	38831	501	146	174	4981	59098	56852	64747	808	17	188	64	140	286	51804	187	1511	90
Area 8	205605	40942	484	142	173	5169	59323	56279	61245	821	15	201	56	142	292	55307	194	1570	83
Trench 1	227819	36356	429	153	157	4839	76546	48588	64386	828	15	197	54	131	299	44520	169	1702	99
Trench 2	203159	37913	440	157	180	4936	78424	43817	61497	796	16	223	44	144	299	45337	198	1646	96
Trench 3	206626	32813	456	198	182	6051	78087	45352	67859	851	19	269	51	129	405	54635	210	1559	101
Trench 4	203645	39705	465	178	196	5791	79816	51724	64920	886	19	256	56	173	428	53127	213	1606	96
Trench 6	185953	44659	425	203	193	5114	80799	42192	63820	794	18	220	55	151	384	50462	201	1780	93

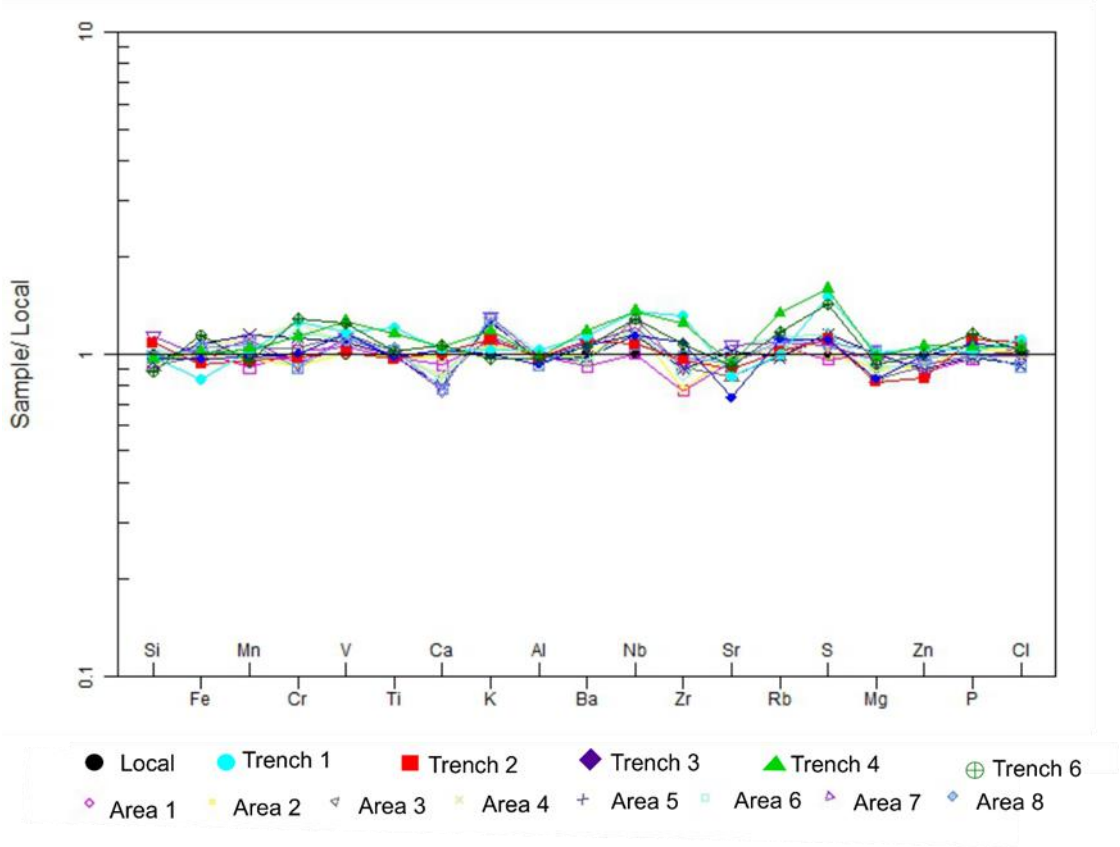

Figure 74: Spider plot of calcsilicate rocks from in-situ p-XRF analysis from areas shown in Figure 56 compared with local calcsilicate rock, normalised to local rock. As it was shown earlier in the chapter that each hillfort has a distinct fingerprint, other hillforts have been omitted from this chart.

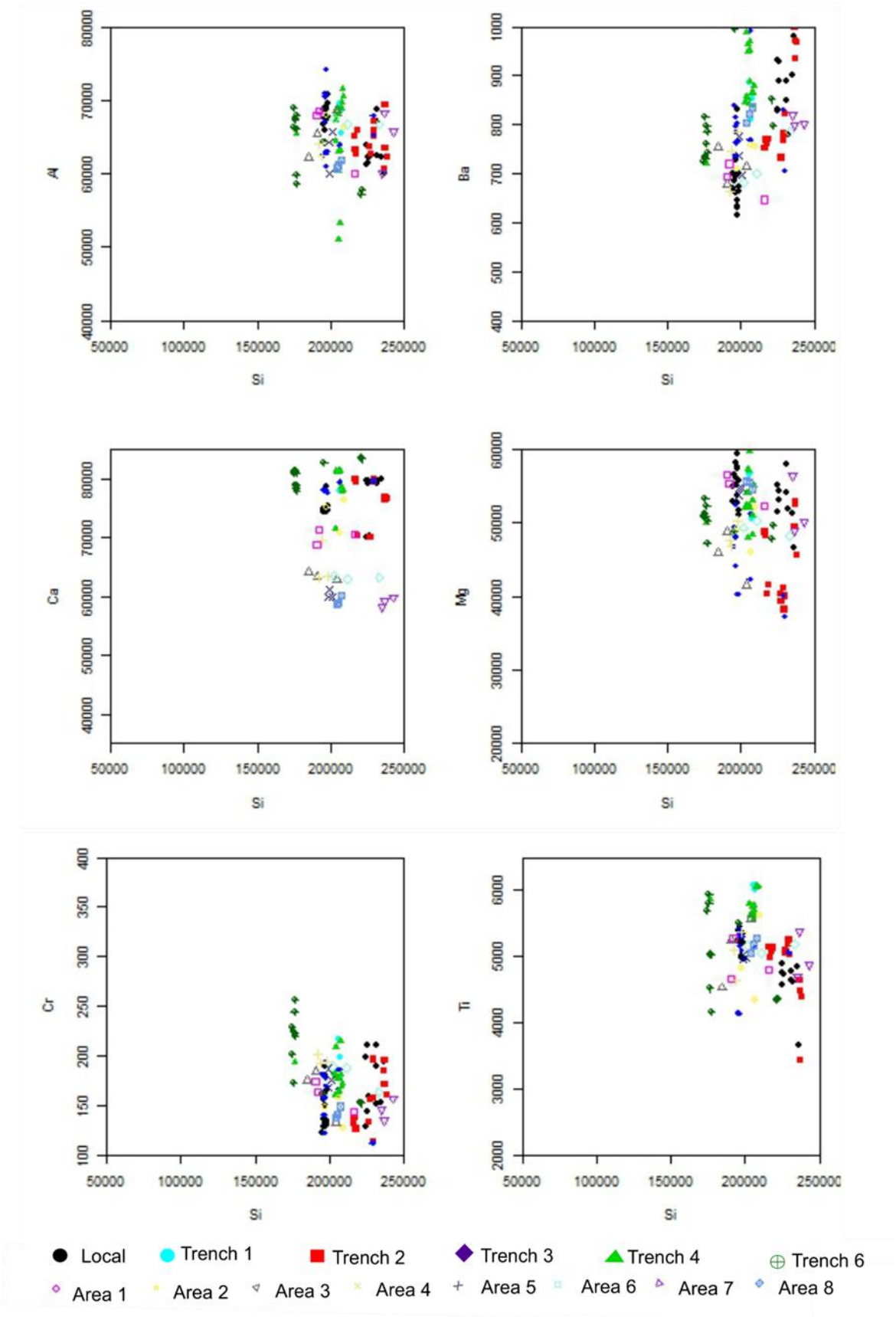

Figure 75: Bivariate plots of calcsilicate rocks from in-situ p-XRF analysed from areas shown in Figure 56 compared with the local calcsilicate rock.

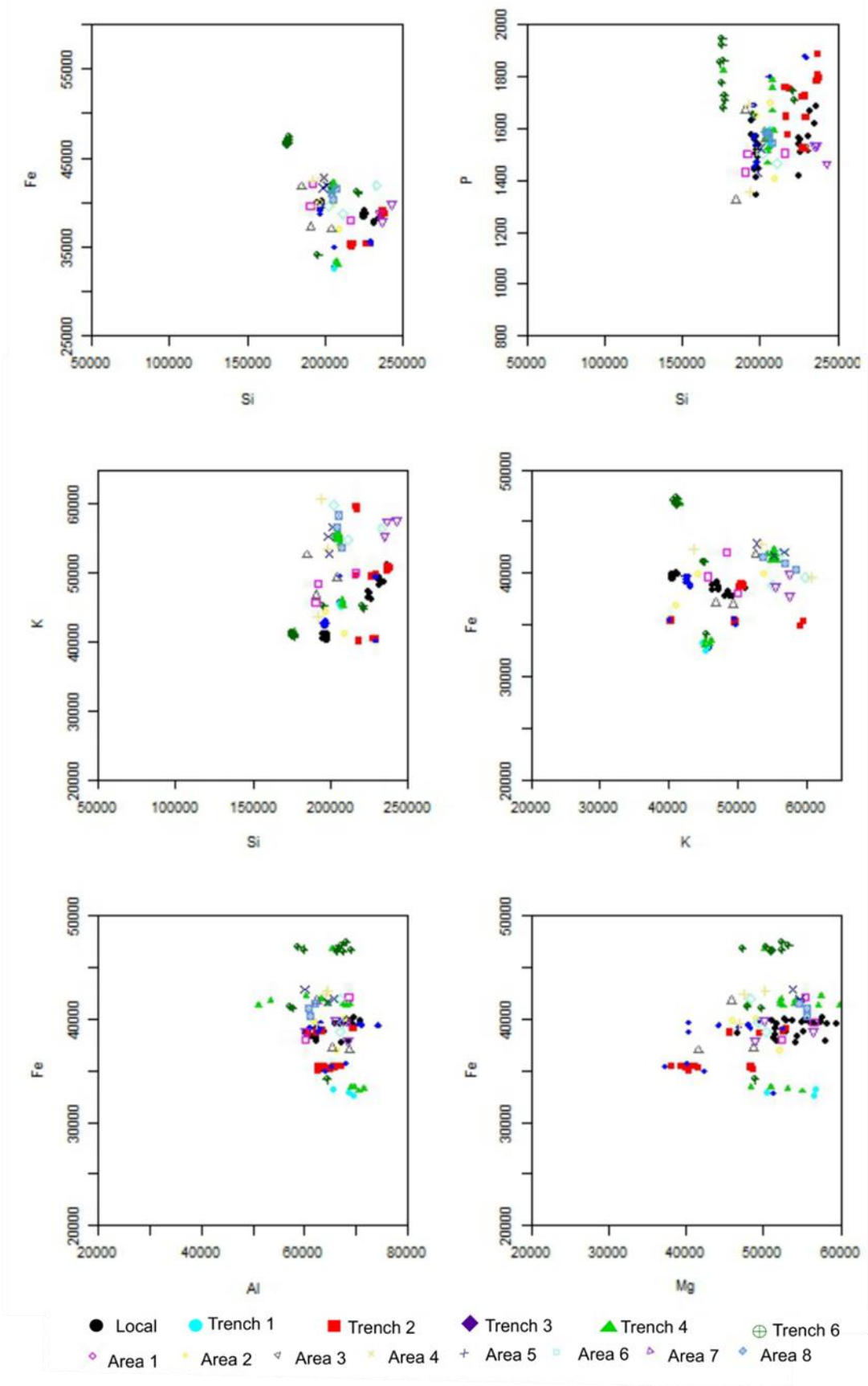

Figure 76: Bivariate plots of calcsilicate rocks from in-situ p-XRF analysed from areas shown in Figure 56 compared with the local calcsilicate rock.

As residue from the burn would also be incorporated into the ash and tumble, soils from trench 6 were analysed using p-XRF and compared with soil sampled from the local area. As each of the soils were from a known secure context in the trench, the differences as we go down the stratigraphy could be determined (Table 34). These results were plotted as a spider chart, normalised to local soil, to visually determine the changes in soil composition when going down the stratigraphy Figure 77. In contrast with the melt results, there is a slight drop in sulphur. Soils 1020 and 1021 show a substantial increase in phosphorus. Manganese has changed over all the soils, with some highly increased and one decidedly decreased. Chlorine mainly shows a reduction across all the soils. There are also smaller changes in most of the other elements.

Table 34: p-XRF results for soils collected from trench 6.

SAMPLE	Ti	Ca	K	Al	P	Si	Cl	S	Mg	Fe	Ba	Nb	Zr	Sr	Rb	Pb	Mn	Cr	V
Units	%	%	%	%	%	%	ppm	%	%	%	ppm	ppm	ppm	ppm	ppm	%	ppm	ppm	ppm
Base average	4330	18255	15144	50685	2816	252327	474	2208	13190	25321	346	13	275	85	77	19	771	175	115
dd16 1004 average	4342	18324	15223	52058	2947	253544	346	2163	15729	25729	368	14	274	86	75	21	733	179	123
dd16 1005 average	4221	22766	15529	58214	3022	243353	718	1803	20521	29248	257	13	239	85	62	12	1208	219	136
dd16 1006 average	4168	21695	12952	54136	2872	234411	512	2312	15448	33023	246	11	211	122	63	12	1169	439	125
dd16 1008 average	3651	13721	16176	57507	2408	206690	536	2388	9840	31000	387	11	220	147	73	14	174	207	120
dd16 1011 average	4121	21308	13374	65914	3146	221439	435	2069	20321	37749	342	12	217	79	65	15	1638	258	147
dd16 1015 average	3688	21507	14153	67270	3336	220265	244	2011	19369	28638	530	14	229	78	76	14	951	220	116
dd16 1016 average	4089	21436	14136	70811	3824	225791	369	1519	20172	32873	387	13	232	86	69	11	699	235	135
dd16 1017 average	4957	14554	18960	78791	3611	239412	222	1529	14243	32200	366	15	234	109	92	11	504	187	146
dd16 1020 average	3938	21481	14693	60478	8058	241839	151	1844	18605	28928	450	12	241	86	71	20	2711	156	119
dd16 1021 average	4069	23591	13483	66119	7743	222634	220	1170	23530	34011	544	12	228	84	66	11	1687	206	140

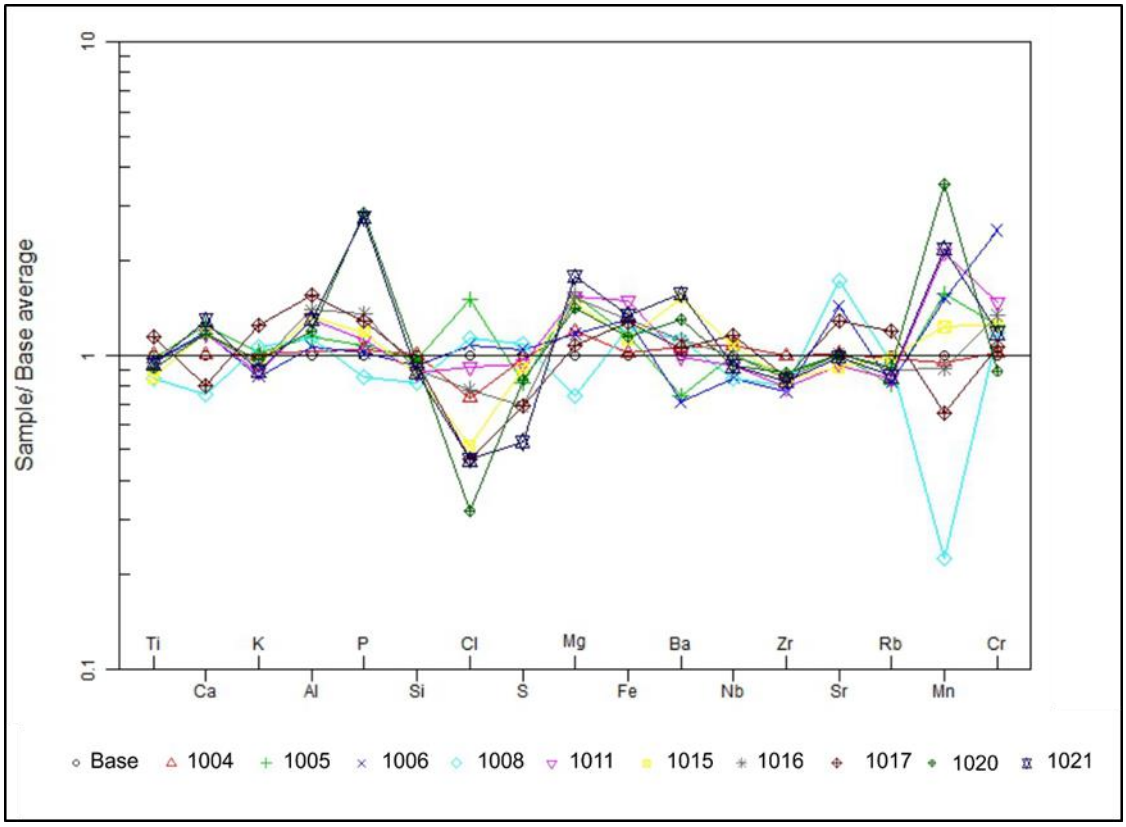

Figure 77: Spider graph of p-XRF soils, compared to the soil from outside the burnt area to determine if there are any fluxes detectable.

p-XRF analysis was carried out on the melted pelite portion of the clasts from each trench. The results were averaged and presented in Table 35. Figure 78 shows the change in the elemental composition of each of the pelitic melts compared with the local pelitic rock. In each of the trenches, the silicon has increased, whilst iron has decreased. This was expected from the SEM-EDS data that showed that the iron has migrated into the surface of the vesicles. Titanium also shows a drop. Calcium, potassium, aluminium and phosphorus all show a small increase.

Table 35: Average p-XRF results from melt areas from trench 1 to 6.

Sample	Si	Fe	Mn	Cr	Ti	Ca	K	Al	Ba	Nb	Mg	Zn	P
Units	%	%	ppm	ppm	%	%	%	%	ppm	ppm	%	ppm	%
Local	278892	52101	622	181	4828	31355	28681	76100	827	14	39082	162	1468
Trench 1	318727	47153	637	184	4435	33434	30872	80123	812	16	36538	166	1597
Trench 2	335546	48736	644	177	4014	34829	31182	78623	845	17	38290	164	1689
Trench 3	308627	48766	624	186	4002	33758	28764	84526	864	15	42209	155	1593
Trench 4	326574	47998	632	183	4264	34657	33085	83205	884	13	35954	159	1667
Trench 6	325466	49273	644	174	4174	33956	30125	83548	818	14	37247	161	1633

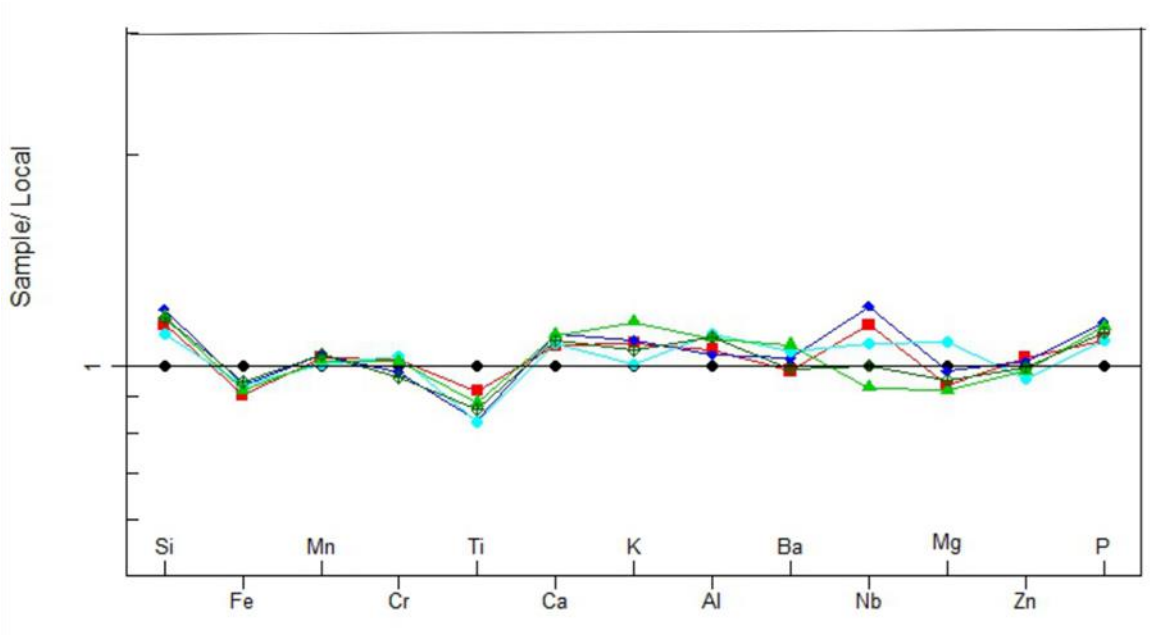

Figure 78: Spider plot of the p-XRF results from melted pelitic areas of clasts from trenches 1 to 6.

5.1.3 Scanning Electron Microscopy (SEM)

Analysing the basic mineralogy using SEM-EDX showed that the melt material is an alkali-aluminosilicate in which plagioclase feldspar phenocrysts were forming. Fractured quartz crystals, with degraded edges, were common. Calcsilicates were also observed in the melt material.

Figure 79 shows a typical SEM-EDS image of a vitrified clast slice mounted onto a glass petrology slide. Area A shows a quartz crystal fracturing in the melt and just above this crystal is quartz material that has been ripped off of the crystal and is dissolving into the melt mixture (Area B). The melt mixture appears to have been a dense, slowly slowing mixture of the melted original pelitic rock and the degrading quartz and olivine crystals. The vesicles (Area C) are mainly off-spherical to ellipsoid and have sometimes joined together during the melting event. This suggests a viscous liquid where the bubbles have not been able to easily escape to the surface (Area D). The surface edge of this clast does not show much sign of degradation or weathering despite being buried for over two-thousand years. There are slight signs of micro-pitting on the edges but nothing substantial.

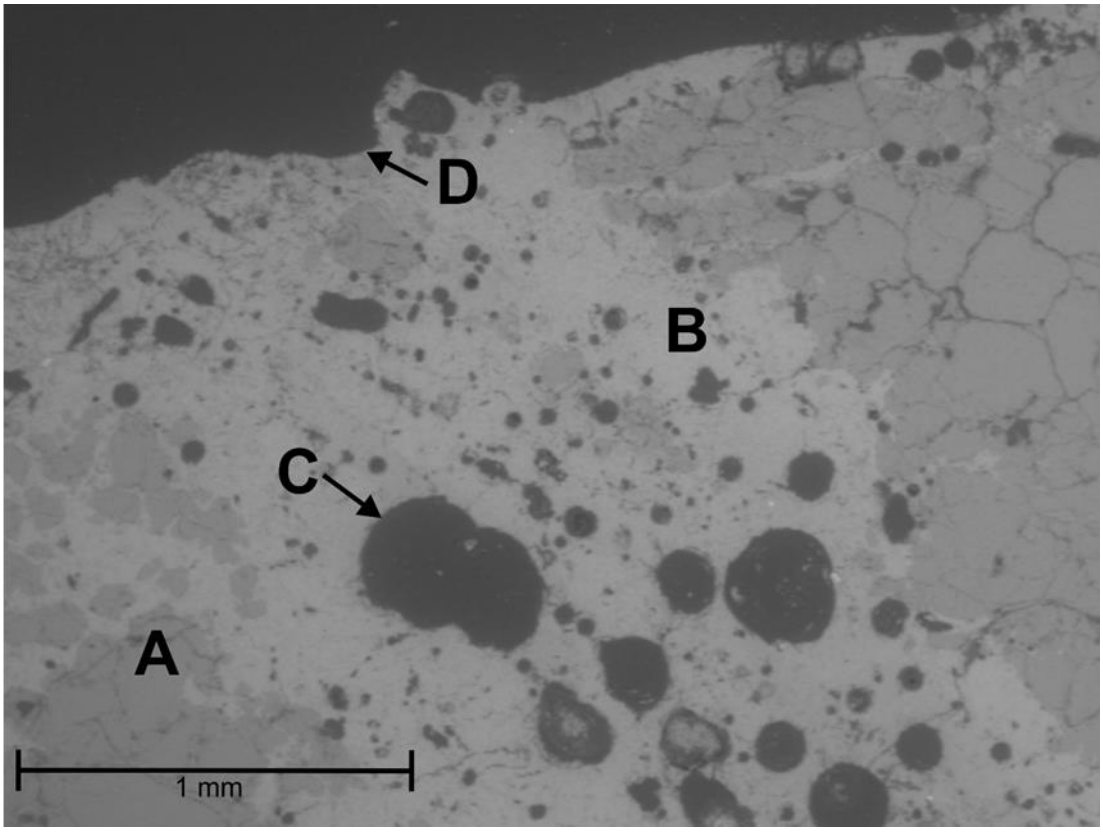

Figure 79: SEM-EDS image of vitrified clast petrology slide.

The temperature of the melt was calculated from the SEM measurements of the magnesium and iron movement from the olivine crystals into the melted rock. Using the Leeman and Scheidegger, (1977) equation (Equation 1: Leeman and Scheidegger calculation (Leeman and Scheidegger, 1977)) with the results presented in Table 36.

As with the experimental melts, the temperatures produced to give a range with the readings from magnesium giving a slightly higher calculated temperature than the iron. Figure 80 illustrates the range in calculated temperatures with Figure 81 showing the average temperature overall and for each trench. This gives an average temperature of 1153˚C for the vitrification temperature of Dun Deardail.

There is little change between temperatures calculated between trenches and Figure 80 shows the range from the calculated results from magnesium and iron, along with the overall average for each. As only the southern and western remains were excavated, only temperatures can be given for these areas. As shown in Figure 81, the average figures are similar around the rampart remains.

Table 36: Temperature of vitrification as per the Leeman and Scheidegger equation (1977), Equation 3.

trench no	Sample	Mg(ol)	Mg(gl)	Fe(ol)	Fe(gl)	T, Mg(˚C)	T, Fe(˚C)
1	DDV3	2.26	0.56	3.71	0.65	1295	979
1	DDV7	5.57	1.34	2.98	0.73	1287	1040
1	DDV13	6.08	1.50	7.59	2.89	1294	1130
2	DDV21	4.03	0.49	6.91	1.88	1121	1060
2	DDV23	2.18	0.57	10.59	3.57	1310	1104
2	DDV27	2.44	0.32	4.54	1.81	1137	1140
2	DDV28	4.46	0.68	12.11	2.56	1172	1012
2	DDV29	2.79	0.42	10.94	2.87	1169	1053
3	DDV47	2.76	0.59	6.15	1.45	1256	1033
3	DDV48	4.73	1.01	16.22	3.67	1255	1025
4	DDV53	2.26	0.56	7.61	1.82	1295	1035
4	DDV61	5.97	1.64	7.08	2.29	1324	1095
4	DDV68	5.47	1.49	3.87	0.99	1322	1048
4	DDV79	3.70	1.05	3.33	1.24	1334	1125
6	DDV91	3.88	0.91	5.07	1.22	1280	1037
6	DDV102	3.24	0.64	4.78	1.17	1235	1040
6	DDV111	2.32	0.43	3.04	1.20	1219	1138
6	DDV116	4.92	0.75	4.44	1.08	1172	1039
6	DDV124	4.62	0.60	4.29	1.10	1135	1049

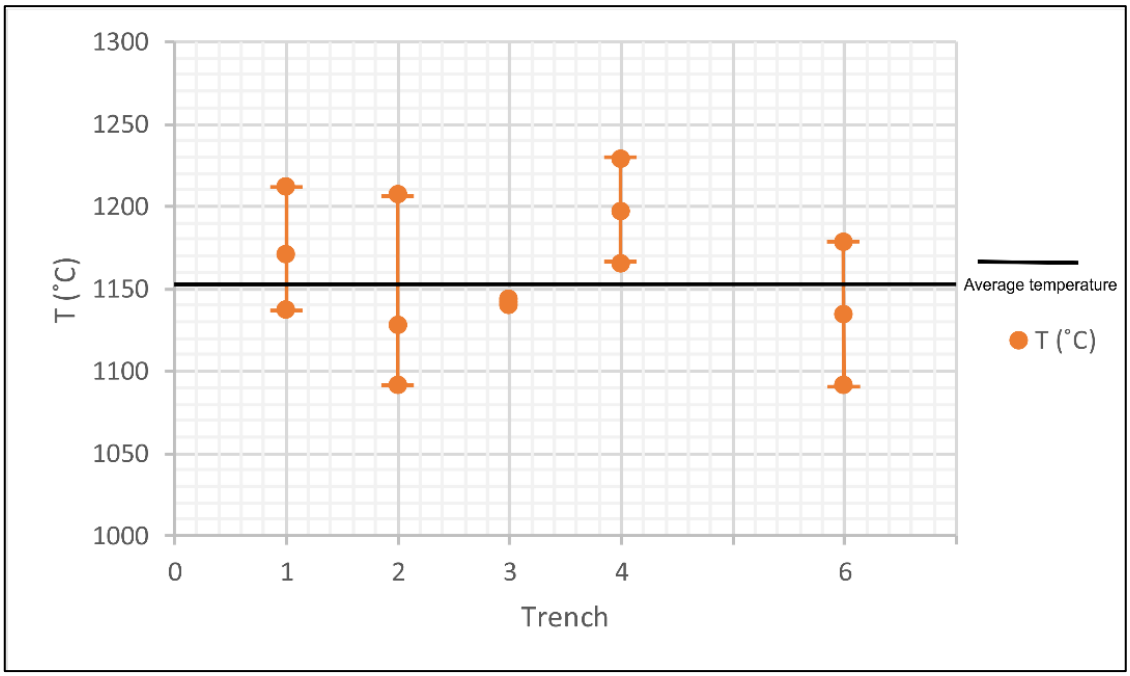

Figure 80: Dun Deardail temperature range using the Leeman, W P and Scheidegger, (1977) equation for magnesium and iron movement from olivine to melt.

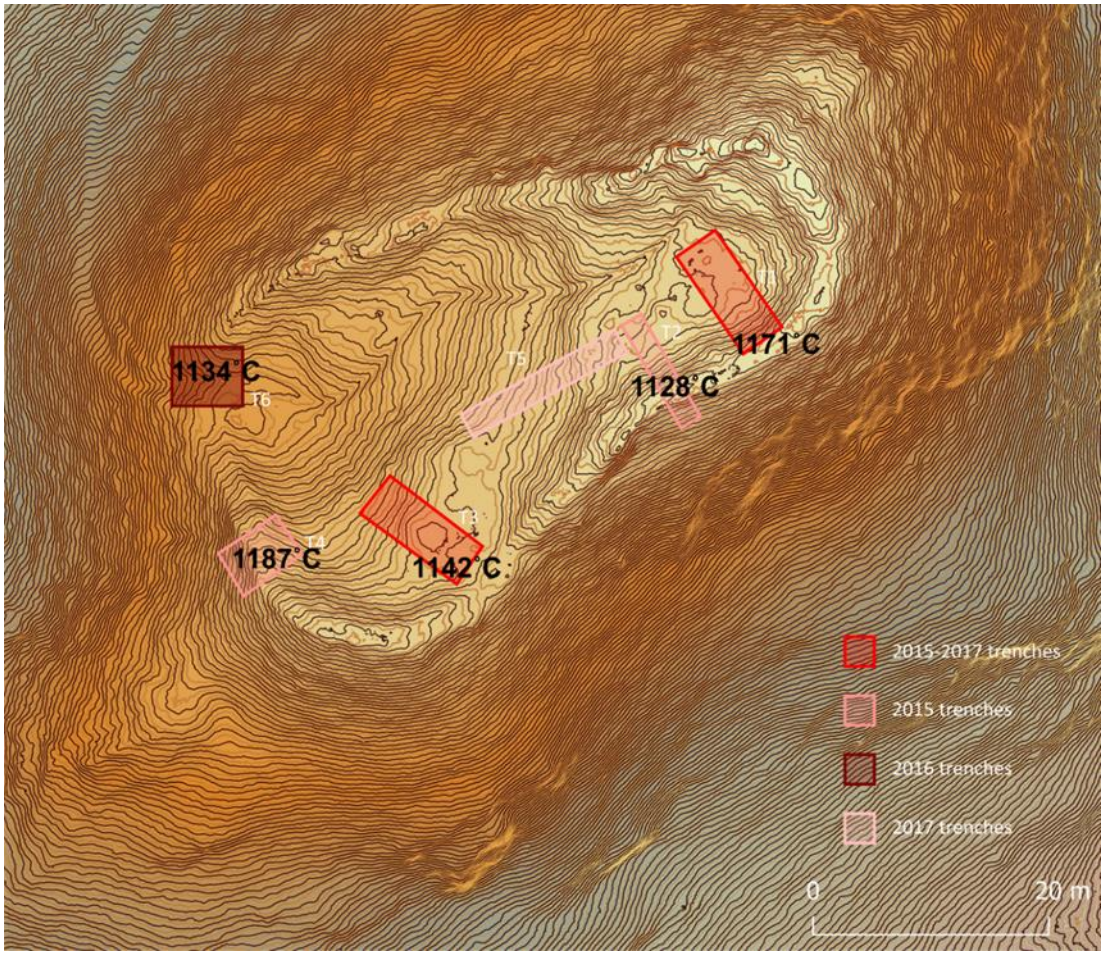

Figure 81: Average calculated temperature (˚C) around the from each of the trenches analysed

SEM results (Table 37) show the difference between the elemental analysis of the melted areas of clasts, from each of the trenches examined, and the results from the local rock. This allows observation into whether there are any traces of potential fluxes within the melt, as was to be shown possible in Chapter 4 – Experimental melts results.

Figure 82 shows the average SEM results for each trench, plotted as a spider plot, with the results normalised to local rock results to allow for direct comparison with that rock and to also allow the differences between the trenches to be easily visualised. These results show a slight lowering of magnesium, potassium, titanium and iron in all of the trenches, whereas calcium levels are slightly elevated. A slight change in Aluminium is also observed in all of the trenches. The most substantial change across the trenches and compared with the local rock is with sulphur. These results are significantly increased in all trenches, except for trench 1, where the results are lower.

Table 37: SEM results (% of total elemental quantity) for the melted material from vitrified samples from excavated trenches compared with the local rock.

Trench	Sample	Na	Mg	Al	Si	P	S	K	Ca	Ti	Fe	total
Local	DDL1	5.90	4.17	19.04	45.80	0.53	0.98	3.33	9.30	1.82	9.11	100
Local	DDL2	5.46	3.15	15.42	49.31	0.45	0.98	4.24	7.41	2.14	11.44	100
Local	DDL3	5.61	3.88	14.98	45.48	0.79	3.11	3.91	13.74	3.95	4.55	100
Local	DDL4	4.66	3.44	12.49	60.92	0.75	0.98	1.87	5.64	0.98	8.26	100
1	DDV3	4.43	1.39	18.65	61.84	0.97	0.97	2.30	6.69	1.16	1.61	100
1	DDV7	6.62	2.87	24.80	47.56	0.26	0.32	2.27	12.01	1.73	1.56	100
1	DDV13	5.84	3.03	21.88	45.42	0.59	0.36	2.99	12.34	1.72	5.84	100
2	DDV21	5.58	0.98	21.39	45.69	0.54	5.34	2.80	12.35	1.56	3.76	100
2	DDV23	2.35	1.41	7.73	54.30	0.69	4.99	1.83	16.77	1.11	8.82	100
2	DDV27	2.63	0.79	9.21	57.64	0.49	5.53	1.62	16.70	0.96	4.44	100
2	DDV28	2.78	1.58	8.82	56.33	0.54	4.08	1.96	16.68	1.26	5.97	100
2	DDV29	6.52	0.81	22.97	45.02	0.42	5.10	2.05	10.88	0.71	5.51	100
3	DDV47	3.02	1.54	9.27	57.44	0.52	5.89	2.27	15.50	0.78	3.78	100
3	DDV48	2.55	2.41	6.95	54.80	0.95	6.50	1.52	14.24	1.33	8.74	100
4	DDV53	5.33	1.26	15.37	55.04	0.38	3.36	3.57	8.55	3.02	4.11	100
4	DDV61	4.91	3.40	12.69	53.01	0.70	6.86	2.53	9.02	2.14	4.75	100
4	DDV68	4.41	3.07	16.88	47.62	0.35	4.14	2.33	17.06	2.10	2.04	100
4	DDV79	3.13	2.85	8.91	59.65	0.49	0.90	2.66	16.98	1.06	3.37	100
6	DDV91	3.16	2.32	9.04	58.86	0.89	0.64	2.09	18.15	1.74	3.11	100
6	DDV102	5.93	1.66	15.37	57.97	0.49	0.52	4.97	7.07	2.96	3.04	100
6	DDV111	3.26	1.04	9.44	59.85	0.36	0.65	2.49	17.96	2.05	2.90	100
6	DDV116	4.66	1.71	11.90	57.08	0.66	8.18	4.32	7.33	1.69	2.47	100
6	DDV124	5.90	1.46	18.10	54.02	1.27	0.85	4.83	8.15	2.73	2.68	100

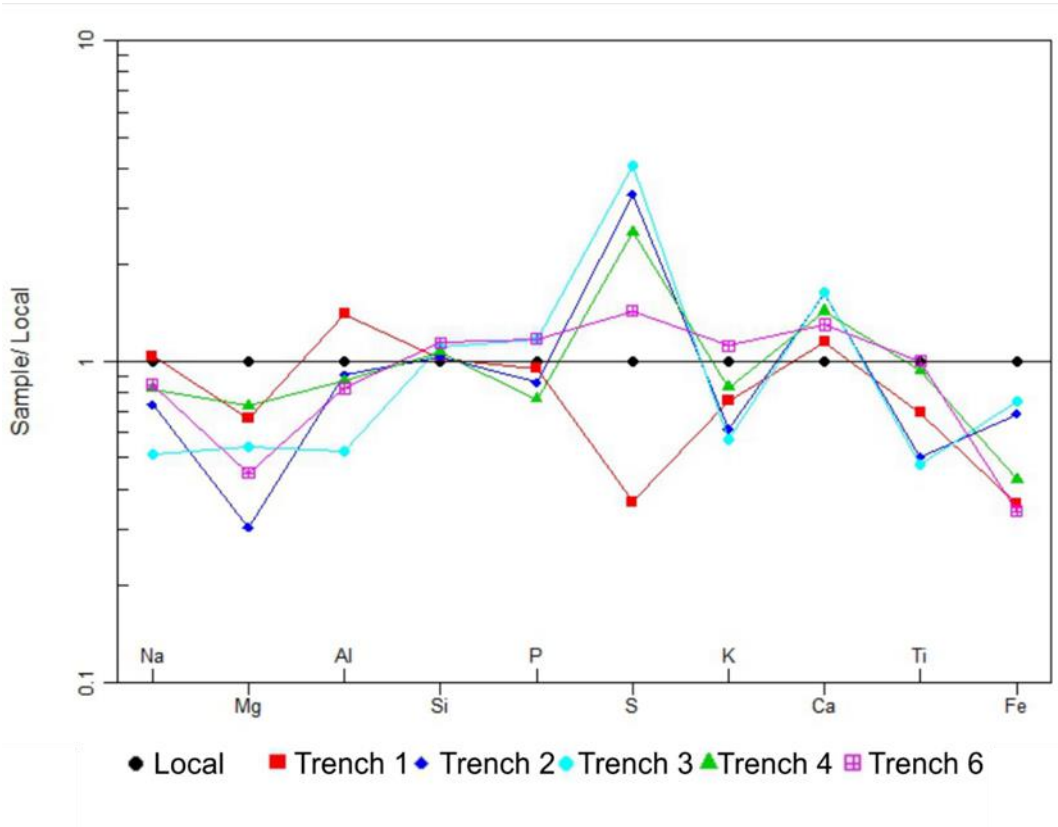

Figure 82: Spider graph

Figure 83 suggests that unreacted iron is coating the vesicles, and this is suggestive of an anoxic environment. This concurs with the results found in the petrology samples.

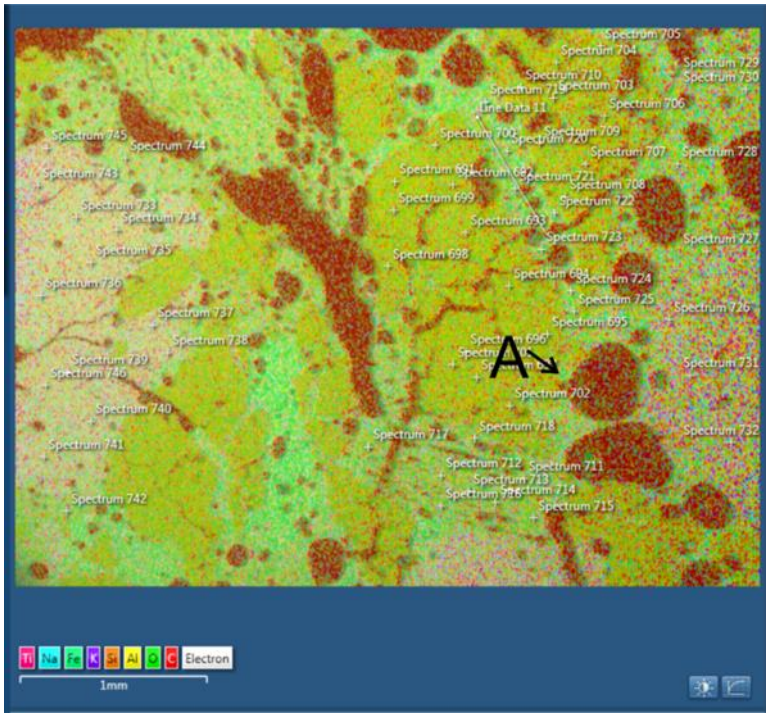

Figure 83: SEM-EDS false colour image showing iron coated vesicles.

5.1.4 Petrology

Figure 84 and Figure 85 illustrate the slides produced from the vitrified rocks and also how these slides look under a petrological microscope. Many slides were produced and observed under the microscope but, for clarity and brevity, only one example has been shown in this thesis each case, for each hillfort. A link to show further examples of these slides and microscope images can be found at the start of the Appendix section.

Figure 84: DDV28 thin section and rock slice

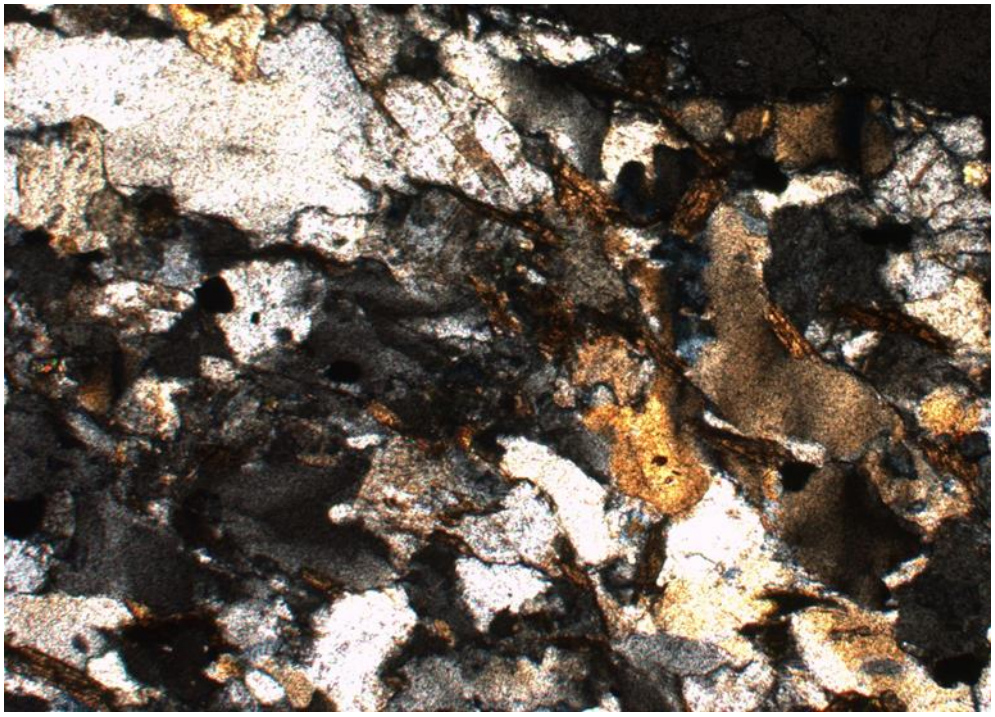

Figure 85: Example PPL thin section image from Dun Deardail.

Figure 86 illustrates how similar the composition of the rocks used in constructing Dun Deardail are and confirms that the rocks are pelitic in nature. Figure 87 confirms that the carbonate rocks that have been used in the construction are calcsilicates and calcareous pelite. This allowed an informed choice of rock, which is representative of the building lithology of Dun Deardail, and these were used in the experimental melts.

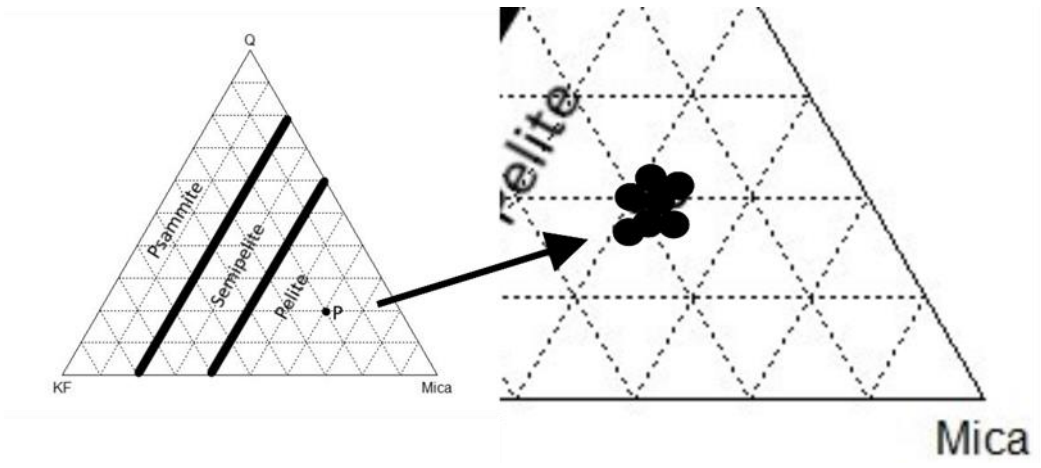

Figure 86: As the rocks are very similar, they are shown as one point on the original ternary; however, when zooming in negligible differences are observed.

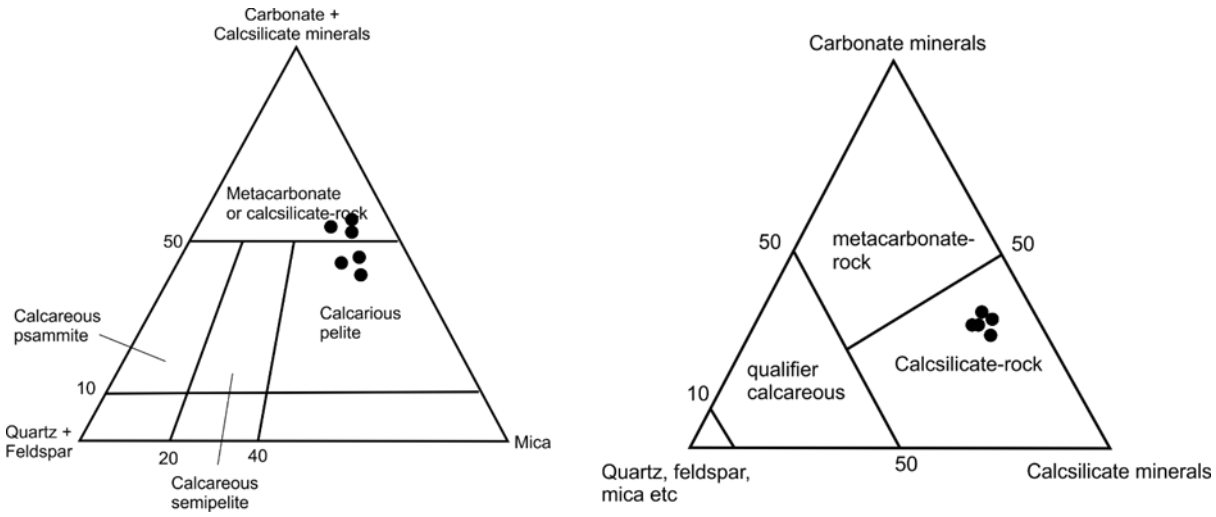

Figure 87: Ternary diagrams classifying the carbonate portions of the clasts.

The rock and thin section shown in Figure 84 is typical of what was observed during petrological analysis. The melt areas can be seen to contain minerals that would be formed at over 800˚C (Table 38). Olivine is beginning to fracture and degrade, with the edges of the crystal moving into the surrounding melting material (Figure 89). The calcitic areas have heated to cause dehydration, and this has made the rock flaky. This suggests a temperature of over 550˚C (Ihli et al., 2014). Calcsilicate in area C has boiled, and the biotite was showing growth suggesting temperatures over 800˚C. These temperatures are quite low and vague; however, relict ilmenite, magnesioferrite and pyrite formation suggest a temperature of closer to 1100˚C, (Morad, S. and Aldahan, 1986). Damaged quartz is also observed in the thin section. Quartz on its own will generally have a melting point of around 1650-1750°C (Deer et al.,1992) however, when combined with other minerals, such as biotite, this temperature may be reduced to 1150˚C, (Kresten et al., 2003). As the sample contains both biotite and quartz, this also constrains the vitrification temperature to 1150˚C or above. Youngblood et al., (1978) suggested that the plagioclase laths were remnant from the pelite, in these samples, it appears that the plagioclase is reforming from the melt as the edges of the crystals show no damage, and there is no apparent fracturing of the crystals, as is observed in the olivine and quartz.

Figure 88:Thin section and cut rock this was produced from.

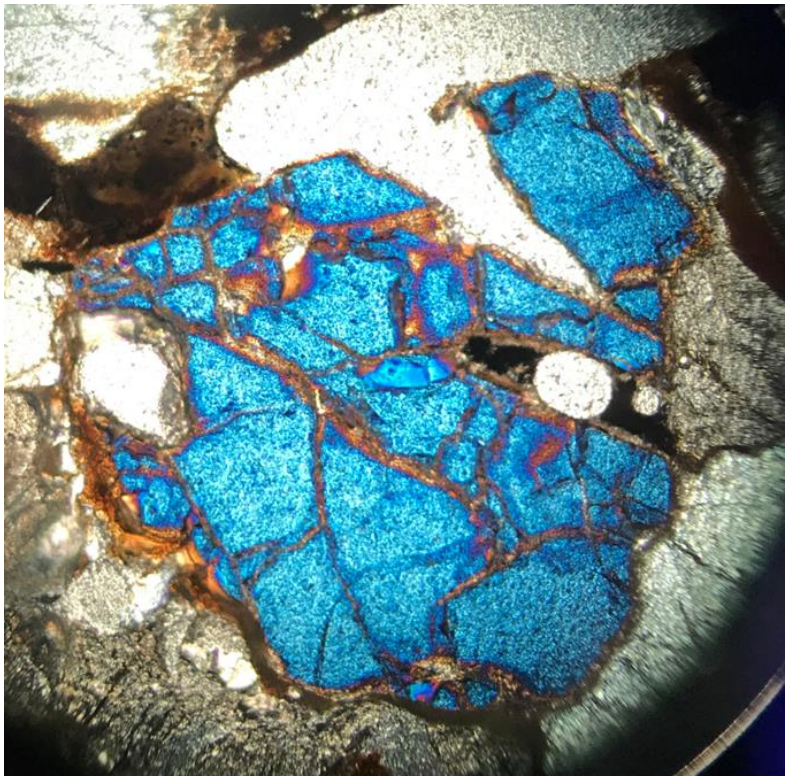

Figure 89:Slide in XPL showing fractured olivine crystal.

Table 38:Petrological analysis of DDV28

Sample: DDV28 **Site:** Dun Deardail		
Area A (%): biotite 30 quartz 20 cordierite 10 plagioclase 10 olivine 10 relict ilmenite 5 pyrite 5 magnesioferrite 5 charcoal 5 metallic vesicle coating	**Area B (%):** calcite 60 quartz 30 biotite 10	**Area C (%):** quartz 40 calcite 30 biotite 30
General comments: Melt area (Area A) is quite dark and glassy making it difficult to differentiate some of the minerals in the melt mix. Flakes of charcoal are visible throughout the melt area. Can see the edges of the quartz being dissolved into the melt, leaving raggy edges on the crystals. Olivine crystals are damaged due to the heat and the endes are showing dissolution into the melt. Many crystals damaged due to the melt flow and heat. There are also new crystals forming that are small and in different alignments to each other. In area B the calcite is dehydrated and friable. The calcsilicate in area C shows signs of boiling and contains many vesicles. Biotitle crystals are forming in places and are in varying alignments.		

5.2 Secondary case study sites

5.2.1 Visual

The visual analysis of the secondary case study hillforts was investigated using visual onsite analysis. Hand samples were available for Craig Phadrig, Knockfarrel, The Torr and The Knock. Site visits to the comparison hillforts were undertaken to make a visual appraisal of both the local geology, within 1km, and the construction material of the hillfort. Table 39 shows the lithology of the material used to construct the hillfort and the local geology. In each of the hillfort sites, the hillfort contains rocks that visually are from local sources. In vitrified hillforts, such as Knockfarrel, the conglomerate contained pelitic and schistose rocks and these are what has melted to create the vitrified melt that that glues the clasts together during the vitrification process.

Table 39: Visual comparison between local geology and hillfort composition for comparison hillforts.

Hillfort	Lithology	Local lithology
Dun Deardail	pelite, calcsilicates, granite, quartzite and quartz	pelite, calcsilicates, granite, quartzite and quartz
Craig Phadrig	granite, sandstone, gneiss and quartzite	basalt and sandstone
Knock Farril	gneiss, schist, quartzite and sandstone	conglomerate
Ord Hill	conglomerate	conglomerate
The Torr	semipelite and psammite	semipelite and psammite
Torr Dhuin	granulite with biotite and basalt	granite gneiss, amphibolite and psammite
Dunagoil	basalt, conglomerate, sandstone	sandstone, basalt and conglomerate
Auld Hill	basalt, sandstone and quartz	sandstone, mudstone, and quartz microgabbro dyke
The Knock	sandstone	sandstone and basalt

Figure 90 illustrates a section from the destroyed hillfort rampart of The Torr, Shielfoot. Various states of rock vitrification processes can be observed in this one clast. These include full vitrification, with many vesicles in the dark centre area of the rock, burnt rock that has reddened and oxidised, red granitic rock that has been made friable through heat exposure, rock that has been cracked open in the heat and the surrounding original building materials. Observations on the different material show the same damage to the calcitic and granitic elements of the clasts and vitrification features of the pelitic material here at The Torr as was observed at Dun Deardail. These vitrification features were similar at all the vitrified hillforts visited and suggested that the burn conditions for each of the vitrification fires at the different sites were comparable.

Figure 90: Vitrified and heat damaged rocks at The Torr, Shielfoot.

Visually, there are cracked and fractured rocks in all of the vitrified hillforts visited, but there was no sign of exploded rock within the melt, as was observed in laboratory furnace experimental melts. This suggests that the burn was a slow long one. The outside of the clasts is often glassy, suggesting rapid cooling of the outside of the rocks and this could have held in the heat, potentially allowing the melting processes to continue inside the vitrifying structure. Figure 91 illustrates the situation at The Torr, Shielfoot where the rocks are heat damaged, dehydrated and fractured but have not exploded.

The vitrified rocks also mirror the scenario at Dun Deardail where the vitrified rocks do not show significant signs of weathering compared with modern glass, which shows far more significant signs of weathering within thirty years (Le Bourhis, 2014).

Figure 91: Heat damaged rock at The Torr, Shielfoot.

Dun Deardail was constructed with stone ramparts, and a rubble core with an internal timberlacing and construction materials used local lithology. Visual analysis documents that the vitrified hillforts compared were also constructed in this manner. Knockfarrel, Figure 92, also shows timber casts preserved in the vitrification. This timberlacing evidence can be observed in other vitrified hillforts visited, as shown in Table 59.

By their manner, the hillforts compared were all constructed using rock materials; however, not all hillforts that were burnt were vitrified. This can be shown by The Knock. The Knock, Figure 93, was built using predominantly sandstone, shows signs of a large scale fire, but no sign of vitrification was detected during the excavation in 2016 (Lang, 2016). This illustrates that not all of the hillforts that were set on fire were built with material that would readily vitrify.

Figure 92: Vitrification on Knockfarrel, showing wood casts preserved in the solidified rock.

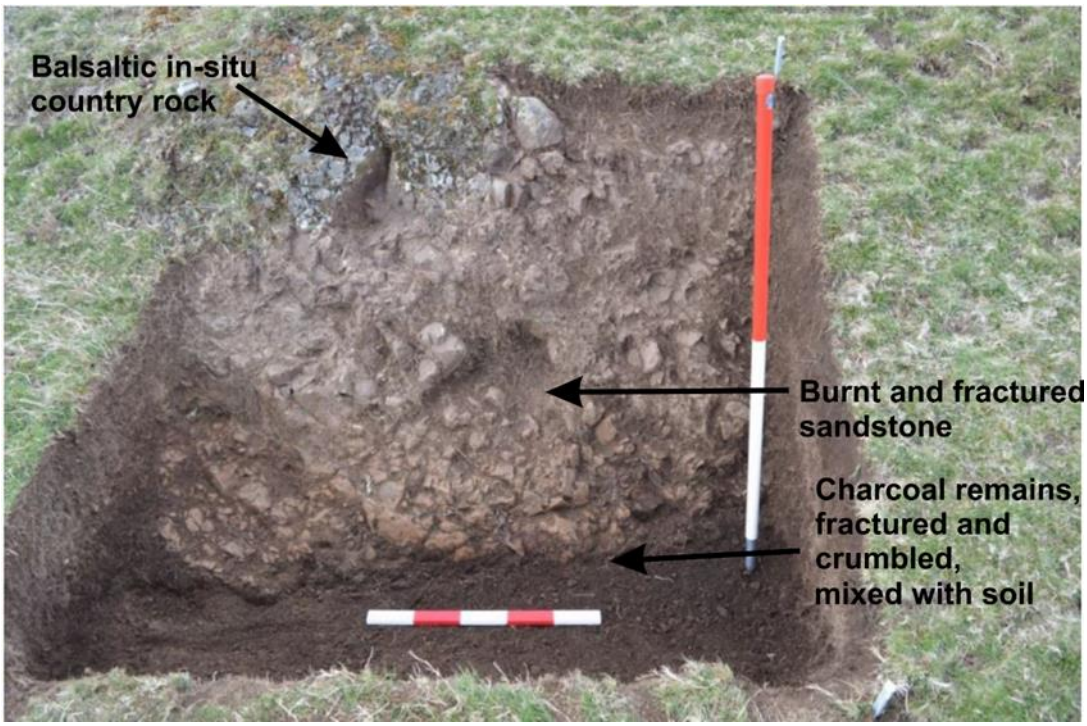

Figure 93: Excavation of The Knock showing the burnt sandstone structure in position with the in-situ basalt and soil layer (Lang, 2016)

From the excavations of Dun Deardail and Craig Phadrig, and site visits to the other secondary case study hillforts, Table 40 can be constructed to compare the construction

type of each of the hillforts used in this research. This demonstrates that the hillfort construction was similar across the hillforts surveyed. Timberlacing is a common stabilising construction method. Outer walls filled with rubble core for rampart construction also appears to be a favoured method of construction for the hillforts surveyed.

Table 40: Table illustrates the structure of the comparable hillforts.

✓- has been found, x – no indication of this feature, ? – this cannot be determined without excavation.

Hillfort	timberlacing	Stone ramparts	Rubble core	Lithology	Local lithology	Signs of vitrification
Dun Deardail	✓	✓	✓	pelite, calcsilicates, granite, quartzite and quartz	pelite, calcsilicates, granite, quartzite and quartz	✓
Craig Phadrig	✓	✓	✓	granite, sandstone, gneiss and quartzite	basalt and sandstone	✓
Knock Farril	✓	✓	✓	gneiss, schist, quartzite and sandstone	conglomerate	✓
Ord Hill	?	✓	✓	conglomerate	conglomerate	x
The Torr	✓	✓	✓	semipelite and psammite	semipelite and psammite	✓
Torr Dhuin	?	✓	✓	granulite with biotite and basalt	granite gneiss, amphibolite and psammite	✓
Dunagoil	?	✓	✓	basalt, conglomerate, sandstone	sandstone, basalt and conglomerate	✓
Auld Hill	?	✓	✓	basalt, sandstone and quartz	sandstone, mudstone, and quartz microgabbro dyke	✓
The Knock	✓	✓	✓	sandstone	sandstone and basalt	x

5.2.2 p-XRF

The geochemical analysis was undertaken, using p-XRF as per Chapter 3, on laboratory samples from Craig Phadrig, The Torr and Knockfarrel. These analyses were concentrated on the pelitic, calcsilicate and quartz areas of the clasts and their comparison with the local geology.

Table 41 gives the p-XRF results for pelitic hillfort and local rock samples from Craig Phadrig, The Torr and Knockfarrel. Using these a spider plot, Figure 94, was constructed. This allows the determination of a fingerprint for each area. Figure 94 illustrates that each of the different areas shows a distinct pattern, with the local geology and hillfort geology being comparable. Table 42 gives the p-XRF results for calcsilicate hillfort and local rock samples from Craig Phadrig, The Torr and

Knockfarrel. Using these a spider plot, Figure 95, was constructed. Table 43 gives the p-XRF results for quartz hillfort and local rock samples from Craig Phadrig, The Torr and Knockfarrel. Using these results, a spider plot, Figure 96 was constructed.

Using the information generated from the p-XRF data, a fingerprint pattern can be determined for each hillfort. Craig Phadrig pelite shows lower levels of iron and higher manganese and zirconium than the other sites. The notable differences in the calcsilicates are a lower trend in vanadium, titanium, calcium and barium, with the manganese being higher. The slight lowering of the calcium values in the quartz also provides a fingerprint for lithology local to the Craig Phadrig area. Knockfarrel pelitic material contains more barium and strontium than the other hillfort sites examined, whereas the niobium is significantly lower in the calcsilicate samples. In quartz samples from the area, sulphur is significantly lower than other sites examined. A distinguishing feature for The Torr pelitic samples is that the barium is significantly lower than other areas and the aluminium and chromium higher. In the calcsilicate samples, the calcium is decidedly lower, whereas the zirconium is high. All of the calcsilicate samples show lower zinc compared with Dun Deardail. The main distinguishing feature for The Torr quartz samples phosphorus is found at a much lower quantity than other sites.

Table 41: Average unmelted pelite p-XRF results for local rocks from Dun Deardail, Craig Phadrig, The Torr and Knockfarrel compared to pelite rock samples used in the construction of Craig Phadrig (CPV). The torr, (TTV) and Knockfarrel (KF).

Sample	Si	Fe	Mn	Cr	Ti	Ca	K	Al	Ba	Nb	Zr	Sr	Rb	Mg	Zn	P
Units	%	%	ppm	ppm	%	%	%	%	ppm	ppm	ppm	ppm	ppm	%	ppm	%
DD local	278892	52101	622	181	4828	31355	28681	76100	827	14	259	142	133	39082	162	1468
CP local	373698	27325	985	90	5430	13645	21197	61317	477	19	517	196	169	13980	79	960
TT local	271658	24620	392	78	2710	25457	35125	52777	1043	12	321	266	106	9310	42	1029
KF local	298364	56375	462	284	6021	7243	32856	130834	201	22	301	177	146	18599	143	1222
CPV1	377604	22786	995	90	5568	15581	21890	68583	478	17	656	218	179	14274	75	902
CPV8	370968	27054	923	96	5355	14066	18851	66630	466	18	589	189	187	12258	79	963
CPV13	408949	22023	993	89	5286	14489	21316	56539	450	16	566	195	172	13427	89	935
CPV14	374139	27177	807	99	5132	14394	21109	56394	464	15	630	199	173	13754	75	930
CPV15	338790	27768	970	90	5889	13375	22688	65156	465	21	586	192	173	13769	77	962
CPV18	313485	23646	881	93	6009	14793	21454	64349	432	22	666	188	185	13740	72	982
TTV1	276548	25431	402	84	2365	25644	34476	52346	980	9	334	278	97	8965	37	1043
TTV2	285354	24627	421	82	2543	24597	36442	56434	1023	10	302	301	101	8854	39	1197
TTV3	278998	25132	399	79	2569	24589	35469	55629	1055	7	356	307	89	8902	47	1085
TTV4	278745	25113	404	82	2786	25830	34197	55899	1177	8	339	299	107	9056	48	997
TTV5	281547	24786	433	88	2534	25385	34784	56137	980	6	326	297	119	9126	35	1064
TTV6	281453	24980	421	87	2768	26311	37109	55882	1010	7	322	303	84	9453	44	983
TTV7	278923	24867	399	84	2898	25753	35265	55973	1043	9	348	311	97	9355	43	1008
KF1	297023	55746	462	255	5946	7204	32632	129124	148	20	328	162	148	18719	126	1225
KF2	293740	56739	443	267	6125	7388	33455	127354	215	23	334	176	152	18742	131	1342

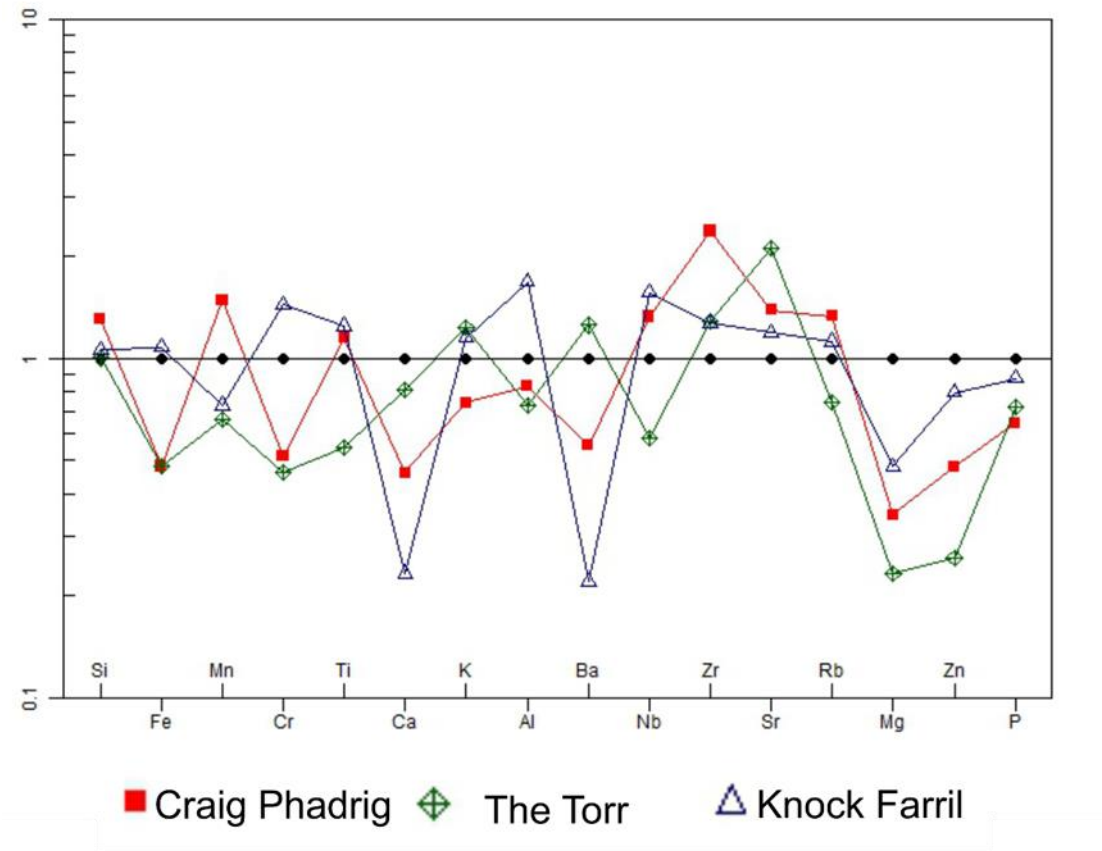

Figure 94: Spider chart illustrating average pelite p-XRF results for local rocks from Craig Phadrig, The Torr and Knockfarrel compared to pelite rock samples used in the construction of Craig Phadrig, The torr and Knockfarrel, with results compared with p-XRF results from Dun Deardail local samples to determine the difference.

Table 42: Average calcsilicate p-XRF results for local rocks from Dun Deardail, Craig Phadrig, The Torr and Knockfarrel compared to calcsilicate rock samples used in the construction of Craig Phadrig (CPV). The torr, (TTV) and Knockfarrel (KF).

SAMPLE	Si	Fe	Mn	Cr	V	Ti	Ca	K	Al	Ba	Nb	Zr	Sr	Rb	S	Mg	Zn	P	Cl
Units	%	%	ppm	ppm	ppm	%	%	%	%	ppm	ppm	ppm	ppm	ppm	%	%	ppm	%	ppm
DD local	210399	39143	449	157	155	4981	75950	43773	66122	764	14	205	60	129	269	54212	201	1532	91
CP local	325027	29115	827	194	81	3757	39241	24082	72196	431	13	343	170	80	372	61483	38	760	186
TT local	445633	21645	475	101	100	5564	33884	25633	44337	556	6	164	155	84	735	84252	22	666	247
KF local	345373	30300	375	99	181	7711	13566	24657	75464	745	27	986	184	131	519	73228	17	904	306
CPV1	316609	27509	830	182	98	3725	40064	20442	77772	441	16	334	180	98	350	65102	37	713	204
CPV8	316581	27952	851	192	79	3142	34033	20862	74151	387	12	360	173	92	352	68103	29	785	176
CPV13	362130	28892	845	185	84	3947	45736	25736	75003	535	10	315	164	90	319	64475	44	783	175
CPV14	384378	27731	888	177	93	3012	47576	25847	75340	483	12	320	163	77	379	66622	36	819	189
CPV15	335464	28547	819	189	91	3749	47927	27384	72846	444	10	368	155	83	375	61947	37	783	221
CPV18	356273	28645	816	179	89	3388	48273	24744	77345	473	14	348	189	79	351	63182	45	773	198
TTV1	402842	28463	482	99	104	5637	39465	25365	46574	563	4	144	173	92	738	79463	21	606	252
TTV2	427563	24273	401	94	108	5511	40118	24385	49573	528	5	173	134	84	699	81352	23	617	264
TTV3	456722	22881	442	103	116	5365	40163	25499	48510	583	2	144	155	86	748	81332	19	700	277
TTV4	437829	21909	472	105	109	5349	39846	26453	49255	592	7	184	128	94	714	78936	18	619	296
TTV5	443556	24389	422	93	114	5646	39745	24658	49274	556	7	168	143	91	731	79360	25	643	285
TTV6	436971	22553	484	97	98	5585	32971	24531	48875	538	4	149	155	82	713	79489	29	641	259
TTV7	527516	21284	428	107	107	5634	34264	24152	45266	527	2	175	112	89	781	79463	23	676	274
KF1	341287	30562	347	86	167	7705	12313	24337	76230	719	23	1009	161	118	564	74259	10	892	301
KF2	334575	29833	355	92	152	7829	13526	25342	77811	738	25	1010	181	132	555	74294	12	994	335

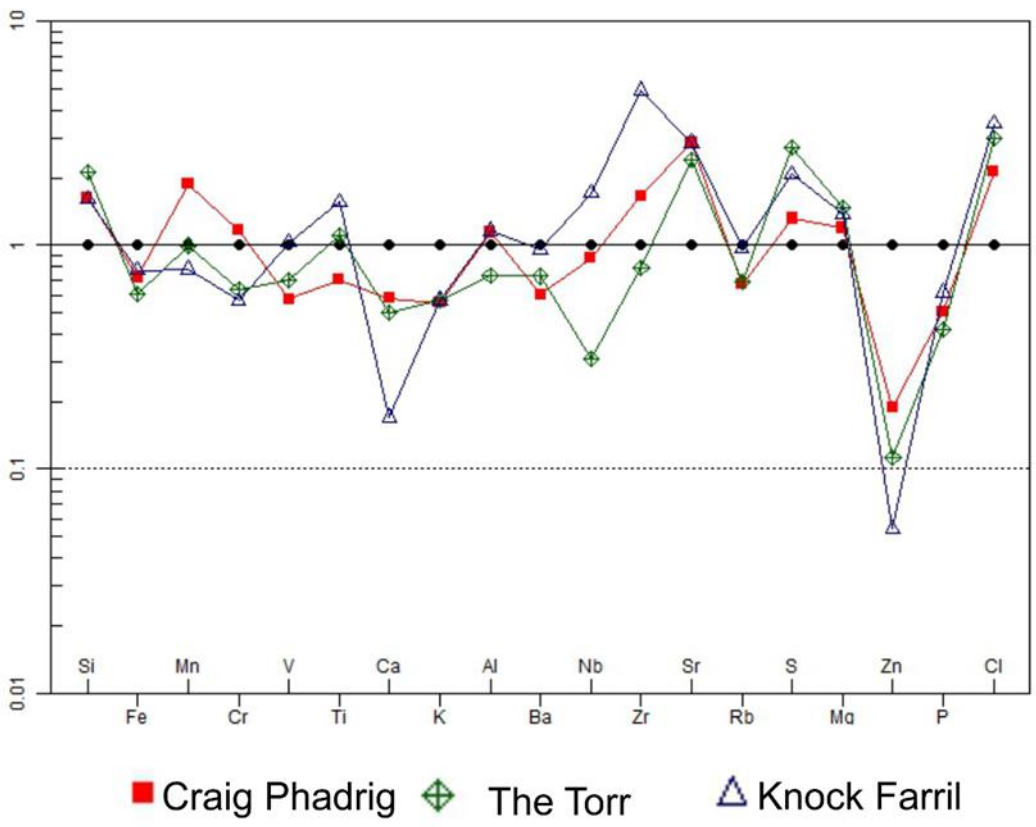

Figure 95: Spider chart illustrating average calcsilicate p-XRF results for local rocks from Craig Phadrig, The Torr and Knockfarrel compared to calcsilicate rock samples used in the construction of Craig Phadrig. The torr and Knockfarrel, with results compared p-XRF results from Dun Deardail local samples.

Table 43: Average quartz p-XRF results for local rocks from Dun Deardail (DD), Craig Phadrig (CP), The Torr (TT) and Knockfarrel compared to quartz rock samples used in the construction of Craig Phadrig (CPV). The torr, (TTV) and Knockfarrel (KF).

Sample	Si	Fe	Ti	Ca	K	Al	Ba	S	P
Units	%	%	%	%	%	%	ppm	%	%
DD average	459970	362	46	200	2516	8350	200	520	868
CP local	408767	476	78	165	3546	7425	419	334	476
TT local	397650	385	47	183	3005	6392	523	422	103
KF local	386576	528	59	264	4026	9452	264	201	285
CPV1	396287	472	75	175	3318	7436	427	325	498
CPV8	387650	415	79	168	3548	7143	453	354	498
CPV13	379729	483	84	175	3318	7342	427	372	472
CPV14	397583	444	81	177	3499	7591	448	379	457
CPV15	381275	428	77	173	3562	7624	396	361	456
CPV18	398759	492	75	169	3565	7526	398	355	471
TTV1	398563	305	44	196	2983	6423	564	462	98
TTV2	401833	338	49	199	2954	6634	528	427	89
TTV3	402574	317	39	201	2865	6452	553	484	95
TTV4	398465	362	36	195	2915	6680	582	436	98
TTV5	391638	349	39	189	2969	6589	555	427	104
TTV6	401736	333	40	190	3003	6456	588	439	101
TTV7	400825	315	37	205	3012	6741	528	444	113
KF1	389576	537	65	274	4185	8952	264	196	301
KF2	389625	563	69	266	4083	8994	251	179	309

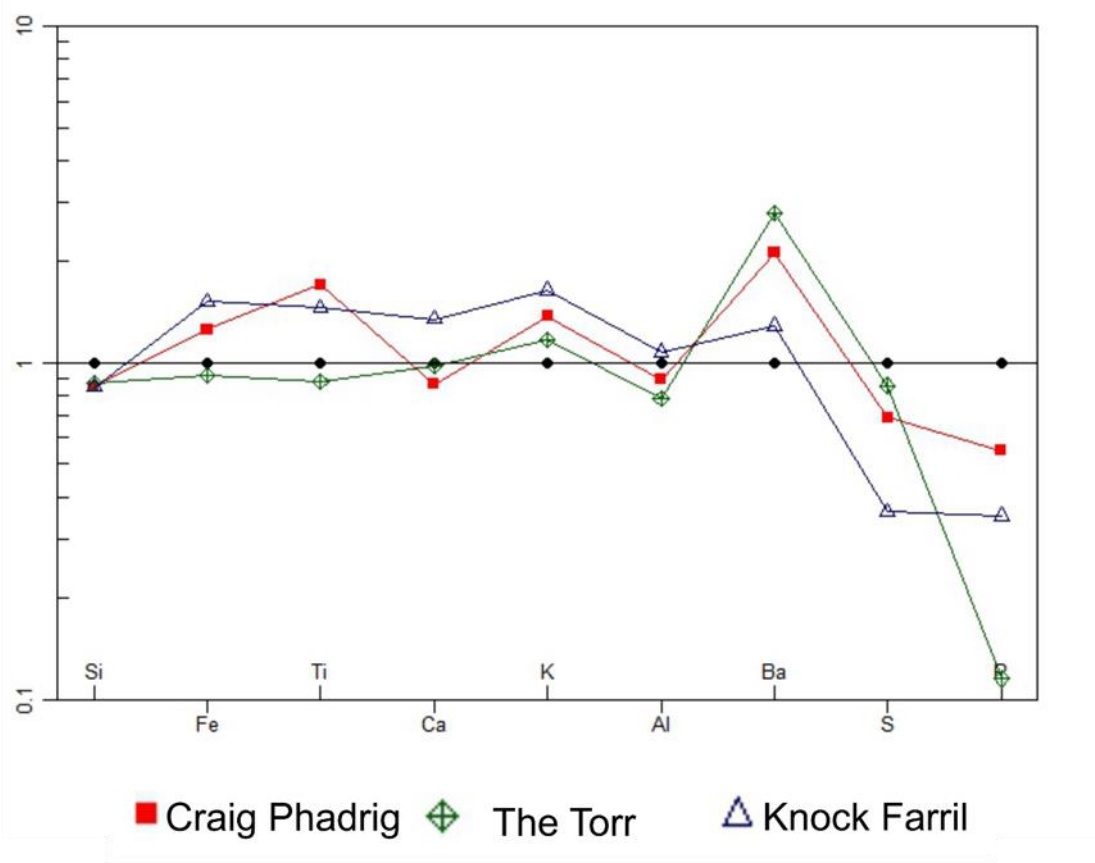

Figure 96: Spider chart illustrating average quartz p-XRF results for local rocks from Craig Phadrig, The Torr and Knockfarrel compared to quartz rock samples used in the construction of Craig Phadrig. The torr and Knockfarrel, with results compared to p-XRF results from Dun Deardail local samples.

p-XRF analysis of the vitrified areas of the pelitic melt material from Craig Phadrig, The Torr and Knockfarrel were compared with that from Dun Deardail (Table 44). The spider plots, shown in Figure 97, show no distinct variation between the elements in the unmelted hillfort pelite, the local rock and the vitrified melt rock. The silicon values in the melt are a little varied as this was dependent on how much of the quartz melted into the melt mix and this would be varied as it would depend on how much quartz was touching the pelite melt.

Table 44: p-XRF results for melted areas of pelite in comparison hillforts.

Sample	Si	Fe	Ti	Ca	K	Al	Ba	S	P
Units	%	%	%	%	%	%	ppm	%	%
CP local	373698	27325	5430	13645	21197	61317	13980	79	960
TT local	271658	24620	2710	25457	35125	52777	9310	42	1029
KF local	298364	56375	6021	7243	32856	130834	18599	143	1222
CPV2	453074	27546	5463	13547	19982	64778	13874	82	983
CPV3	478566	27536	5467	15364	19762	64758	13419	79	972
CPV16	469823	24785	5621	13875	20997	64823	12984	84	945
CPV17	477566	25887	5656	15652	20864	59574	12873	77	951
CPV19	399983	25864	5724	14766	20875	58715	14723	89	987
CPV20	396427	26745	5826	15427	19658	59974	13974	84	951
TTV10	385639	25787	2697	24567	34658	52143	9425	29	1022
TTV11	382943	26764	2699	26499	35682	54629	9417	32	999
TTV13	348653	24536	2828	26744	34565	55963	9573	43	985
KF3	356743	56435	6012	7577	33452	134723	19236	128	1311
KF4	356495	56788	5983	7853	33988	136432	18264	151	1349

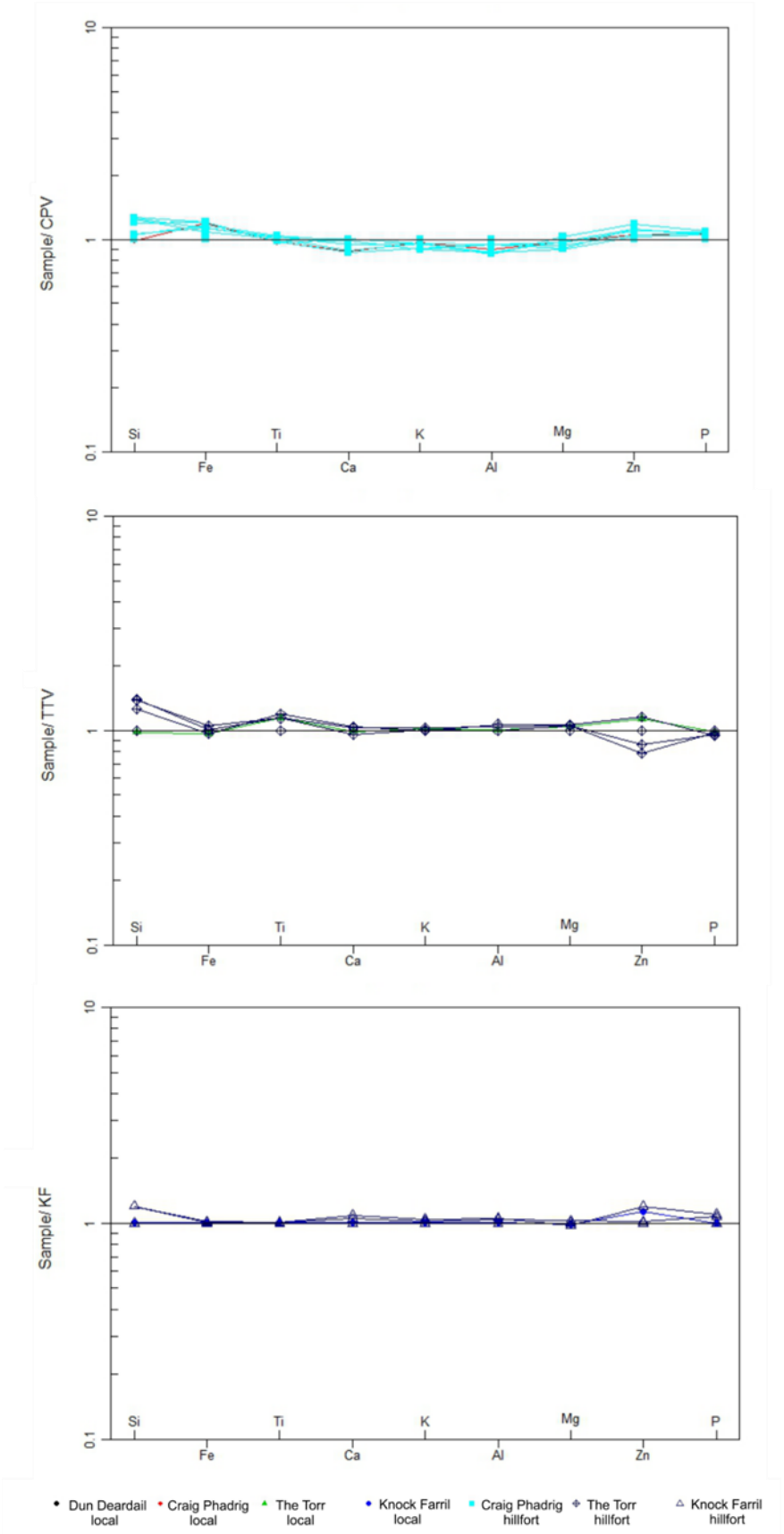

Figure 97: Spider plots of vitrified areas of pelite compared to unmelted areas of hillfort pelite, with local rock added for comparison.

During excavation, it was determined that The Knock was not vitrified and so the p-XRF analysis of the burnt excavated samples have been compared to the local rock (Table 45). The rocks analysed were randomly chosen, with 10 bagged samples removed from the storage box and analysed by p-XRF.

Table 45: p-XRF analysis of excavated samples from The Knock compared with local rock.

SAMPLE	**Si**	Fe	Ti	K	Al	Zr	Sr	Rb	Ba
Units	%	%	%	%	%	ppm	ppm	ppm	ppm
KH SS	331124	11526	1069	29488	49309	58.35	23.72	47.86	553
KH03	330193	11408	1095	28488	48585	52.78	27.78	53.62	287
KH05	333218	10989	1078	29360	48288	54.89	26.78	47.88	423
KH06	337316	11588	1045	28958	45877	55.21	27.39	46.01	365
KH09	331823	11384	992	29341	49441	61.04	23.22	51.05	340
KH15	335674	11228	1057	27660	47234	54.17	25.49	50.25	453
KH16	335522	10806	990	29696	48916	62.54	27.57	47.96	419
KH19	335317	11384	1151	29463	48970	53.05	26.24	42.02	358
KH20	337786	11254	1067	28200	51090	59.39	22.38	53.69	405
KH21	337756	11169	1056	27910	50845	55.86	23.36	38.89	396
KH26	315321	10585	1410	26425	44640	58.35	25.98	46.57	349

5.2.3 SEM

Table 46 provides the data from the SEM analysis of the pelitic melt portions from clasts from Craig Phadrig, Knockfarrel and The Torr. These results were compared with the SEM analysis from the local lithology found within 1km of each of the sites. From Figure 98, it can be seen that the magnesium abundance dips in each of the hillfort areas. Aluminium and silicon both increase slightly, and titanium and iron abundance drop. Calcium lowers in both the Craig Phadrig and Knockfarrel, whereas the level increases slightly in The Torr samples.

Table 46: SEM data from the pelitic melt areas of Craig Phadrig (CPV), Knockfarrel (KF) and The Torr (TTV) compared with local rock.

Sample	Na	Mg	Al	Si	K	Ca	Ti	Fe
CP local	6.88	9.15	18.85	42.80	6.24	2.59	3.53	9.97
CPV1	6.11	3.57	21.75	49.86	5.92	1.79	3.17	7.83
CPV8	5.25	4.80	18.12	49.43	7.60	3.15	3.43	8.22
CPV13	6.25	1.82	20.46	52.56	6.53	2.86	2.89	6.64
CPV14	6.97	0.87	21.32	53.54	6.04	0.84	2.82	7.59
CPV15	5.68	2.15	23.51	49.99	5.72	0.74	3.58	8.62
CPV18	6.27	1.89	22.34	49.41	5.86	1.41	3.30	9.54
Sample	Na	Mg	Al	Si	K	Ca	Ti	Fe
KF local	6.31	6.04	17.24	49.27	5.47	7.08	2.49	6.09
KF1	4.49	2.78	15.84	57.61	5.37	7.05	2.26	4.60
KF2	5.34	1.97	18.08	58.44	6.44	5.52	0.59	3.63
Sample	Na	Mg	Al	Si	K	Ca	Ti	Fe
TT local	5.33	4.05	19.59	47.89	4.66	2.42	5.28	10.78
TTV1	3.17	1.36	18.71	57.89	3.40	2.98	3.54	8.94
TTV2	7.13	0.89	21.06	53.37	4.09	2.70	2.67	8.09
TTV3	5.03	1.15	20.80	49.81	3.42	4.14	5.83	9.81
TTV4	4.98	1.35	17.16	54.05	7.59	3.08	3.08	8.70
TTV5	5.29	1.41	19.65	51.85	5.18	2.50	7.68	6.43
TTV6	5.01	1.05	21.50	51.30	5.50	1.22	5.47	8.95
TTV7	5.10	1.70	18.90	49.05	5.13	1.46	7.99	10.67

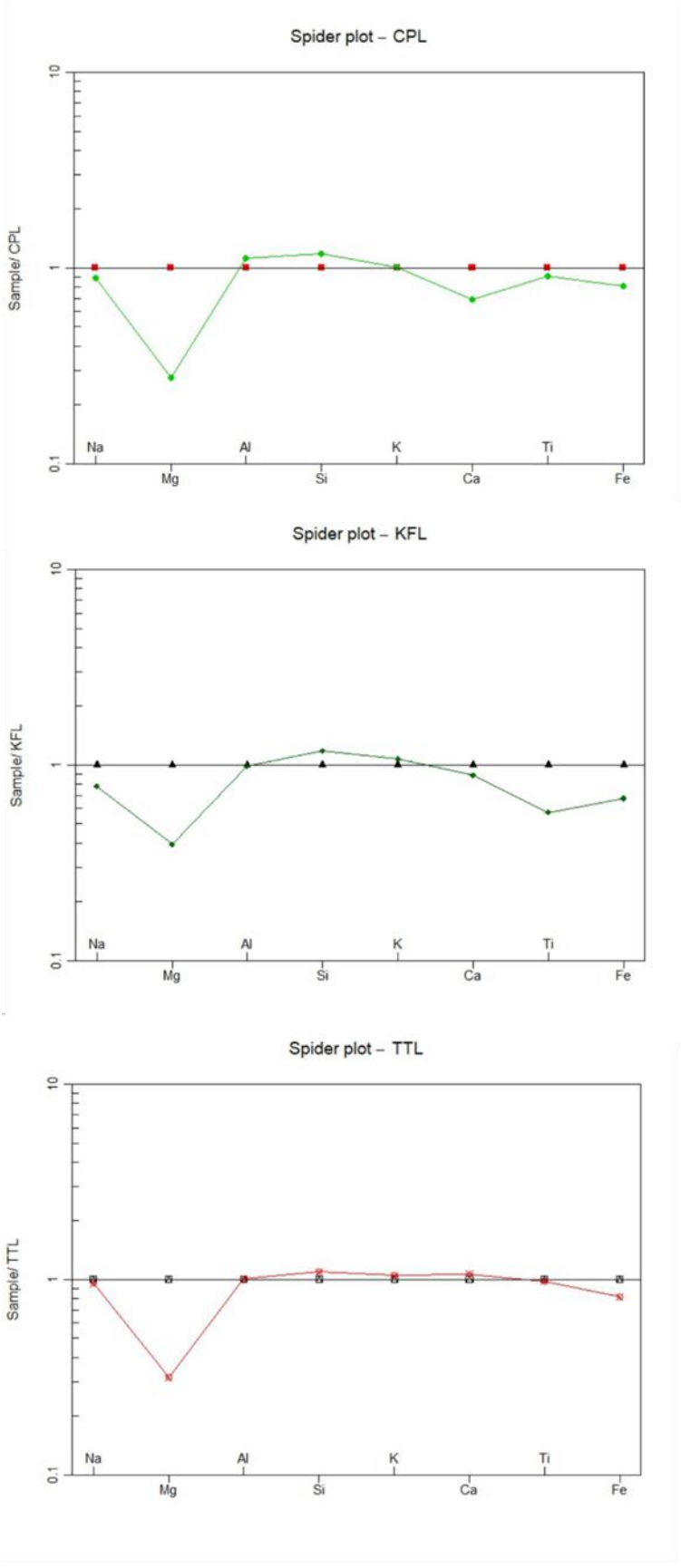

Figure 98: Spider plots from Craig Phadrig, Knockfarrel and The torr showing changes in element abundance compared to the local rock found within 1km of each hillfort.

As per 5.1.3, the Leeman and Scheidegger calculation (1977) (Equation 1: Leeman and Scheidegger calculation (Leeman and Scheidegger, 1977)) was used to give an approximate temperature result from olivine containing melts, for the approximate minimum vitrification temperature of the rocks at Craig Phadrig, The Torr and Knockfarrel, with the temperature spread and range shown in Figure 99. As olivine is a common rock-forming mineral, most samples contained the mineral.

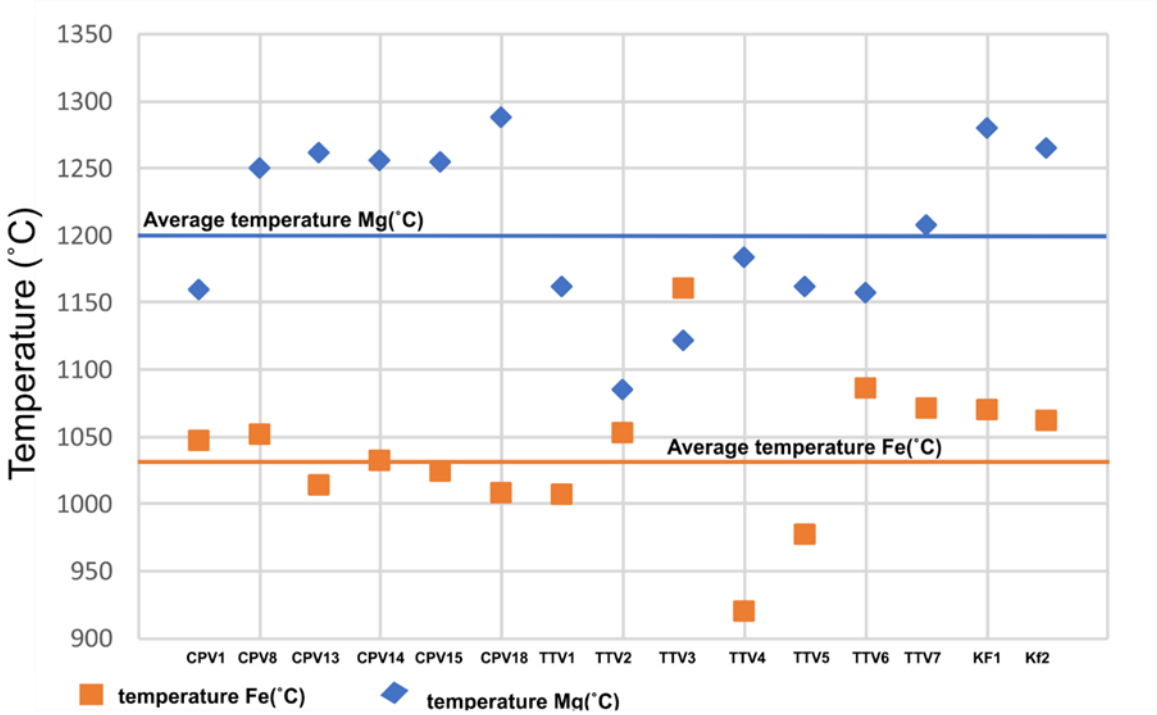

Figure 99: Temperature graph of hillfort samples using Leeman and Scheidegger, (1977) using Fe and Mg difference in olivine and melt of the samples from Craig Phadrig (CPV), The Torr, Shielfoot (TTV) and Knock Farrel (KF)

Table 47 shows the average calculated minimum vitrification temperature calculated for each hillfort. The highest calculated temperature is the highest calculated temperature for each hillfort, which has generally been the value calculated using the movement of magnesium from the olivine into the melt. The fire will have reached a higher temperature than this at times; however, these are the highest minimum melting point temperatures calculated. Just so for the lowest temperatures. The fire temperature will have been lower than this; however, this is the minimum melting temperature calculated for each vitrified hillfort.

Table 47:Average calculated minimum melting temperatures from the comparison hillforts using the Leeman, W P and Scheidegger (1977) equations.

Site	Average T(˚C)	Highest T(˚C)	Lowest T(˚C)
Craig Phadrig	1138	1288	1008
The Torr	1097	1208	920
Knock Farrel	1169	1280	1070
Dun Deardail	1153	1334	979

5.2.4 Petrology

Clasts from four of the vitrified hillforts that we have samples from were used to produce thin section slides for use in petrology and SEM analysis.

As shown in Figure 100, the clast was raised to a high enough temperature for the pelite to boil and melt. Table 48 describes the mineralogical composition of CPV1, an excavated vitrified clast from Craig Phadrig. The vesicles show that the water boiled off the rock and this interpretation is supported by dehydration of the calcite minerals. The spherical, sub-rounded and slightly elongated shape of the vesicles indicate that the rock was moving when molten and the twisted shape may indicate that the clast was still molten when the wall structure and rubble core began to collapse. This vesicle shape also indicates that the melt was viscous, and this prevented many of the bubbles reaching and escaping from the surface of the melted rock. As discussed in 5.1.4: Petrology, the presence of relict ilmenite and pyrite in the sample indicates that the vitrification temperature of the rock was above 1100˚C. The composition of Area A also suggests that the melt was formed in an anoxic environment. Degraded quartz, when mixed with biotite in the pelitic melt suggests a temperature of around 1150˚C. Charcoal fragments, from sub-mm up to around 2mm, are distributed throughout the melted pelite areas, again suggesting that the vitrified material was timberlaced.

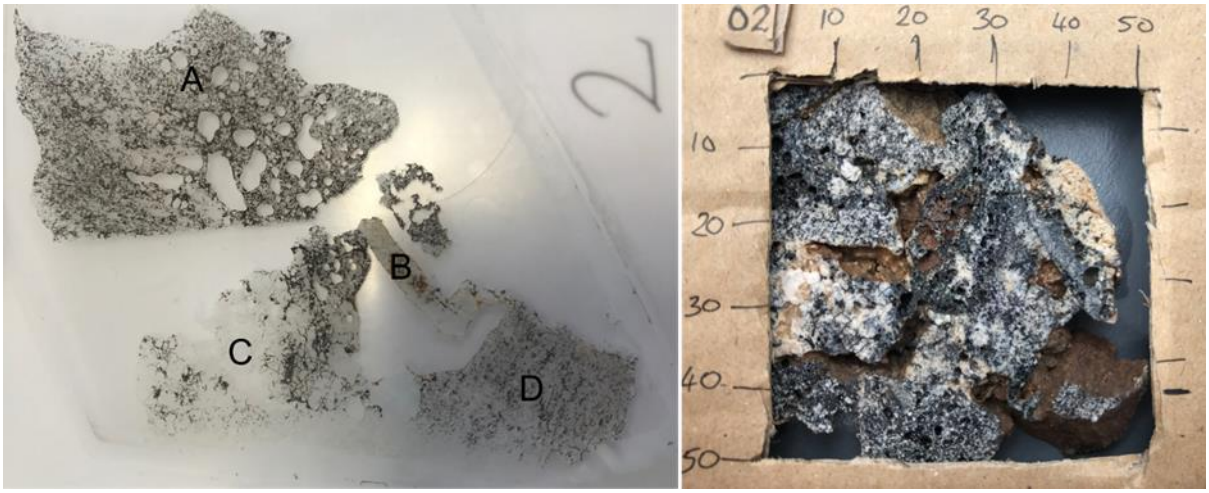

Figure 100: Thin section and cut rock for CPV1

Table 48: Petrology of CPV1 sample from Craig Phadrig.

Sample: CPV1			
Site: Craig Phadrig			
Area A (%): biotite 30 quartz 20 cordierite 10 plagioclase 10 olivine 10 relict ilmenite 5 pyrite 5 magnesioferrite 5 charcoal 5 metallic vesicle coating	**Area B (%):** calcite 60 quartz 30 biotite 10	**Area C (%):** calcite 60 quartz 30 biotite 10 olivine 10 cordierite 10	**Area D (%):** calcite 30 quartz 30 Feldspar 20 biotite 20
General comments: Melt area (Area A) is quite dark in colour and it is difficult to differentiate some of the minerals. Flakes of charcoal, sub-mm to 2mm, are visible throughout the melt area. Can see the edges of the quartz being dissolved into the melt, leaving raggy edges on the crystals. Many crystals damaged due to the melt flow and heat. In area B the calcite is dehydrated and friable. The calcsilicate in area C shows signs of boiling and contains many vesicles. Area D shows signs of deformed layering, melting in the pelitic layers and dehydrating in the calcitic layers.			

Table 49 gives the petrological information gained from thin section CPV15, shown in thin section slide and cut rock in Figure 101. This clast consists of six distinct areas, and each of these will be discussed separately. Area A is a heat altered quartzite. Area B is a heavily vesicular area that has probably been pelitic before the vitrification even and which has been quartz enriched. Area C is a dehydrated layered calcsilicate, where the layering is still evident. Area D has been a pelite containing calcite before vitrification.

This fractured calcite is still evident in the pelitic melt mix. Area E is a dehydrated Metacarbonate. Area F is similar to Area B. All of these suggest anoxic conditions within prolonged hot fire reaching over 1000˚C.

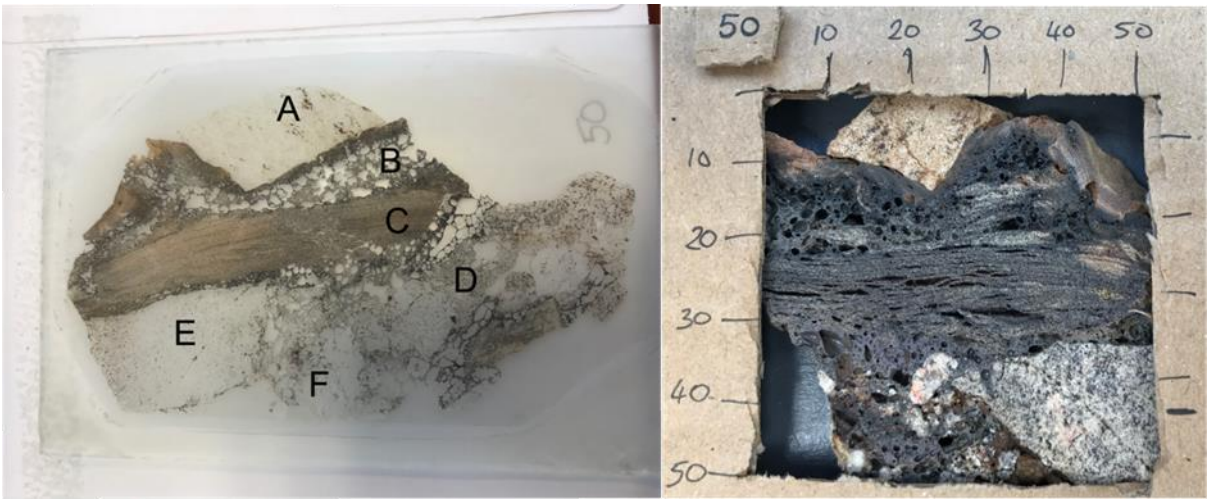

Figure 101: Thin section and cut rock sample for CPV15

Table 49: Petrology of CPV15

Sample: CPV15					
Site: Craig Phadrig					
Area A (%):	**Area B (%):**	**Area C (%):**	**Area D (%):**	**Area E (%):**	**Area F (%):**
quartz 20	biotite 30	biotite 30	biotite 30	calcite 30	biotite 30
calcite	quartz 20	quartz 20	quartz 20	quartz 30	quartz 20
plagioclase 10	cordierite 10	calcite 20	cordierite 10	Feldspar 20	cordierite 10
biotite	plagioclase 10	cordierite 10	plagioclase 10	Biotite 20	plagioclase 10
	olivine 10	plagioclase 10	olivine 10		olivine 10
	relict ilmenite 5	olivine 10	relict ilmenite 5		relict ilmenite 5
	pyrite 5		pyrite 5		pyrite 5
	magnesioferrite 5		magnesioferrite 5		magnesioferrite 5
	charcoal 5		charcoal 5		charcoal 5
	metallic vesicle coating		metallic vesicle coating		metallic vesicle coating

Table 50 describes the three distinct areas observed in the thin section from The Torr, shown as a thin section slide in Figure 102, Area A is a partially melted calcsilicate. Area B is a small heavily vesicular melt area which has probably started as a pelitic rock. Area C is a biotite rich melt that had seeped into the cracks left when the rock was heated and fractured. All of these areas suggest a melt that reached over 1000˚C in anoxic conditions.

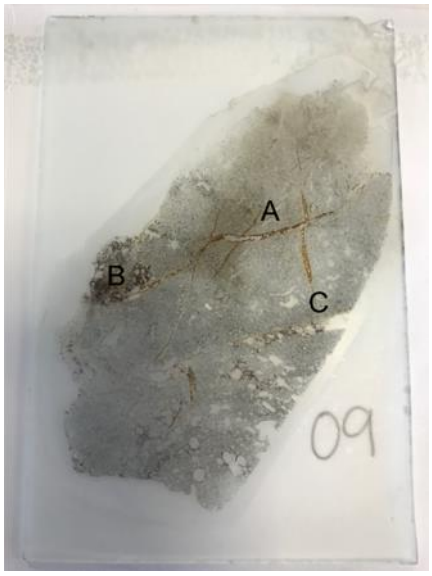

Figure 102: Thin section of TTV02.

Table 50: TTV02 thin-section data from the thin section in Figure 100.

Sample: TTV02 **Site:** The Torr		
Area A (%):	**Area B (%):**	**Area C (%):**
calcite 25 quartz 25 biotite 25 plagioclase 15 olivine 10	biotite 30 quartz 20 cordierite 10 plagioclase 10 olivine 10 relict ilmenite 5 pyrite 5 magnesioferrite 5 charcoal 5 Metallic vesicle coating	biotite melt
General comments: Area A is very dark and glassy		

6 Discussion

This research has investigated the processes and products of vitrification of Iron Age Scottish hillforts through the detailed study of Dun Deardail vitrified hillfort and the targeted study of vitrified hillforts from across Scotland.

Experimental melts results investigated the melting of the local lithology, with different conditions and compositions to replicate some of the conditions that would have occurred during the vitrification process. These experimental melts also determined if the methods that had been proposed for use were fit for purpose or not. Following on from the experimental melts, the provenance of the building material used in the construction and consistency of build of Dun Deardail was investigated to determine if the building materials were local.

The conditions created during vitrification of Dun Deardail, such as the temperatures that the melt reached, and what this meant for the vitrification. Comparison between hillforts takes the Dun Deardail specific results and compares them with vitrified and burnt hillforts in contrasting geological and geographical areas of Scotland. Doing this allowed determination if Dun Deardail was a specific vitrification case, due to build type or construction materials, or if other vitrificated hillforts were of similar construction and vitrification conditions. These analyses also allowed preliminary determination of the state of erosion that the hillfort was in and how this may be further affected by changing weather patterns due to climate change.

6.1 Experimental observations

The purpose of these experimental furnace melts has been two-fold. Firstly, to assess the efficacy of methods for determination of melt temperature, but also to study the effect of vitrification conditions on the melting process and vitrified material under controlled conditions which can then be compared to the evidence seen at the hillforts themselves. The results have been discussed here in the research question order that they answer. This will be discussed in the section after the research questions methods have been verified.

The experimental furnace melting temperatures experiments of the lithologies found in the build of Dun Deardail have been explored in this section.

Five methods of temperature calculation were assessed to have the potential for temperature determination of the melt. Three were instantly dismissed as the samples did not contain any detectable chromium when analysed using SEM. Another type of analysis, such as ICP-OES, may have allowed these temperature calculations to be trialled. As shown in section 4.4, page 76, out of these trails, only one gave a successful approximation of temperature. The Leeman and Scheidegger, (1977) calculation came closest to returning the correct result when the pelite rocks were melted at known temperatures. However, this method will only work in melts that contain olivine as the central part of this calculation is determining differences in iron and magnesium between olivine and the melt. Jung and Pfänder, (2007) equation do not work in this instance as the system is not closed and therefore, the system is not allowed to reach full equilibrium. It is improbable that there would be a completely closed system in any vitrified hillfort situation and therefore this method of temperature determination can be discounted as useful for vitrified hillfort temperature determination. Wan et al. (2008), De Hoog et al. (2010) and Coogan et al. (2014) all were constrained by the same problem. The samples from the area surrounding Dun Deardail did not contain a detectable amount of chromium, using SEM-EDS, and therefore the calculation could not be completed. It would be ideal to be able to rerun the melts using samples containing chromium to determine if any of these methods would give reasonable results for the melt temperatures in vitrified hillforts, however, at present none of the samples used were suitable.

When grain size was investigated, as expected, the smaller the grain then, the easier the sample is to melt. This is important in the melting rubble core of the hillfort as it is likely that there would be midden deposits and eroded rock making its way through the larger rocks in the core. This would have allowed melting to start, and the melt would have then allowed other rock types to begin melting, such as biotite melt on quartz, as shown in the mixed lithology section of this chapter.

The speed of heating and cooling in the vitrifying hillforts was investigated using furnace melts using pelite and calcite mixes and how the materials melt, explode and crack. During the excavation of Dun Deardail, it was noted that the outer walls had cracks in them where the outer fire had been set. However, the inner rubble core remained mainly intact. This suggests a long slow burn and cool down. The melt

experiments show that the calcite explodes and hugely cracks during a fast heat up or cool down furnace cycle. Pelite handles this higher ramp up and down better. However, the crucibles explode during these cycles.

During excavation, it was noted that the rubble core from the ramparts of Dun Deardail consisted of a mixed lithology consisting mainly of pelite, calcsilicate, quartz, calcite and granite. These furnace melting experiments have recreated what happens on to the mixed lithology rubble core during vitrification. Mixing the lithology slightly lowered the temperature that the pelitic rock and quartz melted at. This seems to be especially the case for quartz, where it was difficult to melt quartz as a single rock type where a single lithology melting temperature would be around 1700˚C (Deer et al. 1992). However, it melts more readily when mixed with mica containing rocks. The biotite, in this case, would have reduced the partial melting temperature down to 1150˚C. This has been noticed in both the furnace melting and in the field during excavation. This mixing would have helped the vitrification process and facilitated partial melting vitrification from around 1100˚C.

As fluxes change the energy pathway of a reaction, it has been suggested that fluxes may have been added while building the ramparts to allow for a lower temperature burn to vitrify the structure (Youngblood et al., 1978). This would have been a plausible theory as Iron Age people had an excellent knowledge of fire and smelting. To investigate the effects of flux use and to determine whether the presence of fluxes could be detected in the melt, a series of controlled temperature experiments incorporating fluxes into a pelite rock melt was developed. Different potential fluxes were investigated. Wood and charcoal created the most significant effect on the melting point of the melt and allowed a more consistent burn. Charcoal allows for a long slow, steady burn. Youngblood et al. (1978) suggested that wood and charcoal burn to produce hydrogen and carbon monoxide by:

$$\mathbf{H_2O + C \rightarrow CO + 2H}$$

This would have allowed for a hotter burn than the furnace temperature. Experimental melts seem to confirm that this is the case and is one of the reasons why the rocks with wood or charcoal timbers through them melted when the furnace was set to a lower temperature than that where the wood was not present. Bone and seaweed reduced the

melting point slightly and intensified the burn. Shells added into the rock melt crumble and incorporate into the melt. This left only negligible extra calcium when analysed and did not facilitate the melt in any way. Shells, bones and seaweed may have been added to the rubble during construction as part of the midden pile disposal. Burnt bone was unearthed during the excavation of Dun Deardail in all of the trenches (Cook, 2015). No evidence for seaweed was uncovered during excavation (Cook and Heald, 2016), and with shell, the effect on the melt characteristics of the rock was so negligible that it is unlikely that they were intentionally added. Seaweed was only mentioned once (Nisbet, 1974), in a fleeting reference and the chance of it surviving the burn and melt event is probably too small to leave imprints in the solidified vitrified rock that it can probably be discounted. XRF analysis showed no significant difference in the melt. The fluxes can be detected using p-XRF. However, none of the fluxes tested left a unique fingerprint and so while the presence of additional elements in the p-XRF results may suggest flux use, they cannot tell us which one or ones are present.

The charcoal, as detailed with the fluxes, made a small reduction in the melting point, however, attempting to seal in the material using mud did not work particularly well due to gas building up during melting and this gas cracked the seal. Petrology has shown to be a good determinate of oxidation state. During the insulation experiments where the rocks were insulated, and the heat source switched off, the insulated samples cooled at a slower rate allowing the melting to continue further during cool down, as these took longer to cool, and the heat stayed in longer.

6.1.1 Conclusion of experimental melts

It has been shown that when a mixed lithology cluster of rocks are melted together, some of the minerals from the melt mix together to form a new elemental composition of the rock. This prevents direct use of the p-XRF on the melt to show similar elemental composition of the melted rocks in the vitrified hillfort compared to the rocks in the local area. However, the unmelted components can be analysed by p-XRF as the changes do not occur during heating only. The rocks must be melted to change the elemental composition. Therefore, when analysing the clasts and rocks for provenance, the unmelted part must be the portion analysed and compared to local rocks, from outwith the hillfort area, for provenance. So yes, it has been shown that, with caution, that the methods that have been used in provenance analysis are suitable for use.

During experimental melt experiments, Leeman and Scheidegger (1977) geochemical calculation gave the closest result for known melt temperature and would be suitable for melt temperature determination of vitrified hillforts, with the proviso that the melt contained olivine. This will allow determination of the excavated samples from Dun Deardail and other vitrified hillforts that have been used in this research. Further studies would need to be carried out using different chromium detection methods to allow research into further geochemical temperature determination.

Controlled experimental melts have shown that fluxes do change how the melt proceeds and the residual elements in the solidified melt. The bones especially allowed the melt to happen at a lower temperature, even when the ratio of bone to rock was low. However, even if the presence of bone can be detected, and that its influence on the melting temperature is known, it cannot be determined if the bone was added intentionally to lower the melting temperature of the rock or if this was just incidental, such as the dumping of the midden into the rubble core during construction.

The data gathered here using experimental melts support the use of the methods chosen and may provide some insight into the processes surrounding vitrification in Scottish Iron Age hillforts.

6.2 Dun Deardail provenance and material proportions

The results presented in this chapter have provided enough data for the research questions to be answered. It has been shown that all hillforts in this study have a distinct geochemical fingerprint, and this can be used to show provenance.

The provenance of the materials used to construct Dun Deardail were analysed using a range of geochemical, petrological and visual analysis. If the provenance was found to be local, then there is a lower chance that the rocks were preselected for their melting ability. If the rocks were found to be from further afield, where other suitable building material would have been available closer, then this may suggest selective rock choice. However, absolute intent cannot be confirmed only suggested.

As the silicon and olivine fragment into the melt of the vitrified material, for provenance, the p-XRF analysis had to be carried out on the unmelted portions of the clasts. Leger et al., (1962) showed that there would be increased quartz and sometimes feldspar in the melt in a vitrified hillfort. Research by Winkler, (1967) also agreed that

in-situ melting of minerals created chemical variations in the glass, with (Youngblood et al., 1978)Youngblood et al., (1978) stating that the vitrification in these hillforts had been partial melting and therefore, from this, the geochemical analysis could not be performed on the melt to determine provenance. This was confirmed by performing the experimental furnace melts in section experimental melts. These melts confirmed a partial melting of the rocks, with increased proportions of quartz and biotite; however, a different quantity of these elements entered the melt, depending on the edge area of each of the quartz crystals and partial melting. The geochemical analysis of the clasts from Dun Deardail confirmed that the unmelted clasts shared a similar elemental signature to that of the local rocks.

Visual assessment of Dun Deardail determines that the vitrified hillforts analysed in this research were constructed using local rock from within around 1km from the site location. Those constructing the hillforts would have probably preferred using a source rock from as close as possible to the hillfort site; however, this would not have always been possible. Problems, such as very hard volcanic rock, would make the rock hard to mine and so those constructing the hillfort would have to look further away to find suitable building materials. Helen Nisbet (1975) suggested that Iron Age hillforts would usually be constructed using local lithology, where practical. In the case of Dun Deardail, the lithology that the hillfort was built directly on is calcareous pelite. This rock type would have been difficult to remove from its position and so this constitutes only eighteen percent of the building rock. Almost fifty percent of the rampart and rubble core was built using the pelite, with eighteen percent of the material being calcsilicate, which were both still to be found within half a kilometre of the site. Six percent of the build was found to be granite, which has Ben Nevis, straight across from the hillfort, as its source. There is also a twelve percent proportion of quartz found in the excavated areas. This has also been found to be local in its provenance. Whether using local provenance was the normal status in Scottish hillfort build or if this was a special case has also been studied and this research will be discussed in section 7.4.1.

At Dun Deardail, the results suggest that the rocks are local and not specifically chosen for their fusibility, just that the local lithology happens to be easily vitrified. The location of Dun Deardail might just be a fortunate coincidence, and so it was necessary also to investigate other vitrified hillforts. It could be suggested that hillforts for

vitrifying were built on areas that had a lithology suitable for building, however other hillforts were also researched and showed that not all hillforts, burnt or vitrified, were built on a lithology suitable for vitrification.

The results in this research agree with Youngblood et al., (1978), who suggested that there was no evidence for selected fusibility in the rock types used to build Iron Age hillforts and states that nothing points towards a systemic choice of rock for easy vitrification. Nisbet (1975) also concurred with this theory and believed that local rock would have been used preferentially wherever possible rather than the lithology being chosen for its potential fusibility. And so, in the case of Dun Deardail, this research suggests that the rock has been chosen for its ease of procurement rather than ease of vitrification.

When the geochemical, petrological and visual results are combined, it can be deduced that the rocks used for both the rampart walls and rubble core were local in origin. Both the major and minor elements in the unmelted rocks are comparable to the local lithology found within the 1.5km of the structure.

Visually, it was determined that the highest percentage of building rock consisted of pelitic, layered calcsilicates and calcareous pelites. This is unsurprising as this is the rocks types that the hillfort is built on and surrounded by. These rocks make good sturdy building material and are also easier to mine from the surrounding landscape compared to the igneous rocks of the Ben Nevis formation. There is also a proportion of quartz and granite in the excavated rocks and in-situ vitrified material. Some of the larger cobble sized quartz pieces, found in the rubble core, show wear marks suggesting that they had been used as tools (Cook, 2015; Cook and Heald, 2016). However, the smaller ones look like they have been naturally broken, with no signs of wear.

Comparing the data generated across the trenches shows that the hillfort was built using the same material around the walls and rubble core. The *in-situ* visual assessment has shown that the same proportion of rock types have been used in the areas of vitrified material in the remains. This suggests that there was a uniform mix of lithologies making up the walls and rubble core of Dun Deardail. Geochemical analysis shows that the elemental composition of the rocks that make up the hillfort is the same all of the way around the rampart and this confirms the results from the visual analysis.

Therefore, it can be recognised that the rocks used to construct Dun Deardail were local.

In Dun Deardail hillfort there is no evidence that the rocks have been chosen for their increased fusibility. However, the local rock in the area surrounding Dun Deardail would naturally be both suitable building materials and also good for vitrification. Rocks appear to have been chosen to provide suitable building material and ease of procurement.

Excavation suggests that the hillfort was vitrified at the end of a use period rather than as a building technique. Ash and charcoal were mixed into the rubble in a way that is suggestive of tumble. Excavation has also proven that Dun Deardail hillfort is of timberlaced construction with two thick drystone walls encompassing a rubble core. Archaeological evidence from the three seasons of excavations also suggests that vitrification was a destructive process.

Observation has shown that the rock constructing the walls and rubble core were mainly pelite, calcsilicates and quartz. A smaller proportion of carbonates and granite were also observed. Geochemical and petrological techniques have shown that the building rocks contain the same major and trace element proportions as the local rocks and therefore are local in origin. Rocks from around the hillfort structure all share the same geochemical fingerprint, and so it can be concluded that they all come from the same local source. They have probably been chosen for their ease of procurement rather than for their increased fusibility. If fusibility was to have been an essential part of rock selection, then the proportions of melting rock to non-melting rock would have been higher, whereas what has been observed is that around 50% of some areas of the walls and rubble core and so this would not have made a stable base and instead would have further decreased the stability of the structure.

6.3 Dun Deardail conditions - temperature

For the purposes of this thesis, Zarzycki (1991) gives a satisfactory definition of glass, as used in this way. Zarzycki states that a glass is an amorphous solid showing glass transition rather than a crystalline transition. This may be furthered by Tammann's (1925) definition of glass formation where they state that glass is a substance that is out of equilibrium as it forms when a liquid cools rapidly enough to bypass the liquidus and

start the freezing process before proper crystallisation can occur and by analytical method, it has been shown here that this is what occurs in the processes of hillfort vitrification.

The temperature and conditions of the rock during the vitrification process must be explored if we are to understand how, and potentially why, the hillfort was vitrified.

Through visual examination, petrological analysis and geochemical calculation the temperature for the vitrification of Dun Deardail has been worked out to be in the region of 1150˚C. Leger et al. (1962) hypothesised that the mineral mix of the melted material in the clasts would have reached over 1000˚C and the research carried out here on Dun Deardail suggests that this is the case. Voldan (1962) suggested that in this type of system, the liquidus temperature would be reached by 1300˚C. As the research presented here calculates that the vitrification only reached around 1150˚C this supports the idea that only partial melting occurred as the solidus temperature of 1000˚C has been passed. All of the vitrified hillforts visually assessed contained vesicles. Brothwell et al. (1974) believed that these vesicles were created by boiling off the interstitial mineral water from the original rocks.

The minimum average vitrification temperatures for each trench fell in the range of 1128-1187˚C, calculated using the Leeman and Scheidegger calculation, (1977). These temperatures are plausible, according to Friend et al., (2007) due to quartz partially melting with biotite and muscovite. This can also be seen in the petrology where relict ilmenite has been observed along with pyrite formation. This combination narrows down the minimum melting temperature to around 1100˚C (Morad and Aldahan, 1986). Huang and Wyllie (1975) also agree with the plausibility of this calculated temperature range where this sort of pelitic material should have a solidus temperature of greater than 1000˚C and a liquidus temperature of greater than 1300˚C. As the calculated minimum melting temperature is in the middle of this range, this suggests that only partial melting has occurred during vitrification. This is also what was observed during the experimental furnace melts. This partial melting is one of the reasons why it was more challenging to find a temperature calculation that worked for the vitrified hillfort rocks being analysed. These temperatures would have been difficult to sustain for an extended period of time. However, Kresten et al. (1993) suggested that a sealed system

would have been created, allowing the water to become a supercritical fluid allowing vitrification to occur at a lower temperature than would typically be expected. This was also backed up during the experimental melts stage of this research. In laboratory furnace experimental melts, it was found that the pelitic material from the area surrounding Dun Deardail had melted by 1150˚C, under simple melting conditions. Creating a sealed system during experimental melts allowed the melt to stay molten for a longer time, with lower energy input. This was highlighted further when wood was added, and a sealed system created. This suggests that the supercritical fluidic system, suggested by Kresten et al. (1993), may be one of the pathways to vitrification of Iron Age hillforts.

6.3.1 Were fluxes intentionally used at Dun Deardail to help the burning process and allow the rocks to melt at lower temperatures than without?

Nisbet (1974) suggested several different types of fluxes that may have been used in the vitrification of Iron Age hillforts and so the analysis was undertaken to try to determine if any trace of these fluxes could be established. Visual analysis of clasts had no trace of any item that may have been used as a flux. Nisbet, (1974) suggested items such as shells or seaweed may have been used as flux materials; however, during the laboratory experimental meltings shells and seaweed ashed and were absorbed into the melted pelitic phase. Therefore, fluxes like these may not be visible. During the 2015-2017 excavations of Dun Deardail, bone was unearthed in most trenches (Cook, 2015; Cook and Heald, 2016; Cook et al., 2017). However, this is not an uncommon occurrence during hillfort excavation, and burnt bone has been found on a large number of sites with signs of human interaction. In the case of Dun Deardail, bone was not found in any of the vitrified clasts. This was not unexpected as during experimental laboratory furnace melting experiments, the bones were reduced to powder and incorporated into the melt. This may mean that the bone components were absorbed into the melt and the ones that remained were not in an area that the pelitic melt mixture coated. During Dun Deardail excavations the bones were found in the soil and no sign of bone prints were observed in the outside of vitrified clasts. Bones were discovered during hillfort excavations by Childe and Thorneycroft, (1937) and it was noted that these bones would have had the capacity to change the burn temperature of the vitrifying fire if the quantity was sufficient. However Ralston, (2006) suggests that these bones may have

just been a decoration on the outside of the hillfort and not used as intentional fluxes. Thus, the intention of bone on hillfort sites, if any, will remain unknown, but the presence of burnt bone in hillfort excavation sites is evident. Experimental melts showed that fluxes reduce the melting temperature of the rocks that they are burned with. Wood and charcoal showed the greatest effect, lowering the temperature by forty degrees, whereas bone and shell showed a reduction of between twenty and forty degrees. Unfortunately, this would be indistinguishable from the charred timberlacing found throughout the structure.

Youngblood et al. (1978) observed no evidence of intentional flux use; however, noticed a slight increase in phosphorus. They suggested comparing the glasses with the original lithology to find fluxes and that this could also be carried out on soils or other organic materials. SEM-EDS analysis of the pelitic melt in the clasts suggests a slight increase of calcium in the melt. Youngblood et al. (1978) suggested that an increase in the calcium content of the melt may suggest an addition of bone into the rubble core. However, this may just have been midden dumping into the rubble core during construction rather than intentional flux use. There is not enough information to imply intent. p-XRF analysis of the soil from trench six shows an enrichment of phosphorus in most of the samples. This increases with depth in the trench. Brothwell et al. (1974) found that this phosphorus enrichment was common in vitrified hillforts. This most likely comes from the reaction of the charred wood with the dehydrating vitrifying pelitic rock.

Friend et al. (2008) found no geochemical sign of fluxes during his investigation of vitrified hillforts, however p-XRF analysis on soils from trench six at Dun Deardail show increased phosphorus in several samples, especially the samples taken from lower down in the stratigraphy. Manganese and chlorine also vary from the baseline values.

The presence of the enriched organic material may just be circumstantial or from midden piles added into the rubble core during hillfort construction. In this case, the increase in phosphorus low down in the stratigraphy of the trench suggests that something is occurring here, however, as stated above, this may be midden remains that have been dumped into the rubble core, or there may have been other reasons why the phosphorus is higher the lower down in the stratigraphy. As shown by experimental furnace melts, the timberlacing would have also had an effect on what elements were

detected in both the soils and the melted clasts. Brothwell et al., (1974) reiterated that just because there has been an enrichment of organic material and a percentage of elemental change, this does not justify any claim that any fluxes were used intentionally to change the melting temperature of the rocks and this appears to be the case at Dun Deardail, where there seems to be a small amount of elemental enrichment in the samples. This is most marked in the soil samples but is still visible in the melted areas of the clasts as well.

6.3.2 What was the oxidation state of the melt inside the vitrifying structure?

It was suggested that the environment inside the melting rubble core was anoxic (Díaz Martínez et al., 2005). Daubrée, (1881) found that iron, and to a lesser degree, nickel and manganese, were in a reduced state in vitrified material. In the case of Dun Deardail, preliminary Mössbauer Spectroscopy has also shown that the iron in the pelitic material has been reduced; however, there were not enough samples with the required amount of iron in them to use this method for the samples from Dun Deardail. Therefore, other methods were used to determine the oxidation state of the vitrifying melt environment. Iron spherules are commonly observed in the vitrified material. This was also replicated during the experimental meltings carried out. SEM-EDS analysis carried out on both experimental furnace melts and excavated samples have shown that the iron surrounding the vesicles is found as iron rather than iron oxide. This shows that the environment was anoxic as if an oxygen-containing environment was in existence, the iron would have easily oxidised. The pure metallic iron nature implies strongly reducing conditions during melting (Youngblood et al., 1978).

The case for a reducing environment is also reinforced by the mineralogy observed in petrology slides. Relict ilmenite is observed in the vitrified material, along with pyrite, suggests that the melt was formed in a reducing environment.

In a reducing environment, the ilmenite reduces to rutile (Dimanche and Bartholomi, 1976) by the pathway below:

$$FeTiO_3 + 2H^+ \rightarrow TiO_2 + Fe^{2+} + H_2O$$

From this, the reduced iron can combine with the sulphide from the plant components to form pyrite (Morad and Aldahan, 1986), by pathway 2 below:

$$FeTiO_3 + 2HS^- \rightarrow TiO_2 + FeS_2 + H_2O + 2e^-$$

The dissolved sulphide in pathway 2 may come from the mildly reducing conditions formed by the degradation of plant roots and other organics that may have been growing on the rampart walls (Weibel, 2003). Hence, the combination of roots and soil in the rampart walls may have produced the anoxic sulphide, which allowed the dissolution of ilmenite and its alteration to pyrite (Berner, 1981). This further suggests a reducing environment during vitrification. As previously shown in the petrology results when scanned and viewed under false colour, the vesicles are often coated in iron. This iron is formed when the pelitic rock reacts in an anoxic environment. This is produced as the Fe^{2+} in formula 2 has a higher mobility potential than the titanium ions, and this precipitates around the edges of the forming vesicles. The p-XRF analysis of the melted material shows an increase in sulphur, compared to the local, unvitrified rock, giving more weight to this model.

This reducing environment is not unexpected and has been recreated by the experimental furnace meltings. The oxidation state would be expected to be reducing as the fire would have used up all of the oxygen, and as the outside has sealed then no more oxygen would have been able to be used, and the water boiled off; hence the vesicles with the smouldering charcoal gives off CO (Youngblood et al., 1978).

$$\mathbf{H_2O + C \rightarrow CO + 2H}$$

This would have left carbon monoxide and hydrogen which would have made the fire burn at a hotter temperature and produced an anoxic environment. This would also have allowed the fire to burn hotter than would have been expected. This also indicates that water would have boiled off from the pelitic material producing bubbles in the melted rock and this would have left carbon monoxide and hydrogen which would have made the fire burn at a hotter temperature and produced an anoxic environment. This is demonstrated in the vitrified remains of Dun Deardail as shown by the vesicles in the excavated clasts. Therefore, this appears to be the pathway that the melt has taken at Dun Deardail.

6.3.3 Has the burn been fast or slow?

Experiential furnace melts showed that if the calcitic rocks were heated too quickly that they exploded rather than just cracking. The outside of the vitrified clasts are generally a glass showing that after the external source of heat had been extinguished the outer cooled quickly. This suggests that a skin had formed when the rock was still boiling, similar to the way thick gravy will form a skin while still bubbling on the cooker. As shown by the petrology, the glassy melt is particularly dense and difficult to see through, and this suggests a viscous melt and slow cooling period. The shape and abundance of the vesicles in all of the vitrified samples also confirm a dense glass and therefore, a slow cool-down period (Le Bourhis, 2014). The petrology also indicated that plagioclase had time to crystallise out, and therefore the inside of the melt mixture gluing the clasts together must have taken a greater time to solidify allowing crystals time to form. This would have been caused by the insulating effect that the solidified outer would have created. Colloquially, this would have been a tea-cosy effect keeping the inner warm.

Voldan, (1962) demonstrated that the diffusion of heat through a dense material would have been a slow process, and so for hillforts with walls of several metres thick, this should be the case. Experiential furnace melts showed that if the calcitic rocks were heated too quickly that they exploded rather than just cracking. Observation of the melt in the clasts from Dun Deardail has shown that the clasts have a glassy outside with a vesicle filled inner. This is even more closely highlighted in petrological samples, where the opaque glasses are particularly dense, showing a viscous melt and a slow cooling period. Le Bourhis (2014) also noticed this effect in modern mass-produced glass, where it is a property that glassmakers try to avoid. The glassy texture of the outside suggests that the outside of the melted structure cooled quickly retaining the heat inside, allowing the vitrification process to continue after the fires had regressed. This was another mechanism that allowed a greater degree of melt inside the clasts than would otherwise be expected. Experimental furnace melting has shown that this outer skin would have allowed the melted material inside to remain molten for a longer period of time and this allows the melt to continue to form crystals. This crystal development is also detected in petrological slides from the Dun Deardail clasts and in

this case, the melt is forming new plagioclase crystals. The speed of the heating and cooling is also shown by the lack of explosive features in the calcitic rock. The calcitic rocks are cracked and do not particularly show any signs of explosive fracturing.

6.3.4 Are these temperatures and conditions consistent around the hillfort?

Temperatures calculated from each of Dun Deardail's excavated trenches suggests a similarity in minimum burning temperature. Petrology and SEM-EDS data calculations show that there is a negligible difference in temperature between the west, south and east sides of the remaining rubble core. Observation indicated that the degree of melting is similar around the rubble core remains. This suggests that the fire burned equally around the hillfort. p-XRF results show that oxidation levels were similar around the rubble core. This is further backed up by observations from SEM-EDS, where the vesicles were coated with elemental iron, and so this indicates that a reducing environment would have been present throughout the burnt structure. Kresten et al. (1993) suggested that vitrification may have been accomplished in stages rather than in one massive burning event. However, if this was the case, then it would be more likely that the resulting temperatures and conditions would have been different in each area of the hillfort vitrified. This is not what has been observed at Dun Deardail. As Kresten et al. (1993) was writing about Early Medieval vitrified hillforts, perhaps the technique they suggested for vitrification at Broborg was different from that used at Dun Deardail. This may have been an attempt by the builders of Broburg to copy something they observed on their travels to Scotland but the technique used to vitrify the Scottish hillforts was unknown to them so they may have improvised.

Whether the temperature of the melt around the rampart was equal all around could point towards whether the fire was accidental or intentional. An area with a higher calculated temperature or a much greater degree of vitrification could show that the area was vitrified intentionally. Analysis showed that the temperatures calculated using the Leeman and Scheidegger calculation, (1977) calculation, are similar across all the trench areas indicating a consistency to the burn conditions. Mineral assemblages were also found to be similar, suggesting similar maximum temperatures of burn to achieve melt. In a petrological slide from every trench, relict ilmenite is present, and rutile is forming. The quartz is also showing signs of damage and is starting to breakdown, and so this also ties the temperature of each trench to approximately 1150˚C. This similarity

of the temperature and conditions around the hillfort suggests that the vitrification event was carried out in one single large event rather than several small vitrification events, as suggested by Kresten et al. (1993).

6.3.5 Have rampart building rocks been chosen for their increased fusibility?

In Dun Deardail hillfort there is no evidence that the rocks have been chosen for their increased fusibility. However, the local rock in the area surrounding Dun Deardail would naturally be both suitable building materials and also good for vitrification. Rocks appear to have been chosen to provide suitable building material and ease of procurement. To verify if this is normal for hillfort construction, other hillforts must be compared to Dun Deardail. Excavation also suggested that the hillfort was vitrified at the end of a use period rather than as a building technique. Ash and charcoal were mixed into the rubble in a way that is suggestive of tumble.

6.3.6 Was the build of Dun Deardail such that it facilitated easier vitrification of the hillfort?

The evidence suggests that the build of Dun Deardail did facilitate easier vitrification of the hillfort. However, this does not imply intention. The timberlacing provided the internal fuel and allowed the fire to spread through the walls and into the rubble core. This facilitated the vitrification by allowing heat into the core and producing the carbon monoxide and hydrogen to increase the temperature of the burn. This is further highlighted by the lack of vitrification in the wall separating the upper and lower areas of Dun Deardail. This wall was not timberlaced, did not contain a rubble core and showed no sign of there having been any timber superstructure on top (Cook et al., 2017). This suggests that at least one of these elements is important in vitrification as the fire did not spread along this wall and there is no sign of any vitrification anywhere on its length. Driver, (2016) calculated the quantity of wood that a typical timberlaced hillfort would have contained and this amount would have made a substantial contribution to the internal fuel to keep the fire burning. During the excavation of Dun Deardail, the horizontal beams appeared to be set at around one and a half metre intervals. If this was the same all around the hillfort and for the height of the hillfort, this would have made a substantial amount of fuel. With Dun Deardail having a rough perimeter of just over one hundred meters and built to a height of six meters, this could mean around four hundred timbers may have been used in the construction of Dun

Deardail. This is a vast quantity of fuel and would have most definitely allowed the hillfort to burn for a prolonged period.

An increase in the sulphur content of the melted rock may indicate that there was root growth infiltrating the rampart. Weibel (2003) suggested that organic matter may interact with the rock to produce sulphur in fluvial deposits in warm and wet environments. One of the mechanisms that may have been in place at Dun Deardail if the hillfort was standing for several decades before it was burned to the ground. This may suggest that vitrification was an end of that period of use for Dun Deardail, rather than a constructional tool, as suggested by Brothwell et al., (1974) and Kresten et al., (1993).

Combining the results from the experimental furnace meltings, the laboratory analysis of the excavated material and the results from the excavation itself, it would suggest that the structure of Dun Deardail did facilitate its vitrification. Whether intentional or accidental remains an unknown quantity, but it does appear to be an end of this stage of its life process. Christison et al. (1905) and Youngblood et al. (1978) did not think that the glass results showed any answer to whether vitrification was a constructional or destructive event. However, the combination of laboratory, experimental and excavation appears to suggest otherwise.

Experimental furnace melts have shown that having wooden beams through the structure, as well as a superstructure on top, provides fuel and an atmosphere that helps the vitrification process. The beams also transfer the heat through the walls and rubble core, both transversally and longitudinally. This allowed the spreading of the heat even when the original heat source was on the outside of the structure. Excavation showed that Dun Deardail was built as a timberlaced hillfort with a suggestion of a large wooden structure on top (Cook et al., 2017). However, this may just have been to give the structure greater stability rather than to ensure a good and even burn. The fluxes that may have been used in the rubble core may have just been from midden items in the rubble core, such as shells and bones, or may have been decoration on the outer walls, as suggested by Ralston, (2006). Therefore, no intention has been determined in any of the analysis to prove or disprove the question of whether Dun Deardail was built to facilitate easier vitrification. However, Dun Deardail provided another piece of evidence as to whether the build type of the ramparts assisted with vitrification. There is

a lack of vitrification in the wall that separated the upper and lower citadel in the hillfort interior. Carbon dating has shown that the walls are synchronous and so this wall has not been built after the vitrification event (Cook et al., 2017). However, this wall shows no sign of vitrification. The main differences between this wall and the hillfort rampart are that this was built as a single wall, with no rubble core and no timberlacing. This suggests that the build type of the wall was an important part of the vitrification process.

Unfortunately, there have been no recent large scale burning since Mainland in 2001 (Ritchie, 2018). Therefore, in this research, the closest to a large-scale burn that has been explored was the experimental furnace melts. The experimental furnace melts show that having timberlacing does improve the burn quality of the vitrification. It also shows that having different fluxes in the mix helps to allow the melt to occur at a slightly lower temperature. None of these, however, show that ease vitrification was the goal when planning and building the hillfort.

6.3.7 Dun Deardail conclusion

The research presented here indicates that the average minimum melt temperature at Dun Deardail was 1153˚C; however, the fire used to create this would have periodically risen to higher temperatures. There are also trace elements that could indicate the use of fluxes in the construction or destruction of the hillfort, however, it is unknown if these have just been midden deposits dumped into the rubble core during construction or into the timber that would have been stacked against the hillfort to burn it down. Slight traces can identify that the fluxes may have been present; however, they cannot prove intent if any. The melt mix was found to be anoxic, and this could suggest that this was either an intentional design, to make the fire burn longer and create supercritical fluid reactions that allowed the fire to burn hotter than would be if it was open. This anoxic environment may also have been created by the reaction of the mineralogy of the pelitic rock with a plant root network that may have grown in the time between the building of Dun Deardail and its destruction by fire. This may also indicate that vitrification is an end of life process rather than a constructional process. However, the anoxic environment may just have been that all the oxygen has been used up during the burning, and as the melt sealed no other oxygen could get in to continue the reaction. If this is the case, then there would be no indication of intent or nor or even if this was a

constructional or a destructive process. Comparing what has been seen at Dun Deardail to experimental melts, it can be concluded that the burn even of Dun Deardail was long and strong. The extent of the melt would have needed the rock to remain molten for many days, probably over a week, and this burn would have taken a bit to get going and then held at a high temperature inside the rubble core. The construction type of Dun Deardail was timberlaced and so probably contained over four hundred timber beams in its structure. This would have been plenty for a long, continued burn. Glass analysis from the vitrified clasts appear to concur with this theory of a long, continued burn. Analysis has indicated that the conditions were similar around the rampart during the vitrification. This suggests just one significant burning event rather than a series of short vitrification attempts over small areas of the rampart.

Vitrification has made the structure more structurally sound than would have been expected from a modern glass melt. After over two thousand years, the glasses within the clasts remain structurally sound whereas modern glasses have begun to weather within just over thirty years. Again, this does not suggest either way whether vitrification was a constructional process to strengthen the walls or a destructive process at the end of its life. All it shows is that the structure is sound and weathering well and heritage organisations should not be overly concerned about the erosion of the remains of Dun Deardail.

6.4 Comparison of Dun Deardail and other case study sites

To fully understand Dun Deardail, its conditions of vitrification must be understood in a broader Scottish context. This is especially important as much of the lithology surrounding Dun Deardail would already be easy to vitrify and so would be a good choice to build with whether vitrification was a long-term goal or not. Other hillforts that are sited on not such ideal conditions also have to be considered to ensure that the research is comprehensive and representative of the Scottish Iron Age vitrified hillfort scene.

6.4.1 Was Dun Deardail unique in its provenance of building materials or are other Scottish vitrified hillforts similar?

As shown in section 6.2, the ramparts of Dun Deardail have been constructed using locally available materials. This was confirmed both by visual analysis of the rocks and by geochemical analysis. The geochemistry, as shown in the spider plots, shows a

distinct fingerprint for each hillfort and its local geology. This fingerprinting has shown that the rocks used in the examined hillforts have been locally sourced.

The conglomerates used in hillforts, such as Knockfarrel, have produced the gneiss, schist, quartzite and sandstone needed for the vitrification process. This finding is probably unsurprising as local rocks would have been much easier to transport to the site than rocks from a distance away.

Nisbet (1975) suggested that, where possible, hillforts would be built using the local rock. However, it appears that where the local rock was not easy to use, then rock from further afield was used. This is evident in The Knock where the hillfort was built on basalt, which would be too difficult to extract due to its hardness, but the hillfort was built using red sandstone from the bottom of the hill that the hillfort was built on. Rock that is easier to mine and transport would have been preferable to rock that had to be transported a long distance. This appears to be the case for the hillforts in this research. The Knock, 1km north of Largs, Ayrshire, was constructed using local red sandstone at the bottom of the hill that it sits on instead of the pyroclastic basaltic rock that it was built on. This was probably because the sandstone was far easier to mine than attempting to remove the basalt. The sandstone would not have been easy to vitrify, and in this case, the hillfort was burned, but no sign of vitrification was observed during excavation, and so it appears that the material was not chosen to its ability to melt easily. Knockfarrel has also been constructed using the local conglomerate rock. The conglomerate in the local rock allowed for easier mining of the construction materials.

Geochemically, each hillfort area, showed its own elemental fingerprint, and this allows confirmation that local rocks were used in hillfort construction. There appears to have been no preferred geochemistry or lithology selected for rampart construction.

6.4.2 Have the same temperatures been required for vitrification of Dun Deardail compared with other vitrified hillforts in Scotland?

The rocks at Dun Deardail were calculated to have an average maximum temperature of 1153˚C. Temperature calculations show that the average maximum melting temperatures for the comparison hillforts analysed compared to Dun Deardail are found to be in the same region. Petrology of the samples also agrees with this conclusion; however, petrology only give an approximate temperature range, in this case, higher

than 1000˚C, but the minerals present, mixed melt and strain formations are similar. Youngblood et al. (1978) believed that the degree of vitrification varied between sites, and this is supported by observations taken during vitrified hillfort site visits. They also believed that every vitrified hillfort temperature would fit into the range of 1000-1300˚C. Results calculated from all four hillforts analysed fall into this range. However, Friend et al., (2016) found that from calculations, this range would have been in the range of 850-950˚C, which is slightly lower than the lower range of temperatures calculated for the hillforts analysed in this research.

6.4.3 Were fluxes found in Dun Deardail also found in other Scottish vitrified hillforts?

As no samples of soils were recovered from any of the comparison hillforts, then the glass must be looked at to determine if any fluxes are identifiable (Youngblood et al., 1978).

As discussed previously, Nisbet (1974) documented several fluxes that may have been used in vitrified hillforts. Unfortunately, no soil samples were available for any of the comparison hillforts. At Dun Deardail SEM analysis on the melted material showed a slight increase in calcium, leading to the possibility of bones being used in the rubble core. However, neither Craig Phadrig nor Knockfarrel showed this increase. Samples from The Torr showed a slight increase in calcium. There are no other signs of flux use in any of the vitrified material. This does not confirm that no fluxes were in use, just that no trace of them has been preserved in the melt. The flux use in these samples remains an unknown quantity.

6.4.4 Were the oxidation states of the melt inside the vitrifying structures alike?

Just as the oxidation state of Dun Deardail vitrification proved to be anoxic, the data shows that this is also the case at Craig Phadrig, Knockfarrel and The Torr. Unoxidized iron surrounds the vesicles and, as this had not reacted with oxygen, this would have been formed in a reducing environment (Youngblood et al., 1978). As shown for Dun Deardail, the formation of pyrite from ilmenite, as showing with relict ilmenite and forming pyrite in petrology analysis (Berner, 1981). Again, this agrees with the experimental laboratory melts carried out. As with the SEM-EDS samples from Dun Deardail, the vesicles in the clast interiors are coated with unreacted iron. This suggests

that there was an anoxic environment inside of the burning remains as the rock was melting. Again, this is identical to the conditions that have been found at Dun Deardail. Also, the disintegration of ilmenite and the formation of rutile, as observed in the petrological samples showed that this environment was reducing.

6.4.5 Was the burn fast or slow?

As with Dun Deardail, visual assessment of the hillforts visited has suggested that each of these hillforts also had a long and slow burn. With the vast quantity of beams contained in the timberlaced ramparts, the core would have stayed molten for over a week. When compared with results obtained during the experimental laboratory melts, the sample would have been molten for at least eight days. A skin would have formed over the molten material and retained the heat inside the core. This would have allowed partial melting reactions to occur and kept the molten material in between the liquidus and solidus temperatures. Rocks that did not melt have cracked and fractured rather than exploding, in the way that the rapidly heated rocks did during the experimental furnace melts. As with Dun Deardail, the plagioclase had time to begin to recrystallise and so the melt time must have been long. If it was a short time melt, the plagioclase would be breaking down and fracturing, but this is not what was observed in the thin section petrology.

Large modern building fires, such as the Bank Buildings in Belfast or the Glasgow Art School, also burned for days, even though firefighters were attempting to put each of the fires out (BBC News, 2019; BBC Scotland News, 2019). Both of these fires were also accidental and contained enough construction material fuel to allow the fire to burn and then smoulder for days.

6.4.6 Have the construction methods used for Iron Age Scottish hillfort aided vitrification?

Dun Deardail was found to be a timberlaced, rubble cored twin-walled hillfort, built using local rocks. This build was also found in the other hillforts used for comparison, whether they were vitrified or just burnt. The timberlacing would have helped the heat spread through the ramparts and also provided fuel for the combustion to continue. All of the vitrified hillforts that have been investigated have been built using material that was reasonably easy to melt. In the case of The Knock, this was constructed using red sandstone and therefore when it was burnt the silica bonds remained strong as they did

not contain the biotite or other mica minerals, that would have allowed the silicon to melt at a lower temperature (Kresten et al., 2003). The vitrified hillforts researched in this study were constructed using timberlacing encompassed with a large, two drystone wall construction on the outer and inner faces of the rampart and a rubble core inside.

6.5 Processes of vitrification in Scottish Iron Age hillforts

The soil core taken during season three of the Dun Deardail excavations showed signs of two large burning events. As these burning events have been dated as around one hundred and fifty years apart. It has been suggested that these burning events represent the building and then the destruction of Dun Deardail, where the first burning would be the clearing of the hillfort building site and surrounding areas once the timber had been cut for hillfort construction and the second would be the vitrification burn. (Cook et al., 2017). This concurs with the suggestion that the formation of the sulphurous elements found in the melt, which allowed the formation of rutile, was formed by the presence of roots that had been infiltrating the rampart structure. These roots would have taken many years to penetrate through to the rubble core and so suggests that the hillfort stood for many years before its destruction. When combined, both of these forms of evidence suggest that vitrification was not used as a constructive process. It was, in fact, a destructive process. Whether accidental or intention is still an unknown quantity. However, vitrified hillfort excavations are generally low on finds. This was evident at Dun Deardail, The Knock and Craig Phadrig. A dagger, a melting crucible and some grain were the main non-lithological finds in three seasons of excavation. It appears that the hillforts were cleared of goods and possessions before they were set alight. This suggests that the vitrification fires were an intentional event, perhaps an end of life ceremony, a ritual closure, rather than an accident or malicious destruction by an opposing army. Geochemical analysis has shown that these vitrification events were one single event at each of the hillforts examined. Analytical results at Dun Deardail give findings that are too similar around the rampart for the vitrification to have been carried out at different times.

This destructive burning event was found to have occurred at an average temperature of 1150˚C. The fire would have reached far higher temperatures for short periods of time; however, this higher temperature would not have been sustained. The build of the hillforts studied would have facilitated an easier route to vitrification. The construction

techniques used in the hillforts seem to be similar in that they are both timberlaced with rampart structure containing a rubble core of local rock. This timberlacing has facilitated the spread of heat and allowed anoxic conditions to occur within the rampart structure. The length of time that hillfort stood before vitrification has also helped with the vitrification. The timberlacing would have also acted as a flux for the fire. Experimental melts have shown that the wood would have both created a supercritical fluid system, allowing the vitrification to occur at a lower temperature, and produced carbon monoxide allowing vitrification reactions to occur. Bones, most likely from midden material disposed of in the rubble core during construction, may also have allowed the melt to have occurred at a slightly lower temperature.

The lithology was found to be crucial to vitrification, and this may be why fires at hillforts such as Dun Deardail produced great vitrification whereas hillforts, such as The Knock, which were constructed using local sandstone, have been found to be burnt but vitrification did not occur. Therefore, it can be concluded that these hillforts were constructed using material that would be easy to work with rather than lithologies that would be easy to vitrify. It has been found that the rock types used are local in each of the hillforts examined, all within two kilometres of the hillfort site, and most were from even closer.

6.6 Variability vitrified hillforts

Following on from the Youngblood et al., (1978) classification of hillforts, the geochemically analysed hillforts can be categorised into the three groups according to the melt glass mineral properties compared to the local rock (Table 51). This shows a distinct mineralogical difference between the melt in the vitrified areas of the remains.

Table 51: Analysed vitrified classification according to Youngblood et al., (1978).

	hillfort melt groups		
	Group 1	**Group 2**	**Group 3**
hillfort	Dun Deardail	The Torr	Knockfarrel
	Craig Phadrig		

6.7 Erosion and stability of vitrified hillforts

The long-term future of hillforts such as Dun Deardail has been questioned by heritage authorities, such as HES. The examination of erosion on vitrified material has been highlighted as one of the Dun Deardail project objectives and as a concern for HES

(AOC Archaeology Group, 2015). This was highlighted in the ScARF report on the Iron Age (Hunter and Carruthers, 2012). SEM-EDS and visual analysis show that the glasses that makeup Dun Deardail show little degradation, even on the outer surfaces and in the fissures on the clasts. This is in contrast to the findings of McLoughlin et al. (2006) who found that modern glass begins to degenerate within thirty-two years of burial.

Charles and Hillig (1962) provided a pathway for the usual corrosion of silicate glasses. They hypothesised that the silicate degrades as:

$$Si\text{-}O\text{-}Si + H_2O \rightarrow Si\text{-}OH + HO\text{-}Si$$

This pathway shows the transformation of a siloxane bond into two silanol groups leaving a silicate gel instead of a crystal structure and this gel is easy to weather. This is especially prevalent at edges of the exposed crystals or cracks and flaws in the crystal make-up. This corrosion mechanism allows the cracks to extend and edges to degrade further and is a self-propagating reaction which continues the weathering of the glass.

However, as previously shown, the vitrified glasses of Dun Deardail do not show much weathering. Part of the reason behind the vitrified hillfort glass being so resilient may be due to the increased calcium levels found in the glassy melt mixture that glues the clasts together. This calcium works as an inhibitor to ion movement in the glass.

According to Bourhis (2014), in normal glass weathering:

$$\mathbf{Si\text{-}O\text{-}Si + OH^- \rightarrow Si\text{-}OH + {^-O\text{-}Si}}$$

However, the relatively immobile calcium ions retard this reaction and hinder the movement of other ions in the melt system. This retardation of the normal glass weathering process may indicate why Iron Age vitrified hillforts have not weathered as one would expect glass to. This may also be the reason why they are still very much in evidence in the Scottish landscape, despite over two thousand years of weathering and corrosion, both above and below ground, and several periods of reuse.

6.8 Conclusion

Provenance and conditions are similar across the vitrified hillforts included in this study. The hillforts visited all were constructed of local rock. Construction materials all appear to be the local rock types that are accessible and easiest to mine. This is

unsurprising as if a structure can be built in an easier fashion, but still look impressive and be functional, then why would you make it more difficult than it has to be?

Minimum temperatures of vitrification have been found to be around 1100˚C for all vitrified hillforts examined. The comparison vitrified hillforts all appear to have had a long and slow burn; however, this does not answer the question around if the vitrifying fire was accidental or intentional. Only that it lasted days. The material contained inside of the hillfort would probably have been enough to sustain the fire for a long while, like largescale fires in modern times, and also the pelitic mix melt would have sealed in the hot interior rocks allowing melting to continue after the fire was extinguished.

Building materials also seem to be crucial. Sandstone appears to be more challenging to melt itself compared to those constructed with rocks containing lower temperature melt materials, such as pelite.

So, bringing these results together, it would appear that Dun Deardail is not unique in its construction, provenance or conditions of vitrification. Given the correct materials and conditions, vitrification could occur over days on any hillfort site, however, why this did not happen on every burnt site that fits the same criteria as Dun Deardail is still an unknown quantity.

To fully understand Dun Deardail, its conditions of vitrification must be understood in a broader Scottish context. This is especially important as much of the lithology surrounding Dun Deardail would already be easy to vitrify and so would be a good choice to build with whether vitrification was a long-term goal or not. Other hillforts that are sited on not such ideal conditions also have to be considered to ensure that the research is comprehensive and representative of the Scottish Iron Age vitrified hillfort scene.

Nisbet (1975) suggested that, where possible, hillforts would be built using the local rock. However, it appears that where the local rock was not easy to use, then rock from further afield was used. This is evident in The Knock where the hillfort was built on basalt, which would be too difficult to extract due to its hardness, but the hillfort was built using red sandstone from the bottom of the hill that the hillfort was built on. Rock that is easier to mine and transport would have been preferable to rock that had to be transported a long distance. This appears to be the case for the hillforts in this research.

The Knock, 1km north of Largs, Ayrshire, was constructed using local red sandstone at the bottom of the hill that it sits on instead of the pyroclastic basaltic rock that it was built on. This was probably because the sandstone was far easier to mine than attempting to remove the basalt. The sandstone would not have been easy to vitrify, and in this case, the hillfort was burned, but no sign of vitrification was observed during excavation, and so it appears that the material was not chosen to its ability to melt easily. Knockfarrel has also been constructed using the local conglomerate rock. The conglomerate in the local rock allowed for easier mining of the construction materials.

Geochemically, each hillfort area, showed its own elemental fingerprint, and this allows confirmation that local rocks were used in hillfort construction. There appears to have been no preferred geochemistry or lithology selected for rampart construction.

Youngblood et al. (1978) believed that the degree of vitrification varied between sites, and this is supported by observations taken during vitrified hillfort site visits. They also believed that every vitrified hillfort temperature would fit into the range of 1000-1300˚C. Results calculated from all four hillforts analysed fall into this range. However, Friend et al., (2016) found that from calculations, this range would have been in the range of 850-950˚C, which is slightly lower than the lower range of temperatures calculated for the hillforts analysed in this research.

As no samples of soils were recovered from any of the comparison hillforts, then the glass must be looked at to determine if any fluxes are identifiable (Youngblood et al., 1978).

As with the SEM-EDS samples from Dun Deardail, the vesicles in the clast interiors are coated with unreacted iron. This suggests that there was an anoxic environment inside of the burning remains as the rock was melting. Again, this is identical to the conditions that have been found at Dun Deardail. Also, the disintegration of ilmenite and the formation of rutile, as observed in the petrological samples showed that this environment was reducing.

The vitrified hillforts researched in this study were constructed using timberlacing encompassed with a large, two drystone wall construction on the outer and inner faces of the rampart and a rubble core inside.

7 Conclusions

This research has brought together excavation, field analysis, experimental laboratory furnace melts, petrology and geochemical analysis for the first time in vitrified hillfort analysis.

Using visual and geochemical methods it has been determined that all of the studied hillforts have been constructed using materials from within a 2km radius of the site. Sites that do not use material directly beside where the hillfort was constructed often have a constraint of the adjacent rock would be difficult to remove rather than difficult to vitrify. Therefore, there is no evidence found at Dun Deardail or any of the comparison sites that the building materials have been chosen for their ability to melt. The evidence provided from the analysis conducted for this research shows that it is more likely that the materials were chosen locally for ease of mining.

Geochemical analysis has shown that the analysed hillforts fall under a range of groups from the Youngblood et al., (1978) classification of hillforts. There was a distinct mineralogical difference between the melt in the vitrified areas of the remains in each of the hillforts and therefore variability in the mineralogy of vitrified hillforts exist. So even though the major factors in the success of vitrifying a hillfort appears to be lithology and build, variabilities in the mineralogy do still exist and this may account for the wide spread of vitrified hillforts in Scotland.

Experimental melts show that lithology is key to successful vitrification. This was also noted in the field where The Knock showed definite signs of burning, but no sign of even partial vitrification was evident. Hillforts constructed using rock that has lower melting temperature and a mixture of rock types have a higher chance of vitrification; however, there must be other mechanisms at work during the vitrification process. This is highlighted by the differences in vitrification between Craig Phadrig and Ord Hill. Both were constructed from similar rock types and are in the same area; however, only Craig Phadrig is fully vitrified. A full excavation of Ord Hill would be able to tell if there were differences in the timberlacing or internal structure of the ramparts. Field sampling has shown that all the hillforts included in this research have been built using rock that can be found within 1.5km of their outer ramparts. This would have been for ease of construction. Hillforts for samples further away were built on or beside rock that

was not too difficult to mine. Temperatures of melt were determined using a combination of petrology and geochemical calculation, averaging 1140˚C across all vitrified hillforts sampled. This temperature corresponds with the results determined in the laboratory furnace experimental melts.

This long-lasting vitrification event would have been helped by the timberlaced structure as the timberlacing allowed heat to be transported through to the rubble core of the ramparts, created extra fuel for the fire and allowed the anoxic environment of vitrification to develop. This was noted during excavations of Dun Deardail where the timberlaced rampart had vitrified whereas an adjoining wall, which was not timberlaced, showed no signs of vitrification. This shows that the timberlaced construction is an important part of whether vitrification will occur.

When the results from the flux added experimental melts were compared with those from the excavated hillfort samples it reinforces that there was no purposeful addition of fluxes to produce vitrification and that the trace element analysis result changes are from the timberlacing and midden deposits disposed of in the rubble core of the ramparts. This suggests that the vitrification was an unintentional side effect of the burning of the hillfort and that the hillfort construction and design meant that there was no need for fluxes for vitrification to occur.

Three seasons of excavation combined with laboratory experimentation and analysis suggests that the Dun Deardail was burned at the end of this period of its use. The lack of artefacts unearthed during excavation suggest that the hillfort had been cleared of its contents before the fire was started. If people were rushing from a burning hillfort or a hillfort which had been captured by an enemy who were planning to destroy it, they would not have had time to remove all of their goods. Therefore, this suggests that the hillfort was burned down intentionally by its users in a pre-planned fire at the end of that period of the hillforts use and reinforces the theory presented here that vitrification was not the aim of the burning the hillfort, only a side effect.

The stability of the vitrified glasses was not in the original research questions; however, this research has also shown that the vitrified glass, surrounding the clasts, is more resilient to erosion than modern glass. This stability has allowed the ruins of the vitrified hillforts to be preserved in a recognisable state and points towards the

protection of vitrified structures for the future. However, the exposed dehydrated calcitic areas of the remains are showing signs of degradation. If climate change brings warmer temperatures, higher rainfall levels and decreased pH in rainwater then this may cause an erosional problem with the calcitic areas. The further weathering and erosion of these areas may cause the calcitic areas to weather out and expose new areas of the rampart remains to the elements. In the long term this may cause harm to the stability of the hillforts. And so, if Dun Deardail is taken as a prime example of Scottish vitrified hillforts, there are two mechanisms going on with their erosion. The calcium enriched glasses are protecting and strengthening the structure in the vitrified areas whereas the exposed, dehydrated calcitic areas are at risk of being damaged by predicted climate change weather patterns. This research will be able to help to determine a preservation strategy for historic protection agencies and should be continued to its full potential.

7.1 Limitations of study

Samples from Dun Deardail were chosen through trenches, that was determined in the Dun Deardail Archaeological Project method statement, (AOC Archaeology Group, 2015). This means that were being dug, and removal sampling could only be done in these areas. An ideal sampling plan would have allowed samples from a fully representative portion of the hillfort. However, the areas not sampled were deemed too steep to excavate safely, and in any hillfort excavation, there are bound to be areas that are not suitable for excavation. However, this can be compensated for. p-XRF measurements in other areas on Dun Deardail were able to be taken and visual analysis was performed on all hillforts visited and this has allowed analysis of the complete rampart ruin.

There were also limitations with excavated laboratory samples. Samples larger than 25cm in diameter were unable to be cut using the laboratory saw, and therefore larger samples will not have been analysed using SEM or petrology. However, most of the samples excavated were smaller than this, so this was not particularly restrictive. Visual analysis and surface p-XRF analysis were able to be undertaken and so this was not a major constraining factor.

A limited range of hillforts was covered in this PhD. A continuation of this project, excavating and analysing samples from further hillforts, would add depth to the findings of this thesis. An ideal situation for this would be for further funding to be

obtained to further the findings, possibly as a postdoctoral position. This would be especially useful as ScARF has highlighted a case for researching erosion on historical monuments to determine methods of preservation for future generations.
Due to the nature of the samples, it was not wholly possible to have completely heterogeneous samples, and therefore there are differences in results between samples and between different instrumental techniques. This is also exacerbated by differing detection limits of various techniques. This possibility of error is low between samples, as shown in the experimental melts results chapter, but it is essential to acknowledge that it exists. Also due to the nature of the melt, where more quartz and other minerals enter the melt, the direct comparison of the melts will have a higher level of error than comparison between burnt, heated or natural rocks.

For temperature calculations, several methods were considered. However, the final choice came down to available minerals and completeness of equilibrium. In other samples containing a different range of minerals and in different circumstances, some of the other methods trialled during the experimental melts may have worked and given temperature results comparable to the results determined using Leeman and Scheidegger, (1977). Other methods of elemental determination, such as ICP-OES should be considered as the next stage to this research. Again, ideally, continuation could occur if suitable postdoctoral funding could be sought.

These limitations have been highlighted to acknowledge their existence; however, they do not detract from the findings presented.

7.2 Further research

The ideal scenario would be to continue to build up a database of vitrified hillfort analysis to allow further comparison. With over sixty known vitrified hillforts, this would allow further comparisons to be made between sites. Continued research into erosion on vitrified hillforts would also be beneficial. This would allow conservation practices to be tailored to the developing situation. Further research on fire dynamics and heat transfer would further the information already possessed of how the fire spread and persisted. Further analytical techniques should also be undertaken including ICP-MS to further determine the temperature in samples that do not have olivine but do contain chromium and XCT would allow the internal structure of the clasts without them having to be cut. Mössbauer spectroscopy analytical methods should be

investigated further using iron-rich samples as this would allow a third method of temperature determination for samples with differing iron oxidation state ratios. It would be envisaged that postdoctoral funding will be applied for to continue and further develop this research.

8 Bibliography

AOC Archaeology Group, 2015, Dun Deardail Archaeological Project Method Statement Dun Deardail.:

Armit, I. & Ralston, I.B.M., 1997, The Iron Age, *in* Scotland after the Ice Age, Edinburgh, Edinburgh University Press.

Armit, I., 2005, Celtic Scotland: London, Batsford.

Arne, D.C., Mackie, R.A. & Jones, S.A., 2014, The use of property-scale portable X-ray fluorescence data in gold exploration: advantages and limitations: Geochemistry: Exploration, Environment, Analysis, v. 14, p. 233–244.

Avery, M., Sutton, J. & Banks, J., 1967, Rainsborough, Northants, England: Excavations 1961-65: Proceedings of the Prehistoric Society, v. 33, p. 207–306.

Avery, M., 1993, Hillfort Defences of Southern Britain, 3 vols: Oxford, BAR British Series 231.

BBC News, 2019, Primark fire in Belfast accidental, says fire service: BBC News, https://www.bbc.co.uk/news/uk-northern-ireland-48707632 (accessed September 2019).

BBC Scotland News, 2019, “Final phases” of Glasgow art school fire investigation: BBC Scotland News, https://www.bbc.co.uk/news/uk-scotland-glasgow-west-48636706 (accessed September 2019).

Berner, R.A., 1981, A New Geochemical Classification of Sedimentary Environments: Journal of Sedimentary Research, v. 52, p. 359–365.

BGS NERC, 2018, iGeology app from iTunes, produced by Flying Meat inc, Version 4.0:

Bourhis, E. Le, 2014, Modern Methods for Analysing Archaeological and Historical Glass Mechanical Properties of Glass Bio-Glasses Glasses and the Glass Transition:

Le Bourhis, E., 2014, Ageing of Glass, *in* Glass: Mechanics and Technology, Verlag, Wiley-VCH Verlag, p. 191–210.

Brothwell, D.R., Bishop, A.C., and Woolley, A.R., 1974, Vitrified forts in Scotland: A problem in interpretation and primitive technology: Journal of Archaeological Science, v. 1, p. 101–107, doi:10.1016/0305-4403(74)90020-X.

Caldwell, D.H., Ewart, G., Triscott, J., Cullen, I.S., Franklin, J.A., Hunter, F., and Paterson, L., 1998, Auldhill, Portencross: Archaeological Journal, v. 155, p. 22–81, doi:10.1080/00665983.1998.11078846.

Charles, R.J. and Hillig, W.B., 1962, The Kinetics of Glass Failure by Stress Corrosion, *in* Union scientifique continentale du verre, Charleroi, Belgique.,.

Childe, V.G. & Graham, A., 1943, Some notable prehistoric and medieval monuments recently examined by The Royal Commission on Ancient and Historical Monuments of Scotland.: Proceedings of the Antiquaries of Scotland, v. 77, p. 38–39.

Childe, V.G., and Thorneycroft, W., 1937a, The Experimental Production of the Phenomena Distinctive of Vitrified Forts: Proceedings of the Society, v. v.

Childe, V.G., and Thorneycroft, W., 1937b, The Vitrified Fort at Rahoy, Morven, Argyll: Proceedings of the Antiquaries of Scotland, v. I, p. 23–43.

Christison, D., Anderson, J. & Ross, T., 1905, Report on the Society's excavations of forts on the Poltalloch Estate, Argyll, in 1904-1905: Proceedings of the Society of Antiquaries of Scotland, v. 39, p. 270–285.

Christison, D., 1898, Early fortifications in Scotland : motes, camps, and forts: Edinburgh, Blackwood.

Christison, D., 1889, The Duns and Fortsof Lorne, Nether Lochaber, and the Neighbourhood: Proceedings of the Society of Antiquaries of Scotland, v. 23, p. 368–432.

Christison, D., 1899, The Forts, @Camps@ and Other Field-Works of Perth, Forfar, and Kincardine: Proceedings of the Antiquaries of Scotland, p. 43–120.

Christison, D., 1893, The Prehistoric Forts of Ayrshire: Proceedings of the Society of Antiquaries of Scotland, v. 27, p. 381–405.

Coogan, L. a., Saunders, a. D., and Wilson, R.N., 2014, Aluminum-in-olivine

thermometry of primitive basalts: Evidence of an anomalously hot mantle source for large igneous provinces: Chemical Geology, v. 368, p. 1–10, doi:10.1016/j.chemgeo.2014.01.004.

Cook, M., 2015, Dun Deardail Hillfort , Lochaber : Year 1 Archaeological Excavation Data Structure Report Dun Deardail Hillfort , Lochaber : Data Structure Report.:

Cook, M., and Heald, A., 2016, Dun Deardail Hillfort , Lochaber : Year 2 Archaeological Excavation Data Structure Report Dun Deardail Hillfort , Lochaber : Data Structure Report.:

Cook, M., Heald, A., and Shaw, G., 2017, Dun Deardail Hillfort , Lochaber : Year 3 Archaeological Excavation Data Structure Report Dun Deardail Hillfort , Lochaber : Data Structure Report.:

Cotton, M.A., 1954, British Camps with Timber-laced Ramparts: Archaeological Journal, v. 111, p. 26–105.

Curwen, E.C., 1932, Excavations at Hollingbury Camp, Sussex: Antiquities Journal, v. 12, p. 1–16.

Daubrée, R.A., 1881a, Examen de materiaux prevenant des forts vitrifies de Craig Phaidrig, prb Inverness (Ecosse), et de Hartmannswillerkopf (Haute-Alscace): Revue Archaeologique, v. 42, p. 36–40.

Daubrée, R.A., 1882, Examen des materiaux des forts vitrifies de Chateau-Meignan (Mayenne) et du Puy-de-Gaudy (Creuse): Revue Archaeologique, v. 42, p. 275–278.

Daubrée, R.A., 1881b, Examen mineralogique et chimique de materiaux provenant de quelques forts vitrifies de la France: Revue Archaeologique, v. 41, p. 18–28.

Deer, W. A., Howie, R. A. and Zussman, J., 1992, An Introduction to the Rock-Forming Minerals.: London, Longman Scientific & Technical.

Díaz Martínez, E., Soares, A.M.M., Kresten, P., and Glazovskaya, L., 2005, Evidence for wall vitrification at the Late Bronze Age settlement of Passo Alto (Vila Verde de Ficalho, Serpa, Portugal): Revista portuguesa de Arqueologia, v. 8, p. 151–161.

Dimanche, F. and Bartholomi, P.(, 1976, The Alteration of Ilmenite in Sediments:

Mining and Science Engineering, v. 8, p. 187–200.

Dixon, P., 1976, Crickley Hill 1969-72, *in* Harding, D.W. ed., Hillforts. Later prehistoric Earthworks in Britain and Ireland, London, Academic Press, p. 162–76.

Dobres, M.-A. and Robb, J., 2000, Agency in archaeology: London, Routledge.

Driver, T., 2016, The Hillforts of Cardigan Bay: Herefordshire, Logaston Press.

Duff, D.G., 1961, Vitrified Forts - How were they built? Scots Magazine, p. 254–257.

Eskola, P., 1920, The Mineral Facies of Rocks: Norsk Geologisk Tidsskrift, v. 6, p. 143–194.

Feacham, R., 1966, "The hillforts of Northern Britain," *in* Rivet, A.L.F. ed., The Iron Age in Northern Britain, Edinburgh, Edinburgh University Press, p. 59–88.

Fraser, J., 1906, Vitrified Fort of Knockfarrel: Trans Inverness Sci Soc Fld Club, v. 6, p. 288–291.

Friend, C.R.L., Charnley, N.R., Clyne, H., and Dye, J., 2008, Experimentally produced glass compared with that occurring at The Torr, NW Scotland, UK: vitrification through biotite melting: Journal of Archaeological Science, v. 35, p. 3130–3143, doi:10.1016/j.jas.2008.06.022.

Friend, C.R.L., Dye, J., and Fowler, M.B., 2007, New field and geochemical evidence from vitrified forts in South Morar and Moidart, NW Scotland: further insight into melting and the process of vitrification: Journal of Archaeological Science, v. 34, p. 1685–1701, doi:10.1016/j.jas.2006.12.007.

Friend, C.R.L., Kirby, J.E., Charnley, N.R., and Dye, J., 2016, New field, analytical data and melting temperature determinations from three vitrified forts in Lochaber, Western Highlands, Scotland: Journal of Archaeological Science: Reports, v. 10, p. 237–252, doi:10.1016/j.jasrep.2016.09.015.

Ge, L., Lai, W., and Lin, Y., 2005, Influence of and correction for moisture in rocks, soils and sediments on in situ XRF analysis: X-Ray Spectrometry, v. 34, p. 28–34, doi:10.1002/xrs.782.

Gebhard, R., Guggenbichler, E., Häusler, W., Riederer, J., Schmotz, K., Wagner, F.E.,

and Wagner, U., 2004a, Mössbauer study of a celtic pottery-making kiln in Lower Bavaria: Hyperfine Interactions, v. 154, p. 215–230, doi:10.1023/B:HYPE.0000032099.47440.f6.

Gebhard, R., Häusler, W., Moosauer, M., and Wagner, U., 2004b, Remnants of a bronze age rampart in upper Bavaria: A Mössbauer study: Hyperfine Interactions, v. 154, p. 181–197, doi:10.1023/B:HYPE.0000032076.38155.f7.

Geddes, G.F. & Hale, A.G.., 2010, RCAHMS: The Archaeological Landscape of Bute.:

Gütlich, P., Eckhard, P. & Trautwein, A.X., 2011, Mössbauer Spectroscopy and Transition Metal Chemistry: Heidelberg, Springer.

Hall, G., Page, L., and Graeme, B.-C., 2012, Canadian Mining Industry Research Organization (Camiro) Exploration Division: , p. 1–215.

Hamilton, J.R.C., 1966, Forts, Brochs and Wheel-Houses, *in* The Iron Age in Northern Britain, Edinburgh, Edinburgh University Press, p. 111–130.

Hanle, A., 1960, Der Donnersberg. III. Reihe der Mitteilungen der Pollichia 7. Pollichiamuseum Bad Dtirkheim: 112–126 p.

Harding, D.W., Ralstone, I. & Burgress, D.W.I., 1995, Dunagoil, Isle of Bute (Kingarth Parish), Survey: Disc Esc Scot,.

Harding, D.W., 1997, Forts, Duns, Brochs and Crannogs: Iron Age Settlements in Argyll, *in* Ritchie, G. ed., The Archaeology of Argyll, Edinburgh.

Harding, D.W., 2012, Iron Age Hillforts in Britain and Beyond: Oxford, Oxford University Press.

Headland Archaeology, 2011a, A Topographic Survey of Five Pictish Forts in the Highlands. Report to the Forestry Commission of Scotland.:

Headland Archaeology, 2011b, Knock Farril, Fodderty and Ord Hill, Knockbain: Topographic Survey for the Forestry Commission.:

Helz, R.T., 1976, Phase relations of basalts in their melting ranges at P,,, = 5kb. Part II. Melt compositions: Journal of Petrology, v. 17, p. 139–193.

Hewison, R.J.K., 1893, On Prehistoric Forts of the Island of Bute: PSAS, v. 27, p. 281–

293.

Hodder, I., 2011, Human-thing entanglement: towards an integrated archaeological perspective: Journal of the Royal Anthropological Institute, v. 17, p. 154–177, doi:10.1111/j.1467-9655.2010.01674.x.

De Hoog, J.C.M., Gall, L., and Cornell, D.H., 2010, Trace-element geochemistry of mantle olivine and application to mantle petrogenesis and geothermobarometry: Chemical Geology, v. 270, p. 196–215, doi:10.1016/j.chemgeo.2009.11.017.

Huang, W.-L. and Wyllie, P.J., 1975, Melting reactions in the system NaAlSi,O,-KAlSi,O,- SiO, to 35 Kb., dry and with excess water: Journal of Geology, v. 82, p. 737–748.

Hunter, F., and Carruthers, M., 2012, Iron Age Scotland : ScARF Panel Report.:

Ihli, J., Wong, W.C., Noel, E.H., Kim, Y.Y., Kulak, A.N., Christenson, H.K., Duer, M.J., and Meldrum, F.C., 2014, Dehydration and crystallization of amorphous calcium carbonate in solution and in air: Nature Communications, v. 5, p. 1–10, doi:10.1038/ncomms4169.

Ingold, T., 2011, Being Alive. Essays on Movement, Knowledge and Description: London, Routledge.

Janoušek, V., Farrow, C.M., and Erban, V., 2006, Interpretation of whole-rock geochemical data in igneous geochemistry: Introducing Geochemical Data Toolkit (GCDkit): Journal of Petrology, v. 47, p. 1255–1259, doi:10.1093/petrology/egl013.

John B. Smith, 1895, Prehistoric man in Ayrshire: London, Elliot Stock.

Jones, G.T., Bailey, D.G., and Beck, C., 1997, Source Provenance of Andesite Artefacts Using: Journal of Archaeological Science, p. 929–943.

Jung, S., and Pfänder, J.A., 2007, Source composition and melting temperatures of orogenic granitoids: constraints from CaO/Na2O, Al2O3/TiO2 and accessory mineral saturation thermometry: European Journal of Mineralogy, v. 19, p. 859–870, doi:10.1127/0935-1221/2007/0019-1774.

Keddie, W., 1868, On the remains of a vitrified fort or site, in the island of Cumbrae,

with notes on the vitrified forts of Berigonium, Glen Nevis, Craig Phadrick, Portencross and Bute: Transactions of Glasgow Archaeological society, v. 1.

Kresten, P., Goedicke, C., and Manzano, a, 2003, TL-dating of vitrified material: Geochronometria, v. 22, p. 9–14, http://www.geochronometria.pl/pdf/geo_22/Geo22_2.pdf.

Kresten, P., Kero, L., and Chyssler, J., 1993, Geology of the vitrified hill-fort Broborg in Uppland, Sweden: Gff, v. 115, p. 13–24, doi:10.1080/11035899309454825.

Lang, C., 2016, The Knock Vitrified Fort, N. Ayrshire: Site survey and archaeological excavation of the southern ramparts.:

Leeman, W P and Scheidegger, K.F., 1977, OLIVINE/LIQUID DISTRIBUTION COEFFICIENTS AND A TEST FOR CRYSTAL-LIQUID EQUILIBRIUM: Earth and Planetary Science Letters, v. 35, p. 247–257.

Leger, L., Bray, J. & Plumat, E., 1962, Phenomenes de diffusion a la peripherie de grains de silice en contact avec du verre sodo-calcique en fusion, *in* In (American Ceramic Society, compiler) Advances in Glass Technology, New York, NY, Plenum Press, p. 175–189.

Lemière, B., 2018, A review of pXRF (field portable X-ray fluorescence) applications for applied geochemistry: Journal of Geochemical Exploration, v. 188, p. 350–363, doi:10.1016/j.gexplo.2018.02.006.

Lock, G. & Ralston, I., 2017, Atlas of Hillforts [online]: , p. https://hillforts.arch.ox.ac.uk/.

MacCulloch, J., 1814, ., *in* Transactions of the Geological Society of London, Vol. ii,.

MacKenzie, W.S. and Guilford, C., 1980, Atlas of Rock-Forming Minerals in Thin Section: Harlow, Longman Scientific & Technical.

MacKenzie, G., 1857, Notice of the Ord Hill of Kessock. 22nd December 1924: Archaeologia Scotica, v. 4, p. 194–195.

Mackie, E.W., 1967, Walls in Iron Age Forts : , p. 69–71.

MacLeod, G.W., 2018, Petrology thin section production at University of Stirling:,

http://www.thin.stir.ac.uk/category/methods/ (accessed January 2019).

Mann, L.M., 1925, Note on the Results of the Exploration of the Fort at Donagoil: Transactions of the Buteshire Natural History Society, v. 9, p. 54–60.

Mann, L.M., 1915, Report on the Relics Discovered During Excavations in 1913 at Cave at Dunagoil, Bute, and in 1914 at the Fort in Dunagoil, Bute (with suggestions as to the probable history and chronology of the site): Transactions of the Buteshire Natural History Society, v. 8, p. 61–86.

Marshall, J.N., 1915, Preliminary Notes on some Excavations at Dunagoil Fort and Cave: Transactions of the Buteshire Natural History Society, v. 8, p. 42–86.

McLoughlin, S. D.; Hand, R. J.; Hyatt, N. C.; Lee, W. E.; Notingher, I.; McPhail, D. S.; Henderson, J., 2006, The long term corrosion of glasses: analytical results after 32 years of burial at Ballidon: Glass Technology - European Journal of Glass Science and Technology, v. 47, p. 59- 67(9).

Miles, D., Palmer, S., Lock, G., Gosden, C., & Cromarty, A.M., 2003, Uffington White Horse and its Landscape., *in* Investigations at White \horse Hill, Uffington 1989-95, and Tower Hill Ashbury, 1993-4, Oxford, Oxford, Oxford Archaeology Thames Valley Landscapes Monograph No 18.

Miller, H., 1858, The Cruise of the Betsy, with Ramblings of a Geologist:

Morad, S. and Aldahan, A.A., 1986, Alteration of Detrital Fe-Ti Oxides in Sedimentary Rocks: Geological Society of America Bulletin, v. 97, p. 567–578.

Nisbet, H.C., 1974, A Geological Approach to Vitrified Forts, Part I: Science & Archaeology, v. 12, p. 3–12.

Nisbet, H.C., 1975, A Geological Approach to Vitrified Forts, Part II: Science & Archaeology, v. 15, p. 3–16.

Noble, G., and Brophy, K., 2011, Ritual and remembrance at a prehistoric ceremonial complex in central Scotland: Excavations at Forteviot, Perth and Kinross: Antiquity, v. 85, p. 787–804, doi:10.1017/S0003598X00068319.

Paton, V.A.., 1928, Notes on a vitrified fort at “An-Cnap,” Sannox, Arran, and vitrified stones at mid Sannox, Arran, and at Pennymore, Furnace, Loch Fyne.: Proceedings

of the Antiquaries of Scotland, v. 62, p. 239–245.

Pennant, T.A., 1772, A Tour of Scotland MDCCLXIX: London, R. White.

Peteranna, M., and Birch, S., 2015, Craig Phadrig hillfort, Inverness: archaeological evaluation Data Structure Report:, www.aocarchaeology.com.

Ralston, I., 2006, Celtic Fortifications: Stroud, Tempus Publishing.

Ralston, I., 2004, The Hill-Forts of Pictland Since "The Problem of the Picts": Rosemarkie, Groam House Museum.

Ramsey, M.H., Potts, P.J., Webb, P.C., Watkins, P., Watson, J.S., and Coles, B.J., 1995, An objective assessment of analytical method precision: comparison of ICP-AES and XRF for the analysis of silicate rocks: Chemical Geology, v. 124, p. 1–19, doi:10.1016/0009-2541(95)00020-M.

Ritchie, M., 2009, Dun Deardail Fort, Glen Nevis, Highland (Kilmallie Parish), conservation management: Disc Esc Scot, v. New Ser 10, p. 101–102.

Ritchie, M., 2018, The Archaeology of Dun Deardail: Inverness, Forestry Commission Scotland.

Robertson, S., 1999, Rock classification, metamorphic rocks.:

Ross, W., 1880, Blain's History of Bute, *in* William Ross Rothesay 1995, 65,.

Ross, A., 1915, Dun-Dhearduil and Tor-Duin hill forts: Trans Inverness Sci Soc Fld Club, v. 7, p. 23–27.

Sanderson, D.C.W., and Placido, F., 1985, Scottish vitrified forts: b a c k g r o u n d and potential for tl dating: Nuclear Tracks Radiation Measurement, v. 10, p. 799–809.

Shackley, M.S. (Ed.), 2011, X-Ray Fluorescence Spectrometry (XRF) in Geoarchaeology: London, Springer.

Strickertsson, K., Placido, F., and Tate, J.O., 1988, Thermoluminescence Dating Of Scottish Vitrified Hillforts: Nuclear Tracks Radiation Measurement, v. 14, p. 317–320.

Tammann, G., 1925, The States of Aggregation, Van Nostrand: New York.

Thomas, R., 1997, Land, Kinship Relations and the Rise of Enclosed Settlements in the First Millennium BC Britain: Oxford Journal of Archaeology, v. 16, p. 211–18.

Tytler, A.F., 1790, Accounts of Some Extrordinary Structures on Tops of Hills in the Highlands: Transactions of the Royal Society Edinburgh, v. II, p. 3.

Voldan, J., 1962, Schmelzen und Kristallisieren von basischen Eruptivgesteinen, *in* (American Ceramic Society, compiler) Advances in Glass Technology, New York, NY, Plenum Press, p. 382–396.

Wallace, T., 1921, Archaeological Notes: Trans Inverness Sci Soc Fld Club, v. 8, p. 106–107.

Wallace, T., 1918, Notes on the parish of Petty: Trans Inverness Sci Soc Fld Club, v. 8, p. 87–136.

Wan, Z., Coogan, L.A. and Dante, C., 2008, Experimental calibration of aluminum partitioning between olivine and spinel as a geothermometer: American Mineralogist, v. 93, p. 1142–1147.

Weibel, R., 2003, Alteration of detrital Fe-Ti oxides in Miocene fluvial deposits, central Jutland, Denmark: Bulletin of the Geological Society of Denmark, v. 50, p. 171–183.

Wentworth, C.K., 1922, A Scale of Grade and Class Terms for Clastic Sediments Author (s): Chester K . Wentworth Published by : The University of Chicago Press Stable URL : http://www.jstor.org/stable/30063207 .: The journal of Geology, v. 30, p. 377–392, doi:10.1086/622910.

Wheeler, R.E.M., 1954, The Stanwick Fortifications, North Riding of Yorkshire: Oxford, Society Antiquaries London.

Williams, J., 1777, An Accountof Some Remarkable Ancient Ruins, Lately Discovered in the Highlands and northern Parts of Scotland: In a series of letters to G.C.M. Esq.: Edinburgh.

Winkler, H.G.F., 1967, Petrogenesis of Metamorphic Rocks: New York, NY, Springer Verlag.

Woodham, A.A., 1955, A Survey of Prehistoric Monuments in the Black Isle:

Proceedings of the Society of Antiquaries of Scotland, v. 88, p. 65–93.

Yoder, H.J., and Tilley, C.E., 1962, Origin of Basalt Magmas: an Experimental Study of Natural and Synthetic Rocks Systems: J. Petrol., v. 3, p. 342–532.

Youngblood, E., Fredriksson, B.J., Kraut, F., and Fredriksson, K., 1978, Celtic vitrified forts: Implications of a chemical-petrological study of glasses and source rocks: Journal of Archaeological Science, v. 5, p. 99–121, doi:10.1016/0305-4403(78)90027-4.

Zarzycki, J., 1991, Glasses and the Vitreous State: Cambridge, Cambridge University Press.

Appendix

All supplementary data and further images and graphics can be found at the short form URL: http://tiny.cc/d1d6hz

Appendix A – Wentworth Scale for Rock Classification

Table 52:Wentworth scale for rock size classification (Wentworth, 1992).

>256 mm	Boulder
64 - 256 mm	Cobble
4 - 64 mm	Pebble
2 - 4 mm	Granule
I - 2 mm	Very coarse sand
0.5 - I mm	Coarse sand
0.25 - 0.5mm	Medium sand
0.125 - 0.25mm	Fine sand
0.0625 - 0.125mm	Very fine sand
0.004 - 0.0625mm	Silt
<0.004mm	Clay

Appendix B – p-XRF calibration data

Table 53: p-XRF analysed elements from NIST2780, NIST2709a, CCRMP till4, RCRA and SiO2 reference standards.

RCRA

Element	As	Ba	Cd	Cr	Pb	Se	Ag
Unit	ppm	ppm	ppm	ppm	ppm	ppm	ppm
Amount	**500**	**630**	**500**	**500**	**500**	**500**	**500**
average	**845**	**608**	**474**	**435**	**522**	**448**	**472**
recovery	169	97	95	87	104	90	94
RSD	21.24	37.61	16.52	29.00	12.05	8.41	18.65
%RSD	2.51	6.18	3.49	6.67	2.31	1.88	3.95

SiO2

Element	Si
Unit	%
Amount	99.8
recovery	98.76
Average	98.56
RSD	0.31
%RSD	0.31

NIST2780

Element	Al	Ca	Fe	Pb	K	S	Zn	Sb	Cr	Mo	Nb	Rb	Si	Zr	Ti	Ba	Cu	Mn	Pb	Sr	V
Unit	%	%	%	%	%	%	%	ppm	ppm	ppm	ppm	ppm	%	ppm	%	ppm	ppm	ppm	%	ppm	ppm
Amount	8.87	0.195	2.784	0.577	3.38	1.263	0.257	160	44	11	18	175	31	176	0.699	993	215.5	462	0.577	217	268
average	6.952089	0.245065	2.873985	0.508342	3.292647	1.615994	0.19413	149.1511	71.81168	7.785156	16.014	170.3709	19.39083	159.6829	0.600513	1001.561	174.1421	357.0375	0.508342	153.4928	326.949
recovery	**78.37756**	**125.6744**	**103.2322**	**88.10082**	**97.41559**	**127.9488**	**75.5368**	**93.21945**	**163.2084**	**70.77415**	**88.96667**	**97.35479**	**62.55105**	**90.72891**	**85.91025**	**100.8621**	**80.80838**	**77.28085**	**88.10082**	**70.73399**	**121.9959**
RSD	321.787	141.881	170.419	38.11328	379.6527	136.6767	30.57879	14.4599	17.5833	1.832906	1.279146	3.490952	1415.615	2.722767	93.17952	43.79394	10.54039	53.31929	38.11328	2.465806	28.61754
%RSD	**1.66915**	**5.789524**	**0.592971**	**0.749757**	**1.153032**	**0.845775**	**1.575174**	**9.6948**	**19.15149**	**23.54359**	**7.987674**	**2.049031**	**0.730044**	**1.705109**	**1.551666**	**4.37257**	**6.052752**	**14.93381**	**0.749757**	**1.606464**	**8.752907**

CCRMP till 4

Element	Ba	Mo	Nb	Rb	Bi	As	Pb	W	Cu	Fe	Mn	Cr	Ti	P	S
Unit	ppm	ppm	ppm	ppm	ppm	ppm	ppm	ppm	ppm	ppm	ppm	ppm	ppm	ppm	ppm
Amount	395	16	15	161	40	111	50	204	237	39700	490	53	4840	880	800
average	471.6313	10.55161	16.46255	154.085	53.92845	214.7958	44.87124	265.8681	240.5278	41291.75	357.4413	98.96858	4089.2	3450.352	1445.738
recovery	119.4003	65.94754	109.7503	95.70497	134.8211	193.5098	89.74248	130.3275	101.4885	104.0094	72.9472	186.7332	84.4876	392.0854	180.7173
RSD	43.89659	1.692591	1.154096	3.241809	4.186258	9.783198	4.325118	29.33163	12.09562	213.7931	47.9896	24.5128	91.30968	119.3001	169.1642
%RSD	9.307396	16.04108	7.010436	2.103909	7.762614	4.554649	9.638953	11.0324	5.028782	0.517762	13.42587	24.76826	2.232947	3.45762	11.70089

NIST2709a

Element	Al	Ca	Fe	P	K	Si	Ti	Ba	Cr	Pb	Mn	Sr	V	Zr	As	Rb	Zn
Unit	%	%	%	%	%	%	%	ppm	ppm	ppm	ppm	ppm	ppm	ppm	ppm	ppm	ppm
Amount	7.37	1.91	3.36	0.0688	2.11	30.3	0.336	979	130	17.3	529	239	110	195	10.5	99	103
average	3.432871	1.91563	3.472725	0.337117	1.733978	17.93315	0.312406	882.4403	170.2582	14.78028	389.5536	155.2296	175.1051	122.4816	23.11576	85.53583	85.71941
recovery	46.57898	100.2948	103.3549	489.9952	82.17904	59.1853	92.97799	90.1369	130.9679	85.43512	73.63962	64.94962	159.1864	62.81107	220.1501	86.39983	83.22273
RSD	1038.248	346.9258	234.0865	108.158	347.0646	1274.716	106.3553	37.55006	20.84455	2.378501	58.71741	2.774079	31.5202	2.236205	4.847302	1.71433	6.418097
%RSD	3.024429	1.811027	0.674072	3.208325	2.001552	0.710816	3.404392	4.255252	12.2429	16.0924	15.073	1.787082	18.00074	1.825748	20.96969	2.004225	7.487332

Appendix C – Supplementary graphs and tables, including statistics

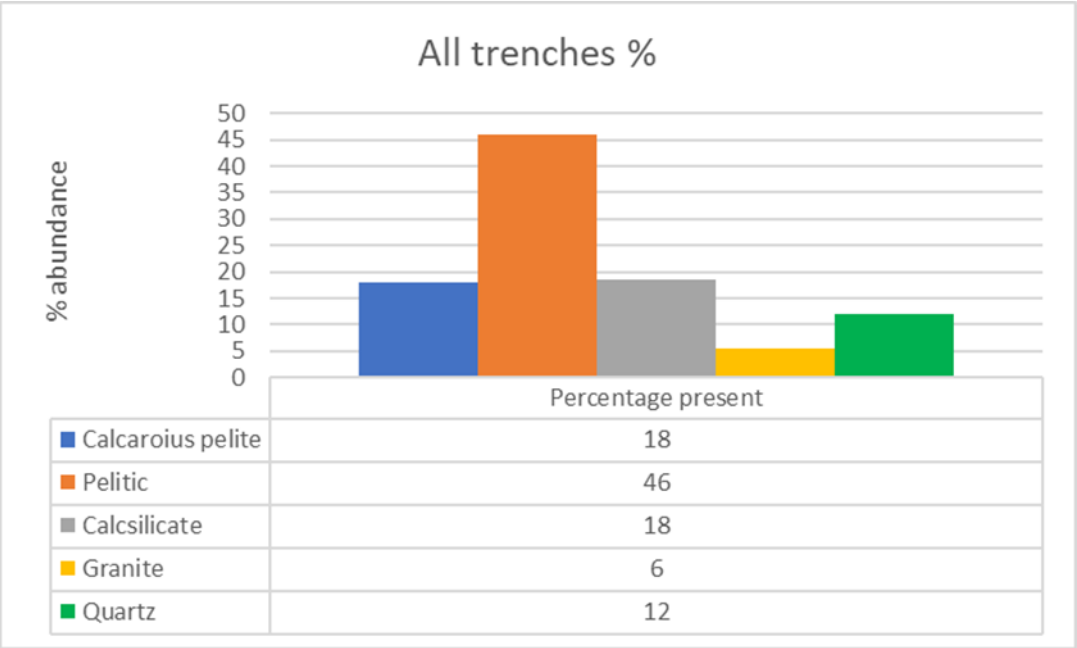

	Percentage present
Calcaroius pelite	18
Pelitic	46
Calcsilicate	18
Granite	6
Quartz	12

Figure 103: % abundance of rock types found in excavated clasts from trenches and surrounding rampart

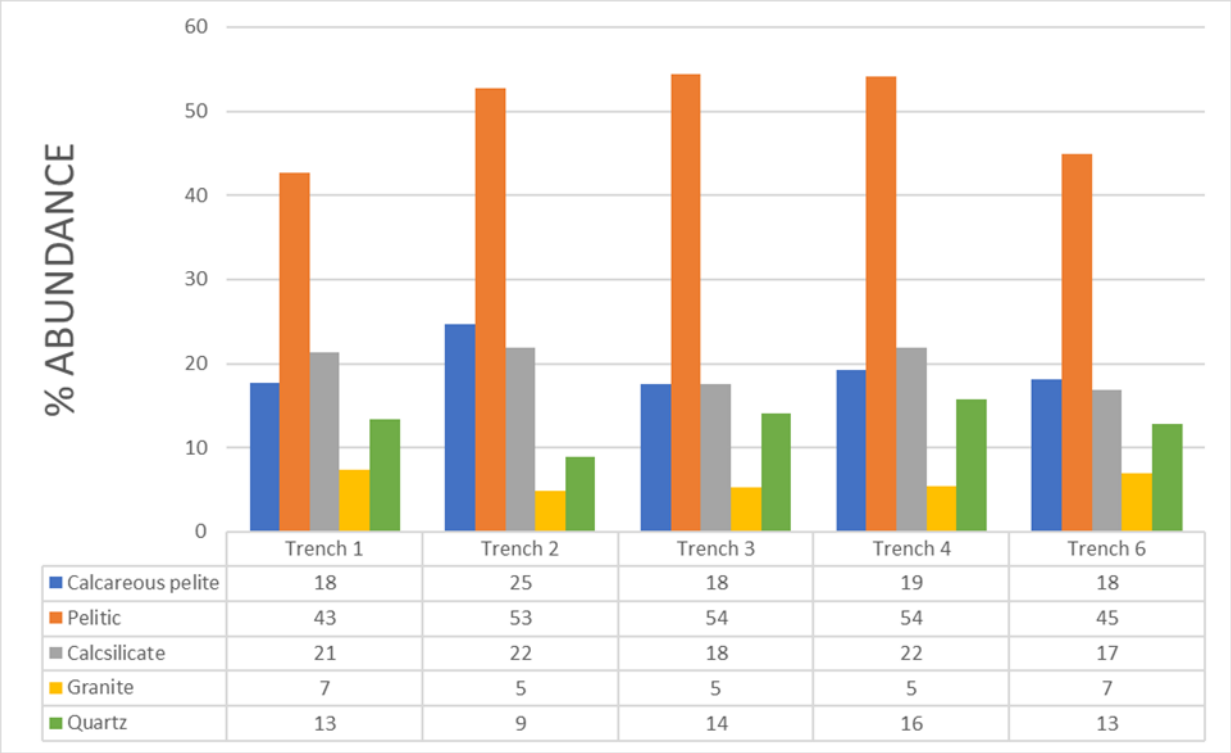

	Trench 1	Trench 2	Trench 3	Trench 4	Trench 6
Calcareous pelite	18	25	18	19	18
Pelitic	43	53	54	54	45
Calcsilicate	21	22	18	22	17
Granite	7	5	5	5	7
Quartz	13	9	14	16	13

Figure 104: Lithological composition of the excavated vitrified material across all trenches.

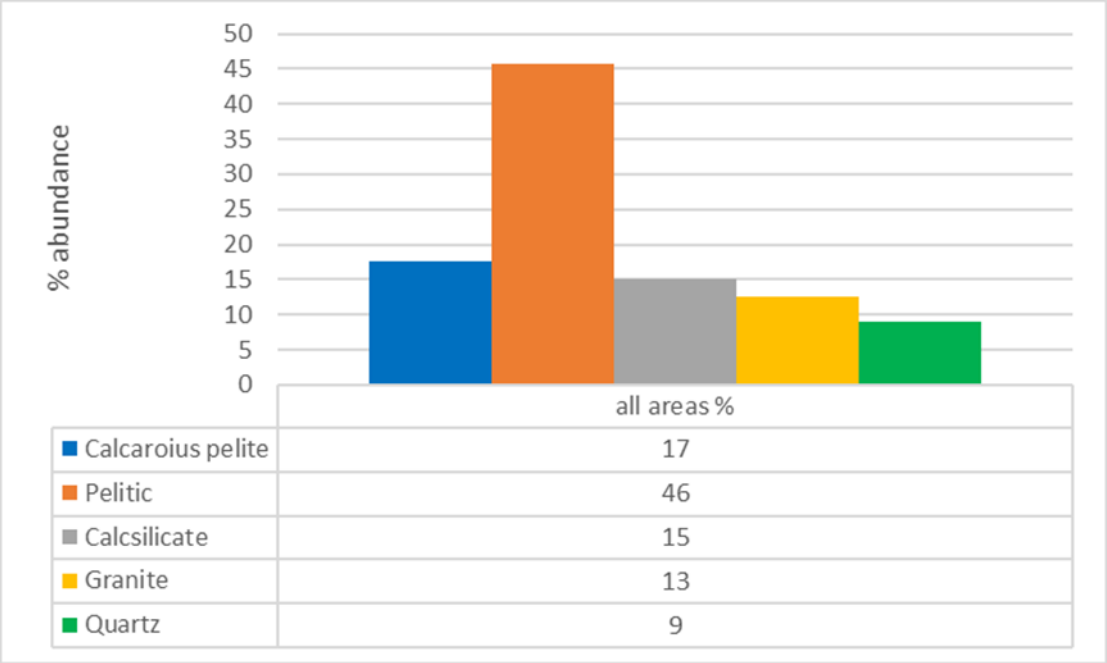

Figure 105:Bar graph of lithology type for all areas (1-8), in %

Table 54:Table showing the results of visual analysis of each area and trench, figures are in area %.

Lithology	Area 1	Area 2	Area 3	Area 4	Area 5	Area 6	Area 7	Area 8	Trench 1	Trench 2	Trench 3	Trench 4	Trench 6
calcareous pelite	17	18	17	16	18	18	18	18	24	25	21	25	26
Pelitic	45	45	45	47	46	46	47	47	43	53	54	54	45
Calcsilicate	15	17	16	16	16	15	14	13	21	22	23	22	21
Granite	15	12	14	12	13	11	11	13	17	15	17	15	17
Quartz	8	8	9	9	8	10	10	11	13	13	11	13	11

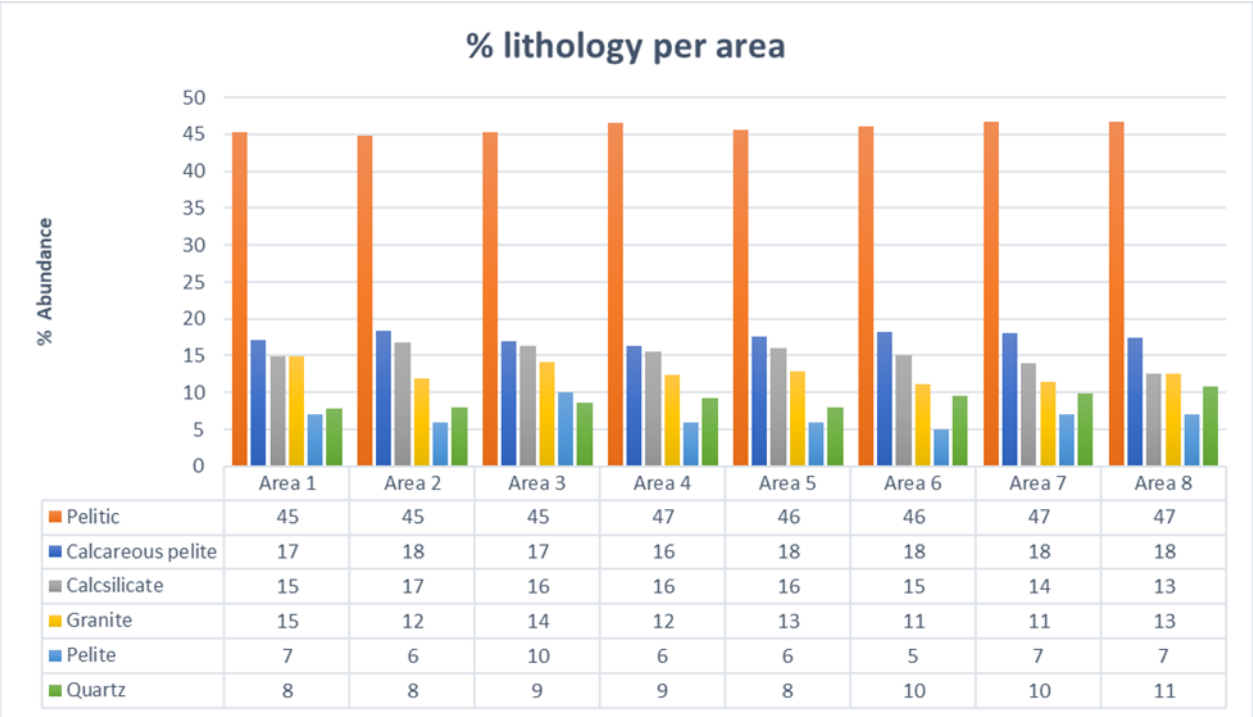

Figure 106: Bar chart of the visual lithology (in area %) of in-situ areas and excavated trenches.

Table 55: Bar chart of the lithology (in area %) of in-situ, shown in Figure 56, produced from data in Table 23.

	calcareous pelite	Pelitic	Calcsilicate	Granite	Quartz
Area 1	17	45	15	15	8
Area 2	18	45	17	12	8
Area 3	17	45	16	14	9
Area 4	16	47	16	12	9
Area 5	18	46	16	13	8
Area 6	18	47	14	11	10
Area 8	18	47	13	13	11
Trench 1	24	43	21	17	13
Trench 2	25	53	22	15	13
Trench 3	21	54	23	17	11
Trench 4	25	54	22	15	13
Trench 6	26	45	21	17	11

Table 56: XRF elemental data on average pelitic rock measured from each trench

sample	Si	Fe	Mn	Cr	Ti	Ca	K	Al	Ba	Nb	Zr	Sr	Rb	Mg	Zn	P
Local	278892	52101	622	181	4828	31355	28681	76100	827	14	259	142	133	39082	162	1468
RSD	27430	2949	70	8.8	600	5371	3327	4566	88	2.4	38	23	29	6373	20	239
%RSD	9.84	5.66	11.30	4.87	12.42	17.13	11.60	6.00	10.69	17.17	14.60	16.45	22.03	16.31	12.53	16.30
Trench 1	305360	58016	627	186	4300	32180	29750	86710	815	15	249	148	144	36538	154	1505
RSD	16856	7306	68	10	896	3901	3806	6479	110	4	24	31	33	5653	34	190
%RSD	5.52	12.59	10.90	5.11	20.83	12.12	12.79	7.47	13.47	22.90	9.82	20.67	22.73	15.47	22.16	12.62
Trench 2	318164	50413	649	180	4087	30115	30191	80499	861	14	282	152	132	38290	157	1527
RSD	11843	2993	94	8.8	417	4259	3909	8066	80	3.0	43	32	36	3976	23	388
%RSD	3.72	5.94	14.43	4.87	10.20	14.14	12.95	10.02	9.25	21.47	15.27	21.11	27.50	10.38	14.98	25.39
Trench 3	274545	50862	614	182	3980	26842	26557	88696	953	19	284	157	121	42209	153	1360
RSD	6939	3067	71	1.9	347	5498	2612	6957	39	0.3	24	34	2.7	3410	23	131
%RSD	2.53	6.03	11.58	1.07	8.72	20.48	9.83	7.84	4.09	1.77	8.52	21.52	2.23	8.08	15.10	9.67
Trench 4	309548	52845	623	180	4327	32156	32310	85230	867	15	237	154	127	35954	144	1468
RSD	27602	3912	71	6.4	478	5331	4894	5776	42	3.3	42	26	14	3713	22	273
%RSD	8.92	7.40	11.36	3.56	11.04	16.58	15.15	6.78	4.80	22.15	17.70	16.67	10.76	10.33	15.56	18.62
Trench 6	301639	54284	647	180	4222	31056	27769	85801	807	13	251	158	131	37247	159	1416
RSD	32353	3666	43	11	495	4892	4767	4566	149	2.8	33	19	12	4271	18	284
%RSD	10.73	6.75	6.62	5.88	11.71	15.75	17.17	5.32	18.44	21.10	13.32	12.13	9.20	11.47	11.56	20.02

Table 57: XRF elemental data on average quartz rock measured from each trench

sample	Si	Fe	Ti	Ca	K	Al	Ba	S	P
Local	459970	362	46	200	2516	8350	200	520	868
Stdev	29816	23	5.6	26	293	361	21	41	67
%RSD	6.48	6.46	12.25	13.15	11.66	4.33	10.61	7.96	7.71
Trench 1	463494	326	44	194	2661	8806	183	536	864
Stdev	8136	21	4.0	23	191	660	27	24	51
%RSD	1.76	6.48	9.23	11.74	7.16	7.49	14.68	4.55	5.89
Trench 2	462100	346	41	178	2771	8884	198	528	852
Stdev	8714	15	4.8	12	223	149	5.4	35	52
%RSD	1.89	4.37	11.82	6.54	8.05	1.68	2.71	6.67	6.08
Trench 3	470778	379	38	204	2888	8911	180	489	847
Stdev	4842	57	0.5	3.0	87	112	7.5	0.5	42
%RSD	1.03	15.04	1.33	1.47	3.00	1.26	4.18	0.10	4.96
Trench 4	448477	349	47	190	2472	9046	167	543	885
Stdev	14732	15	3.2	11	312	540	17	30	35
%RSD	3.28	4.22	6.70	6.01	12.63	5.97	10.06	5.51	3.94
Trench 6	449522	376	44	203	2550	8483	189	553	914
Stdev	22970	17	2.6	14	202	720	18	27	25
%RSD	5.11	4.41	5.88	6.91	7.92	8.49	9.46	4.95	2.73

Table 58: p-XRF elemental data on average calcsilicate rock measured from each trench

SAMPLE	Si	Fe	Mn	Cr	V	Ti	Ca	K	Al	Ba	Nb	Zr	Sr	Rb	S	Mg	Zn	P	Cl
Local	210399	39143	449	157	155	4981	75950	43773	66122	764	14	205	60	129	269	54212	201	1532	91
RSD	16134	752	41	28	17	386	2809	3754	3154	112	1.9	59	6.1	6.1	32	2888	24	79	5.1
%RSD	7.67	1.92	9.17	17.58	11.07	7.74	3.70	8.58	4.77	14.66	13.25	28.69	10.23	4.73	11.74	5.33	11.99	5.13	5.61
Trench 1	227819	36356	429	153	157	4839	76546	48588	64386	828	15	197	54	131	299	44520	169	1702	99
RSD	7898	1632	55	27	26	485	3742	6361	2226	96	1.2	43	1.6	5.8	46	5087	16	108	6.5
%RSD	3.47	4.49	12.84	17.44	16.25	10.03	4.89	13.09	3.46	11.64	7.73	21.81	2.89	4.40	15.43	11.43	9.18	6.33	6.50
Trench 2	203159	37913	440	157	180	4936	78424	43817	61497	796	16	223	44	144	299	45337	198	1646	96
RSD	11750	2229	39	26	23	578	684	2712	16216	68	1.5	14	6.0	10	69	4635	23	133	4.7
%RSD	5.78	5.88	8.79	16.74	12.77	11.71	0.87	6.19	26.37	8.52	9.14	6.28	13.65	6.69	23.19	10.22	11.81	8.05	4.92
Trench 3	206626	32813	456	198	182	6051	78087	45352	67859	851	19	269	51	129	405	54635	210	1559	101
RSD	758	303	70	16	19	35	223	236	1700	31	1.2	3.9	0.8	3.3	15	2922	5.1	26	5.6
%RSD	0.37	0.92	15.24	8.00	10.40	0.57	0.29	0.52	2.51	3.66	6.12	1.44	1.50	2.53	3.74	5.35	2.44	1.69	5.61
Trench 4	203645	39705	465	178	196	5791	79816	51724	64920	886	19	256	56	173	428	53127	213	1606	96
RSD	7501	4105	41	16	21	180	2607	4975	5829	67	2.6	11	2	26	36	3162	20	102	7.4
%RSD	3.68	10.34	8.75	8.77	10.60	3.10	3.27	9.62	8.98	7.62	13.53	4.10	4.04	15.14	8.48	5.95	9.48	6.36	7.67
Trench 6	185953	44659	425	203	193	5114	80799	42192	63820	794	18	220	55	151	384	50462	201	1780	93
RSD	17541	3993	34	36	16	644	1898	1815	4301	74	1.8	6.4	2.0	15	57	1802	30	95	4.4
%RSD	9.43	8.94	7.89	17.53	8.38	12.59	2.35	4.30	6.74	9.33	9.95	2.91	3.70	9.87	14.82	3.57	14.66	5.34	4.68

Table 59: p-XRF results for pelitic rocks from examined sites around the rampart from in-situ analysis.

sample	Si	Fe	Mn	Cr	Ti	Ca	K	Al	Ba	Nb	Zr	Sr	Rb	Mg	Zn	P
Local	278892	52101	622	181	4828	31355	28681	76100	827	14	259	142	128	39082	162	1468
RSD	27430	2949	70	9	600	5371	3327	4566	88	2.4	38	23	25	6373	20	239
%RSD	9.84	5.66	11.30	4.87	12.42	17.13	11.60	6.00	10.69	17.17	14.60	16.45	19.76	16.31	12.53	16.30
Area 1	244811	50035	554	175	4404	29598	27866	77524	800	16	268	140	96	42488	144	1640
RSD	23894	2210	21	10	331	4013	6245	3263	73	2	23	21	17	3002	14	166
%RSD	9.76	4.42	3.72	5.89	7.52	13.56	22.41	4.21	9.16	14.54	8.58	14.95	17.43	7.06	10.05	10.14
Area 2	272155	48003	640	172	5213	35405	23808	73437	763	15	235	128	103	48549	158	1386
RSD	13620	700	8.1	11	307	1105	2779	3594	44	1.9	30	13	27	4239	20	120
%RSD	5.00	1.46	1.27	6.22	5.90	3.12	11.67	4.89	5.70	13.12	12.88	10.44	26.02	8.73	12.37	8.69
Area 3	249895	47916	602	179	4779	37286	24912	69650	788	15	232	155	123	47049	136	1650
RSD	15709	1623	18	2.1	402	3531	2683	10371	35	1.1	13	27	10	3960	13	107
%RSD	6.29	3.39	2.96	1.17	8.41	9.47	10.77	14.89	4.40	7.59	5.60	17.70	7.99	8.42	9.29	6.51
Area 4	250278	50723	566	175	4573	37720	26855	73720	888	17	229	135	122	39882	152	1577
RSD	17983	2348	47	2	418	3138	3351	3940	55	1.7	38	33	25	1569	21	70
%RSD	7.19	4.63	8.37	1.27	9.14	8.32	12.48	5.34	6.16	9.84	16.76	24.40	20.27	3.93	13.87	4.43
Area 5	285111	45201	552	182	4342	34066	27044	72596	775	17	252	169	132	43719	165	1612
RSD	21249	2534	25	6.6	229	2067	2088	4952	33	2.4	44	25	5.1	3038	25	88
%RSD	7.45	5.61	4.50	3.63	5.28	6.07	7.72	6.82	4.24	13.89	17.42	15.01	3.87	6.95	14.89	5.47
Area 6	225808	48327	595	189	4660	34854	26223	76328	844	16	256	139	141	46461	137	1512
RSD	8459	1952	30	6.1	566	2154	2908	2157	42	2.8	28	9	11	3071	15	150
%RSD	3.75	4.04	5.03	3.22	12.15	6.18	11.09	2.83	4.97	17.08	10.97	6.29	8.08	6.61	10.89	9.94
Area 7	259220	50342	603	184	4696	33551	26628	78080	897	17	277	126	125	48855	152	1670
RSD	19308	3315	39	3.4	245	1953	2888	1773	97	1.5	29	21	19	1826	19	38
%RSD	7.45	6.58	6.47	1.85	5.22	5.82	10.84	2.27	10.77	9.34	10.49	16.99	15.40	3.74	12.38	2.28
Area 8	267238	48222	573	179	4515	33390	22997	73520	779	18	267	122	122	49241	155	1650
RSD	31045	3845	33	4.1	534	623	1998	4135	100	2.1	39	9.3	17	868	17	201
%RSD	11.62	7.97	5.84	2.31	11.83	1.87	8.69	5.62	12.78	11.57	14.74	7.62	14.03	1.76	11.27	12.18

Table 60: p-XRF results for pelitic rocks from examined sites around the rampart with statistics removed for clarity

sample	Si	Fe	Mn	Cr	Ti	Ca	K	Al	Ba	Nb	Zr	Sr	Rb	Mg	Zn	P
Local	278892	52101	622	181	4828	31355	28681	76100	827	14	259	142	128	39082	162	1468
Area 1	244811	50035	554	175	4404	29598	27866	77524	800	16	268	140	96	42488	144	1640
Area 2	272155	48003	640	172	5213	35405	23808	73437	763	15	235	128	103	48549	158	1386
Area 3	249895	47916	602	179	4779	37286	24912	69650	788	15	232	155	123	47049	136	1650
Area 4	250278	50723	566	175	4573	37720	26855	73720	888	17	229	135	122	39882	152	1577
Area 5	285111	45201	552	182	4342	34066	27044	72596	775	17	252	169	132	43719	165	1612
Area 6	225808	48327	595	189	4660	34854	26223	76328	844	16	256	139	141	46461	137	1512
Area 7	259220	50342	603	184	4696	33551	26628	78080	897	17	277	126	125	48855	152	1670
Area 8	267238	48222	573	179	4515	33390	22997	73520	779	18	267	122	122	49241	155	1650

Table 61: p-XRF results for quartz rocks from examined sites around the rampart

sample	Si	Fe	Ti	Ca	K	Al	Ba	S	P
Local	459970	362	46	200	2516	8350	200	520	868
RSD	29816	23	5.6	26	293	361	21	41	67
%RSD	6.48	6.46	12.25	13.15	11.66	4.33	10.61	7.96	7.71
Area 1	459028	353	66	176	2709	8593	163	523	837
RSD	24575	30	12	14	189	434	13	28	70
%RSD	5.35	8.52	18.90	8.24	6.96	5.05	7.95	5.45	8.35
Area 2	461593	330	47	185	2599	8127	173	550	841
RSD	27429	20	4.3	12	167	295	19	35	38
%RSD	5.94	5.99	9.05	6.53	6.41	3.63	11.05	6.39	4.56
Area 3	444066	401	42	161	2644	8079	186	507	919
RSD	32423	2.9	1.8	27	126	138	6.6	11	6.3
%RSD	7.30	0.72	4.19	16.56	4.75	1.71	3.57	2.16	0.68
Area 4	477028	354	47	168	2594	8218	182	468	859
RSD	17113	15	2.6	15	147	157	5.2	21	10
%RSD	3.59	4.13	5.55	8.91	5.67	1.92	2.84	4.53	1.18
Area 5	477436	375	44	167	2753	8015	198	545	762
RSD	9630	34	2.4	14	80	65	6.0	19	17
%RSD	2.02	9.11	5.57	8.57	2.92	0.81	3.03	3.48	2.21
Area 6	452961	388	51	174	2549	8612	217	513	838
RSD	32732	13	3.6	8.6	217	268	10	15	14
%RSD	7.23	3.33	6.98	4.94	8.51	3.11	4.83	2.95	1.64
Area 7	422529	360	47	184	2667	7968	190	510	852
RSD	7973	18	6.5	7.7	69	33	30	12	17
%RSD	1.89	5.05	13.90	4.20	2.60	0.42	15.96	2.30	1.96
Area 8	405428	381	46	210	2682	8148	188	523	879
RSD	5438	12	2.9	11	145	69	2.9	17	17
%RSD	1.34	3.24	6.28	5.30	5.39	0.85	1.57	3.17	1.95

Table 62: p-XRF results for calcsilicate rocks from examined sites around the rampart

sample	Si	Fe	Mn	Cr	V	Ti	Ca	K	Al	Ba	Nb	Zr	Sr	Rb	S	Mg	Zn	P	Cl
Local	210399	39143	449	157	155	5022	75950	43773	66122	751	14	205	60	129	269	54212	201	1532	91
RSD	16134	752	41	28	17	280	2809	3754	3154	104	1.9	59	6.1	6.1	32	2888	24	79	5.1
%RSD	7.67	1.92	9.17	17.58	11.07	5.57	3.70	8.58	4.77	13.80	13.25	28.69	10.23	4.73	11.74	5.33	11.99	5.13	5.61
Area 1	199509	39911	407	161	164	4921	70213	48063	65517	687	14	158	57	138	258	54763	177	1480	96
RSD	11801	1669	9	12	16	265	1049	1779	3865	30	1.3	38	6.1	2.1	22	1766	5	34	1.4
%RSD	5.91	4.18	2.09	7.76	9.83	5.38	1.49	3.70	5.90	4.41	8.98	23.83	10.76	1.55	8.35	3.22	2.60	2.30	1.46
Area 2	204425	38886	435	144	157	4935	74181	46408	65275	741	17	159	59	130	268	49136	186	1583	93
RSD	5321	1429	29	13	18	525	2376	5368	2660	23	1.4	13	3.1	9.0	8.0	2461	0.9	127	1.4
%RSD	2.60	3.67	6.57	8.81	11.19	10.65	3.20	11.57	4.08	3.08	8.04	8.36	5.26	6.94	2.99	5.01	0.51	8.04	1.50
Area 3	192978	38630	469	164	180	5119	63417	49579	65406	715	18	187	51	127	303	45396	184	1519	93
RSD	8086	2215	27	23	1.5	435	479	2370	2609	31	1.2	7.5	7.5	1.2	6.0	2965	10	145	3.8
%RSD	4.19	5.74	5.82	13.86	0.84	8.51	0.76	4.78	3.99	4.39	6.82	3.99	14.63	0.93	1.97	6.53	5.34	9.51	4.10
Area 4	194517	41555	498	196	166	5039	65434	52589	63600	732	16	186	58	136	285	48212	184	1522	89
RSD	2310	1442	9.1	4.0	19	296	2886	7043	883	51	0.8	7.0	2.8	0.8	12	1444	6.4	137	2.0
%RSD	1.19	3.47	1.82	2.06	11.52	5.87	4.41	13.39	1.39	6.96	4.99	3.77	4.76	0.59	4.11	3.00	3.45	9.01	2.25
Area 5	199326	42161	516	177	169	4988	60332	54925	63370	738	16	185	61	126	310	54428	180	1494	84
RSD	1012	501	12	7.8	18	22	653	1641	2439	32	2.1	8.7	4.1	2.6	10	415	5.9	44	1.9
%RSD	0.51	1.19	2.31	4.44	10.79	0.45	1.08	2.99	3.85	4.37	12.58	4.73	6.69	2.09	3.16	0.76	3.27	2.94	2.24
Area 6	215295	40118	455	180	175	5139	63233	57053	67010	722	17	179	63	146	307	49304	189	1501	90
RSD	13067	1340	17	12	7.3	59	164	2085	318	45	0.5	10	3.3	2.2	7.1	822	11	27	2.1
%RSD	6.07	3.34	3.77	6.41	4.15	1.15	0.26	3.65	0.47	6.24	2.83	5.79	5.21	1.48	2.32	1.67	5.91	1.82	2.29
Area 7	238066	38831	501	146	174	4981	59098	56852	64747	808	17	188	64	140	286	51804	187	1511	90
RSD	3389	829	2.1	9.0	6.8	297	711	1007	3447	10	1.2	10	2.5	8.4	12	3268	8.6	33	5.8
%RSD	1.42	2.13	0.41	6.15	3.91	5.96	1.20	1.77	5.32	1.18	7.48	5.23	3.88	6.00	4.06	6.31	4.62	2.19	6.41
Area 8	205605	40942	484	142	173	5169	59323	56279	61245	821	15	201	56	142	292	55307	194	1570	83
RSD	1549	503	3.7	4.8	7.4	99	604	1958	465	13	0.8	10	2.2	3.4	19	476	5.4	18	3.4
%RSD	0.75	1.23	0.77	3.36	4.25	1.91	1.02	3.48	0.76	1.60	5.44	5.14	3.86	2.39	6.35	0.86	2.76	1.17	4.08

Table 63: p-XRF data from the melted area of the mix melts.

Sample		Zn	Fe	Ti	Ca	K	Al	P	Si	Mg
original	Average	62	34073	4685	1480	39051	94410	1058	272251	7838
	SD	4	166	121	48	943	1748	45	5999	497
	%RSD	6.96	0.49	2.58	3.21	2.42	1.85	4.21	2.20	6.34
1150 mix melt	Average	67	33963	4685	1493	39687	94288	1060	269916	7664
	SD	2	377	121	30	525	705	27	4889	312
	%RSD	3.57	1.11	2.58	2.00	1.32	0.75	2.57	1.81	4.07
1250 mix melt	Average	63	33991	4685	1515	40067	92483	1005	293913	6964
	SD	5	159	121	17	452	504	11	2256	39
	%RSD	7.89	0.47	2.58	1.13	1.13	0.55	1.06	0.77	0.57
1350 mix melt	Average	64	32283	4685	1518	39840	90079	985	333517	5910
	SD	6	336	121	40	191	381	8	5617	48
	%RSD	8.87	1.04	2.58	2.60	0.48	0.42	0.81	1.68	0.82

Table 64: p-XRF results for the flux incorporating melts

SAMPLE		Zn	Fe	Ti	Ca	K	Al	P	Si	Mg
Original	Average	62	34073	4685	1480	39051	94410	1058	272251	7838
	SD	4	166	121	48	943	1748	45	5999	497
	%RSD	6.96	0.49	2.58	3.21	2.42	1.85	4.21	2.20	6.34
Charcoal	Average	57	33108	4714	1732	48183	91747	1520	267370	8729
	SD	7	1373	95	23	1038	1057	53	10780	187
	%RSD	12.47	4.15	2.02	1.34	2.15	1.15	3.46	4.03	2.14
Wood	Average	58	32820	4429	1685	44868	92174	1476	251442	8661
	SD	4	923	232	43	1335	787	32	8360	120
	%RSD	7.41	2.81	5.25	2.53	2.98	0.85	2.16	3.32	1.38
Bones	Average	72	35265	4661	1642	42208	96249	1649	253145	8780
	SD	3	467	104	35	570	2388	71	6381	397
	%RSD	4.56	1.33	2.23	2.16	1.35	2.48	4.32	2.52	4.53
Shell	Average	62	34941	4609	1584	40509	92912	1204	274321	8507
	SD	4	1684	166	34	1296	156	19	2614	30
	%RSD	6.69	4.82	3.60	2.16	3.20	0.17	1.55	0.95	0.35
Seaweed	Average	79	35463	4455	1628	41092	94873	1371	279476	8664
	SD	3	469	69	35	576	936	70	4136	91
	%RSD	3.88	1.32	1.54	2.17	1.40	0.99	5.14	1.48	1.05

Table 65: p-XRF results for soils collected from trench 6.

SAMPLE	Ti	Ca	K	Al	P	Si	Cl	S	Mg	Fe	Ba	Nb	Zr	Sr	Rb	Pb	Mn
Units	%	%	%	%	%	%	ppm	%	%	%	ppm	ppm	ppm	ppm	ppm	%	ppm
Base average	4330	18255	15144	50685	2816	252327	474	2208	13190	25321	346	13	275	85	77	771	175
Base RSD	48	257	99	1173	125	1476	16	43	2098	94	56	0.3	4.1	1.7	1.4	57	25
Base %RSD	1.12	1.41	0.65	2.31	4.42	0.58	3.31	1.97	15.91	0.37	16.07	2.55	1.48	2.04	1.84	7.34	13.98
dd16 1004 average	4342	18324	15223	52058	2947	253544	346	2163	15729	25729	368	14	274	86	75	733	179
dd16 1004 RSD	83	235	242	741	61	900	16	33	2328	212	17	0.9	4.4	1.1	1.4	46	23
dd16 1004 %RSD	1.92	1.28	1.59	1.42	2.06	0.35	4.59	1.52	14.80	0.82	4.67	6.77	1.60	1.32	1.87	6.26	12.72
dd16 1005 average	4221	22766	15529	58214	3022	243353	718	1803	20521	29248	257	13	239	85	62	1208	219
dd16 1005 RSD	71	309	217	1070	122	1319	29	47	2562	85	39	1.4	3.0	1.9	1.6	44	28
dd16 1005 %RSD	1.68	1.36	1.40	1.84	4.04	0.54	4.09	2.59	12.48	0.29	15.03	10.68	1.26	2.20	2.56	3.63	12.94
dd16 1006 average	4168	21695	12952	54136	2872	234411	512	2312	15448	33023	246	11	211	122	63	1169	439
dd16 1006 RSD	93	222	248	929	135	1549	17	47	1626	129	18	0.7	3.2	2.5	2.1	54	22
dd16 1006 %RSD	2.22	1.02	1.92	1.72	4.69	0.66	3.27	2.05	10.53	0.39	7.20	6.60	1.50	2.04	3.38	4.58	4.95
dd16 1008 average	3651	13721	16176	57507	2408	206690	536	2388	9840	31000	387	11	220	147	73	174	207
dd16 1008 RSD	66	191	289	889	77	1690	25	44	1971	205	30	0.8	2.7	2.5	1.6	38	17
dd16 1008 %RSD	1.81	1.39	1.79	1.55	3.19	0.82	4.65	1.85	20.03	0.66	7.80	7.47	1.25	1.71	2.13	21.76	8.33
dd16 1011 average	4121	21308	13374	65914	3146	221439	435	2069	20321	37749	342	12	217	79	65	1638	258
dd16 1011 RSD	53	310	239	1554	105	1120	18	34	3036	193	22	1.0	4.0	1.6	1.4	52	18
dd16 1011 %RSD	1.29	1.45	1.79	2.36	3.33	0.51	4.12	1.64	14.94	0.51	6.44	8.75	1.83	2.03	2.22	3.16	6.90
dd16 1015 average	3688	21507	14153	67270	3336	220265	244	2011	19369	28638	530	14	229	78	76	951	220
dd16 1015 RSD	81	361	210	1292	105	1008	22	37	2544	182	37	1.2	3.1	1.7	1.8	73	19
dd16 1015 %RSD	2.19	1.68	1.48	1.92	3.14	0.46	9.02	1.82	13.13	0.63	7.03	8.43	1.35	2.23	2.39	7.64	8.63
dd16 1016 average	4089	21436	14136	70811	3824	225791	369	1519	20172	32873	387	13	232	86	69	699	235
dd16 1016 RSD	50	282	196	1927	151	1084	24	31	2048	159	30	1.4	2.0	1.5	2.7	46	15
dd16 1016 %RSD	1.22	1.32	1.39	2.72	3.96	0.48	6.63	2.05	10.15	0.48	7.84	11.22	0.88	1.71	3.84	6.57	6.44
dd16 1017 average	4957	14554	18960	78791	3611	239412	222	1529	14243	32200	366	15	234	109	92	504	187
dd16 1017 RSD	68	276	358	915	84	1417	13	26	2348	176	35	0.7	2.4	1.6	2.5	38	16
dd16 1017 %RSD	1.38	1.90	1.89	1.16	2.33	0.59	5.94	1.73	16.49	0.55	9.51	4.50	1.01	1.49	2.74	7.48	8.78
dd16 1020 average	3938	21481	14693	60478	8058	241839	151	1844	18605	28928	450	12	241	86	71	2711	156
dd16 1020 RSD	48	275	258	1325	149	1058	14	30	1553	206	27	1.1	2.6	1.6	2.3	113	12
dd16 1020 %RSD	1.21	1.28	1.76	2.19	1.85	0.44	8.98	1.64	8.35	0.71	5.96	9.46	1.08	1.88	3.33	4.15	7.44
dd16 1021 average	4069	23591	13483	66119	7743	222634	220	1170	23530	34011	544	12	228	84	66	1687	206
dd16 1021 RSD	38	377	214	1353	113	979	14	36	1706	179	36	1.3	4.3	2.3	0.9	99	8.7
dd16 1021 %RSD	0.94	1.60	1.58	2.05	1.46	0.44	6.56	3.10	7.25	0.53	6.68	10.53	1.89	2.77	1.38	5.84	4.24